Studies on Early Processes in Radiation Chemistry by Means of ESR Spectroscopy and Picosecond Pulse Radiolysis

by Yosuke Katsumura

Nuclear Engineering Research Laboratory
Faculty of Engineering, University of Tokyo
Tokaimura, Ibaraki, Japan 319-11

1980

Preface

Knowledge of the chemical effects produced by high-energy radiation is beginning to be sufficiently well founded for radiation chemistry to be regarded as a distinct scientific discipline. The subjects are related closely with other fields in chemistry because short lived chemical species produced by high-energy radiation are electrons, holes, anions, cations, radicals, and excited states, which react with each other to be formed final products.

It seems that many studies between 1950's and 1960's were mainly based on the measurements by product analyses and steady state techniques. Since the discovery of flash photolysis technique, studies depending on the observations and measurements of dynamic behaviors of the short lived intermediates produced by high-energy radiation appeared and have been developed in radiation chemistry. Today, the time resolution of the techniques reached to picosecond (10^{-12} sec) region.

Although many kinds of techniques have been used in radiation chemistry and new types of techniques will be discovered and applied, both ESR spectroscopy and pulse radiolysis technique have been playing important roles among these techniques. In fact, over one hundred papers entitled "pulse radiolysis" or "ESR" were published in these five years (1975~1979). It seems that these two techniques will be playing important roles in radiation chemistry in future.

The present paper consists of two sections. The one is a study by ESR spectroscopy. In chapter 1, historical survey of ESR spectroscopy in radiation chemistry is reported briefly. Studies on radiolysis of neopentane during electron irradiation, fluoroalkyl nitroxide radicals using spin trapping technique, and spatial distribution of radicals by fast neutron irradiation are reported in chapters, from 2 to 4.

The other section, chapter 5 to 11, is focused on the studies on the formation processes of solute excited states in liquid hydrocarbon by pulse radiolysis technique.

These studies were carried out at Faculty of Nuclear Engineering in Hongo and Nuclear Engineering Research Laboratory in Tokaimura. I would express here my sincere thanks to Professor Yoneho Tabata, Professor Keichi Oshima, Professor Takaaki Tamura and Associate Professor Kenkichi Ishigure, who introduced me into the field of radiation chemistry and encouraged me all the time. I would express sincere thanks to Dr. Hajime Kadoi, Dr. Hirotsugu Shiraishi, Dr. Seiichi Tagawa, Dr. Shingo Matsuoka, Dr. Norihiko Fujita, Mr. Miyoshi Onoue, Mr. Toshio Kawanishi, and Mr. Chihiro Matsuura, who taught me how to carry out the research and encouraged me all the time. I thank Associate Professor Yasuo Itoh for his helpful suggestions. I should also thank to my colleague in our laboratory, especially, Associate Professor Kenzo Miya, Mr. Hitoshi Kabayashi, Mr. Toru Ueda, Mr. Toshiaki Kobayashi, Mr. Hideharu Yanagi and Mr. Masakazu Washio.

I thank Miss. Yasuko Asai for typing of the present paper.

Papers

1) "Electron Spin Polarization Effects in a Study of Transient Hydrogen Atoms in Acidic Ices under Electron Irradiation"
Hirotsugu Shiraishi, Hajime Kadoi, Yosuke Katsumura
Yoneho Tabata and Keichi Oshima
J. Phys. Chem. 78 1336 (1974)

2) "Electron Spin Resonance Studies on Hydrogen Atoms Formed in Pure and Acidic Ices under Electron Irradiation. Motional Narrowing and Electron Spin Polarization Effect"
Hirotsugu Shiraishi, Hajime Kadoi, Yosuke Katsumura
Yoneho Tabata and Keichi Oshima
J. Phys. Chem. 80 2400 (1976)

3) "Electron Spin Resonance Study on the Radiolysis of Neopentane in Solid Phase during Electron Irradiation"
Yosuke Katsumura, Akihiro Fujita, Hajime Kadoi, Kenkichi Ishigure and Yoneho Tabata
Rad. Phys. Chem. 12 69 (1978)

4) "ESR Study on Fluoroalkyl Nitroxide Radicals Using Spin Trapping Technique"
Yosuke Katsumura, Kenkichi Ishigure and Yoneho Tabata
J. Phys. Chem. 83, 3152 (1979)

5) "ESR Study on the Spatial Distribution of Radicals Formed by Fast-neutron irradiation"
Yosuke Katsumura, Masahiro Hamamoto, Hideharu Yanagi and Yoneho Tabata
J. Fac. Eng. Univ. of Tokyo, 35 345 (1979)

6) "Spatial Distribution of Radicals Produced by Fast-neutron Irradiation"
Yosuke Katsumura, Masahiro Hamamoto, Hideharu Yanagi and Yoneho Tabata
Rad. Phys. Chem. in press

7) "A 35 MeV Electron Linear Accelerator Project at Nuclear Engineering Research Laboratory, University of Tokyo"
Yoneho Tabata, Jiro Tanaka, Seiichi Tagawa, Yosuke Katsumura, Toru Ueda and Kenichi Hasegawa
J. Fac. Eng. Univ. of Tokyo, 34 619 (1978)

8) "35 MeV Electron Linear Accelerator at University of Tokyo"
Yoneho Tabata, Seiichi Tagawa, Yosuke Katsumura, Toru Ueda, Kenichi Hasegawa and Jiro Tanaka
J. Atomic Energy Soc. Japan, 20 473 (1978)

9) "The Ultra Fast Process of Picosecond Time Resolved Energy Transfer in Liquid Cyclohexane by Picosecond Single Pulse Radiolysis"
Seiichi Tagawa, Yosuke Katsumura and Yoneho Tabata
Chem. Phys. Letts. 64 258 (1979)

10) "Evidince for Two Fast Formation Processes of Solute Excited States in Liquid Toluene Solutions Studied by Picosecond Single Pulse Radiolysis"
Seiichi Tagawa, Yosuke Katsumura and Yoneho Tabata
Rad. Phys. Chem. 15 287 (1980)

11) "Direct Observation of Energy Transfer from Excited Cyclohexane Molecules to Toluene by Means of Picosecond Pulse Radiolysis"
Yosuke Katsumura, Tadashi Kanbayashi, Seiichi Tagawa and Yoneho Tabata
Chem. Phys. Letts. 67 183 (1979)

12) "Picosecond Pulse Radiolysis Studies on Excitation Processes in Liquid Cyclohexane"
Yosuke Katsumura, Seiichi Tagawa and Yoneho Tabata
J. Phys. Chem. 84 833 (1980)

13) "Studies on Energy Transfer Process in Liquid Toluene by Picosecond Pulse Radiolysis"
Yosuke Katsumura, Tadashi Kanbayashi, Seiichi Tagawa and Yoneho Tabata
to be published

14) "Recent Progress in Radiation Chemistry"
Yoneho Tabata, Seiichi Tagawa and Yosuke Katsumura
Radioisotopes 28 No. 9 548 (1979)

15) "Studies on Scavenging Effect for Faster Formation Process of Solute Excited State in Cyclohexane by Means of Picosecond Pulse Radiolysis"
Yosuke Katsumura, Seiichi Tagawa, Yoneho Tabata
to be published

16) "Studies on Scintillation Emission in Various Kinds of Solvents by Means of Picosecond Pulse Radiolysis"
Yosuke Katsumura, Seiichi Tagawa and Yoneho Tabata
J. Fac. Eng. Univ. of Tokyo in press

17) "Picosecond Pulse Radiolysis Studies on Scintillation Emission in Various Kinds Solvents"
Yosuke Katsumura, Tadashi Kanbayashi, Seiichi Tagawa and Yoneho Tabata
to be published

18) "Picosecond Pulse Radiolysis Studies of Solute Excited State Formation Mechanism in Cyclohexane Solution"
Seiichi Tagawa, Yosuke Katrumura, Tadashi Kanbayashi and Yoneho Tabata
to be published

19) "Picosecond Pulse Radiolysis Studies of Solute Excited State in Several Saturated Hydrocarbon Solvents"
Seiichi Tagawa, Tadashi Kanbayashi, Yosuke Katsumura and Yoneho Tabata
to be published

20) "Excimer Formation of Hexafluobenzene by Means of Picosecond Pulse Radiolysis"
Yosuke Katsumura, Tadashi Kanbayashi, Seiichi Tagawa and Yoneho Tabata
to be published

21) "Bunch Moniters for S-Band Electron Linac"
Masakazu Washio, Shigeki Fukuda, Jiro Tanaka, Isamu Sato, Shozo Anami, Yoneho Tabata, Hitoshi Kobayashi, Yosuke Katsumura, Toru Ueda and Seiichi Tagawa
KEK-79-24 October 1979 P

22) "Study on Fast Processes in Radiation Chemistry by Means of Picosecond Pulse Radiolysis"
Yoneho Tabata, Yosuke Katsumura, Hitoshi Kobayashi, Masakazu Washio and Seiichi Tagawa
Proceedings for the Second International Conference on Picosecond Phenomena, June 18-20, 1980, Massachusetts, USA.

Contents

Chapter 1.

ESR Spectroscopy in Radiation Chemistry

Since 1945, when Zavoisky in the U.S.S.R. observed esr (electron spin resonance) absorption of cupper salts, esr spectroscopy has been widely used in many areas, of course, including radiation chemistry.[1] In principle, esr spectroscopy gives information of radical structure, radical kinetics, intramolecular change of radicals (interconversion, conformational change, et al) and relaxation mechanisms.[2] The development of esr studies in radiation chemistry is closely related to that of the techniques how to produce short lived transient species.

In the present paper, the development of esr studies in radiation chemistry is discussed briefly in connection with both in other fields and techniques how to produce short lived transients.

In 1950's, at 77 K a variety of organic compounds were irradiated by Co^{60} γ-ray and many types of trapped radicals produced in the medium were observed by means of esr spectroscopy. Using this technique, many results were reported but the resolution of esr spectra reported was poor because produced species were frozen tightly in matrices at low temperature. At that time cold finger technique or rotating cryostat method appeared.[3] Those methods were based on observation of frozen short lived radicals.

In 1960's many researchers intended to observe the short lived transient species directly, dynamically and clearly. In 1963 Dixson and Norman[4] produced very active OH radicals, which easily abstract H atoms from solute molecules (for example, $CH_3OH + \cdot OH \rightarrow \dot{C}H_2OH + H_2O$), by the following reaction in aqueous solution,

$$Ti^{3} + H_2O_2 \longrightarrow Ti^{4+} + OH^{-} + \cdot OH$$

They observed many kinds of alcohol radicals in aqueous system with higher resolution than those observed in solid at low temperature. This method has been called a rapid mixing method. This method is extended to polymerization system, and initiation and propagation radicals were observed.[5] This is also applied to co-polymerization system.[6] Another rapid mixing method is developed in liquid hydrocarbon systems as following,

$$R-Li + R'x \longrightarrow Lix + R\cdot + R'$$

Using this method, several transient alkyl radicals were observed.[7]

Similar systems were developed in photolysis system. When aqueous solution containing small amount of H_2O_2 and solute is irradiated by UV light, highly reactive OH radicals are produced and they attack the solute molecules.[8] This method was also applicable to iodide compounds or peroxycompounds.

$$\text{I)} \quad H_2O_2 \xrightarrow{h\nu} \cdot OH$$

$$R + \cdot OH \longrightarrow R\cdot$$

$$\text{II)} \quad RI \xrightarrow{h\nu} R\cdot + I\cdot$$

$$\text{III)} \quad R'OOR' \xrightarrow{h\nu} \cdot OR'$$

$$R + \cdot OR' \longrightarrow R\cdot$$

Henceforth, this photo production of radicals has been widely used for studies on radical structures.

In 1963, another production technique of radicals was introduced by Fessenden and Schuler.[9] They produced short lived radicals by irradiation with electron beam having a energy of 2.8 MeV from van de Graaf accelerator. They successfully observed many kinds of alkyl radicals in liquid hydrocarbon and obtained accurate esr parameters of radicals. Their data has been widely used for considering structure in molecular orbital theories. They also observed anomalous spectra of H atom in liquid methane <u>in situ</u> electron

irradiation. In the case of liquid methane, resonance line at lower side of H atom, which has two resonance lines with 506G separation, indicated not absorption but emission. This observation was not explained at that time. Later these phenomena including abnormal spectra have been called CIDEP (Chemically Induced Dynamic Electron Polarization) in connection with CIDNP (Chemically Induced Dynamic Nuclear Polarization).[10] ESR studies during electron irradiation have been carried out at several places in the world.[11]

In 1968 Smaller et al at Argonne National Lab. made a time resolved ESR spectroscopy equipment with $\sim\mu$ second time resolution. They used not normal 100 KHz field modulation but 2 MHz one. They found that some lines of observed c-pentyl radical produced by electron irradiation of cyclopentane are not absorption but emission.[12] It was also found that the emission line changes to absorption one at $\sim$20 μsec after the electron pulse irradiation. This observation was similar to that of H atom in liquid methane reported by Fessenden in 1963. They also studied the behavior of H atom in aqueous solution and solvated electron in alcohol solutions.[13]

Another unique method, using adduct compounds of urea and thio urea, is developed. A certain molecules such as acetone are stably taken in adducts and radicals produced selectively from guest molecule by γ-irradiation can be observed rather sharply. This method is convenient to observe cation and anion radicals and widely used now.[14]

In 1970's, time resolved esr spectroscopy was developed by Fessenden.[15] Since they used direct amplification method without field modulation, absorption spectra is directly obtained. Anomalous spectra of H atom was explained by modified-Bloch equation based on spin selective reaction. Recently, Trifunac et al used spin echo technique for observation of the polarization effect of short lived transient radicals by pulse radiolysis and laser photolysis.[16] Time resolved esr spectroscopy is also in progress at Nuclear Engineering Research lab. Univ. of Tokyo.

These techniques above mentioned are a direct detection of radicals. However, spin trapping technique[17] is an indirect method. This method is based on the observation of formed stable nitroxide radicals by the reaction between radicals produced in the sample system and nitroso or nitrone compounds as trapping agents. The reaction can be expressed as following,

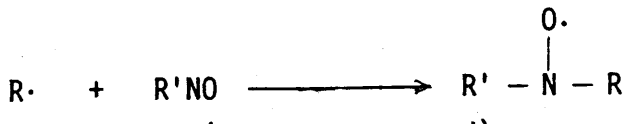

(nitroso compound)

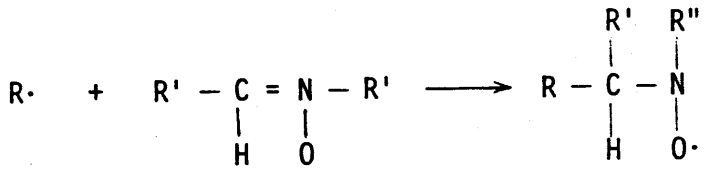

(nitrone compound)

First application of this technique to radiation chemistry is a study on radiolysis of alcohols.[18),19)] When alcohol is irradiated, a formation of alcohoxy radicals were assummed to be produced, but had not been observed. Williams et al observed alcohoxy nitroxide radicals produced in spin trapping agent solution of alcohol in 1970 and confirmed the exsistence of alcohoxy radical produced by irradiation. Recently, at 4K, Iwasaki et al directly observed the alcohoxy radical itself produced by x-ray irradiation.[20)] It seems that this technique has much potential to be applicable to many fields; radiolysis of gases,[21)] liquid and solid,[22)] polymerization, pilolysis, and electolysis.[23)] However, the yields of produced nitroxide radicals in the systems are dependent on the reaction rates between radicals and spin trapping agents. If precise rate constant of scavenging by the trapping agents is not obtained, it is difficult to evaluate the real scope of the reaction.

Recently, the reaction rates of diffirent spin trapping agents with

different kinds of radical were measured and these data help us to evaluate the reaction.[24] There is also another problem that the trapping agents behave like scavengers of electron or hole[25] in radiolysis. Although there are some limitations in the spin trapping technique, this technique will be more widely used because of its convenience.

Since 1950's low temperature technique has been widely used and, now, measurement even at liquid heliqum temperature becomes popular. ENDOR (electron nuclear double resonance) and ELDOR (electron electron double resonance) appeared in the late of 1960's.[26] Not only radiation chemistry but also biochemistry become a big field for application of esr spectroscopy. On the other hand, molecular orbital theory is rapidly developed with increasing digital computers and it becomes easy to calculate the structure of radicals by use of INDO, CNDO method.[27] Now, it is well known that theoretical calculation such as INDO, CNDO strongly supports the experimental results.

In the following, some recent topics using esr technique in radiation chemistry will be discussed.

i) Selective Radical Formation in Solid Phase

Selective radical, cyclohexyl radical, formation was observed at 77 K by irradiation of neopentane containing a small amount of cyclohexane in 1974 by Miyazaki et al in Japan.[29] Independently, similar effect was also observed in Europe in 1974.[30] At that time selective radical formation was explained by energy transfer from solvent to solute.[31] However, two experimental results, selective formation of solute radicals by the photolysis of neopentone-cyclohexane mixture containing HI and selective solute radicals produced by H atom addition to olefins in neopentane by radiolysis, strongly suggested that H atom produced in the matrix by irradiation plays an important role for selective solute radical formation. Today, this

mechanism is widely accepted for selective solute radical formation by irradiation at 77 K. This selective solute radical formation was also observed in another system, n-deutrated decane (n-$C_{10}D_{22}$) containing a small amount of n-decane (n-$C_{10}H_{22}$),[31] tetramethylsilane[32] and xenon matices.[33] However, this selective formation of solute radicals in neopentane matrix could not observed at 4K and above 140K in plastic crystal phase.[34] It is thought that irradiation temperature and phase are very important factors. About this problem, two Japanese groups, Miyazaki et al and Iwasaki et al, have investigated very intensively. However, the precise mechanisms suggested by the two groups were different. Miyazaki's group[35] suggested " hot H atom mechanism " and " channelling mechanism ". On the other hand, Iwasaki's group[36] assumed that not hot but thermal H atom produced by irradiation plays a dominant role for selective reaction. Similar problem in solid rare-gas systems is also investigaged by the two groups.

ii) Radiolysis at Liquid Helium Temperature

In optical absorption spectroscopy radiolysis at liquid helium temperature was frequently done for studying on solvation process of electron in polar systems. In esr spectroscopy, this low temperature technique became popular and much new information is obtained. Iwasaki et al studied on radiolysis of crystalline methanol at 4.2K, and directly found that $CH_3O\cdot$ and $\cdot CH_3$ are formed as a major products. Alcohoxy ($CH_3\dot{O}$) radical was not observed directly before because of its high reactivity and short relaxation times and only exsistance of a alcohoxy radical was confirmed indirectly by spin trapping technique.

In methane containing 0.5 mol% ethane, reactivity of thermal hydrogen at 10-30K was also discussed by Iwasaki.[36] In methane matrix, it is well known that H atom is trapped at 4K. After annealing at 10K, solute ethyl radical was formed by H atom abstraction of solute ethane and consequent

decrease of trapped H atoms were observed. Reactivity of H atoms and spatial distribution of radicals were discussed based on above experimental results. It seems that much more interesting information of early processes in irradiation can be obtained by means of low temperature radiolysis.

iii) Studies on Anion, Cation Radicals using Neopentane, Tetramethylsilane and Fleon Mixture as Matrices

Unstable guest radicals were observed in urea or adamantane adducts, as already written. Recently, unstable cation, anion radicals could be observed using particular matrices.

William et al used tetramethylsilane or neopentane as a matrix and observed halofluoromethane anion radicals (CF_3Cl^-, CH_3Br^-, CF_3I^- et al) having rather sharp lines. In these matrices, the radicals are expected to be rotating rather freely and give sharp esr spectra. Not only halofluoromethane but also halofluorosilane anion radicals (SiF_4^-, SiF_3Cl^- et al)[39] were investigated by them. The structure of these radicals were discussed in connection with the result of molecular calculation such as INDO. Recently, esr spectra of cation radicals and their structures were also reported by Shida et al[40] in fleon mixture matrix.

Although we have little information of the structure about anion and cation radicals except aromatic molecules in solution at present, much more knowledge about anion and cation radicals is expected to be obtained, by means of esr spectroscopy in near future.

References

1) a) R.W. Fessenden; "Advances in Radiation Chemistry" vol. 2 John Wiley & Sons. 1972.

b) A.D. Trifunac and M.C. Thurnauer, p107 in "Time Domain Electron Spin Resonance" John Wiley & Sons, 1979.

2) a) Poole, Jr. C.P.; Electron Spin Resonance — A Comprehensive Treatise on Experimental Techniques, Interscience Publishers, 1967.

b) R.S. Alger; Electron Paramagnetic Resonance: Techniques and Applications. John Wiley & Sons, 1968.

c) A. Carrington and A.D. McLachlan; Introduction to Magnetic Resonance, Harper & Row, 1967.

d) J.E. Wertz and J.R. Bolton; Electron Spin Resonance Elementary Theory and Practical Applications, McGraw-Hill, 1972.

e) G.E. Pake; Paramagnetic Resonance, W.A. Benjamin, Inc., 1962.

3) a) C.K. Jen, S.N. Foner, E.L. Cochran, V.A. Bowers; Phys. Rev. 112 1169 (1958)

b) S.N. Foner, E.L. Cochran, V.A. Bowers, C.K. Jen; Phys. Rev. Lett. 1 91 (1958)

c) J.E. Bennett, A. Thomas; Proc. Roy. Soc. 280A 123 (1964)

4) W.T. Dixson, R.O.C. Norman; Nature 196 891 (1962), J. Chem. Soc., 1964 3625 and J. Chem. Soc., 1964 4850.

5) H. Fisher; Z. Naturforsh., 199 866 (1964)

6) P.O. Kinell, B. Rånby and V. Runnström-Reio, eds.; ESR Applications to Polymer Research, Proceedings of the 22 nd Nobel Symposium, Sweden. 1972.m John Wiley & Sons, 1973.

7) H. Fischer; J. Phys. Chem. 73 3834 (1969)

b) H. Zeldes, R. Livingston; J. Chem. Phys., 45 1946 (1966)

9) R.W. Fessenden and R.H. Schuler; J. Chem. Phys. 39 2147 (1963)

10) a) L.T. Muus, P.W. Atkins, K.A. McLachlan and J.B. Pedersen, eds.; Chemically Induced Magnetic Polarization, D. Reidel Publishing Com., 1977.

b) A.R. Lepley and G.L. Closs, eds; Chemically Induced Magnetic Polarization, Wiley, 1973.

11) Rad. Lab. Univ. of Notre Dame and Argonne National Lab. in USA, Ispra in Italy, Atomic Research in Canada and Univ. of Tokyo in Japan.

12) a) B. Smaller, J.R. Remko and E.C. Avery; J. Chem. Phys. 48 5174 (1968)

b) E.C. Avery, J.R. Remko and B. Smaller; J. Chem. Phys. 49 951 (1969)

13) B. Smaller, E.C. Avery and J.R. Remko; J. Chem. Phys. 55 2414 (1971)

14) Y. Kimura, Doctor Thesis, University of Tokyo, 1974.

15) a) R.W. Fessenden; J. Chem. Phys. 58 2489 (1973)

b) N.C. Verwa and W.R. Fessenden; J. Chem. Phys. 58 2501 (1973)

c) R.W. Fessenden and N.C. Verwa; J. Amer. Chem. Phys. 65 2139 (1976)

d) N.C. Verwa and R.W. Fessenden; J. Chem. Phys. 65 2139 (1976)

e) R.W. Fessenden and N.C. Verwa; Faraday Disc. Chem. Soc. 63 104 (1977)

16) for time resolved esr;

a) A.D. Trifunac and E.C. Avery; Chem. Phys. Letts. 27 141 (1974)

b) A.D. Trifunac and E.C. Avery; Chem. Phys. Letts. 28 294 (1974)

c) A.D. Trifunac and D.J. Nelson; Chem. Phys. Letts. 46 346 (1977)

d) D.J. Nelson, C. Mottley and A.D. Trifunac; Chem. Phys. Letts. 55 323 (1978)

e) A.D. Trifunac, M.C. Thurnauer and J.R. Norris; Chem. Phys. Letts. 57 471 (1978)

by means of spin echo technique;

f) A.D. Trifunac; Chem. Phys. Letts. 59 (1978)

g) A.D. Trifunac; J.R. Norris, and R.G. Lawler; J. Chem. Phys. in press.

17) a) M.J. Perkins; Chem. Soc. Spec. Publ., No.24., 97 (1970)

b) E.G. Janzen; Accounts Chem. Res. 4 31 (1970)

c) C. Lagercrantz; J. Phys. Chem. 75 3466 (1971)

18) J.A. Wargon and F. Williams; J. Amer. Chem. Soc. 94 7917 (1972)

19) a) S.W. Mao and L. Kevan; Chem. Phys. Letts., 24 505 (1974)

b) F.P. Sargent and E.M. Gardy; Can. J, Chem., 52 3645 (1974)

Can. J. Chem. 53 3128 (1975) and Can. J. Chem. 54 275 (1976)

20) K. Toriyama and M. Iwasaki; J. Amer. Chem. Soc. 101 2516 (1979)

21) S. Nagai, K. Matsuda and M. Hatada; J. Phys. Chem., 82 322 (1978)

22) J. Sohoma; the 5 th ICRR, Tokyo, 1979.

23) P.H. Kasai, D. McLeod, Jr.,; J. Phys. Chem. 82 619 (1978)

24) P. Schmidt, K.V. Ingold; J. Amer. Chem. Soc., 99 6434 (1977)

and J. Amer. Chem. Soc., 100 2493 (1978)

25) S. Murabayashi, M. Shiotani and J. Sohma; J. Phys. Chem. 83 844 (1979)

26) L. Kevan and L.D. Kispert; Electron Spin Double Resonance Spectroscopy, John-Wiley & Sons.(1976)

27) J.A. Pople and D.L. Beveridge; Approximate Molecular Orbital Theory, McGraw-Hill, 1970.

28) J.K. Kochi; Advanced in Free Radical Chemistry, vol. 5, p189 ed. G.H. Williams, Academic Press, 1975.

29) T.Miyazaki, T. Wakayama, M. Fukaya, Y. Saitake and Z. Kuri, Bull. Chem. Soc. Jpn., 46 1030 (1973)

30) a) C. Fauquenoit and P. Claes; Bull. Soc. Chem. Belges., 80 323 (1971)

b) T. Gilbro and A. Lund; Chem. Phys. Letts. 27 300 (1974)

31) a) T. Miyazaki, K. Kinugawa and J. Kasugai; Rad. Phys. Chem. 10 155 (1970)

b) M. Iwasaki, K. Toriyama, K. Nunome, M. Fukaya and H. Muto; J. Phys. Chem. 81 1410 (1977)

32) T. Miyazaki, J. Kasugai, M. Wada, and K. Kinugawa; Bull. Chem. Soc. Jpn. 51 1676 (1978)

33) a) M. Iwasaki, H. Muto, M. Fukaya and K. Nunome; J. Phys. Chem. 83 1950 (1979) and J. Phys. Chem. 81 1410 (1977)

b) K. Kinugawa, T. Miyazaki and H. Hase; Rad. Phys. Chem. 10 341 (1977)

34) Y. Katsumura, A. Fujita, H. Kadoi, K. Ishigure and Yoneho Tabata; Rad. Phys. Chem. 12 69 (1978)

35) T. Miyazaki; Bull. Chem. Soc. Jpn. 50 1625 (1977)

36) a) K. Toriyama and M. Iwasaki; J. Phys. Chem. 82 2056 (1978)

b) M. Iwasaki and K. Toriyama; J. Phys. Chem. 83 1596 (1979)

37) M. Iwasaki, K. Toriyama, H. Muto and K. Nunome; Chem. Phys. Letts. 56 494 (1979)

K. Toriyama, M. Iwasaki and K. Nunome; J. Chem. Phys. 71 1698 (1979)

38) a) A. Hasegawa, M. Shiotani and F. Williams; Discus. Faraday Soc. 63 157 (1978)

b) A. Hasegawa and F. Williams; Chem. Phys. Letts. 46 66 (1977)

39) R.I. McNeil, F. Williams and M.B. Yirn; Chem. Phys. Letts. 61 293 (1979)

40) a) K. Egawa, T. Kubodera, T. Kato and T. Shida; the 18 th ESR symposium in Japan, 1979, Sapporo.

b) K. Egawa, T. Kubodera, T. Kato and T. Shida; Chem. Phys. Letts. 68 106 (1979)

Chapter 2.

Electron Spin Resonance Study on the Radiolysis of Neopentane in Solid Phase during Electron Irradiation

Summary

The radiolysis of neopentane was investigated mainly in the plastic crystal phase by means of esr spectroscopy during electron irradiation. In this phase, neopentyl, tert-butyl and tert-pentyl radicals were observed. The formation and decay rates of these radicals were measured, and the G-values of those radicals and the rate constant of the decay were estimated in the plastic crystal phase. In order to elucidate the mechanism of radical formation, the difference in effect of additives between plastic crystal and normal crystal phases was examined. It was found that the radical formation is greatly affected by electron scavengers such as CCl_4 and SF_6 in both phases. On the other hand, the well-known selective radical formation from added alkanes in the crystal phase was not observed in the plastic crystal phase. From the effect of the additives the mechanism of the radical formation in the radiolysis of neopentane was discussed.

Introduction

Neopentane is a spherical molecule and forms plastic crystal phase between the crystal transition point, -133°C, and the melting point, -16°C.[1] In the plastic crystal phase, neopentane molecules rotate freely at lattice points and move around to some extent depending on temperature. Therefore, radicals produced by irradiation are thought to rotate and migrate rather

freely. Esr spectra are much sharper in the plastic crystals than in the normal crystals owing to motional narrowing. The lifetime of radicals becomes shorter and radicals decay quickly in the plastic crystal.

The esr measurements during electron irradiation were reported by Buben et al[2] and Fessenden & Schuler[3], independently. The radiolysis of 2, 2, 3, 3-tetramethylbutane in the plastic crystal was discussed from both esr measurement during electron irradiation and product analysis in our previous paper.[4] In the present work, the production and decay kinetics of radicals in neopentane plastic crystals were investigated through esr measurement during electron irradiation. The radiolysis of neopentane has been investigated at 77 K by means of esr spectroscopy by several investigators.[5] However, the mechanism of the radical formation and the effect of phase on the radiolysis of neopentane was not discussed before. To elucidate the mechanism and the difference of radical formation between both phases, the effect of electron scavengers such as sulfur hexafluoride and carbon tetrachloride was examined.

Recently, Miyazaki et al[6] have reported that the selective radical formation occurs in the radiolysis of neopentane containing a small amount of alkane in the crystal phase. They[7] also found that selective hydrogen atom abstraction occurs in the photolysis of neopentane containing alkane and hydrogen iodide. They concluded that the radicals are formed from the solute alkane by selective hydrogen abstraction of atoms produced in the radiolysis of neopentane. However, the precise mechanism for the selective radical formation is not clear at present. It is expected that comparative measurements in the plastic crystal phase may help to solve this problem. Additives used are cyclohexane, 2, 3-dimethylbutane and isopentane, which are known to give corresponding radicals by the selective hydrogen atom abstraction. Benzene was also used as another additive.

Experimental

Neopentane (>99.9 %) was used as received from Tokyo Kagaku Seiki Co. . 2, 3-Dimethylbutane, cyclohexane, isopentane, benzene, and carbon-tetrachloride were Tokyo Kasei's guaranteed grade. Sulfur hexafluoride was supplied by Asahi Glass Co., Ltd.

Electron accelerator employed is a Dynamitron in Research Center for Nuclear Science and Technology, University of Tokyo, and it was operated at 1.2 MeV.

Dose rate was monitered by the measurement of electron current coming into the cavity, and irradiation dose was measured by the change of optical absorbance of a polymethylmethacrylate plate irradiated.[8] Dose rate was estimated to be 7.5 Mrad/min at 1.0 μA monitered at the esr cavity. The used dose rate was usually in a range of 1 to 100 Mrad/min. Esr spectrometer was a conventional X-band type with 100 KHz modulation. The microwave power was kept low enough to avoid saturation effect. Details of the irradiation system have been reported elsewhere.[4]

Sample material (0.2 cc) was sealed after degassing on a vacuum line in a tube (~4 ϕ) made of special radiation resistant glass with a thermocouple enclosed to detect the sample temperature. Radical concentration was measured by comparing the signal intensity with a Mn^{2+} standard sample which was placed in the cavity away from electron beam path and been calibrated by DPPH solution of known concentration.

Results

I. Identification of radicals and decay kinetics in plastic crystals

Esr spectra measured during electron irradiation of neopentane in the plastic crystal phase at different temperatures at a dose rate of 15 Mrad/min are shown in Fig. 1. There are three types of radicals observed.

Equally separated ten lines and a central broad triplet are assigned to tert-butyl radical (tert-Bu), and neopently radical (neo-Pe), respectively. These radicals were already reported by Fessenden & Schuler.[3] Besides these, a third component was observed. This component was also found to be present in their system by Fessenden & Schuler, but was not identified.[3] This is attributable to tert-pentyl radical (tert-Pe). This assignment is based on the following two results. One is the result of a computer simulation (Fig. 2) and the other is the comparison of the spectrum with one from neopentane containing 2-methyl-2-chlorobutane (2.5 mol%). In this system it is expected that the formation of tert-Pe radical is enhanced by a dissociative electron attachment reaction. The coupling constants of these three radicals are in good agreement with the reported data, except $A_{\beta}^{CH_2}$ of tert-Pe radical which was slightly smaller than the value observed in the radiolysis of liquid isopentane.[3),9)] In these experiments high dose rates are used. However, any appreciable changes of the spectra were not observed with increasing irradiation time. Therefore, the effect of accumulated dose is considered not to be significant in plastic crystal in contrast with the result in crystal phase at lower temperatures. Methyl radical was not observed even at the highest dose rate (∿100 Mrad/min).

The main component of the formed radicals is tert-Bu radical, and the relative intensity ratios of these radicals are dependent on the irradiation temperatures as shown in Fig. 3. With elevating temperature, the relative intensity of tert-Bu radical becomes large, but that of tert-Pe radical is reduced. The temperature dependence of the steady state concentration of tert-Bu radical is shown in Fig. 4. Above -60°C the signal becomes smaller and color centers from the sample tube being to overlap with the signal. The decay order can be determined from dose rate dependence of the steady state concentration. The tert-Bu radical

concentration was found to be proportional to the square root of the dose rate (Fig. 5). The intensity ratio of the components does not change with dose rate at a constant temperature. This indicates that the radicals decay by second order reactions, recombination and/or disproportionation reactions. To confirm the decay order, the decay of tert-Bu radical signal was followed directly by the measurement of the signal peak height after electron beam was stopped. The second order plots are given in Fig. 6. It is seen that the reciprocal plots give fairly good straight lines. Although there are three types of radicals, it is easily shown that the reciprocal plot of one component should give a straight line if the component radicals are assumed to react with each other with the same rate constants.

If it is assumed that all the rate constants of combination reactions are approximately the same, the following equations are derived.

$$\frac{d[R_T]}{dt} = \sum_i P_i I - 2k_t[R_T]^2 \qquad (1)$$

$$\frac{d[R_i]}{dt} = P_i I - 2k_t[R_i][R_T] \qquad (2)$$

where $P_i I$ is production rate of i-th radical, I dose rate, k_t rate constant, of the recombination reactions, $[R_T]$ total radical concentration, and $[R_i]$ concentration of i-th radical. Steady state concentration and decay kinetics are described by following equations.

$$[R_T]_{\text{steady state}} = \left(\frac{\Sigma P_i I}{2k_t}\right)^{1/2} \qquad (3)$$

$$[R_i]_{\text{steady state}} = \left(\frac{I}{2k_t}\right)^{1/2} \cdot \frac{Pi}{\sqrt{\Sigma Pi}} \qquad (4)$$

$$\frac{1}{R_i(t')} - \frac{1}{R_i(0)} = \frac{R_T(0)}{R_i(0)} 2k_t t' \qquad (5)$$

where t' refers to time after electron beams is stopped. These equations show that each steady state radical concentration is proportional to the square root of the dose rate. Following eq. (5) the rate constant k_t can be estimated from the reciprocal plot (Fig. 6) after the correction of the radical concentrations with temperature shown in Fig. 3. An Arrhenius plot of the rate constant k_t for the tert-Bu radical decay was obtained between -104°C and -115°C and this gave the activation energy of 6.5 kcal/mole. Finally, $k_t=(4\pm1)\times10^{13}$ exp(6.9±0.2 kcal/RT) M^{-1} sec^{-1} was determined after correction of line width of spectra.

II. Effect of additives

Difference in the effect of additives between the plastic crystal and the crystal phases was compared. It was found that the electron scavengers give influence in both phases, but hydrocarbons as additives do only in the crystal phase.

Neopentane is known to form normal crystal phase below -133°C. When liquid neopentane was cooled to about -150°C in the cavity of the esr spectrometer, however, it was found that neopentane did not form crystal immediately, but that it was still in the plastic crystal phase even below the transition point. After fifteen or twenty minutes the crystal current of the esr detector diode was observed to be reduced to lower level at the same microwave power condition. This decrease in the crystal current is considered to arise from the decrease of the dielectric loss of neopentane due to the phase transition from the plastic crystal to the crystal. Thus, the transition was readily detected by the reduction of the crystal current. The selective radical formation from the hydrocarbon

as an addtive was observed only when the sample was irradiated after the transition occurred. In all the crystal phase experiments the samples were irradiated after the decrease in the crystal current took place and the esr measurements were made after the electron beam was stopped to avoid the effect of accumulating dose which occurs in crystal phase where the radicals are very stable.

i) Electron scavenger

Electron scavengers were found to affect the radical formation in both crystal and plastic crystal phases. The esr spectra observed in neopentane containing CCl_4 in plastic crystal phase during irradiation are shown in Fig. 7. The spectra change remarkably with temperature. At -124°C its specturm is not symmetic but at -121°C resolved ten lines (A≈6.5G) due to $\cdot CCl_3$ appear at a field ∿10G lower than the center of the matrix radical.[10] This $\cdot CCl_3$ radical is considered to be produced by a dissociative electron attachment reaction. The change of relative radical concentration with the amount of CCl_4 was investigated at -116°C (Fig. 8) in plastic crystal phase. It is seen from the figure that only tert-Bu radical is reduced significantly and the intensity of $\cdot CCl_3$ is proportional to added amounts of CCl_4. This suggests that tert-Bu radical is produced by a different mechanism from neo-Pe radicals. The spectrum obtained in the presence of CCl_4 in the crystal phase is broad but very similar to that in the plastic crystal phase at -130°C (Fig. 7).

The concentration of tert-Bu radical was also reduced by the addition of SF_6 and an electron-attached type anion SF_6^- was formed by irradiation in both phases. The spectrum of SF_6^- was easily identified by a large coupling constant (A_F=143G) and the characteristic second order splitting.[11] The reduction of the tert-Bu radical was not so significant as in the CCl_4 system. This shows that the electron scavenging

efficiency of SF_6 is weaker than CCl_4 in neopentane in both phases.

ii) Hydrocarbons

In the plastic crystal phase, the presence of a small amount of hydrocarbon as an additive did not affect the spectra of radicals obtained during electron irradiation. This is in a marked contrast with the results obtained in the crystal phase as shown below.

The spectra measured in irradiated pure neopentane at about -150°C are shown in Fig. 9(a). At early stage of irradiation the relative intensity of tert-Pe radical is large. With increasing dose, the relative intensity of tert-Bu radical increases and total radical concentration begins to level off.

In the presence of 2, 3-dimethyl butane (3.5 mol%) one of the components of the spectrum is a broad quintet which can be assigned to the $\cdot CH_2CH(CH_3)CH(CH_3)_2$. It is known that 2, 3-dimethylbutane is one of the additives which gives rise to selective solute radical formation.

Cyclohexyl radical was formed selectively in neopentane crystals containing cyclohexane (3.5 mol%) as shown in Fig. 9(b). Cyclohexyl radical in plastic cyclohexane was studied by Ogawa and Fessenden.[12)]

From the pattern of cyclohexyl radical (A_H^{α}=21G, A_H^{β}=40G, $A_H^{\beta'}$=5G) the internal conversion (chair-chair interconversion) was thought to stop in neopentane matrix at -150°C, because no broadening effect of two different β-protons can be seen. With accumulating dose, the intensity of tert-Bu radical became larger but the intensity of cyclohexyl radical decreased. It indicates that cyclohexyl radical is formed more selectively at the early irradiation stage.

The addition of a small amount of isopentane (3.5 mol%) to neopentane showed selective radical formation, too. The selectively formed radical is tert-Pe radical.

In the system of neopentane crystals containing a small smount of benzene, cyclohexadienyl radical is formed selectively (Fig. 9(c)). The spectrum of cyclohexadienyl radical is a triplet (A≈47G) of quartets (A≈10G) of triplets (A≈2.5G). In the outer part of this spectrum, characteristic small triplets are seen, however inner lines of cyclohexadienyl radical are not discriminated easily because of overlapping with matrix radicals. With accumulating dose this triplet decreases in intensity. A similar dose effect has been observed in other alkane mixture systems. The cyclohexadienyl radicals is considered to be formed by addition of H atom to benzene molecule. On the other hand, the radicals observed in the mixture of neopentane and alkane are those of H atom abstraction types. This indicates that H atom plays an important role in the selective radical formation. The changes of total radical and cyclohexadienyl radical concentrations with dose are shown in Fig. 10. It is seen that cyclohexadienyl radical ($\dot{C}_6H_7$) saturates at about 3 Mrad, but matrix radical does not. Now it may be said that the selective radical formation occurs in crystal at the early stage of irradiation and saturates at higher doses. When the sample which showed the selective radical formation in crystal was stored in plastic crystal or liquid phase, all radicals decayed completely. When this sample was reirradiated in crystal phase after recrystalization, the selective radical formation was observed again. This suggests that the special sites of the guest molecules in the crystal phase are attacked selectively by hydrogen atom, and these sites are recovered by the recrystalization of the sample.

Discussion

I. Kinetics in plastic crystal

Three kinds of radicals: tert-Bu, neo-Pe, and tert-Pe radicals were observed in plastic crystal of pure neopentane during electron irradiation.

The dose rate dependence and the decay kinetics indicate that the radicals obey second order decay. In the kinetic treatment mentioned in the foregoing part, it was assumed for the simplification that all the rate constants of the recombination reactions between the radical components are approximately equal. It seems reasonable to consider that the recombination reactions of the radicals are diffusion-controlled in plastic crystal phase. Then, the rate constant is represented by the equation, $k_t=4\pi(\sigma_A+\sigma_B)(D_A+D_B)$, introduced by Smolkowsky, where D_A and D_B are diffusion constants of radicals A and B in neopentane matrix, and σ_A and σ_B are reaction radii defined in terms of the distance across which the reaction can take place between A and B. If in plastic crystal one half of the lattice constant of neopentane, 5.6Å, is used for σ_A and σ_B, and the diffusion constants are approximately equal for the three radicals because of similar molecular dimensions, then k_t's are approximately equal for all recombination reactions, and the diffusion constant of the radicals, D, can be estimated from the plots in Fig. 4. The results is shown in table and the values are of the same order as self-diffusion constants measured by nmr spectroscopy in several plastic crystals.[13] The activation energy for narrowing of tert-Bu radical line width is ∿1 kcal/mol which is the same as the value obtained from rotational correlation time of Raman scattering of neopentane in plastic crystal.[14] These agreements seem to justify the assumption mentioned above.

The G values of tert-Bu, tert-Pe, and neo-Pe radicals were estimated to be ∿0.9, ∿0.3 and ∿0.2, respectively at -155°C in the plastic crystal phase. The G value of tert-Bu is higher than the value, 0.55, in liquid phase reported by Holroyd,[15] and the sum total of these values is smaller than that in crystal phase, G(Total) ∿3.

II. Effect of electron scavengers and mechanism of radical formation

The effect of electron scavengers is quite different from that of hydrocarbon additives. The electron scavengers affect and radical formation in both the crystal and the plastic crystal phases, while the hydrocarbon additives give influences only in the crystal phase. The formation of tert-Bu radical in the plastic crystal is reduced by the addition of CCl_4. This suggests that tert-Bu radical is produced by the neutralization of cations with electrons. In gas or liquid phase, the excited parent ion of neopentane is known to dissociate in 10^{-12} to 10^{-13} sec[16] as indicated in eq. (7). Therefore, the mechanism for the formation of tert-Bu radical is considered as follows,

$$\text{neo } C_5H_{12} \rightsquigarrow C_5H_{12}^{*+} + e^- \quad (6)$$

$$C_5H_{12}^{*+} \longrightarrow \text{t-}C_4H_9^+ + \dot{C}H_3 \quad (7)$$

$$\text{t-}C_4H_9^+ + e^- \longrightarrow \text{t-}\dot{C}_4H_9 \quad (8)$$

The reduction of tert-Bu radical in the presence of the electron scavengers is explained by the competition between electron-ion recombination (equation (8)) and electron scavenging. Since the electron scavengers show a small effect on the formation of neo-Pe radical, neo-Pe radical may be formed by the dissociation of excited neopentane.

$$\text{neo-}C_5H_{12}^* \longrightarrow \text{neo-}\dot{C}_5H_{11} + H \quad (9)$$

In the crystal phase, the hydrogen atoms produced in reaction (9) may attack selectively the guest molecules occupying the special sites in the crystals. The process for the formation of tert-Pe radical is not so clear at present. Neopentyl cation is well known to rearrange to tert-Pe cation.

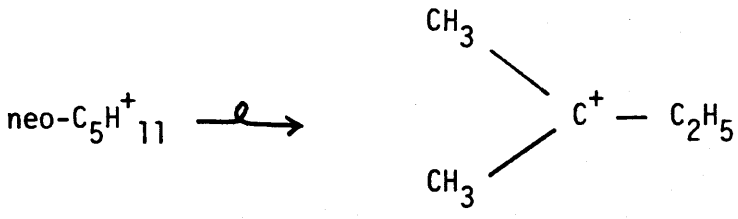

(10)

The neutralization of tert-Pe cation with electron after the rearrangement of neopentyl structure might produce tert-Pe radical. However this mechanism is ruled out because the electron scavengers do not effect the formation of tert-Pe radical. The rearrangement of neo-Pe radical to tert-Pe radical is not likely to occur from a theoretical consideration.[17] It has been reported that the yield of iso-butene in the radiolysis of liquid neopentane is high: G≈1.2.[18] In the presence of CCl_4, an additional radical which has a pattern similar to tert-Pe radical is seen. This may be assigned to $(CH_3)_2\dot{C}CH_2CCl_3$. Therefore, tert-Pe radical may be produced from the reaction (12) between $\cdot CH_3$ and isobutene.

$$neo\text{-}C_5H_{12} \rightsquigarrow neo\text{-}C_5H_{12}^{*} \longrightarrow i\text{-}C_4H_8 + CH_4 \qquad (11\ a)$$

$$\longrightarrow i\text{-}C_4H_8 + \dot{C}H_3 + H \qquad (11\ b)$$

$$i\text{-}C_4H_8 + \dot{C}H_3 \longrightarrow (CH_3)_2\dot{C}C_2H_5 \qquad (12)$$

$$i\text{-}C_4H_8 + \dot{C}Cl_3 \longrightarrow (CH_3)_2\dot{C}CH_2CCl_3 \qquad (13)$$

$$i\text{-}C_4H_8 + H \longrightarrow t\text{-}\dot{C}_4H_9 \qquad (14)$$

A portion of tert-Bu radical may be produced from the addition of hydrogen atom to isobutene as shown in (14).

III. Selective radical formation in crystal

It was found that selective solute radical formation in neopentane containing a small amount of hydrocarbon occurs only in the crystal phase

and not in the plastic crystal phase. Selectively formed radicals are hydrogen atom abstraction type radicals in the cases of neopentane containing 2, 3-dimethyl butane, cyclohexane, and isopentane. Hydrogen atom addition type radical is formed in the neopentane-benzene system. This indicates that the hydrogen atoms attack selectively the guest hydrocarbon molecules in the crystal phase. Miyazaki et al[7] reported that the formation of HD in the photolysis of neopentane containing hydrogen iodide and deutrated isobutane as additives was observed in the crystal phase but not in the plastic crystal phase. This result is consistent with the above observation.

In the case of neopentane-benzene (3.5 mol%) system, the selectively formed cyclohexadienyl radical was about 50 % of the total radical concentration at 1.3 Mrad, and it leveled off at about 3 Mrad. However, the intensity of signal due to matrix radicals increased with increasing dose.

If hydrogen atoms are produced at a constant rate with dose, the saturation effect suggests that the portion of the benzene molecules which are attacked by hydrogen atoms is very small. The saturated concentration of the cyclohexadienyl radical is only $\sim 10^{-3}$ of the benzene concentration. Therefore, most of the benzene molecules are not attacked by hydrogen atoms. When the irradiated sample which arrived once at the saturation point was stored in the form of plastic crystal, and then was reirradiated in the crystal phase, the selective radical formation was again observed. It may be considered from these results that in the crystal phase a portion of the guest molecules occupy the special sites such as defects in the lattice of neopentane, where they are selectively attacked by hydrogen atoms. On the other hand, in the plastic crystal phase there may be no special site because disordered lattice structure

or defects formation may be difficult in the plastic crystal owing to the mobility of the molecules.

Conclusion

The radiolysis of neopentane in the plastic crystal phase was investigated by means of esr spectroscopy during electron irradiation. It was found that neopentyl, tert-butyl, and tert-pentyl radicals are formed and those yields are dependent on temperature in plastic crystal. At -115°C estimated G values of tert-butyl, tert-pentyl and neo-pentyl are $\sim$0.9, $\sim$0.3 and $\sim$0.2, respectively. From the decay kinetics the decay rate constants of the radicals are obtained, $K_t=(4\pm1)\times10^{13}$ exp $(-6.9\pm0.2$ kcal/RT) M^{-1} sec^{-1}. From the effect of electron scavengers as additives, it was concluded that tert-butyl radical may be formed via ionic mechanism. In the presence of hydrocarbon as an additive the selective radical formation from the additive occurs only in the crystal phase but not in the plastic crystal phase. The hydrogen atom produced by irradiation plays an important role in this selective radical formation.

Acknowlegement

We wish to thank Mr. Miyoshi Onoue and Mr. Toshio Kawanishi for their help in the maintenance of the irradiation system and in the operation of the accelerator.

Reference

1) J.G. Aston: " Physics and Chemistry of the Organic Solid State " ed. by D. Fox, M.M. Labes, A Weissenberger, Interscience Publ., New York, 1963, vol. 1, p 543

2) Yu.N. Molin, A.T. Koritskii, N. Ya. Buben, V.V. Voyevodskii; Dokl. Acad. Nauk. SSSR. 123 882 (1958)

3) R.W. Fessenden and R.H. Schuler; J. Chem. Phys. 39 2147 (1963)

4) H. Shiraishi, H. Kadoi, Y. Tabata, K. Oshima; Bull. Chem. Soc. Jpn. 47 1400 (1974)

5) a) B. Smaller and M.S. Matheson; J. Chem. Phys. 28 1169 (1958)
b) F. Thyrion, J. Dodelet, C. Fauquenoit and P. Claes; J. Chim. Phys. 65 227 (1968)
c) J. Lin and F. Willams; J. Phys. Chem. 72 3707 (1968)

6) T. Miyazaki, T. Wakayama, M. Fukaya, Y. Saitake, and Z. Kuri: Bull. Chem. Soc. Jap. 46 1030, 1036 (1973)

7) T. Miyazaki and T. Hirayama; J. Phys. Chem. 76 566 (1975)

8) R. Tanaka, S. Mitomo, Y. Oshima; JAERI-memo 4121

9) The tert-pentyl radical has positive temperature coefficient of $A_\beta^{CH_2}$. Smaller $A_\beta^{CH_2}$ may be due to hindered rotation of C_α-$C_\beta H_2 CH_3$ in plastic crystal phase. P.J. Krusic and J.K. Kochi; J. Amer. Chem. Soc. 93 846 (1971)

10) A. Hudson, H.A. Hussian; Mol. Phys. 16 199 (1969)

11) R.W. Fessenden and R.H. Schuler; J. Chem. Phys. 45 1845 (1966)

12) S. Ogawa and R.W. Fessenden; J. Chem. Phys. 41 994 (1964)

13) a) E.O. Stejskal, D.E. Woessner, T.C. Farrar and H.S. Gutowsky; J. Chem. Phys. 31 55 (1959)

b) R. Folland, R.L. Jackson and J.H. Strauge; J. Phys. Chem. Solids 34 1713 (1973)

14) R.C. Livingston, W.G. Rothshild, J.J. Rush; J. Chem. Phys. 59 2498 (1973)

15) R.A. Holroyd; J. Phys. Chem. 70 1341 (1966)

16) P. Ausloos; Mol. Photo. Chem. 4 39 (1972)

17) J.W. Witt, " Free Radical Rearrangement " in " Free Radicals " ed. J.K. Kochi. A Wiley-Interscience Publ., New York, 1973 vol. 1, p 333. Chap. 8

18) A.V. Chadwick and J.N. Sherwood; " Diffusion Process " ed. by J.N. Sherwood, A.V. Chadwick, W.M. Muir and F.L. Swinton, Goldon and Breach, New York, p475 (1971)

Table

Rate constants and diffusion constants in neopentane plastic crystal. Diffusion constants are derived from Smolkowsky eq.

Temperature (°C)	$k_t(M^{-1}\cdot sec^{-1})$	$D(m^2\cdot sec^{-1})$
-133 (t.p.)	$^{*}6.2 \times 10^{2}$	3.8×10^{-17}
-100	$^{*}7.6 \times 10^{4}$	4.3×10^{-15}
- 50	$^{*}6.9 \times 10^{6}$	3.9×10^{-13}
- 16 (m.p.)	$^{*}5.4 \times 10^{7}$	3.1×10^{-12} **

* calculated from extrapolation using $k_t=4\times10^{13}\exp(-6.9\ kcal/RT)M^{-1}\cdot sec^{-1}$ obtained experimentally between -105°C and -115°C.

** $0.5\sim2.5\times10^{-13}$ $m^2\cdot sec^{-1}$ at melting point for triethylenediamine, 3-Azabicyclononane, and Norbornane which from plastic crystal.[13)b)] $10^{-12}\sim10^{-13}$ $m^2\cdot sec^{-1}$ for close-packed metal is reported.[18)]

Figure Captions

Fig. 1 The esr spectra of neopentane measured during electron irradiation at a dose rate of 15 Mrad/min in the plastic crystal and stick diagrams of tert-butyl (a), neopentyl (b) and tert-pentyl (c) radicals. The symbols indicated in tert-butyl radical lines are used in Fig. 5 (dose rate dependence)

Fig. 2 Computer simulated spectrum. A_{β}^{H}=22.7G for tert-Bu radical. A_{β}^{H}=16.0 and 22.5G for tert-Pe radical. A_{α}^{H}=22.8G for neopentyl. Intensity ratios of tert-Bu, tert-Pe, and neo-Pe radical are 128, 25.6, and 20, respectively.

Fig. 3 The change of relative intensity of tert-butyl (o), tert-pentyl (x) and neo-pentyl (•) radical with temperature.

Fig. 4 The variation of steady state concentration of tert-butyl radical with temperature at a dose rate of 15 Mrad/min in plastic crystal.

Fig. 5 Dose rate dependence of tert-butyl radical concentration at -103°C and -83°C. The symbols indicated are the same components of the spectra of tert-butyl radical in Fig. 1.

Fig. 6 Reciprocal plot of tert-butyl radical decay.

Fig. 7 The esr spectra of neopentane containing CCl_4 (2.8 mol%) at -130°C, -124°C, and -121°C. Dose rate is 15 Mrad/min.

Fig. 8 Change of relative intensity ratio of tert-butyl (•), neopentyl (o), tert-pentyl (▲) and $\dot{C}Cl_3$ (▼) radicals as a function of CCl_4 concentration at -116°C.

Fig. 9 (a) The esr spectra of irradiated pure neopentane at -150°C in crystal.

——: 0.61 Mrad (Gain 1000) ----: 2.9 Mrad (Gain 300)

(b) The esr spectra of irradiated neopentane containing cyclohexane (3.5 mol%) at -150°C.

——: 0.9 Mrad (Gain 3000) ----: 8.8 Mrad (Gain 500)

(c) The esr spectra of irradiated neopentane containing benzene (3.5 mol%) at -150°C.

——: 1.3 Mrad (Gain 1000) ----: 7.4 Mrad (Gain 100)

Fig. 10 Radical concentration vs dose for pure neopentane and neopentane containing additives in crystal phase at -150°C.

▼: 3.5 mol%, 2,3-dimethylbutane o: 3.5 mol%, isopentane

Δ: 3.5 mol%, benzene x: 3.5 mol%, cyclohexane

o: pure neopentane ▲: cyclohexadienyl radical in neopentane containing 3.5 mol% benzene.

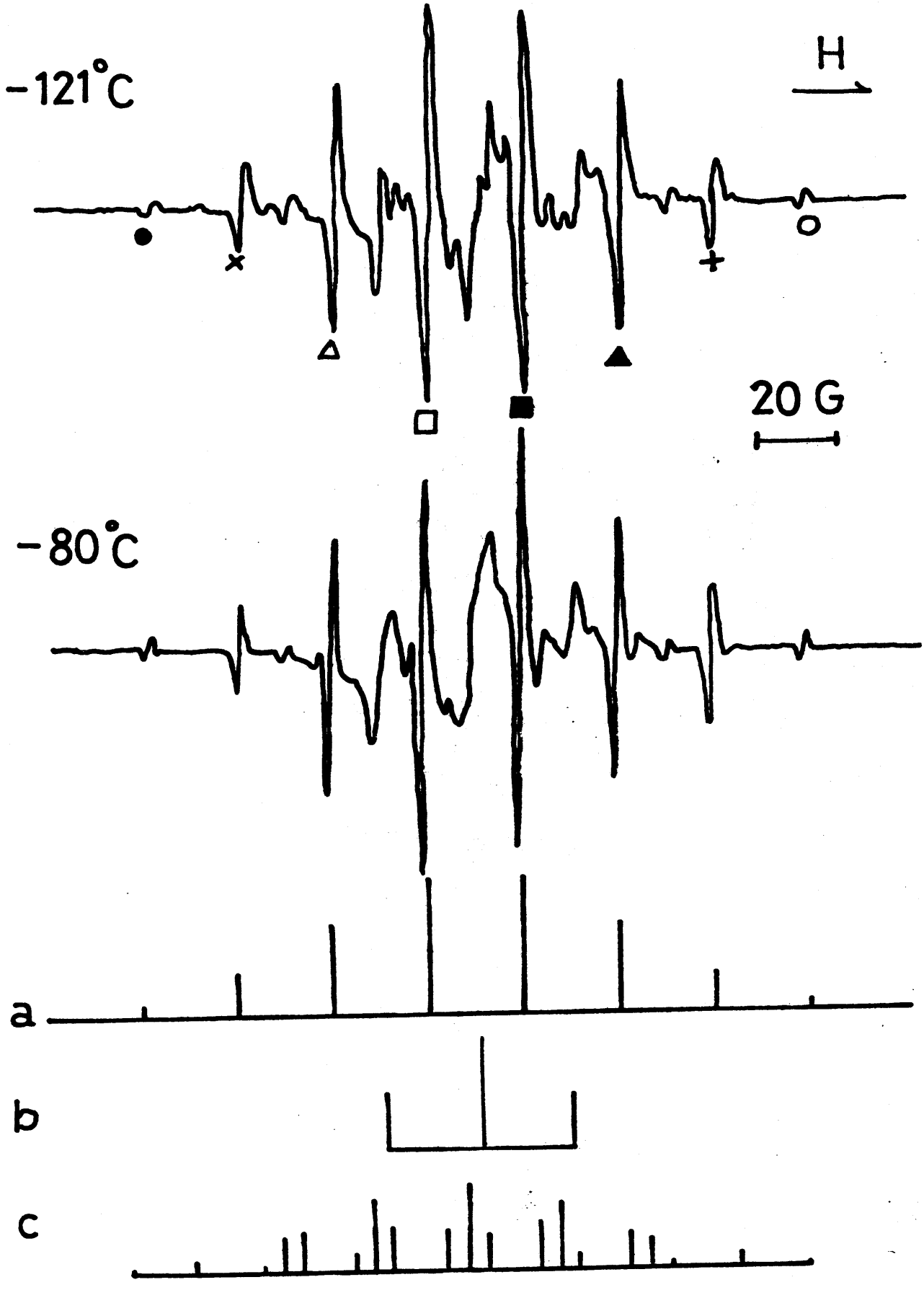

Fig.1

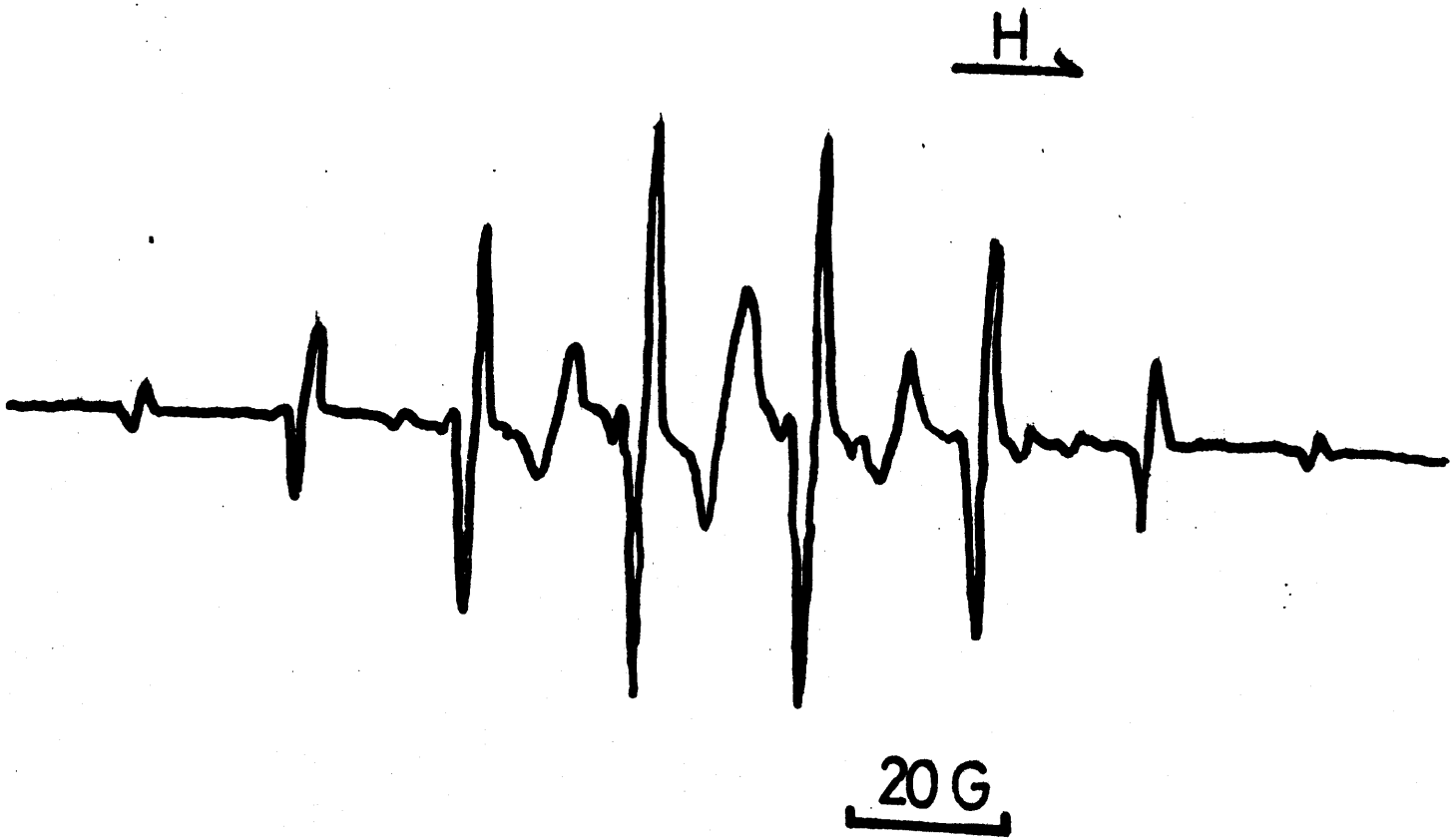

Fig. 2

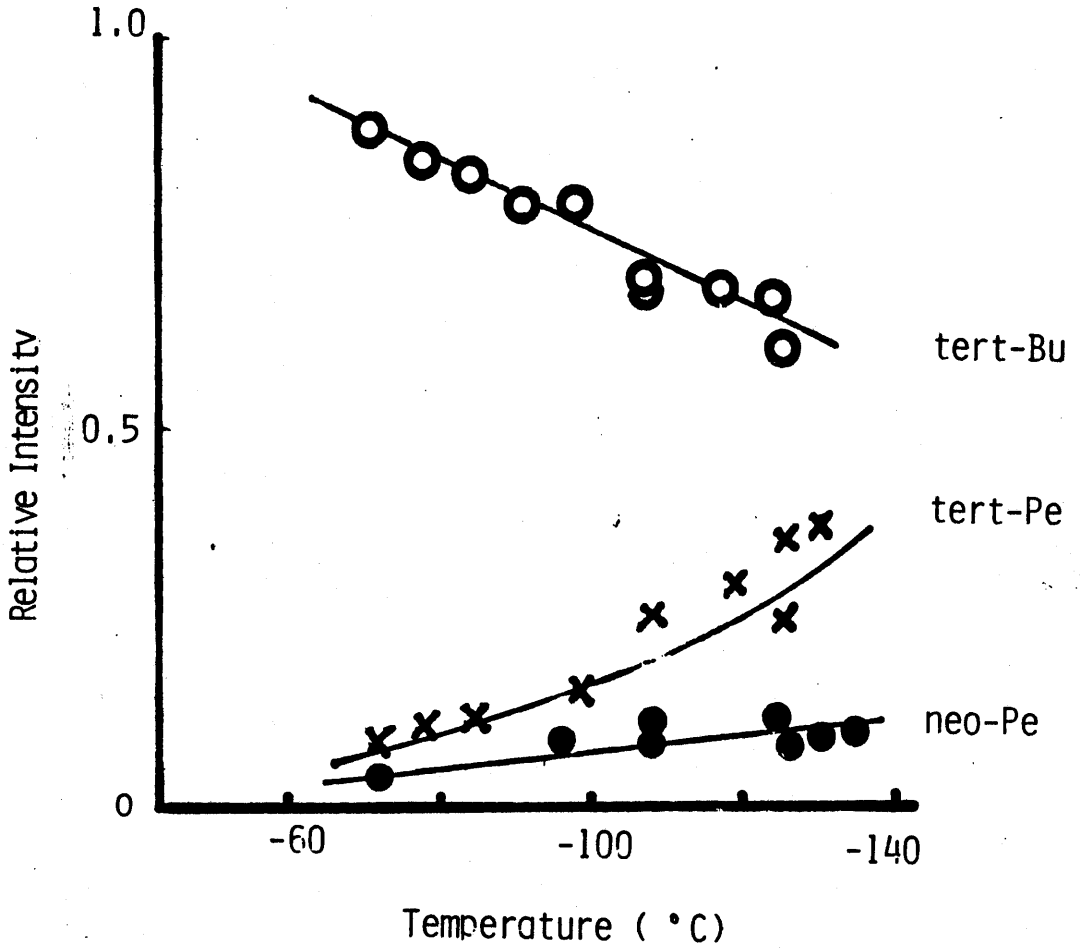
1.0
0.5
0
Relative Intensity
tert-Bu
tert-Pe
neo-Pe
-60
-100
-140
Temperature (°C)

Fig.3

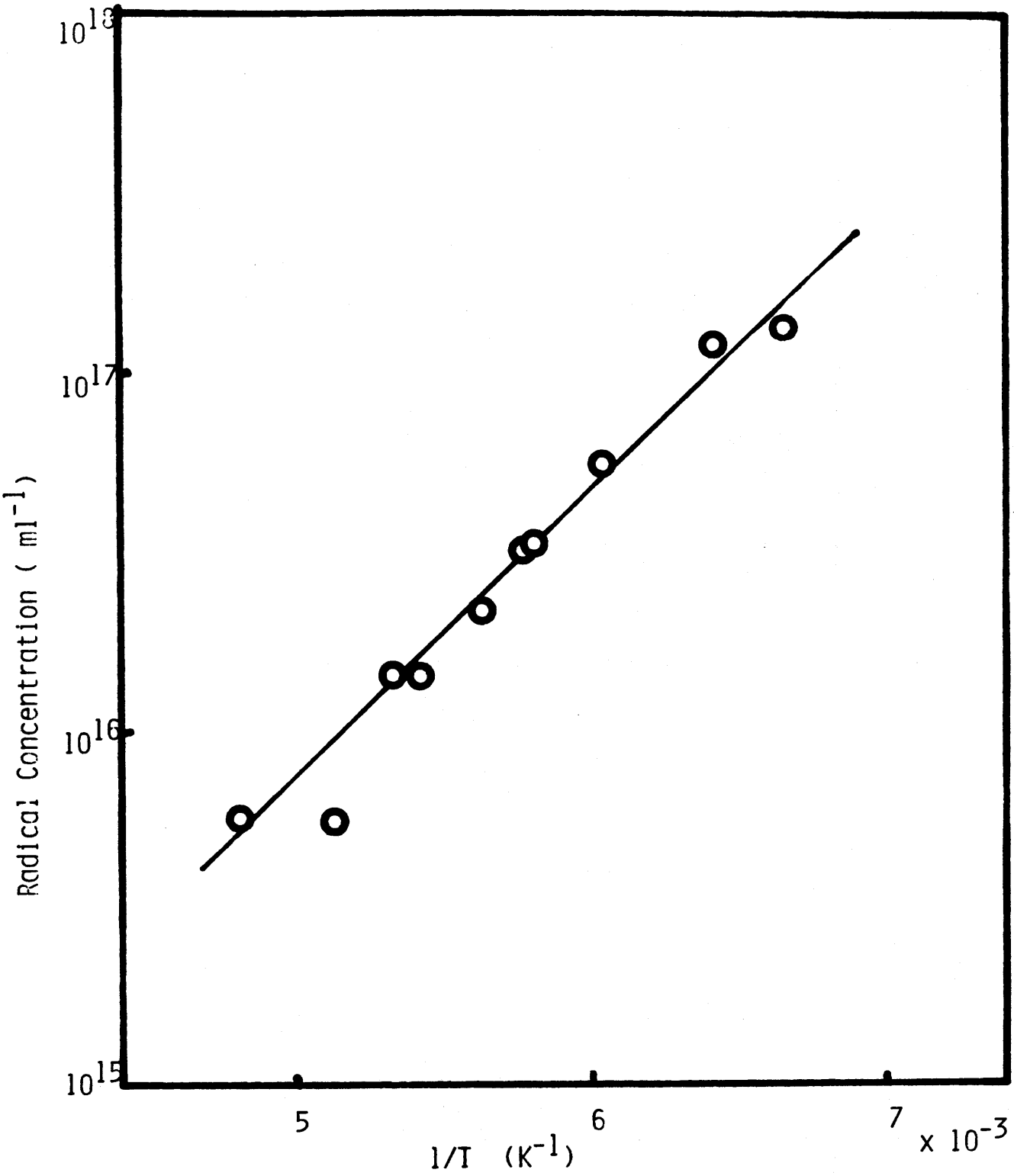
10^{18}
10^{17}
10^{16}
10^{15}
Radical Concentration (ml^{-1})
5
6
7
x 10^{-3}
1/T (K^{-1})

Fig.4

Fig. 5

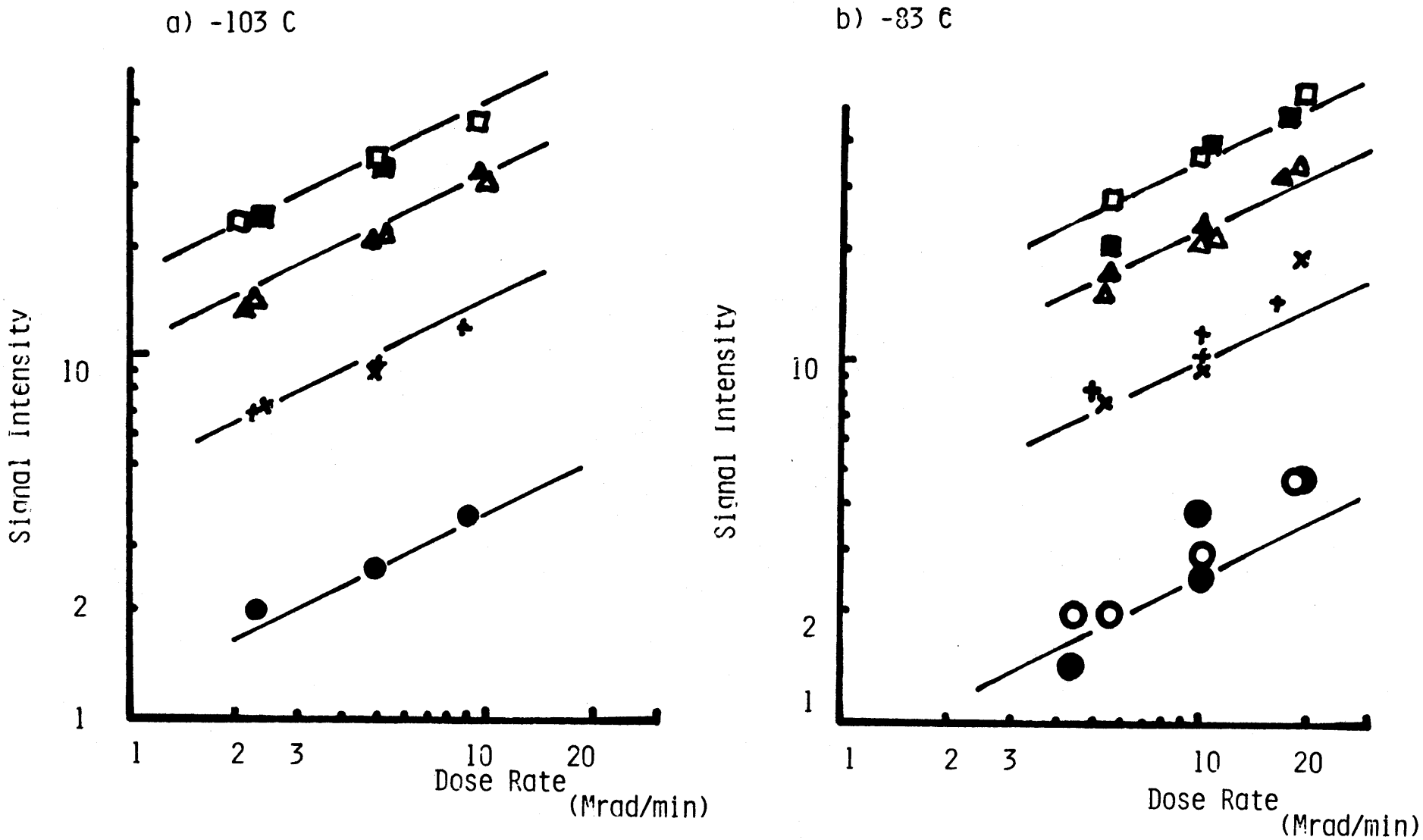
a) -103 C
b) -83 C
Signal Intensity
10
2
1
1
2
3
10
20
Dose Rate
(Mrad/min)

Fig.5

Fig. 6

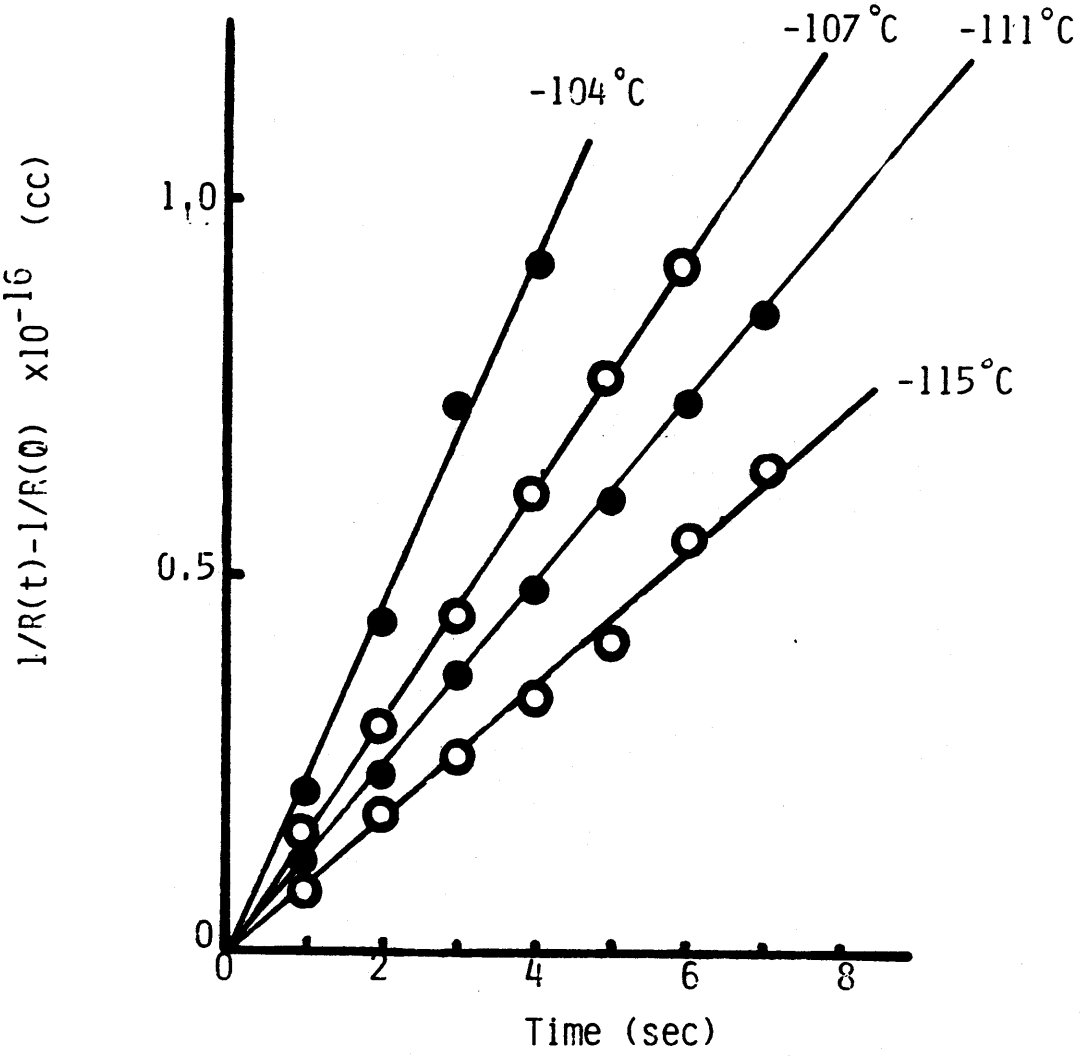

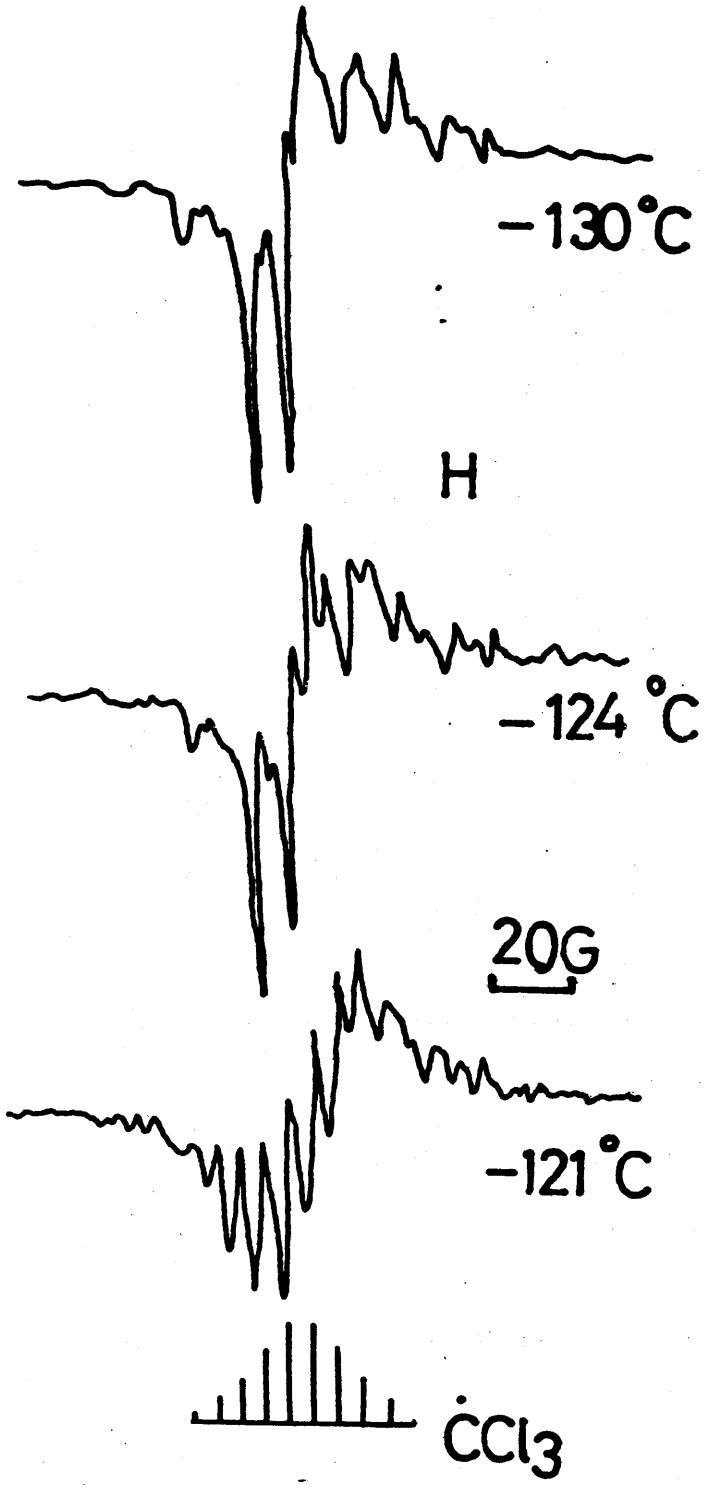

Fig.7

Fig.8

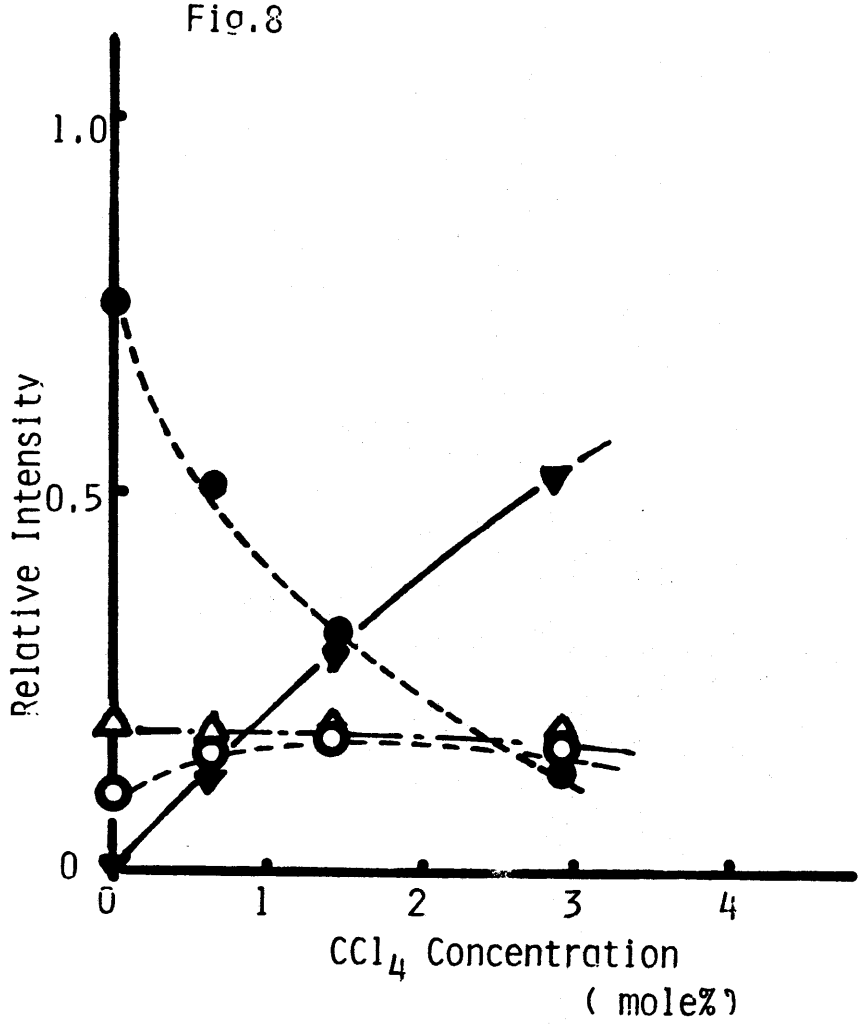

Fig. 9 a)

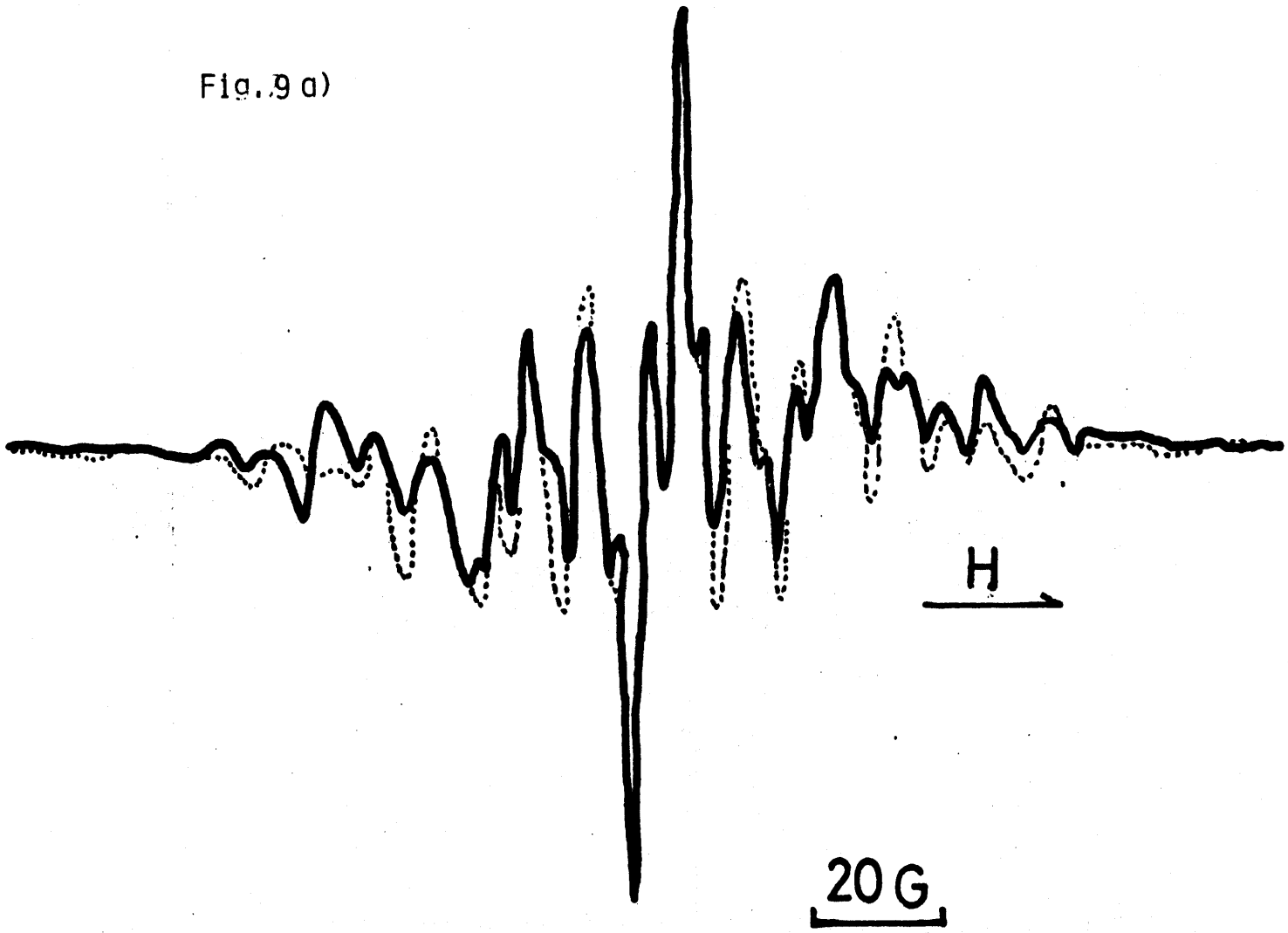

Fig.9 b)

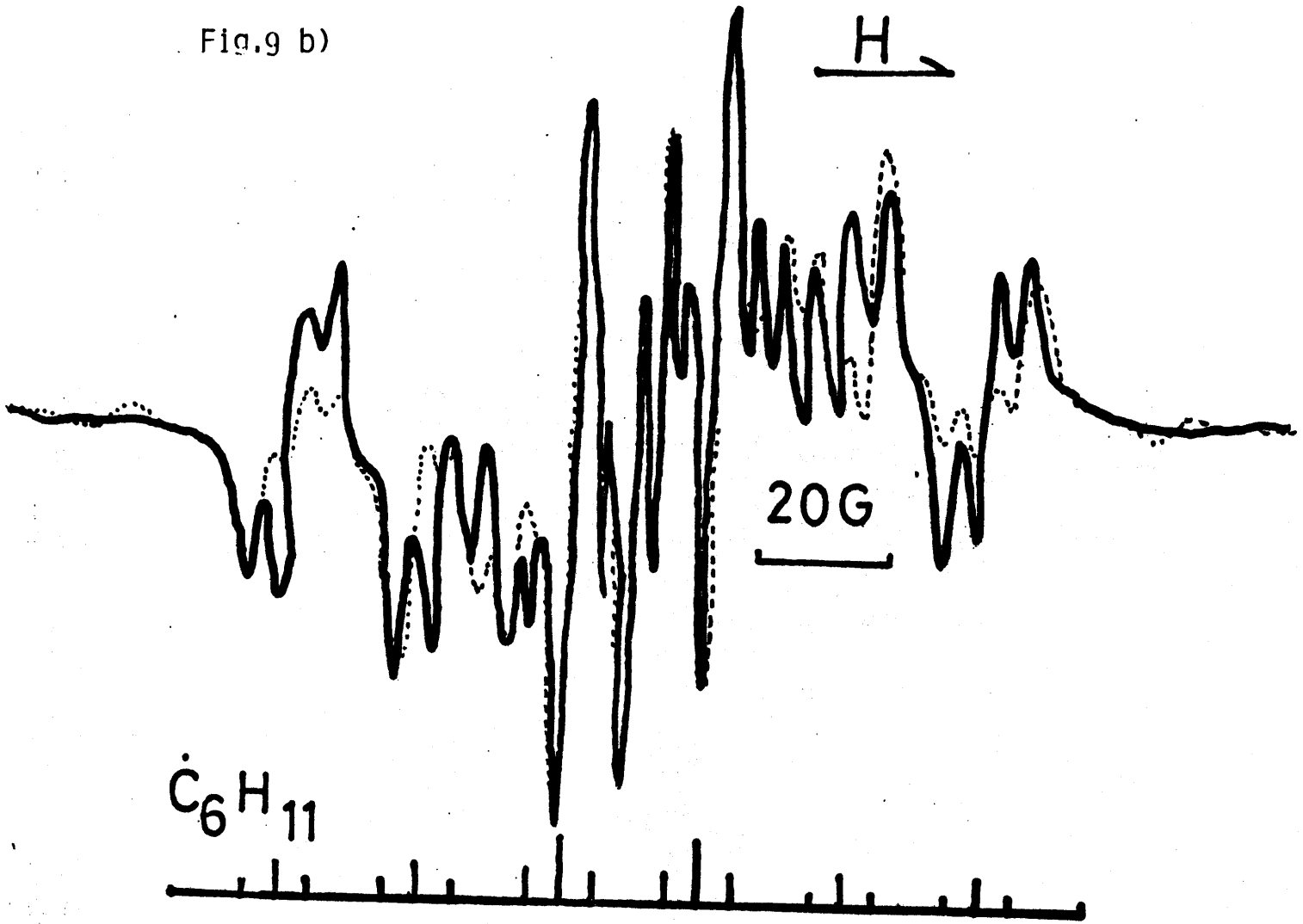

Fig. 9 c)

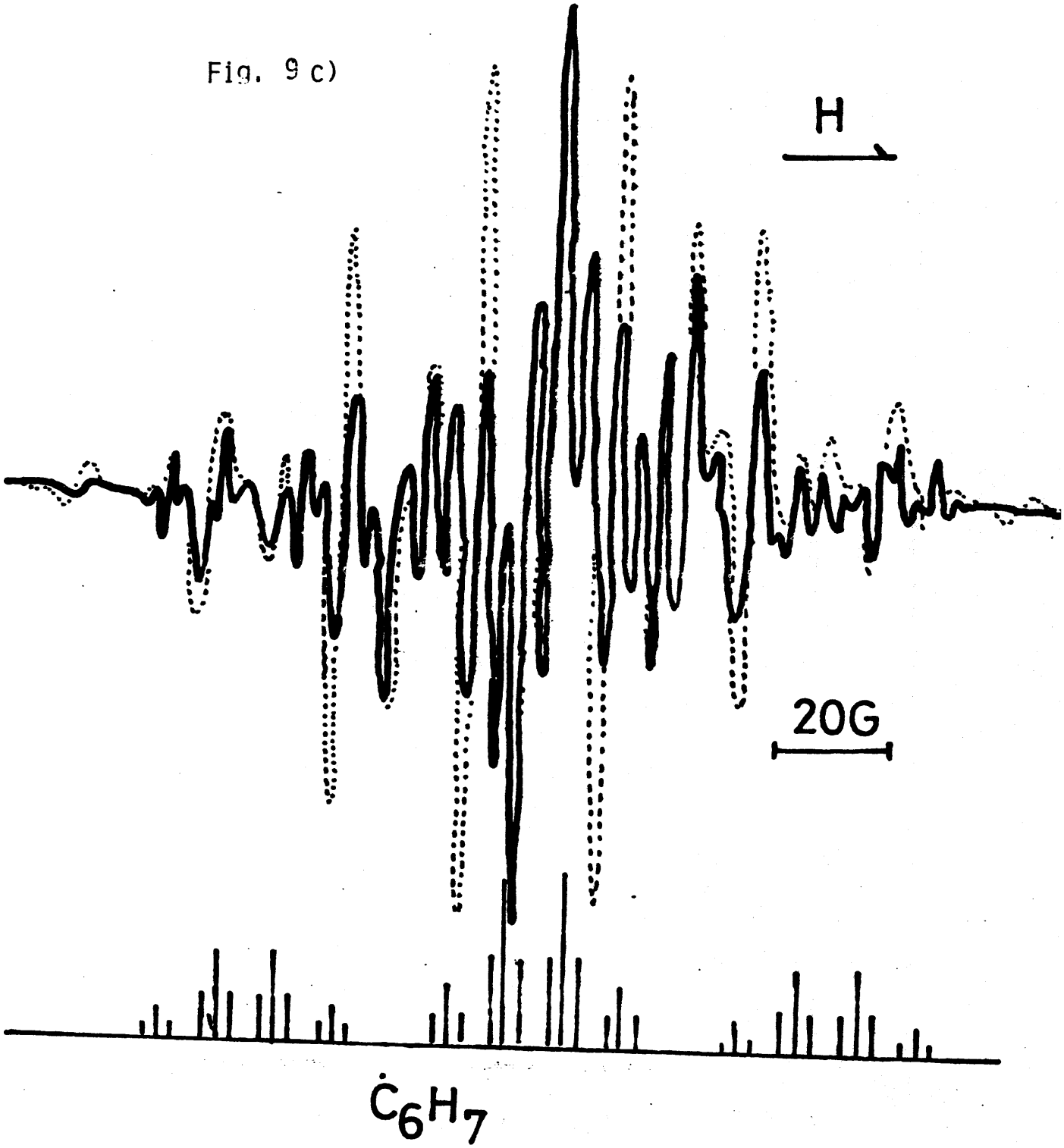

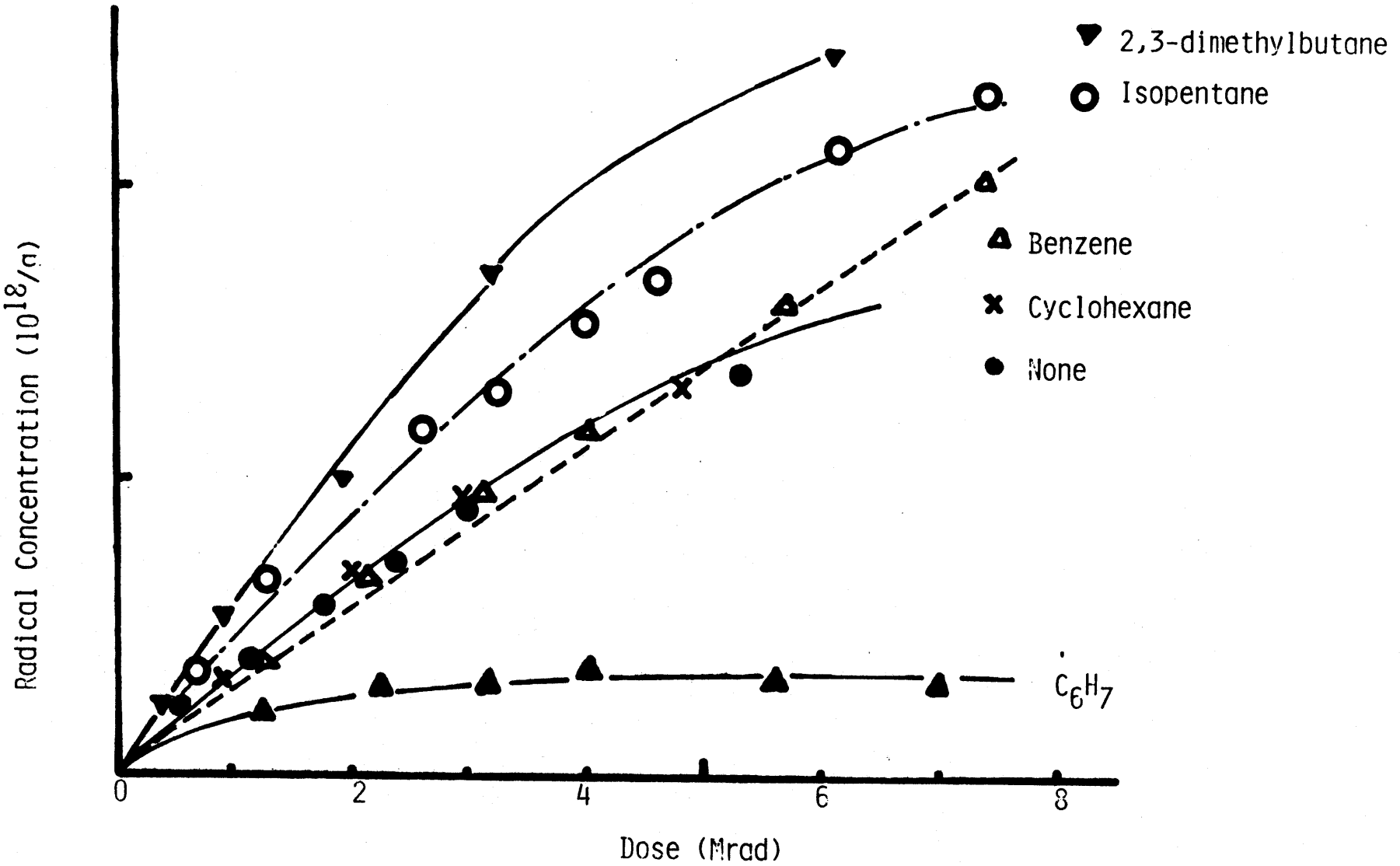
2,3-dimethylbutane
Isopentane
Benzene
Cyclohexane
None
C_6H_7
Radical Concentration (10^{18}/g)
0
2
4
6
8
Dose (Mrad)

Fig.10

Chapter 3.

ESR Study of Fluoroalkyl Nitroxide Radicals Using the Spin Trapping Technique

Summary

Many types of spin adducts produced by the photolysis of a mixture of fluoroalkyl iodides and spin trapping agents in solution were investigated by means of esr spectroscopy. It was found that not only esr patterns but also A_F^β values depend significantly on temperature. INDO calculations were carried out to get information about the structure of the spin adducts, the magnitudes of A_F and A_N, and internal rotations of fluoroalkyl groups. The temperature dependencies of both esr pattern and A_F^β value were attributed to the restricted rotation or torsional oscillation of the fluoroalkyl groups about the nitrogen-carbon bond. The structure of nitroxide radicals, the magnitudes of A_F^β and A_N, and the stable conformations of these spin adducts are discussed.

Introduction

Recently, the spin trapping technique has been found to be useful to detect and identify short lived intermediate radical species.[1,2] It is expected that fluoroalkyl radicals may be easily identified by their esr spectra since spin adducts of the fluoroalkyl radicals are chracterized by large fluorine coupling constants, in contrast with the adducts of alkyl radicals. Perfluoroalkyl nitroxide radicals have been investigated by

Klabunde[3] and Konaka et al[4]. They found that the β-fluorine coupling constant changes with temperature. The spin trapping technique has been applied to identify the fluoroalkyl radicals produced from fluorocarbons by γ-irradiation by the present authors. Both coupling constants and esr spectra themselves of the spin adducts of fluoroalkyl radicals were temperature dependent. Therefore, it was necessary to investigate those temperature dependencies as the first step of our studies. Various types of fluoroalkyl spin adducts have been investigated systematically. They were produced by the photolysis of fluoroiodides in the presence of trapping agents: three different nitroso compounds, such as nitrosobenzene, 2-methyl-2-nitrosopropane and 2-methyl-2-nitrosobutanone-3. The main advantage of nitroso compounds is that the information concerning the structure of the trapped radical is more easily obtained from the spectrum of the nitroso-adducts than in the case of nitrone compounds. It is also interesting to investigate the structure of nitroxide radicals, especially concerning planarity and internal rotations.

SCF INDO calculations[5] have been carried out to determine the structure of many types of radicals. In order to get information about the conformation of nitroxide radicals, the coupling constants of nitrogen and fluorine atoms, and the potential barrier of internal rotations of the fluoroalkyl groups, INDO calculations have been carried out in the present work.

Experimental

Three different spin trapping agents, nitrosobenzene (NB), 2-methyl-2-nitrosopropane (BNO) and 2-methyl-2-nitrosobutanone-3 (MNB) were used. NB was purchased from Tokyo Kasei Co., Ltd. BNO and MNB were prepared according to Perkins et al[6] and Aston et al[7], respectively.

Fluoroalkyl iodides used were ICF_3, ICF_2CF_3, $ICF(CF_3)_2$, $ICFHCH_2CF_3$, $ICFHCF_2Cl$, $ICF_2CH_2CF_3$ and ICF_2CF_2Cl. ICF_3 and $ICF(CF_3)_2$ were employed as

commercially available from Peninsula Research Co. ICF_2CF_3 was received from Asahi Glass Co., Ltd. $ICFHCH_2CF_3$ and $ICF_2CH_2CF_3$ were prepared by the addition of CF_3I to $CFH=CH_2$ and $CF_2=CH_2$ (Matheson Gas Products), respectively, induced by UV-radiation[8]. $ICFHCF_2Cl$ and ICF_2CF_2Cl were prepared by the thermal addition of ICl to $CFH=CF_2$ and $CF_2=CF_2$ (Matheson Gas Products), respectively, in a high pressure autoclave[9].

The solvents which dissolve the nitroso compounds were chosen. In the NB and BNO systems, iso-pentane was usually employed as the solvent, and for the low temperature measurements, propane was also used. In the MNB system, dichloromethane was used, since MNB is insoluble in iso-pentane and propane. These solvents are Tokyo Kasei's guaranteed grade. About 10 vol% of fluoroalkyliodide was dissolved in a solvent including about 10 mM of the spin trapping agent, and then the sample was degassed in an esr tube by connecting a vacuum line. The tube was placed in an esr cavity and irradiated by an ultra high pressure mercury lamp (Ushio 150 W) for a few minutes. Esr spectra were measured with a JEOL P-2X spectrometer in the temperature range between -180°C and room temperature (~20°C).

The photolysis of isopentane, propane or dichloromethane solutions containing both spin trapping agent and fluoroalkyl iodide led to the formation of stable fluorinated nitroxides. One example is:

$$CF_3I \xrightarrow{h\nu} \cdot CF_3 \qquad (1)$$

$$\dot{C}F_3 + \text{C}_6\text{H}_5\text{N=O} \longrightarrow CF_3-\dot{N}(O)-\text{C}_6\text{H}_5 \quad (CF_3\text{-NB}) \qquad (2)$$

For simplicity, the spin adduct of CF_3 radical trapped by NB is indicated as

CF_3-NB in the following section.

It has been reported[1] that nitroso compounds are degraded by photolysis and nitroxide radicals are formed as a result of the reaction between nitroso compounds themselves. However, in the presence of alkyliodide, only nitroxide radical adducts between the fluoroalkyl radicals and spin trapping agents were observed, and the formation of the nitroxide radicals from the degradation of trapping agents were negligible under the present conditions.

Results

1. CF_3 spin adducts

The esr spectra of the simplest fluoroalkyl radical, trifluoromethyl radical, trapped by NB, BNO and MNB are shown in Fig. 1. The spectra show a characteristic triplet of quartets due to the coupling of the nitrogen atom and three equivalent fluorine atoms. In the case of CF_3-NB, additional lines from ortho, metha and para protons of the benzene ring are observed. The values of A_F^β and A_N of these spin adducts are slightly dependent on temperature. The value of A_F^β is about 10 G.

It is known that A_N values of alkyl radicals trapped by NB, BNO and MNB are ∿12 G[10], ∿15 G[11] and ∿15 G[11], respectively. The observed A_N values of fluoroalkyl radical adducts (see Table. II) are ∿20 % smaller than those of non-fluorinated radical adducts. The reduction of A_N may be attributable to the reduction of the spin density of s-orbital on the nitrogen atom due to the high electron affinity of fluorine atoms in the fluoroalkyl groups. Another explanation for the reduction of A_N values will be discussed in the relation to the planarity of the nitroxide radical at the nitrogen atom. (see discussion)

The spectrum of CF_3-MNB shows a selective line broadening below -80°C. The two inner lines of the quartet (1:3:3:1) due to three equivalent fluorine

atoms are broadened at low temperatures. However, other CF_3 spin adducts show no selective line broadening at -100°C. This indicates that the potential barrier of internal rotation around the nitrogen-β-carbon bond of CF_3-MNB is higher than those of other CF_3 spin adducts, and that the internal rotation of CF_3 is limited to a large extent at -80°C.

2. Perfluoroalkyl-MNB spin adducts

Spin adducts of perfluoroalkyl radical trapped by MNB have not been investigated before. The CF_3CF_2-MNB spin adduct also shows the selective line ($M_I^F=0$) broadening as indicated in Fig. 2(a). On the other hand, the spectra of the $(CF_3)_2CF$-MNB spin adduct do not change with temperature (Fig. 2(b)). Hyperfine splitting from γ-fluorines can be seen clearly in both CF_3CF_2-MNB and $(CF_3)_2CF$-MNB spin adducts. The coupling constants of these spin adducts are shown in Table I. It is found that the A_F values of perfluoroalkyl-MNB have no large temperature dependence in contrast with the adduct of BNO reported by Klabunde[3].

3. Fluoroalkyl-NB spin adducts

It was found that most of the esr spectra of the NB adducts have no temperature dependency. Only the CF_2ClCF_2-NB spin adduct shows selective line broadening ($M_I^F=0$) at -20°C (Fig. 3). Esr spectra of fluoroalkyl phenyl nitroxide radicals are shown in Fig. 3. It was also found that the coupling constants of protons in the phenyl group are ∿0.8 G for metha and ortho, and ∿2 G for para protons. The value of A_N is 9∿10 G, which is ∿20 % smaller than that of non-fluorinated spin adducts of NB[11].

It is noted that the splitting by the β-proton is seen in the spectra of the CF_3CH_2CFH-NB spin adduct, while, no splitting by the β-proton is seen in the CF_2ClCFH-NB spin adduct. This difference is discussed in relation to the conformation of these spin adducts.

4. Classification of the spin adducts

Many types of fluoroalkyl radical spin adducts were investigated and the spectral parameters are summarized in Table II. These adducts are classified into N and C groups as shown in Table II. The N indicates that the spectra of spin adducts of the N group are not temperature dependent and the C indicates temperature dependence. The C group consists of three different types of groups, C-1, C-2 and C-3. The C-1 group is characterized by only simple selective line broadening as in the CF_3-MNB spin adduct. The C-2 shows at lower temperatures the complicated spectra which can be assigned to two or more radicals superimposed, but at higher temperature rather simple spectra as in the case of the CF_2ClCFH-BNO spin adduct. An example is shown in Fig. 4. The C-3 group of spin adducts such as CF_2ClCF_2-BNO and CF_2ClCF_2-MNB shows at lower temperatures complicated spectra arising from the coupling of two nonequivalent β-fluorine atoms, and selective line broadening at higher temperatures. It is noted that these changes are reversible with temperature as shown in Figs. 6 and 7.

In the BNO adduct, a large temperature coefficient of A_F^β and a small change of A_N were observed, while a large coefficient of A_F^β with temperature was not observed in the NB and MNB adducts. Most MNB adducts of the fluoroalkyl radicals observed belong to the C group.

It is seen that the spin adducts involving bulky asymmetric substituents tend to show abnormal changes of their esr spectra.

5. $CF_3CH_2CF_2$-BNO spin adduct

A simple selective line broadening effect was observed in $CF_3CH_2CF_2$-MNB spin adduct (Fig. 5(a), (b)). The central lines ($M_I^F=0$) are broadened at -120°C. The lowest temperature was attained by using isopentane as the cooling agent. For the measurements in the liquid phase at lower temperatures propane was used as the cooling solvent, and it was possible to

measure the esr spectra in the liquid phase at temperatures between -170°C and -20°C. At -170°C the spectrum was a normal 1:2:1 triplet owing to the coupling with two equivalent fluorine atoms in the $CF_2CH_2CF_3$ group. With increasing temperature, the inner lines of the spectrum are rapidly broadened and the peak intensity is decreased. The value of A_F gradually becomes smaller at the same time. About -100°C the intensity of the inner lines gradually recovers to the normal ratio 1:2:1.

The values of A_F and A_N and the intensity ratio ($M_I^F=0/M_I^F=\pm1$, where $M_I^F=0$ and $M_I^F=\pm1$ are intensities of a central and outer lines, respectively.) are also shown in Fig. 5(c) as a function of temperature. The A_F values are 31.6 and 26.4 G at -166°C and -40°C, respectively, in propane. The temperature coefficient of A_F value is -40 mG/K . However, A_N is almost constant in the temperature range of -170°C and +30°C.

Both the CF_3CH_2-BNO and CF_3CF_2-BNO spin adducts show no selective line broadening, but they have large negative temperature coefficients of A_F, -19.8 mG/K and -18.1 mG/K , respectively. Many of the fluoroalkyl-BNO spin adducts were found to have negative temperature coefficients of A_F^β.

6. CF_2ClCF_2-BNO and CF_2ClCF_2-MNB spin adducts

A reversible temperature change in the spectrum of CF_2ClCF_2-BNO spin adduct is shown in Fig. 6. At -120°C, the lines are broadened due to slow molecular rotational motion of the adduct in liquid iso-pentane. With increasing temperature, the lines become sharp, and more than one type of adduct appear to exist in the temperature range of -100°C to -80°C. The asymmetric spectra at -100°C and -80°C suggest that two or more nitroxides having different g-factors and different coupling constants are overlapping. At -40°C, the spectra show selective line broadening and A_F is 21.78 G, which is similar to the value of A_F^β in the CF_2CF_3-BNO spin adduct. At -20°C, the line intensities reach a normal ratio, 1:2:1. At the same time the adduct

begins to react and a new radical, having A_N=∿7 G, appears. This new radical may be an acyl-alkyl radical which is produced by a secondary reaction of the CF_2ClCF_2-BNO spin adduct with BNO[12]. The remaining old spin adduct shows the same temperature change as described above.

As shown in Fig. 7, the CF_2ClCF_2-MNB spin adduct also shows a large temperature dependence in the spectrum, but this temperature dependence seems to be rather simple in comparison with that of the CF_3CF_2Cl-BNO spin adduct. At -70°C, the spectrum has six rather broad lines which are probably due to couplings of one of the two β-fluorine atoms and the nitrogen atom. By elevating the temperature, the lines are sharpened; and at the same time, the intensity ratio returns to the normal value, 1:2:1. The spectrum at -70°C, having six lines due to the couplings of one fluorine atom and one nitrogen atom, suggests that the dihedral angles of two fluorine atoms should be ∿90° and ∿30°.

Discussion

Marked changes of both the esr spectral patterns and the coupling constants with temperature were observed in many fluoroalkyl spin adducts. These changes are attributed to the transition between the different conformations or to torsional oscillations of the fluoroalkyl groups. However, the structure of the nitroxide radical is not clearly known at present. There have been few reports describing the structure of nitroxide radicals. To get information about the stable conformation and to evaluate the coupling constants, INDO calculations were carried out for the radicals. The following values as standard bond lengths were used for the calculations: NO=1.24Å, CC=1.54Å, CF=1.36Å, CH=1.09Å (for alkyl) and 1.08Å (for phenyl) and CN=1.47Å[5]. The angle between the two bonds of tetravalent carbon is assumed to be 109.47° (tetrahedral angle). The value of 120° is used for C-C=O in MNB system.

1. Planarity of nitroxide radicals.

For the nitroxide radicals such as $H_2N\dot{O}$[16], $(CF_3)_2N\dot{O}$[13],[14],[15] and $(CH_3)_2N\dot{O}$[16], it has been reported that the structure with the minimum energy is non-planar at the nitrogen atom. In the present system, the spin adducts are rather complex and have bulky substituents. To evaluate the planarity of the nitroxide radical at the nitrogen atom, the INDO calculations for CF_3-BNO and CF_3-NB spin adducts were carried out.

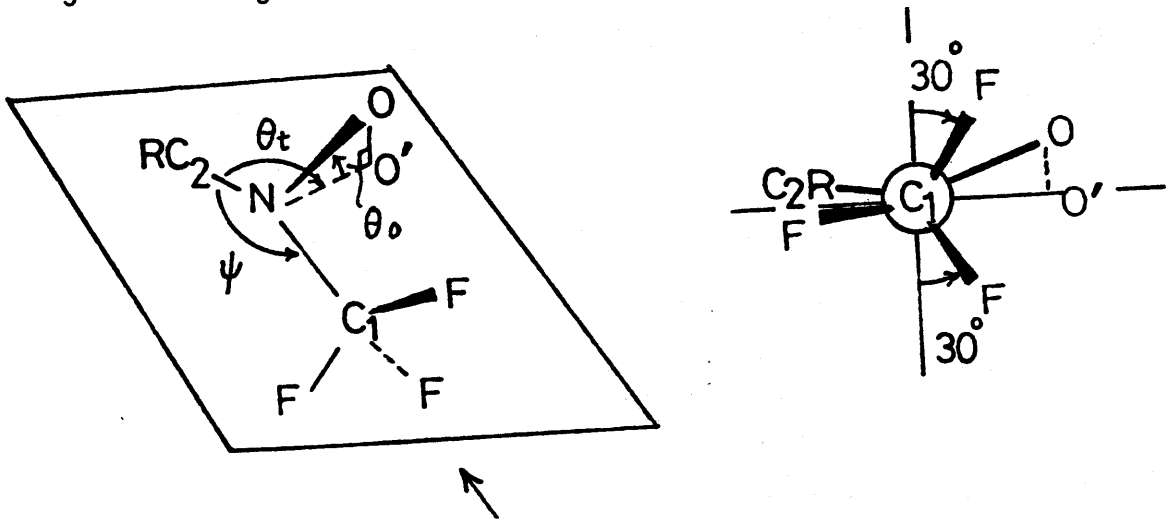

For the structure of the nitroxide radical, C_1, N and C_2 are placed on a Plane, as shown above. In the figure, the point O' is the projection of the O atom to the plane including C_1, N and C_2. The angles of $\angle C_1NC_2$, $\angle C_2NO'$ and $\angle ONO'$ are difined as ψ, θ_t and θ_o, respectively. The angle θ_o indicates the magnitude of non-planarity at the nitrogen center in the nitroxide radical. In Fig. 8 the value of total energy, A_F and spin density of nitrogen s-orbital calculated from the INDO method are indicated as a function of ψ, θ_t and θ_o. It is seen that the larger ψ gives smaller A_F but constant A_N, and larger θ_o gives smaller A_F and larger A_N. It is reasonable that larger θ_o gives larger A_N, because distortion from a planar structure increases the s-character of the nitrogen atom. The geometry of the lowest energy corresponds to a planar structure (θ_o=0) with the angle of ψ and θ_t being 125° and 120°, respectively. The energy change with the

deformation of the oxygen atom from the plane including C_1, N and C_2 is smaller in contrast with the change of ψ and θ_t. Underwood et al[14],[15] reported that the structure of $(CF_3)_2\dot{N}O$ having the minimum energy is non-planar at the nitrogen atom with a low barrier to the inversion. However, our computational results show that the structure having minimum energy is planar. This discrepancy is attributed to the substituents, the tert-butyl group. The fact that no dependence of A_N on temperature was observed is consistent with this conclusion. If the inversion at the nitrogen atom occurs, A_N must be dependent on temperature. This planar structure at the nitrogen atom may cause the reduction of the magnitude of A_N for the fluoroalkyl spin adducts in contrast with non-fluorinated alkyl spin adducts.

The planar structure at the nitrogen atom is adopted for the calculations on other fluoroalkyl spin adducts. The results of the INDO calculations of the CF_3-BNO spin adduct are summarized in Table III. The agreement between the observed and calculated A_F values is fairly good, whereas the calculated A_N is quite different from the observed value. The calculated A_N is derived from the relation $A_N=379.34\ \rho_N^S$ introduced by Pople et al, where ρ_N^S is the spin density in the s-orbital of nitrogen. This relation could not explain the observed A_N values of other spin adducts. A corrected value was obtained from the calculation of ρ_N^S and experimental A_N values of many other nitroxide radicals.[17] The modified relation is $A_N=882\ \rho_N^S$ from the correlation between ρ_N^S and A_N as shown in Fig. 9. This modified relation can explain the observed A_N value of fluoroalkyl spin adducts (see Tables III and IV).

It is well known that the β-hydrogen hyperfine splitting constant is related to both ρ_π and θ, where ρ_π is the electron spin density in a π orbital, and θ is the dihedral angle between the C_β-H bond and the ρ_z orbital of odd electron. It is called the " Heller-McConnell " relation.[18]

$$A_H^\beta = \rho_\pi(B_0 + B_2\cos^2\theta) \quad (3)$$

This relation is applicable to evaluate the magnitude of the β-fluorine coupling constant,

$$A_F^\beta = \rho_N^\pi(B_0 + B_2\cos^2\theta), \quad (4)$$

where ρ_N^π is the spin density in the π-orbital of nitrogen. It was also found that the values of B_0 and B_2 are dependent on ψ. The values of B_0 and B_2 are also dependent on the number of β-fluorine atoms. For the CF_3-BNO spin adduct, the B_0 and B_2 values were evaluated to be ∿-20 G and ∿130 G, respectively. In the case of CF_3-NB, the change of A_F with θ is shown in Fig. 10.

2. Internal rotation of the CF_3 group around the N-CF_3 axis.

Among the three CF_3 spin adducts, only the CF_3-MNB shows the selective broadening effect at lower temperature. This broadening is attributed to the higher energy barrier about the N-CF_3 bond of the CF_3-MNB spin adduct than that of other CF_3 spin adducts. From the INDO calculations, the barrier for the internal rotation of the CF_3 group was found to be ∿0.6 kcal/mole and ∿4 kcal/mole for BNO and MNB spin adducts, respectively. These results seem reasonable judging from our observations, though the absolute values of the barriers may be less reliable because of the limitation of the INDO calculation.

3. Restricted rotation of CF_2R-BNO spin adducts.

It is not known whether the pentafluoroethyl group is freely and rapidly rotating around the carbon-nitrogen bond with respect to the esr measurement frequency or not. Our results seem to show that CF_2R groups, including CF_2CF_3, and not freely rotating about carbon-nitrogen bond because

the CF_2ClCF_2-BNO and $CF_3CH_2CF_2$-BNO spin adducts change their esr patterns with temperature.

It is important to estimate the barrier of rotation about the carbon-nitrogen bond. From the INDO calculations, the change of total energy with ψ and θ_B of the CH_3CF_2-BNO spin adduct was estimated as shown Fig. 11(a), where ψ and θ_B are the angles between β-fluorine atom and the oxygen atom; and CF_3 of tert-butyl and CH_2CF_3, respectively, as shown below.

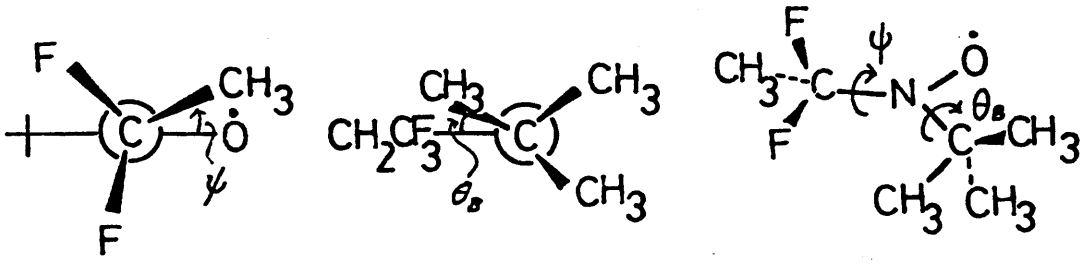

In the case of the CH_3CF_2 group, the high energy barrier may arise from a strong steric interaction between the CH_3 group of CF_2CH_3 and the oxygen atom. It is thought that the CF_2CF_3 group has a higher barrier than the CF_2CH_3 group because the CF bond length (∿1.36Å) is larger than the CH bond length (∿1.09Å), and consequently, the CF_3 group induces larger interaction with oxygen than does the CH_3 group. Therefore, the rotation of CF_2R about the carbon-nitrogen bond may not be free. On the other hand, the internal rotation of the tert-butyl group about the nitrogen-carbon bond may be free because the energy change with θ_B is very small when ψ is nearly 0°, as shown in Fig. 11(a). The conformations of CH_3CF_2-BNO and CF_3CF_2-BNO having minimum total energy obtained from calculation and the coupling constants are summarized in Table IV. The coupling constants from the calculation are in good agreement with the observed values. The fluorine coupling constants in the

adducts show large temperature dependence. It was found that A_N is independent of internal rotation about the carbon-nitrogen bond according to the INDO calculations. The temperature dependent change of A_F may be due to torsional oscillation of CF_2R about the C-N bond, as shown in Fig. 11(b). This change of A_F will be discussed later.

4. Stable conformations of $CF(CF_3)_2$ spin adducts.

In $\dot{C}F(CF_3)_2$ spin adducts of BNO, MNB and NB, the $CF(CF_3)_2$ group may not be rotating freely around the carbon-nitrogen bond. Inspection of a space-filling model of these adducts indicates that the most stable conformation of these adducts is as follows:

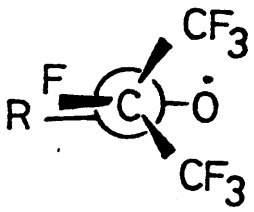

R: C_6H_5, $C(CH_3)_3$ and $C(CH_3)_2\overset{O}{\overset{\|}{C}}CH_3$

This conclusion is supported by INDO calculations. In the case of the $(CF_3)_2CF$-BNO spin adduct, the value of total energy, A_F and ρ_N^S as a function of ψ are shown in Fig. 12. The temperature coefficient of A_F^β will be discussed in the next section.

5. Negative or positive temperature coefficient of A_F.

It is well known that the temperature dependence of A_H^β helps to elucidate the conformation of alkyl radicals.[19]~[21] All the RCF_2-BNO spin adducts except CF_2ClCF_2-BNO have negative temperature coefficients of A_F^β. The conformers having the lowest total energy of the CF_2R spin adducts except CF_2ClCF_2-BNO, -MNB and CH_2CF_3-MNB have two equivalent fluorine atoms. In these conformations, the dihedral angle between fluorine atom and nitrogen

π-orbital is 30°. The distortion from this geometry makes two fluorine atoms non-equivalent. If the distortion angle is defined as ψ, the fluorine coupling constant from the modified Heller-McConnell relation is

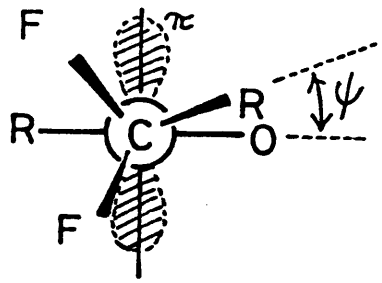

$$A_F = \{B_0 + B_2\cos^2(30 \pm \psi)\}\ \rho_\pi . \qquad (5)$$

When the CF_2R group is torsionally oscillating rapidly, the population averaged A_F is observed. The averaged A_F is written in the following form.

$$\overline{A}_F = \frac{1}{2}\{A_{F+} + A_{F-}\} = \{B_0 + B_2\,(\frac{1}{2} + \frac{1}{4}\cos^2\psi)\}\ \rho_N^\pi$$

$$\leqq (B_0 + \frac{3}{4}B_2)\ \rho_N^\pi = (B_0 + B_2\cos^2 30°)\ \rho_N^\pi \qquad (6)$$

This equation indicates that the distortion from the dihedral angle of 30° gives a smaller $\overline{A}_F$ value. Thus, with increasing temperature the observed A_F becomes smaller owing to the oscillation in the potential well, and consequently the negative temperature coefficient of A_F^β is observed.

From similar consideration, the positive temperature coefficients of A_F^β in $(CF_3)_2CF$-BNO, -MNB and -NB spin adducts can be explained. From inspections of a space-filling models and the INDO calculations, the stable conformation of these adducts is predicted to be one in which the dihedral angle of the β-fluorine atom is 90°. Distortion of the $(CF_3)_2CF$-N bond from stable conformation gives a larger fluorine coupling constant. At higher temperatures, the coupling constant of β-fluorine atom becomes larger. This result is consistent with both the observation and the INDO calculation.

It was found that CF_3CH_2CFH-NB gives an observable separation due to

A_H^β, but CF_2ClCFH-NB spin adduct gives no observable separation (Fig. 3). From both the Heller-McConnell relation ($\cos^2\theta$ law) and the magnitude of A_F and A_H values observed, the stable conformations of CH_2ClCFH-NB and CF_3CH_2CFH-NB are considered to be:

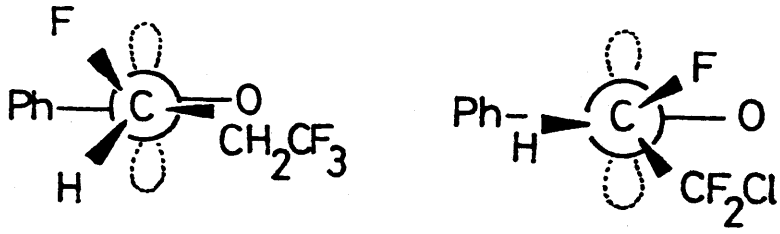

6. $CF_3CH_2CF_2$-BNO spin adduct

This adduct shows the normal 1:2:1 pattern at low temperatures. Selective line broadening occurs between -150°C and 0°C. In the calculation, it is necessary to consider trans and gauche conformations of the $CF_2CH_2CF_3$ group.

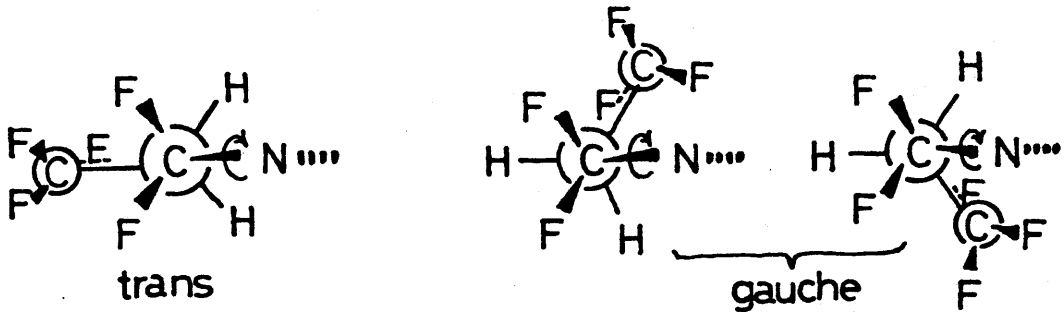

The results are shown in Fig. 13. In the case of trans-$CF_2CH_2CF_3$, the conformation having the minimum total energy has two equivalent fluorine atoms, as shown for conformation A in Fig. 13. On the other hand, in the case of gauche-$CH_2CH_2CF_3$, two different conformations having minimum total energy exist as shown for B and C in Fig. 13. The minimum energy of the trans conformation is lower than that of the gauche conformations. The conformation C is more stable than B.

The behavior of the esr spectral change of $CF_3CH_2CF_2$-BNO is explained in the following manner. At the lowest temperature, -170°C, the observed esr pattern has normal intensity ratios (1:2:1) due to two equivalent fluorine coupling constants. At this temperature, the transition from the conformation A to B and C is thought to be restricted, and the $CF_3CH_2CF_2$-BNO spin adduct stays in conformation A.

With increasing temperature, selective line broadening effect was observed. This means that the interconversion rate among the conformations A, B and C increases, and consequently the coupling constant measured from experimental observation is the population average A_F among the conformations A, B and C. For the interconversion among the conformations A, B and C, the movement of lines due to $M_I^F=0$ is larger than that of the outer lines $M_I^F=\pm 1$. Therefore, the central line is broadened much more than the outer lines. At higher temperatures, the interconversion rate becomes more rapid than the resonance frequency difference, and the intensity ratio becomes the nomal 1:2:1.

It is possible to evaluate the energy difference between these conformations. For simplicity only internal conversions among the conformations A, C and C' are considered. From the INDO calculation for conformation A, the value of A_F=28.4 G is obtained. This A_F obtained for the conformation A from the calculation is smaller than the observed value of A_F, 31.6 G at -160°C, in propane. To explain the dependency of A_F observed, it is necessary to take a A_F value which is larger than 31.6 G. From the INDO calculation for the gauche conformation having ψ=60°, averaged A_F is assumed to be 12 G for the conformation C. By using a value of A_F of 34 G for the conformation A, and an energy difference between the conformation A and C of $\sim$0.5 kcal/mole, the simulated change of A_F with temperature from population averaging is in excellent agreement with the observed one as indicated in

Fig. 5(b). The energy difference of 0.5 kcal/mole obtained from simulation is smaller than that from the INDO calculation between the conformation A and C in Fig. 12. This discrepancy may be due to the intrinsic limitations of the INDO calculation.

7. CF_2ClCF_2-BNO and -MNB spin adducts.

The esr spectra of the CF_2ClCF_2-BNO spin adduct change abnormally with temperature (Fig. 6). The CF_2ClCF_2 group has both trans and gauche conformations. At lower temperatures, the spectrum is asymmetric. This means that the conformers having different g-factors and different coupling constants overlap in the spectrum. With increasing temperature, the exchange rate among these conformers increases and the spectrum changes significantly. At temperatures higher than -60°C the change in the spectra is similar to that of $CF_3CH_2CF_2$-BNO. In the case of CF_2ClCF_2-MNB, the change is rather simple in contrast with CF_2CF_2Cl-BNO. An abnormal esr pattern change was also found in CF_2ClCFH-BNO (Fig. 4) and CF_2ClCFH-MNB. It is thought that these adducts may stay at several different stable conformations and the interconversion rate is slow at lower temperatures.

With increasing temperature, the rate of the interconversion between these conformations increases with respect to the esr measurement frequency and the observed spectra become simple. Therefore, the change in esr pattern with temperature depends on the rate of interconversion defined by the energy difference between the conformers, and depends also on the magnitude of A_F defined by the structure of the conformation. More precise analysis is difficult at present because of the limitation of the calculations and the lack of exact information of the structure of these adducts.

Conclusion

It is found that fluoroalkyl spin adducts show significant temperature dependent change in esr patterns and A_F^β values. On the basis of observations of many types of fluoroalkyl spin adducts and INDO calculations, the origin of these effects were explained. The structure of these spin adducts may be planar at the nitrogen atom and the A_F^β value is assumed to obey the $\cos^2\theta$ law (Heller-McConnell relation). The CF_3 group of spin adducts is assumed to rotate freely around the C-N axis in the CF_3-BNO and -NB spin adducts and restrictedly in the CF_3-MNB spin adduct. The CF_2R and $CF(CF_3)_2$ groups do not rotate freely, but oscillate torsionally around the C_β-N bond. The temperature dependence of the A_F value was explained by restricted oscillation, and the stable conformations of these adducts can be estimated. Spectra such as those of CF_2ClCF_2-BNO, CF_2ClCF_2-MNB,CF_2ClCFH-BNO and CF_2ClCFH-MNB, in which more than one kind of radical seems to overlap, suggest that several stable conformations exist in these adducts and that the interconversion rate between the different conformations is slow at lower temperatures.

Acknowlegement

This research was carried out at the National Universities Laboratory for the Common Use of JAERI Facilities.

All calculations were performed in the HITAC 8700/8800 TODAI CENTER at the University of Tokyo. The INDO program used was CALCULATION OF CNDO AND INDO MOLECULAR ORBITALS + CALCULATION OF LOCALIZED MOLECULAR ORBITALS (Y4/TCCB04N) written by J.A. Pople, D.L. Beveridge, P.A. Dobosh and P.M. Kuznesof, based on Quantum Chemistry Program Exchange.

References and Notes

1) E.G. Janzen; Accounts of Chem. Res., 4, 31, (1971)

2) C. Lagercrantz; J. Phys. Chem. 75, 3466 (1971)

3) K.J. Klabunde; J. Amer. Chem. Soc., 92, 2427 (1970)

4) S. Terabe and R. Konaka; Bull. Chem. Soc. Jpn., 46, 825 (1975)

5) J.A. Pople and D.L. Beveridge, " Approximate Molecular Orbital Theory " McGRAW-HILL, Inc. (1970)

6) R.J. Holman and J.J. Perkins; J. Chem. Soc, (B), 2195 (1970)

7) J.G. Aston, D.F. Mevard and M.G. Haryberry; J. Chem. Soc., 54, 1530 (1932)

8) R.N. Haszeldine and B.R. Steele; J. Chem. Soc., 1199 (1953)

9) R.N. Haszeldine; J. Chem. Soc., 4423 (1952)

10) A. Mackor, Th. A.J.W. Wajor and Th. J. de Boer; Tetrahedron Lett., 19, 2115 (1966)

11) Th. A.J.W. Wajor, A. Mackoe, Th. J. de Boer and J.D.W. Van Voorst; Tetrahedron 23, 4021 (1962)
S. Forshult, C. Lagercrantz and K. Torsell; Acta Chem. Scand., 23, 522 (1969)

12) J.W. Hartgerink, J.B.F.N. Fngberts and Th. J. de Boer; Tetrahedron Lett., 29, 2709 (1971)

13) K. Morokuma; J. Amer. Chem. Soc., 91, 5143 (1969)

14) G.R. Underwood and V.L. Vogel; Mol. Phys., 621 (1970)

15) G.R. Underwood and V.L. Vogel; J. Amer. Chem. Soc., 92, 5019 (1970)

16) I. Morishima, K. Endo and T. Yonezawa; Chem. Phys. Lett., 9, 143 (1971)

17) The coupling constants of $(CF_3)_2\dot{N}O$ and $(CH_3)_2\dot{N}O$ experimentally are reported by W.R. Knolle and J.R. Bolton in J. Amer. Chem. Soc. 91, 5411 (1969) and Morishima et al in J. Phys. Lett. 9, 143 (1971), respectively.

The coupling constants of all spin adducts were calculated by the INDO method in the present work.

18) C. Heller and H.M. McConnell; J. Chem. Phys., 32, 1535 (1960)

19) P.J. Krusic, P. Meakin and J.P. Jessen; J. Phys. Chem., 75, 3438 (1971)

20) J.C. Scaiano and K.U. Ingold; J. Phys. Chem. 80, 275 (1976)

21) J.K. Kochi, " Advances in Free Radical Chemistry, " vol. 5, G.H. Willams, Ed., Academic Press, New York, 1975, P189.

Figure captions.

Fig. 1 Esr spectra of nitroxide formed by the photolysis of CF_3I in the presence of trapping agents.

a) Spectrum of CF_3-$\dot{N}O$-C_6H_5 at -60°c in isopentane.

b) Spectrum of CF_3-$\dot{N}O$-$C(CH_3)_3$ at -60°c in isopentane.

c) Spectrum of CF_3-$\dot{N}O$-$C(CH_3)_2COCH_3$ at -30°c and -80°c in dichloromethane. At lower temperature than -80°c, the lines due to $M_I^F=0$ are broadened.

Fig. 2 Esr spectra of nitroxide formed by the photolysis of perfluoromethyl iodide and perfluoroisopropyl iodide in the presence of MNB in dichloromethane.

a) Spin adduct of CF_3CF_2-MNB observed at 0°c. Even at this temperature the lines due to $M_F^I=0$ are still broadened and splitting of β-F is separately observed.

b) Spin adduct of $CF(CF_3)_2$-MNB observed at 0°c. The change of esr pattern with temperature is not observed.

Fig. 3 Esr spectra of nitroxides formed by the photolysis of fluoroalkyl iodides in the presence of NB in isopentane.

a) Spin adduct of CF_3CH_2CFH-NB observed at -60°c.

b) Spin adduct of CF_2ClCFH-NB observed at -60°c.
A_β^H is observed in (a) but not in (b).

c) Spin adduct of CF_2ClCF_2-NB observed at -20°c. The lines due to $M_F^I=0$ are still broadened even at this temperature.

Fig. 4 Esr spectra of $\dot{C}FHCF_2Cl$ radical trapped by BNO observed -107°c and -78°c in isopentane.

Fig. 5

a) Spectra of $\dot{C}F_2CH_2CF_3$ radical trapped by BNO observed at -160°c and -110°c in propane. At -110°c the lines due to $M_F^I=0$ are broadened.

b) The change of A_F^β, A_N and intensity ratio of the lines ($M_I^F=0/M_I^F=0$) as a function of temperature. The solid lines are in propane and broken lines are in isopentane. Significant broadening effect is seen at ∿100°c in both sovents. Simulated calculation of A_F (see discussion) is also shown as (– – – –).

Fig. 6 Esr spectra of $\dot{C}F_2CF_2CF_3$ radical trapped by MNB observed at various temperatures in isopentane. The change of spectra is reversible between -120°c and -20°c.

Fig. 7 Esr spectra of $\dot{C}F_2CF_2Cl$ radical trapped by MNB observed at various temperatures in dichloromethane. The change of spectra is reverisible between -100°c and +10°c.

Fig. 8 The change of total energy (o), A_F (Δ) are spin density of nitrogen s-orbital (+) calculated from INDO method as a function of θt, θo and ψ, in CF_3-BNO spin adduct.

a) ψ = 125° θo = 0°c (b) θt = 120°c ψ = 125° (c) θt = 120° θo = 0°c

In all cases the dihedral angle of F atom is 30°.

Fig. 9 Correlation between experimental A_N and ρ_N^S calculated by INDO method.[17]

A: $(CF_3)_2\dot{N}O$, B: ph-$\dot{N}O$-CF_3, C: $(CH_3)_2\dot{N}O$, D: CF_3-$\dot{N}O$-$C(CH_3)_2COCH_3$, E: $C(CH_3)_3$-$\dot{N}O$-CF_3, F: $C(CH_3)_3$-$\dot{N}O$-$CF_3CH_2CF_3$, G: $C(CH_3)_3$-$\dot{N}O$-$CF(CF_3)_2$, H: $C(CH_3)_3\dot{N}OCF(CF_3)_2$.

Fig. 10 Change of A_F calculated by INDO method as a function of θ, dihedral angle of β-fluorine atom difined as below, in CF_3-$\dot{N}O$-Ph.

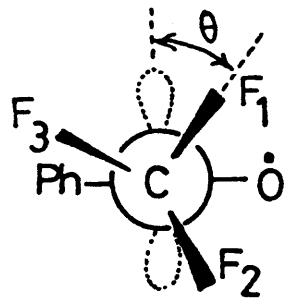

Fig. 11

a) The change of total energy as a function of CF_2CH_3 group (ψ) and tert-butyl group (θ_B).

θ_B is dihedral angle of methyl group in tert-butyl group.

x is the minimum total energy.

b) The change of energy at – – – – indicated in a)

Fig. 12 The change of total energy (o), A_F^{β}(▲), A_F^{γ}(Δ) and spin density at nitrogen s-orbital (+) calculated from INDO method as a function of ψ in $CF(CF_3)_2$-BNO spin adduct.

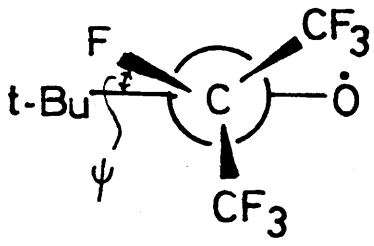

Fig. 13 The change of total energy of trans and gauche conformation as a function of ψ defined as shown in (c). In (b), esr pattern of two fluorine atoms obtained at the conformation A, B and C.

Table I ; Hyperfine splittings of perfluoroalkyl radical trapped by MNB in dichloromethane.

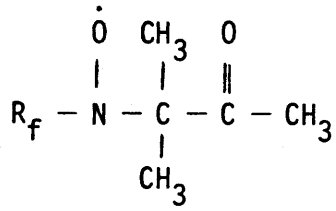

R_f	Temperature (°C)	Hyperfine splitting constants (G)		
		A_N	A_F^β	A_F^γ
CF_3	+ 5	11.51	10.13	—
	- 40	11.35	9.89	—
	- 80	11.32	9.56	—
CF_2CF_3	+ 10	10.89	17.48	0.85
	- 40	10.73	17.40	0.5
	- 80	10.9	17.7	—*
$CF(CF_3)_2$	0	4.02	4.02	2.01
	- 40	3.98	3.98	1.99
	- 80	3.90	3.90	1.95

* No separation is observable at -80°C.

R	$CFHCH_2CF_3$	$CFHCF_2CH_3$	CF_2CH_3	$CF_2CH_2CF_3$	CF_2CF_2Cl	CF_3	CF_2CF_3	$CF(CF_3)_2$
NB 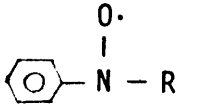	N (-60°c) A_F^β = 44.90G A_H^β = 3.39G A_N = 9.20G $A_N^{o.p}$ = 2.30G A_H^m = 0.48G	N (-57°c) A_F^β = 36.33G A_H^β = — A_N = 9.67G $A_H^{o.p}$ = 2.10G A_H^m = 0.80G	unstable	N (-50°c) A_F^β = 21.29G A_N = 9.81G $A^{o.p}$ = 2.29G A_H^m = 0.78G	C-1 (+25°c) A_F^β = 15.3G A_N = 9.5G $A_H^{o.p}$ = 1.96G A_H^m = 0.78G*	N (+25°c) A_F^β = 10.60G A_N = 9.68G $A_H^{o.p}$ = 1.96G A_H^m = 0.78G*	N (+25°c) A_F^β = 17.29G A_F^α = 0.66G A_N = 9.93G $A_H^{o.p}$ = 1.90G A_H^m = 0.66G*	N (+25°c) A_F^β = 4.95G A_F^α = 1.18G A_N = 10.93G $A_H^{o.p}$ = 1.81G A_H^m = 0.80G*
BNO 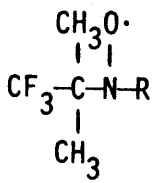	N (-45°c) A_F^β = 53.96G A_H = 1.59G A_N = 12.16G	C - 2	N (0°c) A_F^β = 28.94G A_N = 12.06G	C-1 (+35°c) A_F^β = 25.07G A_N = 12.32G	C-3 (+35°c) A_F^β = 20.23G A_N = 11.26G	N (-60°c) A_F^β = 12.34G A_N = 12.03G **	N (-60°c) A_F^β = 22.65G A_F^γ = 0.22G A_N = 11.31G **	N (-60°c) A_F^β = 1.32G A_F^γ = 2.29G A_N = 12.15G **
MNB 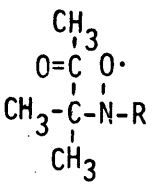	N (-50°c) A_F^β = 50.61G A_H^β = 1.65G A_N = 12.11G	C - 2	N (-50°c) A_F^β = 40.89G×1 A_N = 11.84G ***	N (-50°c) A_F^β = 39.14G×1 A_N = 11.94G ***	C-3 (-50°c) A_F^β = 16.09G A_N = 11.15G	C-1 (-40°c) A_F^β = 9.89G A_N = 11.35G	C-1 (10°c) A_F^β = 17.48G A_F^γ = 0.85G A_N = 10.89G	C-1 (-50°c) A_F^β = 3.94G A_F^γ = 1.97G A_N = 11.89G

* from ref (4)

** from ref (3)

*** it seems that only one fluorine coupling constant

Table III ; Spin densities and coupling constants from INDO calculation of trifluoromethyl-tert-butyl nitroxide radical.

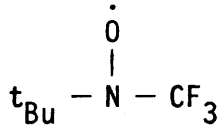

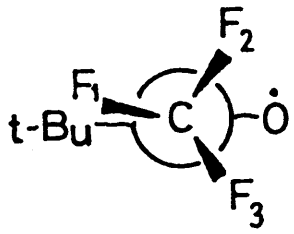

θ_t = 120°

ψ = 125°

θ_o = 0°

atom	ρ_s	ρ_π	A(G)cal	A(G)obs**
O	0.00127	0.7316	11.33	—
N	0.0135	0.2516	5.12 (11.20)*	12.02
C_α	-0.0050	-0.0110	-4.09	—
F_1	-0.0001	-0.0020	-4.26	
F_2	0.0005	0.0066	22.0	
F_3	0.0005	0.0066	22.0	
F_{av}	0.0003	0.0037	13.25	12.34

* corrected value using the modified relation, $A_N = 882\rho_S^N$

** observed at -60°c from ref (3)

Table IV ; Calculated spin densities and coupling constants in $\dot{C}F_2CH_3$ and $\dot{C}F_2CF_3$ trapped by BNO.

atom	ρ_s	ρ_π	Acal(G)	|Aob|(G)	ρ_s	ρ_π	Acal(G)	|Aob|(G)
O	0.0124	0.7137	11.01	—	0.0126	0.7264	11.21	—
N	0.0146	0.2698	12.88[b]	12.06[c]	0.0139	0.2571	12.25[b]	11.31[d]
C_α	-0.0043	-0.0149	-3.52	—	-0.0044	-0.0157	-3.71	—
F_1^β	0.0006	0.0076	28.32	—	0.0006	0.0078	26.06	—
F_2^β	0.0006	0.0076	28.32	—	0.0006	0.0078	26.06	—
F_{av}^β	0.0006	0.0076	28.32	23.94	0.0006	0.0078	26.06	22.65
F^γ	—	—	—	—	-0.0000	-0.0004	-1.45	0.22
$t_{Bu} - \overset{O\cdot}{\underset{\vert}{N}} - CF_2CH_3$			θ_B = 30° ψ[e] = 125° ψ[a] = 0°		$t_{Bu} - \overset{O\cdot}{\underset{\vert}{N}} - CF_2CF_3$		θ_B = 30° ψ = 125° a) = 0°	

a) ψ is defined as the additional deviation from the angle, θ=30°. ψ=0 means that the dihedral angle of β-fluorine atom is 30°.

b) derived from the relation, $A_N = 882\rho_S^N$.

c) present work

d) from ref (3)

e) ψ is defined as the angle between $^tBu - N$ bond and N − CR bond.

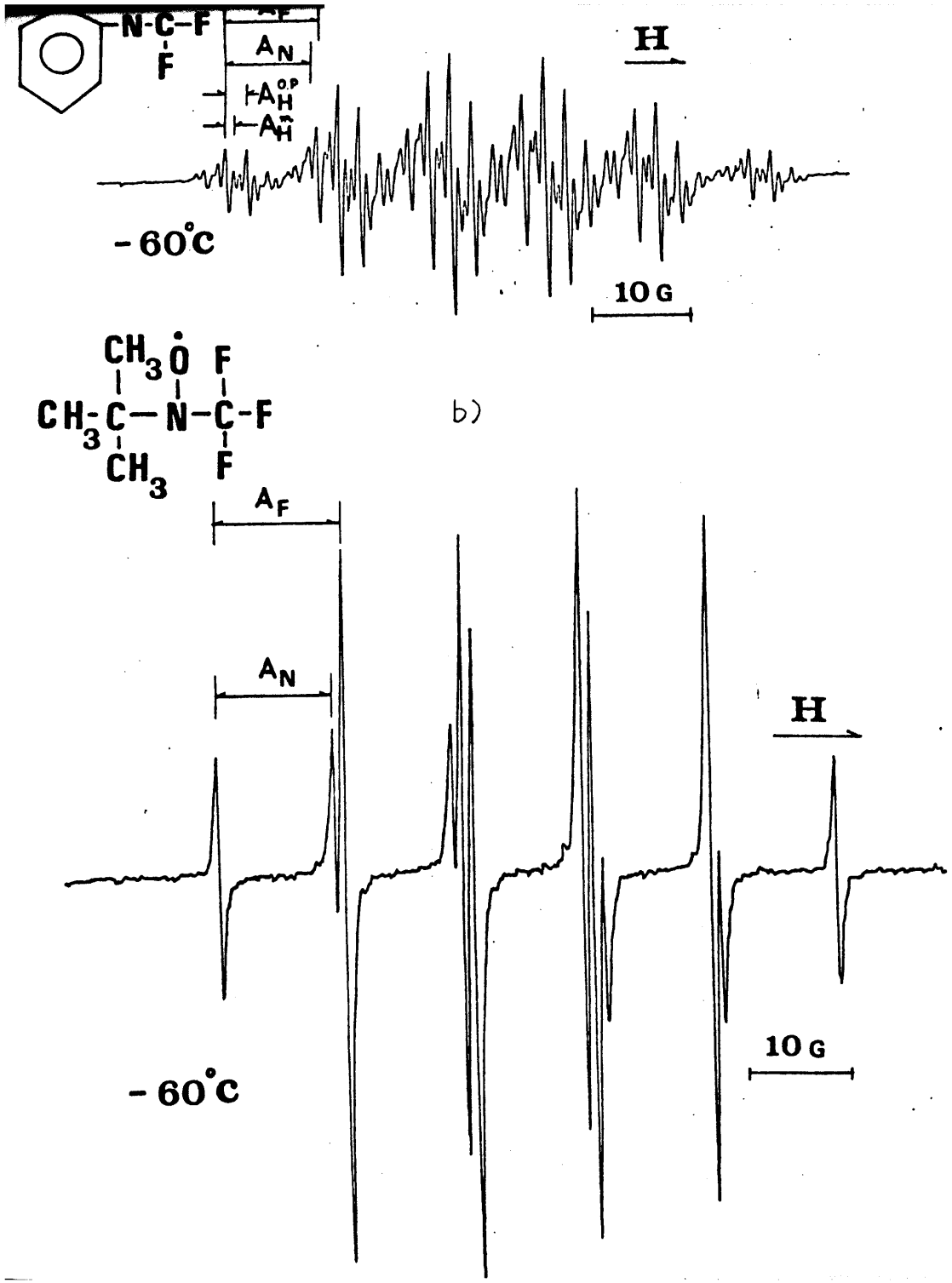
N-C-F
F
A_N
A_H^{op}
A_H^{m}
H
-60°C
10 G
b)
CH_3 O F
CH_3-C-N-C-F
CH_3 F
A_F
A_N
H
10 G
-60°C

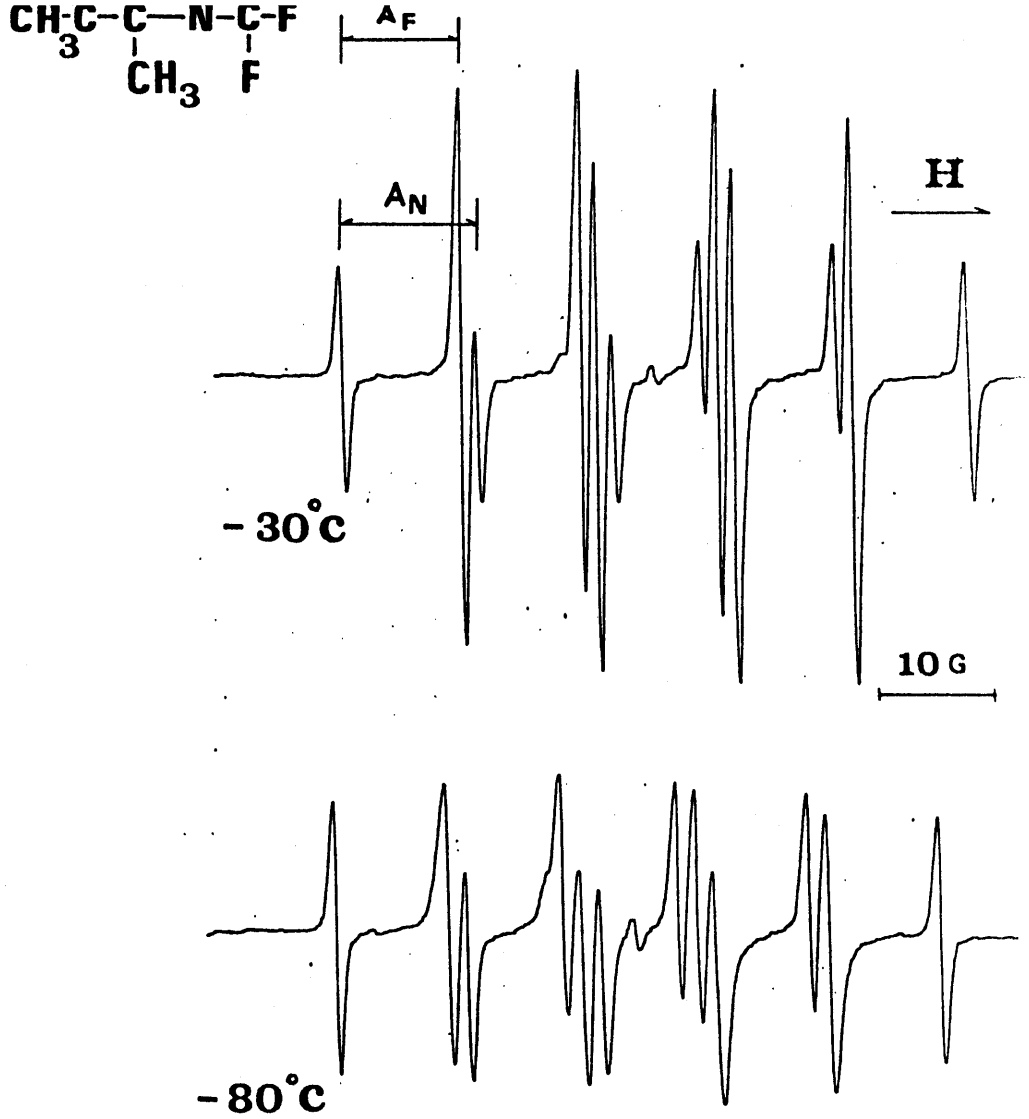
CH_3-C-C-N-C-F
CH_3 CH_3 F
A_F
A_N
H
-30°C
10 G
-80°C

Fig.1 (a),(b) and (c)

a)

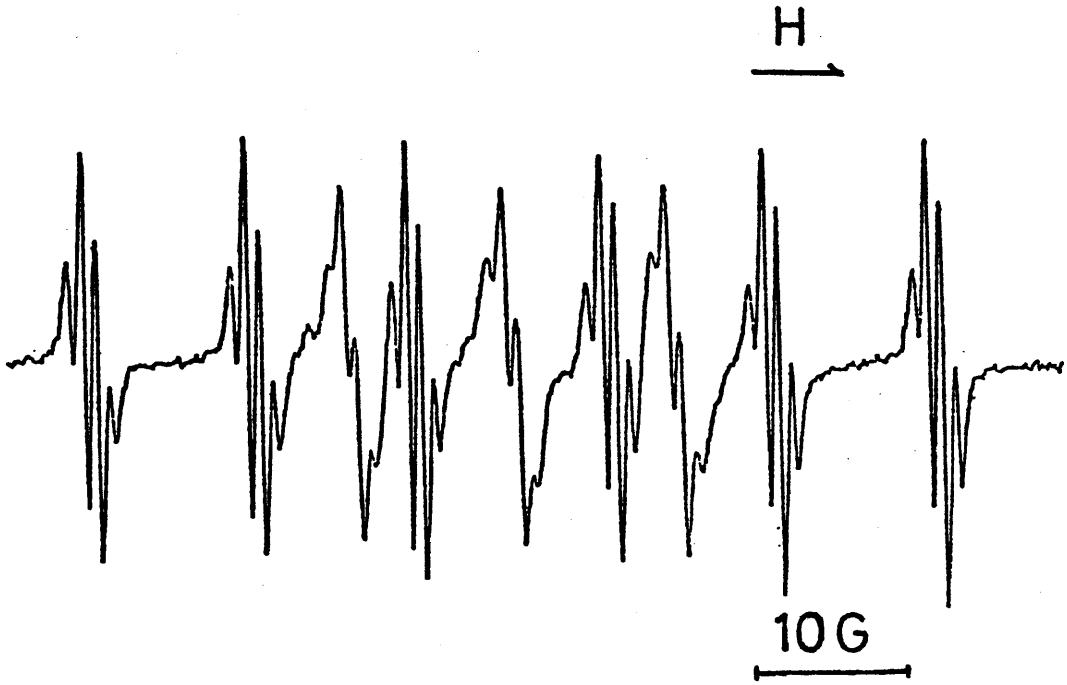

b)

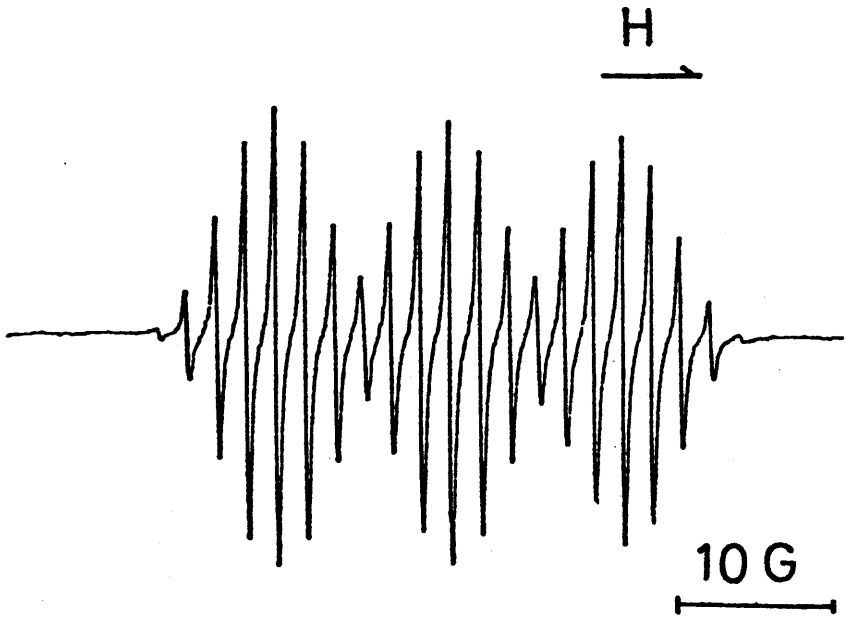

Fig.2 (a) and (b)

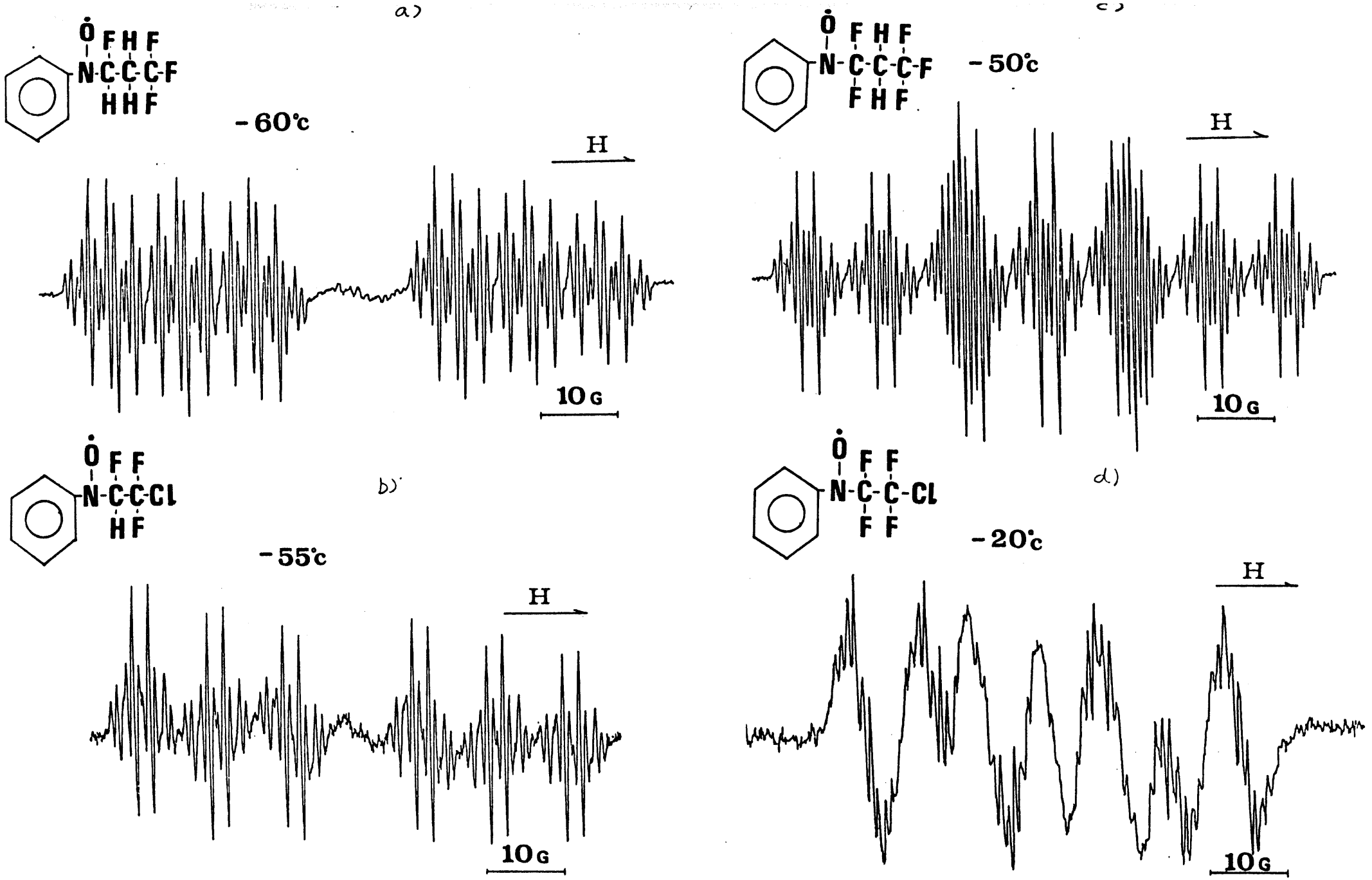

Fig.3 (a),(b),(c) and (d)

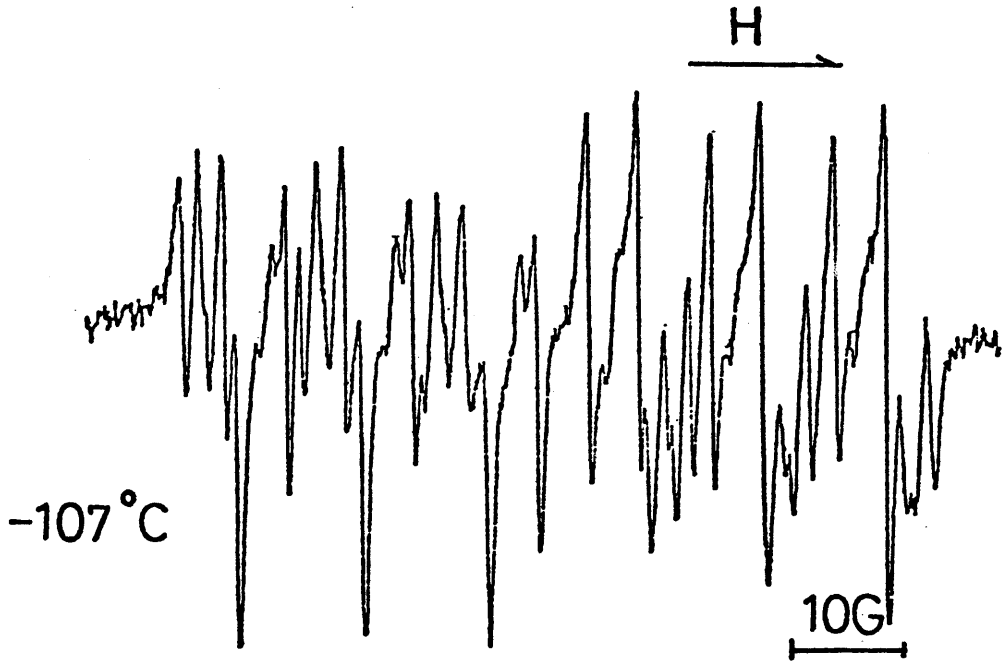

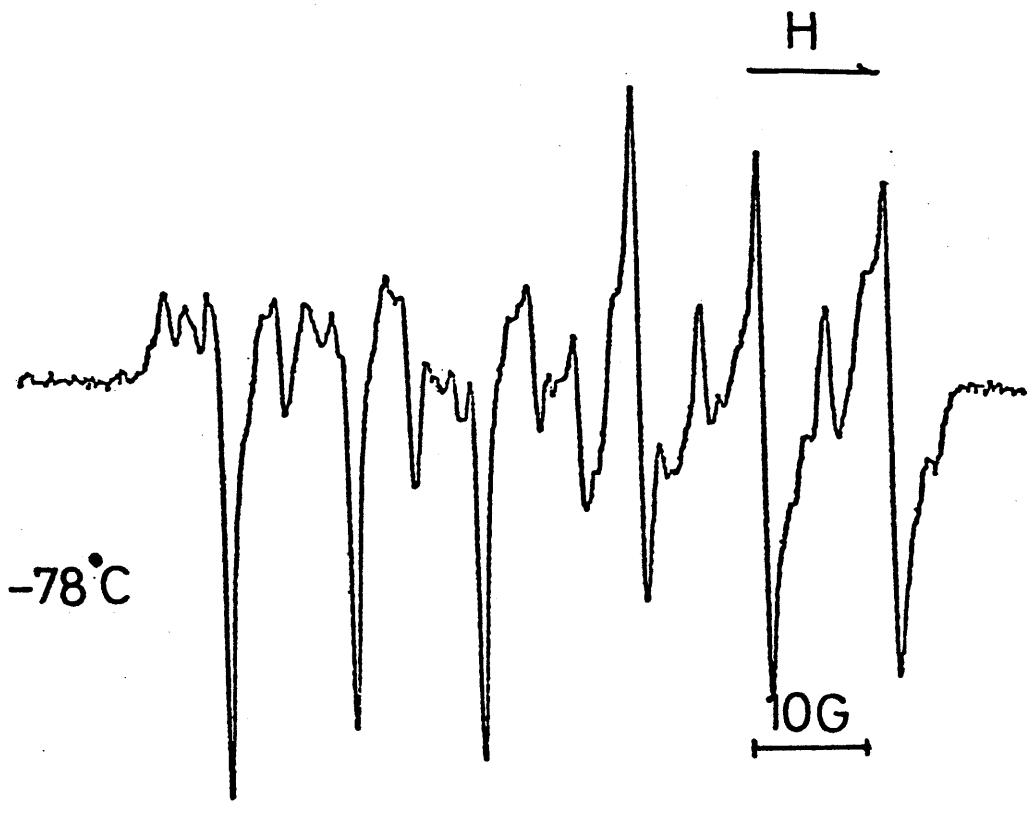

Fig.4

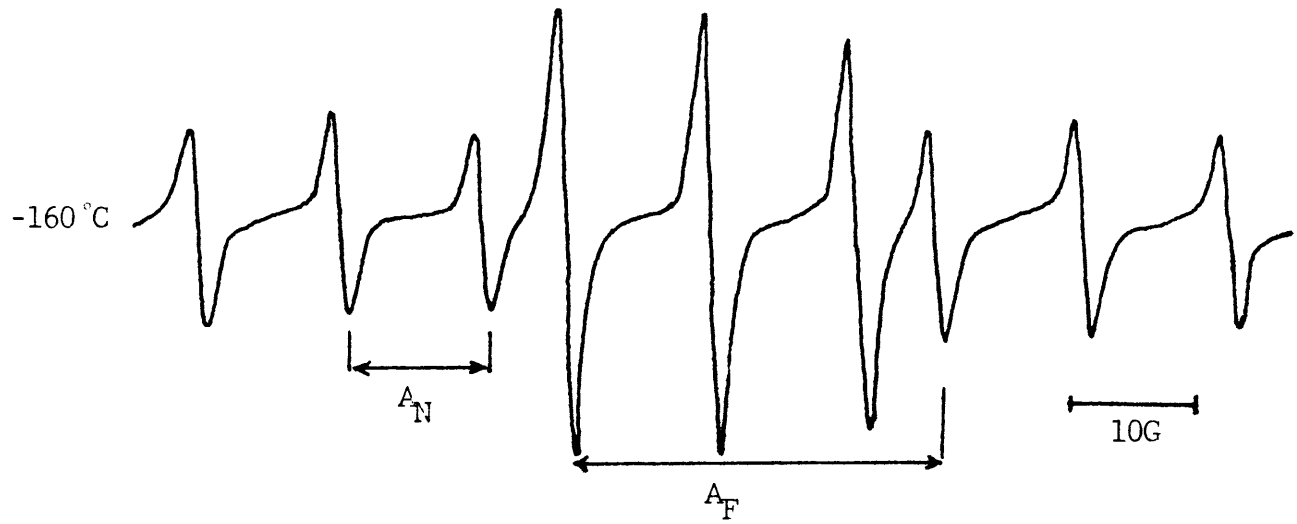

a)

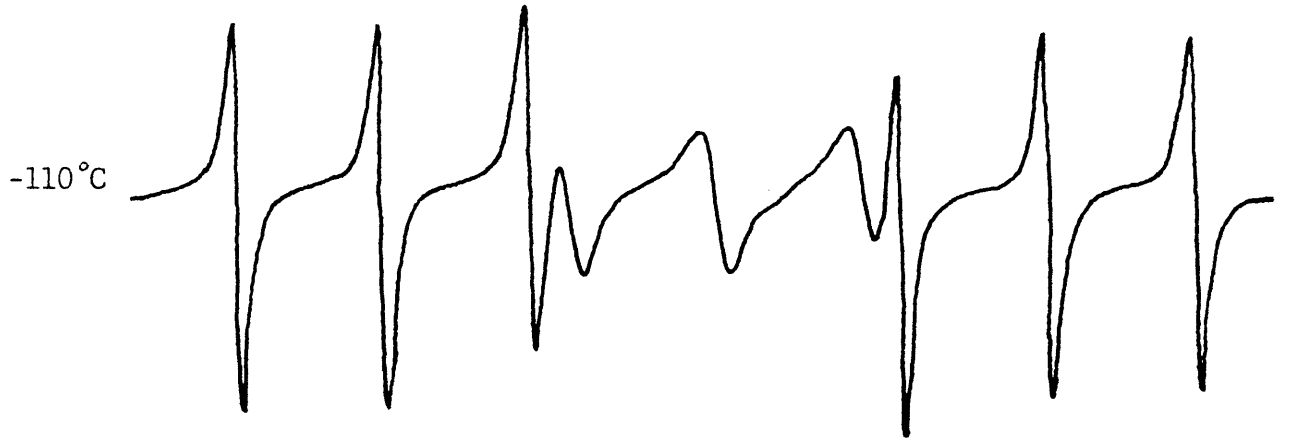

b)

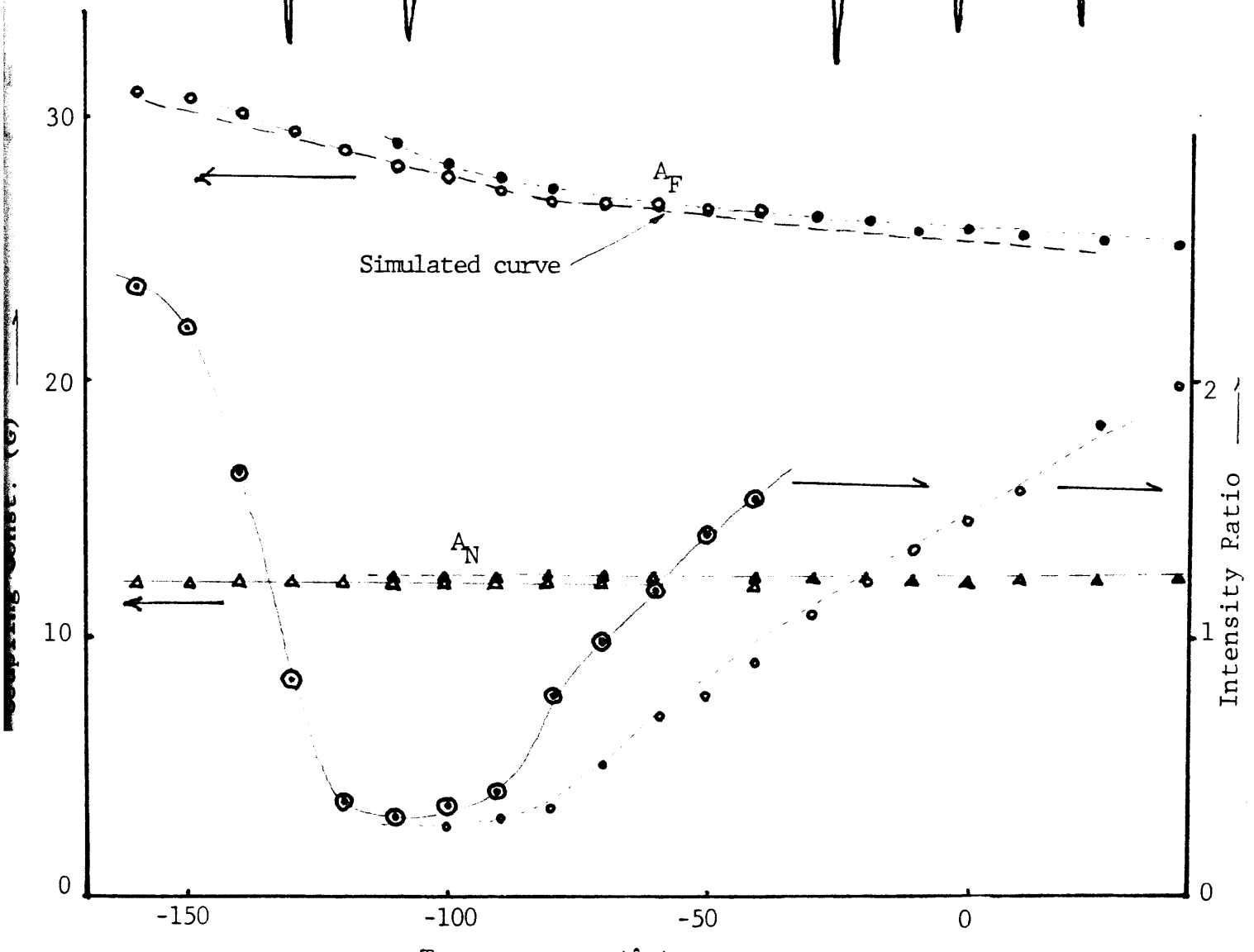

Fig.5 (a) and (b)

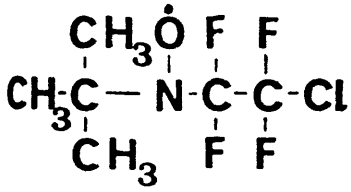

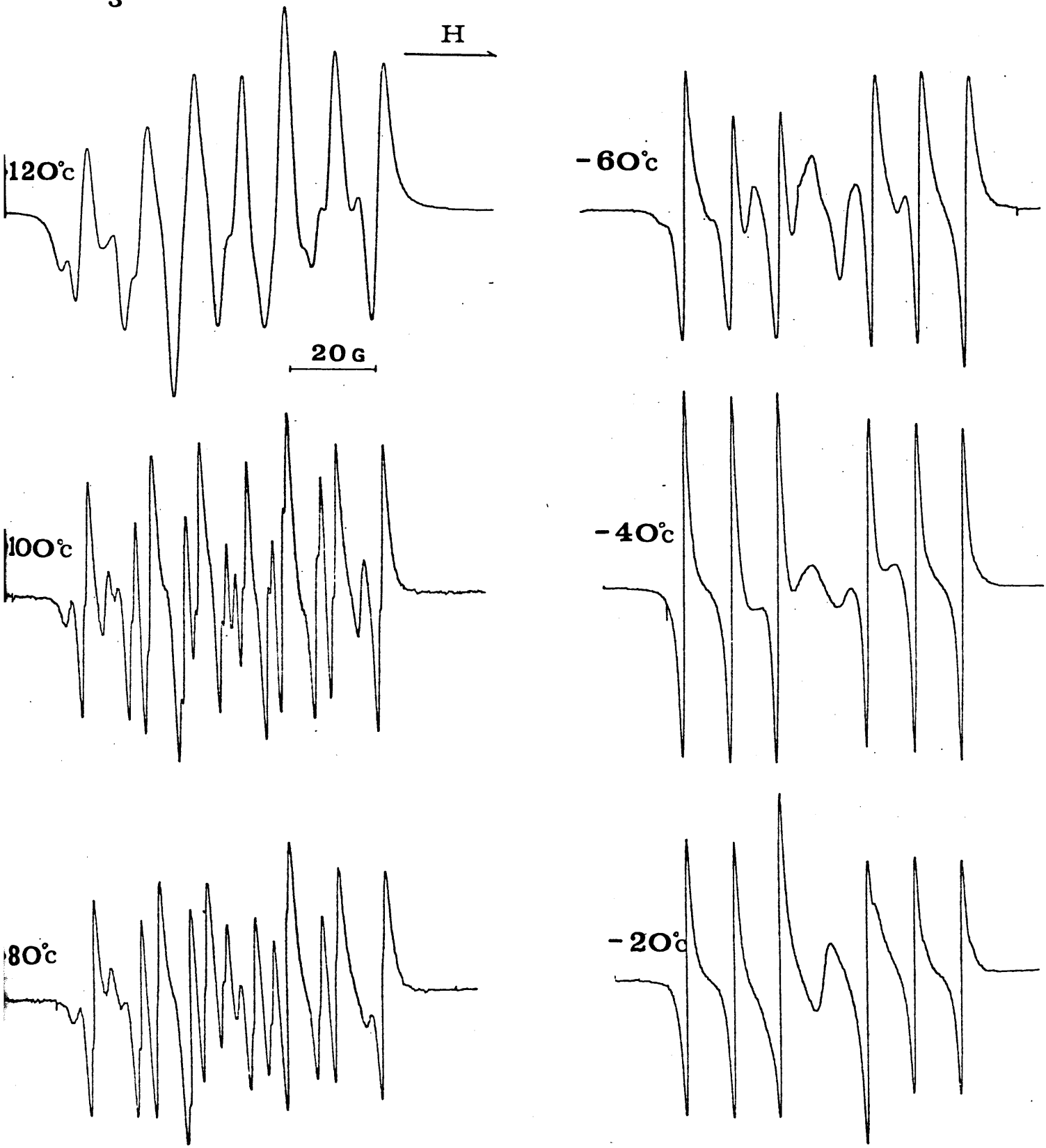

Fig.6

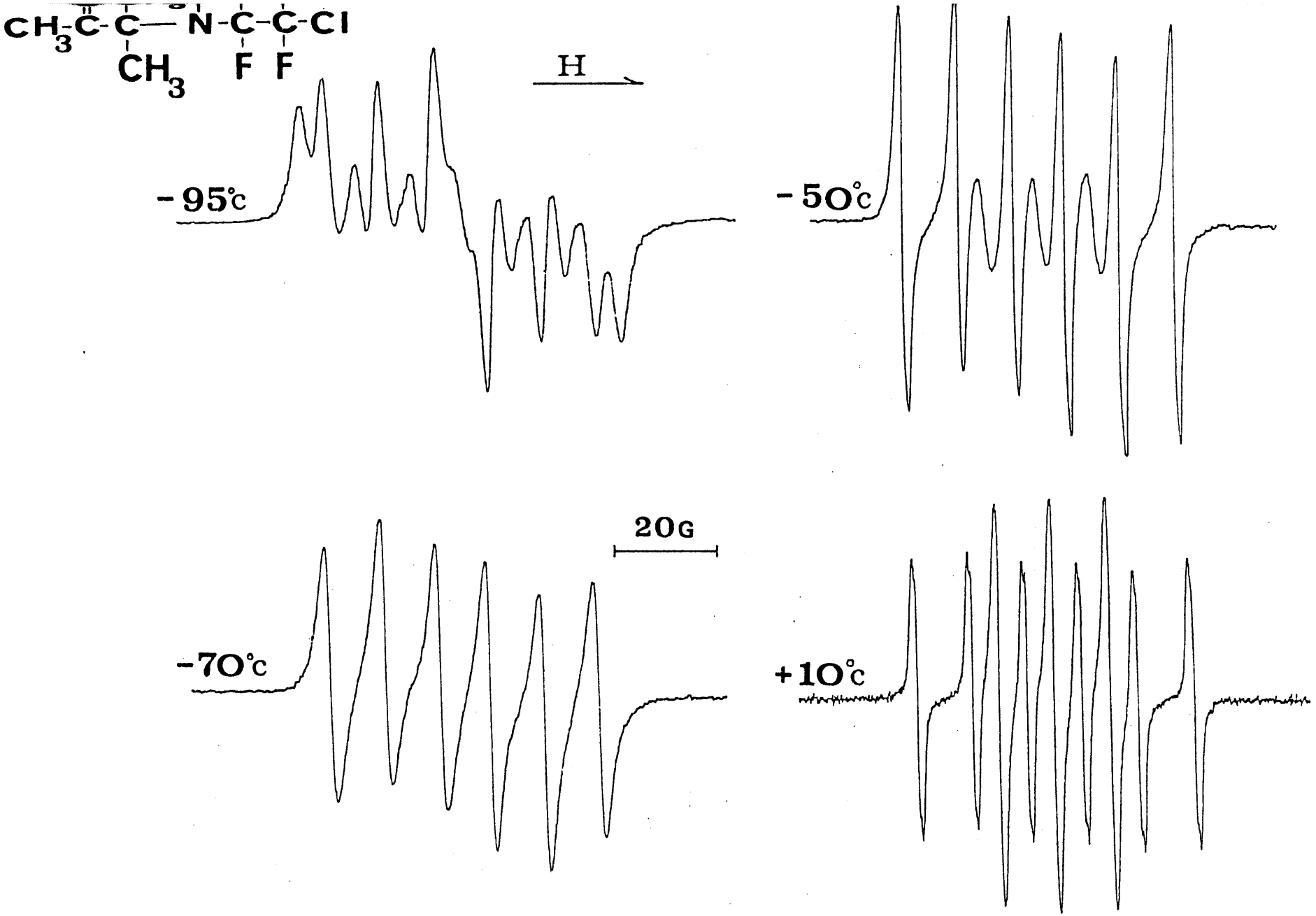

Fig.7

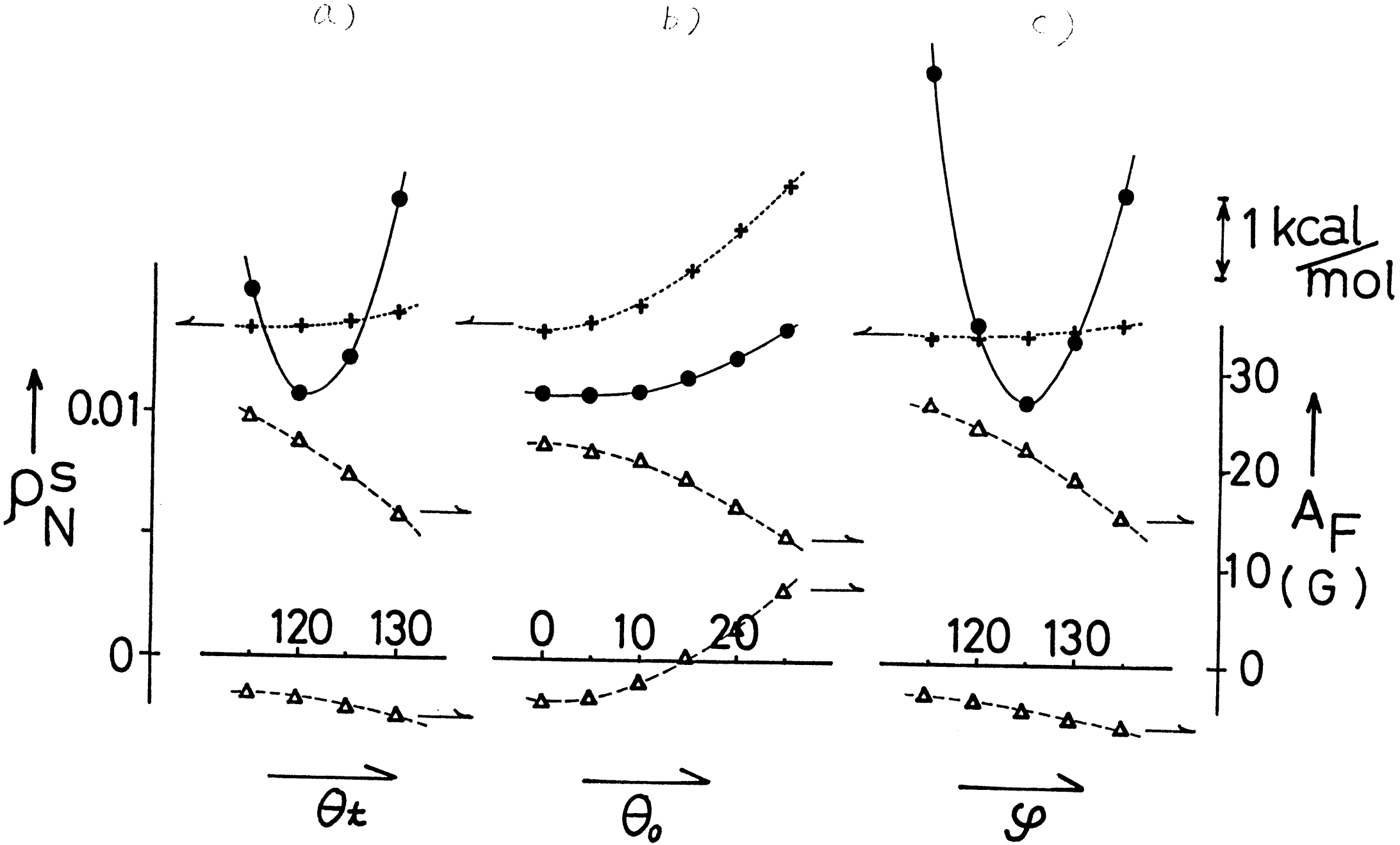
a)
b)
c)
1 kcal/mol
ρ_N^S
0.01
0
120 130
0 10 20
120 130
30
20
10
0
A_F (G)
θ_t
θ_0
φ

Fig.8 (a),(b) and (c)

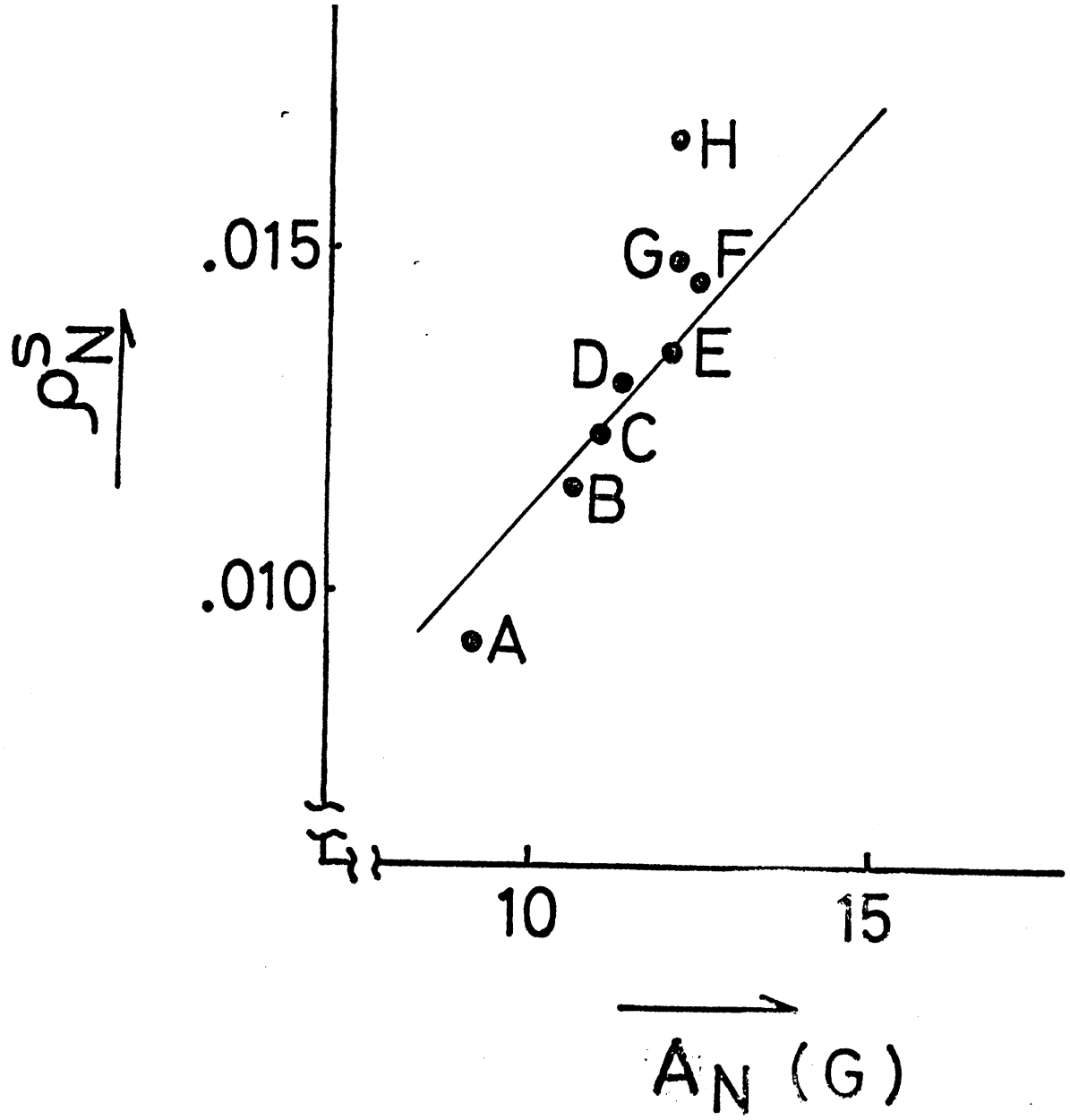

Fig.9

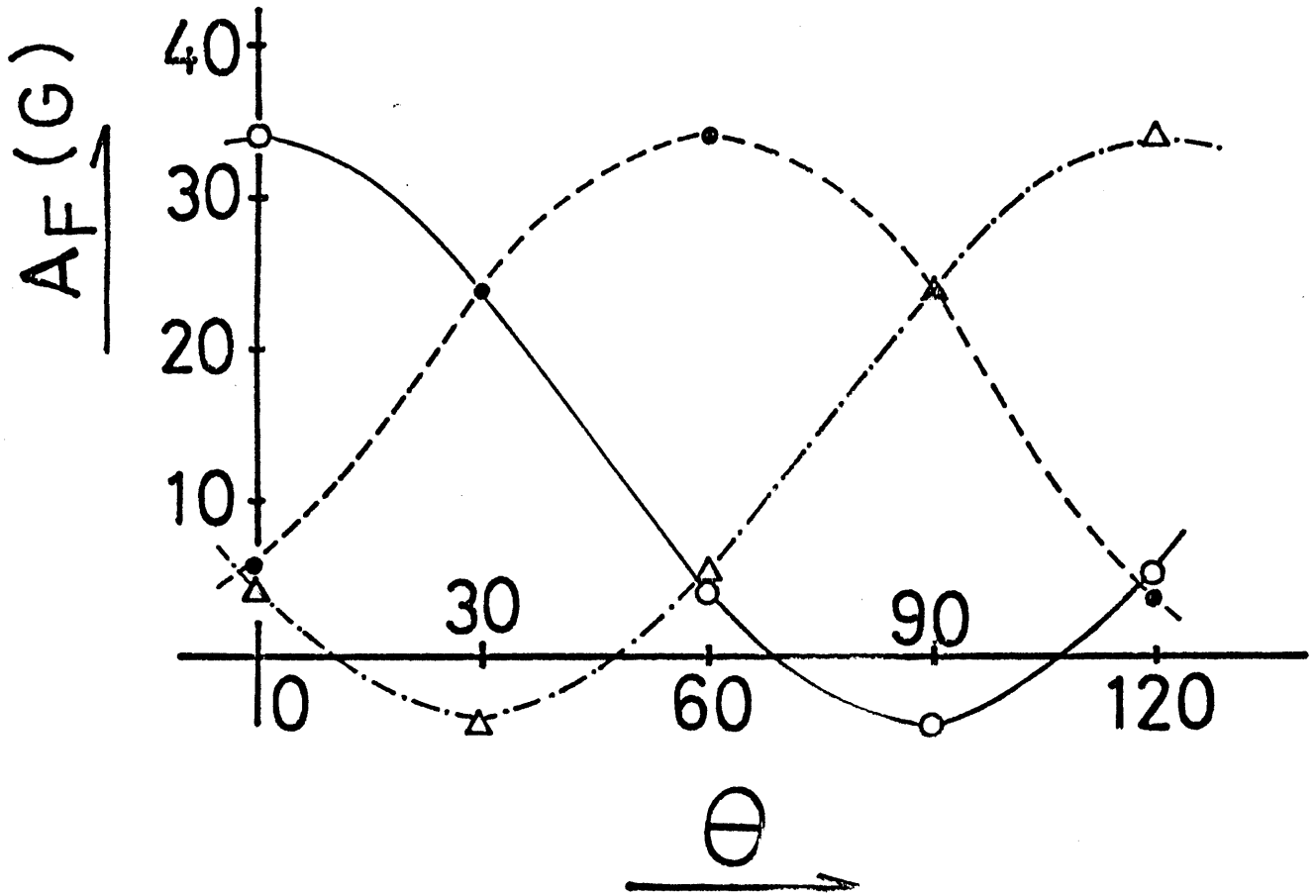

Fig.10

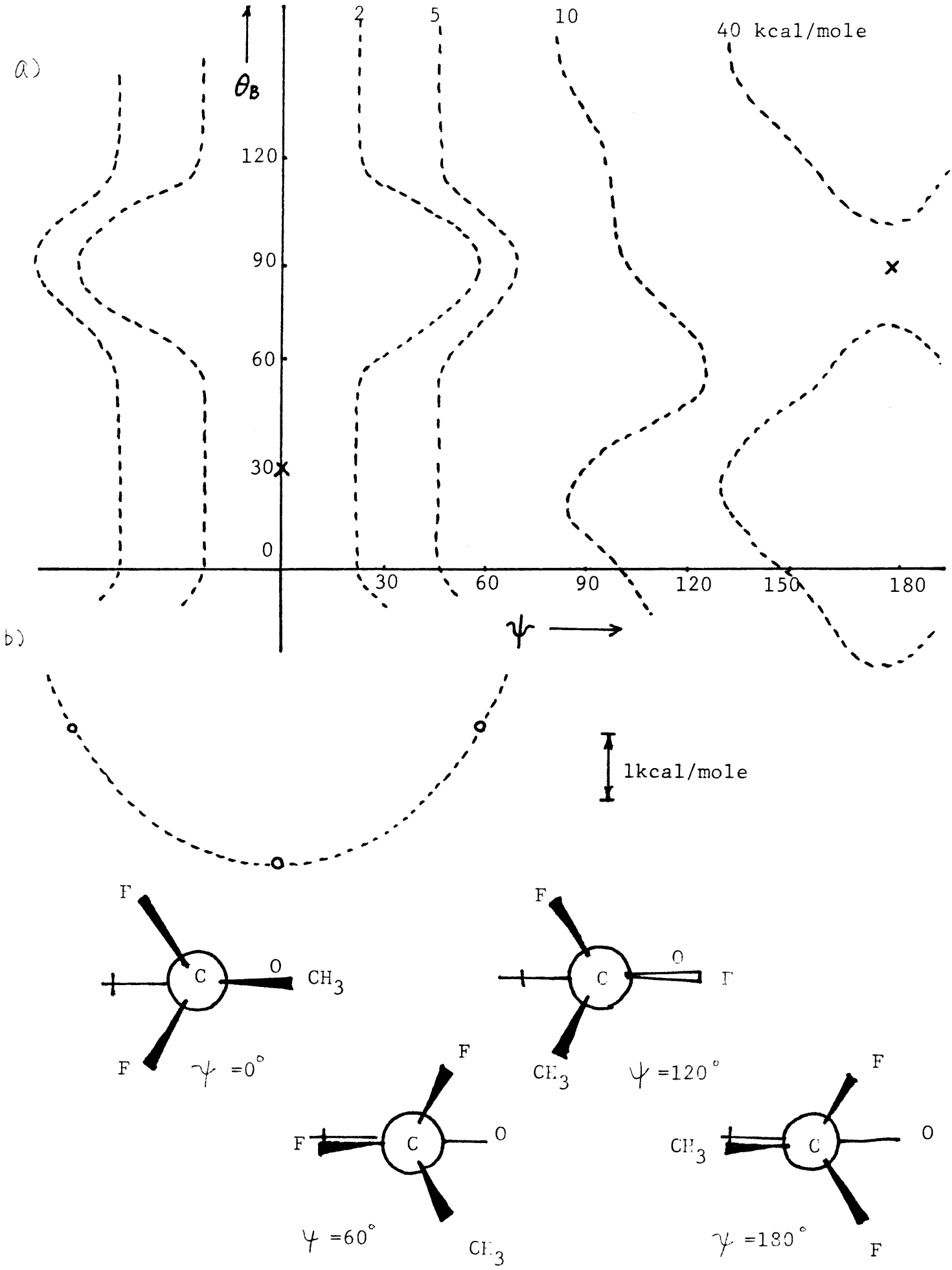

Fig.11 (a),(b) and (c)

Fig. 12

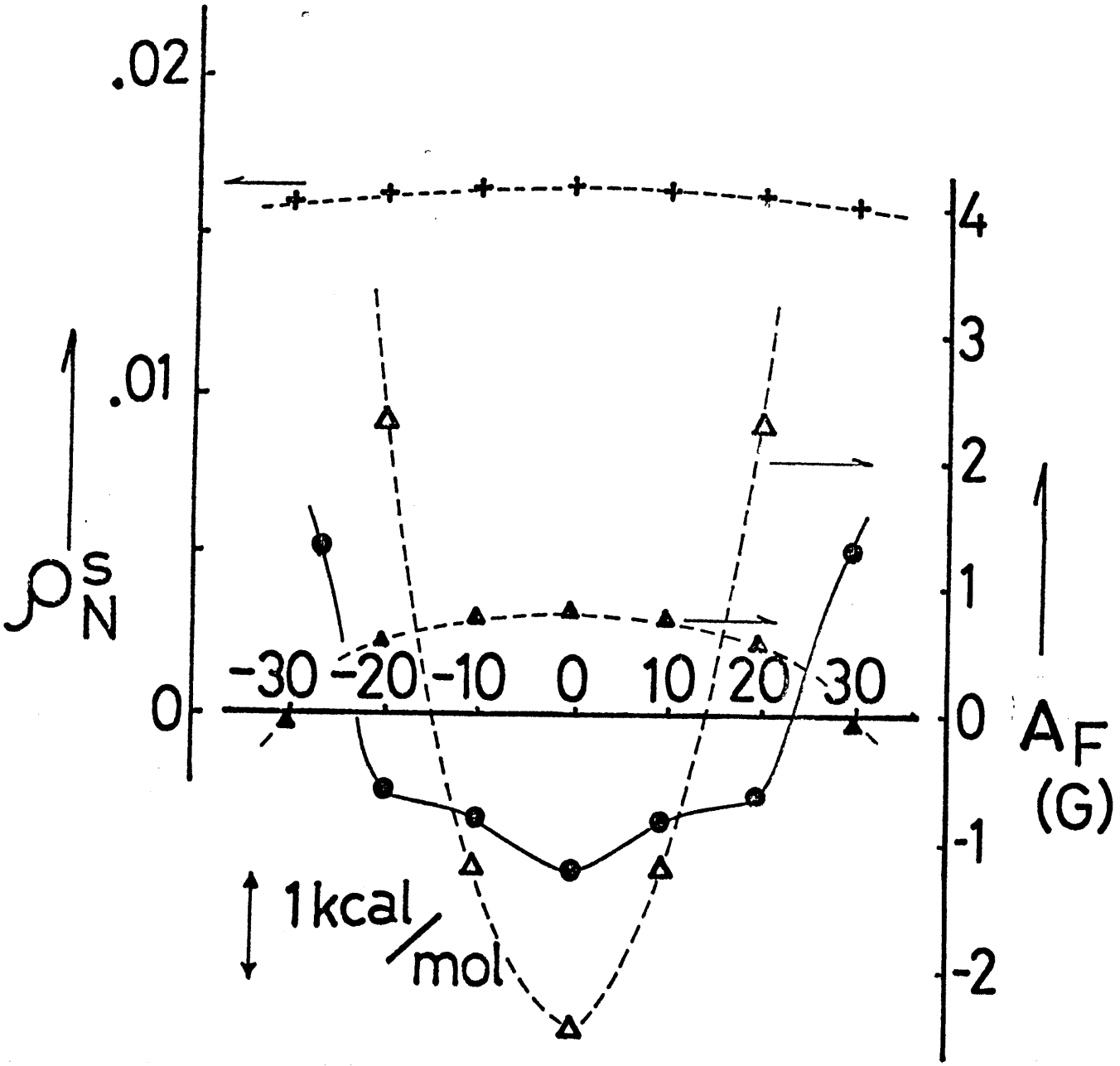

a)

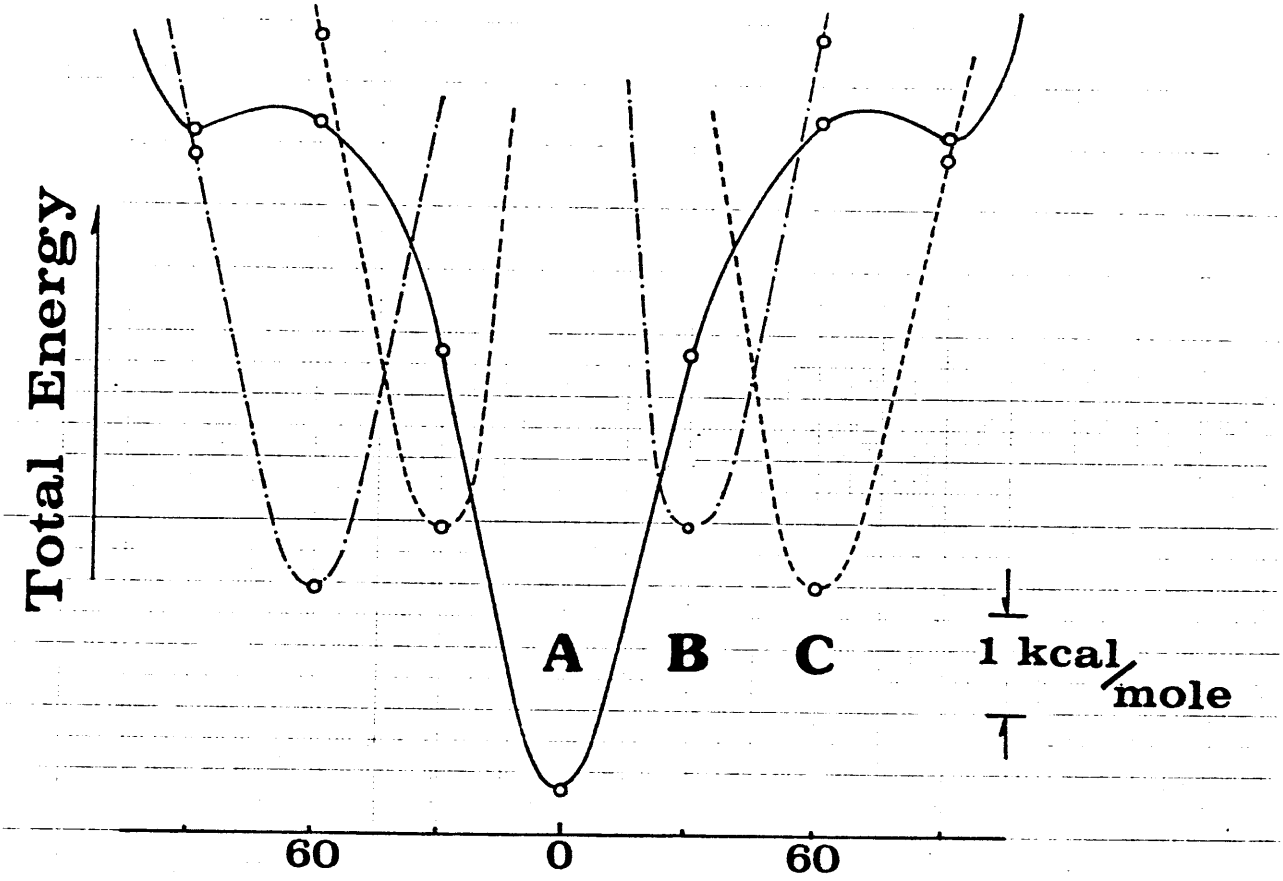
Total Energy
A
B
C
1 kcal/mole
60
0
60

b)

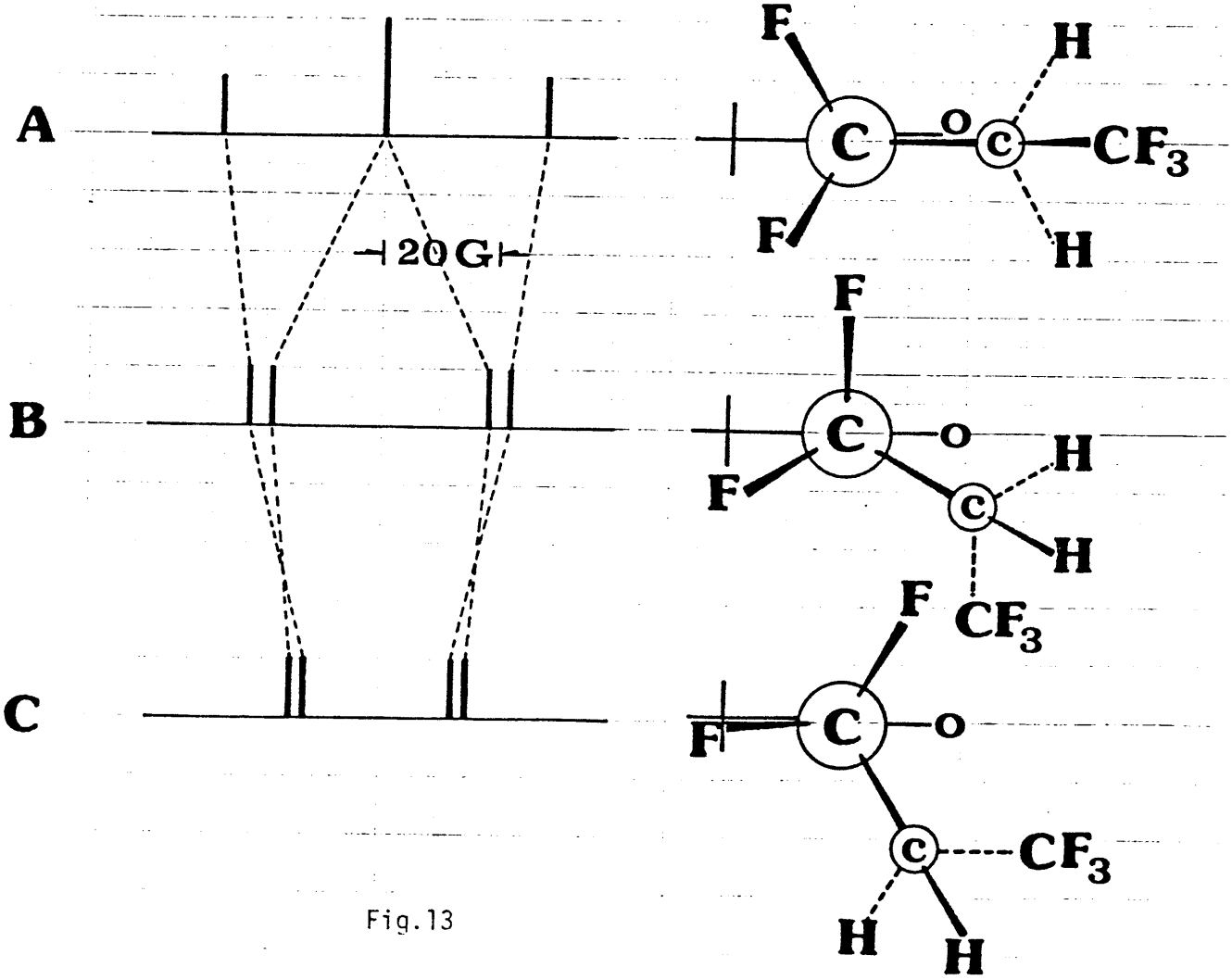
A
B
C
20G
F
H
C
O
C
CF3
F
H
F
C
O
F
H
C
H
F
CF3
C
O
F
C
CF3
H
H

Fig.13

Chapter 4.
Spatial Distribution of Radicals Produced by Fast Neutron Irradiation

Abstract

The linear energy transfer (LET) of ∿0.5 MeV fast neutron in organic compounds is known to be more than 100 times larger than that of Co-60 γ-ray. The local concentration of radicals produced by irradiation with two different kinds of radiation have been evaluated.

Microwave power saturation of electron spin resonance(esr) spectra of radicals formed by fast neutron irradiation in a fast neutron source reactor " YAYOI " at 77K has been measured.

Although esr spectra of irradiated cyclohexane, polymethylmethacrylate and polyethylene show no large difference between neutron and γ-irradiations, power saturations of the esr spectra for the two irradiations are very different. From the saturation characteristics, the spin-spin relaxation time in fast neutron irradiated samples was evaluated to be 3 ∿ 7 times smaller than that of γ-irradiation.

In other words, the local concentration of radicals formed by fast-neutron irradiation is 3 ∿ 7 times higher than that formed by γ-irradiation.

The spatial distributions are discussed in connection with LET of the radiations and structures of spurs in the matrix.

Introduction

Studies on the effects of fast-neutron irradiation of organic materials become more important as the number of nuclear reactors, fusion reactors and other nuclear facilities increases. It is also important to investigate the biological effects of neutron irradiation. However, there are few reports which discuss the effects of linear energy transfer (LET) on the spatial distributions of the radicals produced with different kinds of radiation as determined by esr spectroscopy.

The relaxation times (T_1, T_2) of radicals produced by γ-irradiation in several polymers and their temperature dependences were reported by Yoshida et al[1]. They used only γ-irradiation. Henriksen et al[2] irradiated amino acids and proteins with several types of heavy ion beam and measured their esr spectra, and discussed their results in terms of " thermal spike theory. " They concluded that the thermal spike model for the formation of secondary radicals is not applicable to the radicals produced. Kevan et al[3] irradiated PMMA (polymethylmethacrylate) with γ-rays and 2 MeV protons, and compared the esr spectra and their microwave power saturations for γ and proton irradiations. It was concluded that the local concentration of the radicals produced by proton irradiation is at least 5.9 times higher than produced by γ-irradiation.

Recently, Tabata et al[4,5] investigated the paired radicals produced in *n*-eicosane single crystal by several types of heavy ion irradiation.

The nuclear reactor " YAYOI " at Nuclear Engineering Research Laboratory, University of Tokyo is characterized by a very high fraction of fast neutron flux in the core. The peak of $E\phi(E)$ is $\sim$0.5 MeV, where E and $\phi(E)$ are energy and the flux distribution of neutrons, respectively. Samples of cyclohexane, polymethymethacrylate (PMMA) and polyethylene (PE)

were irradiated in the reactor " YAYOI " at 77K in the present work. The microwave power saturation behavior of radicals trapped in these samples was measured by means of esr spectroscopy and the spatial distribution of radicals produced by the fast-neutron irradiation is discussed in comparison with the radicals produced by γ-irradiation with Co-60 under the same conditions.

Experimental

The details of the fast neutron source reactor " YAYOI " is reported elsewhere[6]. The irradiation system is shown in Fig. 1[7]. The continuous flow type cryostat for irradiation was introduced from the top of the reactor through the shield. The samples in the sample chamber of the cryostat were put at the core centre of the reactor. The cryostat is a simple and convenient one which is capable of providing a wide range of temperature from liquid helium (4K) to room temperature (300K). In our experiment, the irradiations were carried out at $\sim$77K.

The reactor was operated at a power of 500 W for 2.5 hours. The sample chamber was filled with liquid nitrogen and could be pulled out keeping the liquid nitrogen temperature after irradiation. The dose-rate due to fast neutron irradiation was estimated to be 1.05 Mrad/KWh and that due to γ-ray to be 0.08 Mrad/KWh for polyethylene in the reactor[8]. Therefore, the main contribution to the irradiation dose is that caused by fast neutrons.

Cyclohexane was obtained from Tokyo Kasei Co. Ltd. PMMA and PE were washed with xylene and dried. The samples in tubes made of fused silica were evacuated by a vacuum line. By using high purity fused silica, activation of the sample tubes by neutrons could be kept at low level. Cyclohexane was chosen as one of the samples, because virtually only one kind of radical, cyclohexyl radical ($\cdot C_6H_{11}$), is produced by γ-irradiation.

It was found that cyclohexyl radical is also produced in cyclohexane by neutron irradiation. The γ-irradiation was carried out with a Co-60 source at 77K at a dose rate of 0.4 Mrad/hr and a total dose of 1 Mrad was always used. The esr spectra of the samples irradiated by two kinds of radiation were obtained with a Varian E 109 EPR system at the Research Centre for Nuclear Science and Technology, University of Tokyo. The system contains a rectangular cavity (TE 102) with a quartz dewar for liquid nitrogen temperature experiment. The microwave magnetic field, H_1, is estimated by the relation reported by Poole.[9]

The yield of radicals produced in the sample was obtained by using a benzene solution of known concentration of DPPH as the standard.

Result

In order to examine the microwave power saturation, it is important to avoid the rapid passage condition. Therefore, the field modulation frequency must be chosen carefully by comparing among spectra obtained with different modulation frequencies. The frequencies used were 100 KHz, 1 KHz and 270 Hz. It was found that the esr spectra obtained were the same at lower microwave power. The power saturation behavior of electron spin resonance spectra for fast neutron irradiated cyclohexane at 77K was followed by plotting the maximum intensity of the absorption spectra as a function of power. The results are shown in Fig. 2. The power saturations obtained with 270 Hz and 1 KHz modulations are different from that with 100 KHz modulation. Since the spin-lattice relaxation times in irradiated samples were obtained to be of the order of 10 μsec in the present experiment, it was clearly seen that 100 KHz modulation is not applicable to the power saturation experiment. However, by using lower modulation frequencies, S/N ratio of the signal become worse. Considering both the relaxation times

and noise level of signals, 1 KHz modulation was finally chosen. This choice is reasonable with respect to the relaxation times of radicals.

The radicals produced by both fast neutron and Co-60 γ-irradiations showed similar esr spectra and the concentrations caused by $\sim$1 Mrad irradiation were found to be $10^{16} \sim 10^{17}$ spins/g by comparing with the DPPH standard sample. When higher concentration of radicals are produced, overlapping of spurs will become significant and exchange narrowing will be observed as reported in heavy ion irradiations.[3),5)] So, total radical concentrations were kept to be lower than one usually reported. The radical produced in cyclohexane is the cyclohexyl radical as shown in Fig. 3(a). The couplings of the cyclohexyl radical are 21G, and 5G and 40G for one A_{α}^{H} and two A_{β}^{H} due to two kinds of two equivalent protons, respectively. The spectra obtained were composed of $2\times3\times3=18$ lines. From the computer simulation it was found that the Gaussian distribution having $\sim$8G for line width (ΔH)[(10)] is the best fit to the observed spectra at the lowest microwave power condition (0.01 mW) as indicated in Figs. 3(b) and (c). In the case of PE as shown in Fig. 3(d), the alkyl type radicals were dominant and the line width was estimated to be $\sim$11G from the simulation. The couplings of alkyl radicals are 22.4G and 33.1G for one A_{H}^{α} and four equivalent A_{H}^{β}.[(11)]

In irradiated PMMA, esr spectra (Fig. 3(e)) of the radicals produced were the same as reported by Kevan.[(3)] The line width for the best fit to the experimental results was found to be $\sim$6G.

The esr spectra of the radicals produced by two kinds of radiation were very similar to each other, from the points of couplings and linewidths. However, the behaviors of microwave power saturation are different. The changes in the signal intensity at the maximum point of the absorption spectra as a function of microwave power saturation are different. The changes in the signal intensity at the maximum point of the absorption

spectra as a function of microwave power are shown in Fig. 4. Intensities of a particular peak shown in Fig. 3 as ↑ in the first derivatives of the absorption signals are also shown in Fig. 4. The first derivatives of the esr absorption spectra are normally directly obtained in esr measurement. The intensity of the derivative is thought to be one of the parameters for saturation measurement. However, the degree of saturation from the derivatives seems to be enhanced. Another parameter for saturation is total area of the absorption spectrum. This parameter changes almost in the same way as the change of the maximum intensity of the absorption spactra. Finally, the changes in the signal intensity at the maximum point of the absorption spectra as a function of microwave power were used for evaluation of the degree of microwave saturation.

Discussion

The phenomenon of microwave power saturation is characterized by two relaxation times, T_1(spin-lattice) and T_2(spin-spin). If the all spins stay under the same environmental condition, and energy absorbed from the magnetic field is transferred to all spins, the system is called " Homogeneous ". However, such a condition is usually not satisfied for radicals produced by irradiation, because a certain number of spins form a small group called spin packet. In such case, it is considered that each spin packet forms a homogeneous system. Ensembles of spin packets are not homogeneous and form an " inhomogeneous " system. Therefore, the absorption spectrum is expressed by an envelope of many overlapping spin packets, as shown in Fig. 5(a).

Portis[12] extended the saturation theory to inhomogeneous system, and Castner[13] obtained T_1, T_2 of the V center in irradiated alkali-halides using Portis' theory. The lineshape of individual spin packets

is assumed to be Lorentzian, and the distribution of spin packets to be Gaussian. The normalized distributions are written as

$$g(H-H') = \frac{T_2}{\pi} \frac{1}{1+T_2^2(H-H')^2} \tag{1}$$

$$h(H'-H_o) = \frac{1}{\pi^{\frac{1}{2}}} \frac{1}{\Delta H_G} \exp[-(\frac{H'-H_o}{\Delta H_G})^2] \tag{2}$$

where ΔH_G is the Gaussian line width[10] of the inhomogeneous broadening. T_2 of the homogeneous Lorentzian line is obtained from the relation, $\gamma \Delta H_L \cdot T_2 = 1$, where ΔH_L is the line width for half maximum of g(H) for each spin packet. Using the parameter $\underline{a}$ which indicates the degree of inhomogeneous broadening, namely the ratio $\Delta H_L / \Delta H_G$ of the Lorentzian spin packet width to the inhomogeneous Gaussian width, the absorption signal V_R is expressed as follows,

$$V_R = \frac{X}{(1+X^2)^{\frac{1}{2}}} \exp(a^2X^2) \frac{\{1-\Phi(a(1+X^2)^{\frac{1}{2}}\}}{[1-\Phi(a)]} \tag{3}$$

$$X = \gamma H_1 (T_1 \cdot T_2)^{\frac{1}{2}} \tag{4}$$

where $\Phi(aX)$ is the error function.

From eq. (3) the intensity of the absorpiton signal V_R as a function of the reduced microwave field $X=H_1/H_{\frac{1}{2}}$, where $H_{\frac{1}{2}}=\gamma^{-1}(T_1, T_2)^{\frac{1}{2}}$, is calculated and shown in Fig. 5(b). Considering the relation, $H_1 \propto P^{\frac{1}{2}}$, X is Fig. 5(b) is proportional to the square root of the microwave power. The comparison of the experimental results (Fig. 4) with the theoretical curve (Fig. 5(b)) gives the value of $\underline{a}$. Since $\underline{a}$ is the ratio $\Delta H_L / \Delta H_G = \Delta H_L / \sqrt{2} \Delta H$[10], ΔH_G obtained from the simulation of absorption at the lowest microwave power condition without any saturation effect gives the value of ΔH_L and consequently T_2.

The intersection of the line having a slope 1 before saturation with the horizontal line drawn from the point having maximum intensity of saturation curve gives the point A shown in Fig. 5(b). The magnetic field strength at A is H_2^1. If $\underline{a}$ is not very small, $H_{\frac{1}{2}}$ is nearly equal to H_1' which satisfies the equation, $\gamma H_1' = (T_1 \cdot T_2)^{\frac{1}{2}}$ from which T_1 is obtained. This method will be called the " A point method ". From another method we will call the " T_2^* method ",[13] T_1 is obtained independently. From both theoretical consideration and experimental results, the values of $\underline{a}$, T_1 and T_2 were obtained and summarized in Table I.

In the present experiment, an external field modulation of 1 KHz was chosen, as already mentioned. It is easily seen that the 100 KHz modulation usually used is a rather high frequency for the saturation experiment, because the spin-lattice relaxation time (T_1) obtained for PE is a few tens microsecond. Therefore, the field modulation frequency of 1 KHz seems to be very reasonable. The relaxation times obtained are much shorter than the period of the chosen field frequency.

The value of linear energy transfer (LET) of the two types of radiation used, Co-60 and fast-neutron, have been calculated before.[14] The values are summarized in Table II. The value of LET for fast neutron having an energy of $\sim$0.5 MeV is 6$\sim$7 eV/Å and this value is more than 200 times larger than that of Co-60 γ-radiation. Although the above values are for water, they are assumed to be applicable to hydrocarbon system. The effect of fast neutron irradiation is thought to be similar to that of proton irradiation, because neutron-irradiation effects can be explained mainly by the knock-on protons produced by the collision of neutrons in hydrocarbon system. Neutrons have no charge and penetrate materials rather freely. However, the proton itself has a positive charge and penetrates only the surface of materials. Therefore, by irradiation with a rather

low energy proton beam, the radicals produced are localized only at the surface of the sample. Using a 2 MeV proton, the penetration range of the beam is ∿9 μm in water and overlapping of the spurs or tracks should become important.(3)

Since the irradiation effect of fast neutrons can be explained mainly based on the protons ejected internally in the matrix, the distribution of produced radicals is rather homogeneous in contrast with proton irradiation. From the consideration of the penetration range of the particles, the distributions of radicals produced in the matrix by fast-neutron and proton irradiation on a macro-scale are thought to be different.
In spite of the large difference in LET, the values of T_1 show no drastic difference between Co-60 and neutron irradiation in each sample.
This result is similar to that reported by Kevan(3) between γ and proton irradiations. He assumed a priori that T_1 is the same between γ and proton irradiated samples. Although we did not use above assumption, the values of T_1 are obtained to be almost the same between γ and neutron irradiations.

If the same type of radical is produced by two different radiation, the spin-lattice relaxation time (T_1) is assumed to be the same. Because the spin-lattice relaxation time is determined by the interaction between the radical and the surrounding lattice, it is independent of the spatial distribution of radicals.

On the other hand, the spin-spin relaxation time (T_2) is dependent on the distribution of radicals and a higher local concentration of radicals should give a smaller T_2 value. If T_2 is assumed to be mainly due to the dipole-dipole interaction, the ratio of the values of T_2^{-1} indicates the ratio of local concentration of radicals produced. The local concentration ratio of radicals produced by two kinds of radiation is also shown in Table I. The ratios are in the range of 3∿7. These values are thought to be

underestimated because diffusion of radicals may occur to some extent even at 77K and recombination reactions occur between nearest neighbor radicals. Therefore, the distribution of the remaining radicals observed should be less condensed than the true distribution during or immediately after the irradiation. These concentration ratios should be closely related to the characteristics of the sample matrices, because diffusion and trapping efficiency of radicals are thought to be strongly dependent on the matrices. However, this effect may not be evaluated at present. Comparative experiments at 77K and 4K irradiations will give more information. In spite of the large difference in LET, no drastic difference of local concentration between two types of irradiation can be interpreted as follows. Track structure by two different radiations is shown schematically in Fig. 6. γ radiation deposits energy by releasing Compton scattered electrons. The tracks of the latter contain widely spaced ' spurs ' each containing a few radicals in an approximately spherical space of radius a few nm. The radicals are not spread out homogeneously. For proton and neutron irradiation, the spurs are close together. The increase in local concentration is a measure of the extent of spur overlap, and is not directly related to the ratio of LET values. The obtained local concentration is assummed to be that of the regions A and B in Fig. 6. Therefore, the ratio of LET is not the same of that of local concentions in each sample.

The separation of radicals is easily estimated, assuming that the T_2 is determined by the interaction of the dipole-dipole (spin-spin), $E \approx \mu_1\mu_2/r_{12}^3$, where E is the energy of the interaction, μ_1 and μ_2 are the magnetic moments of spin 1 and spin 2, respectively, and r_{12} is the separation of these two spins. If we assume only a pair of two radicals, r_{12} can be calculated from the values of T_2 and the results are also shown in Table I. Of course, the separation of radicals produced by fast-neutron irradiation

is smaller than that by γ-irradiation.

At present, the number of spins (radicals) in one spin packet or each spur is not clear. However, the experiments using single crystals as samples at lower temperature as 4K will give more precise information about LET.

References and Notes.

[1] H. Yoshida, K. Hayashi and S. Okamura; ARKIV FOR KEMI 23 177 (1964)

[2] T. Henriksen, P.K. Horan and W. Snipes; Rad. Res. 43 1 (1970)

[3] W. Kaul and L. Kevan; Proceedings of Third Tihany Symposium on Radiation Chemistry. (1971)

[4] K. Hamanoue, V. Kamantauskas, Y. Tabata and J. Silverman; J. Chem. Phys. 61 3439 (1974)

[5] K. Kimura, M. Ogawa, M. Matsui, T. Karasawa, M. Imamura, Y. Tabata, and K. Oshima; J. Chem. Phys. 63 1979 (1975)

[6] S. An, T. Tamura, A. Furuhashi and H. Wakabayashi; Proceedings of the International Symposium on the Physics of Fast Reactors 1 152 IAEA, Vienna (1973)

[7] H. Yanagi, T. Tamura and Y. Tabata; J. Fac. Eng. of Tokyo 34 639 (1978)

[8] S. Egusa, K. Ishigure, S. Tagawa, Y. Tabata and K. Oshima; Rad. Phys. Chem. 11 129 (1978)

[9] C.P. Poole; " Electron Spin Resonance, A comprehensive Treatise on Experimental Techniques " Interscience Publishers (1967)

[10] The Gaussian shape is expressed as follows

$$g(H) = \frac{1}{\Delta H\sqrt{2\pi}} \exp\left[-\{(H-H_{av})^2/2(\Delta H)^2\}\right]$$

where ΔH and H_{av} are the line width and the center of the resonance line, respectively.

This expression is transformed to eq. (2) using the relation $\Delta\omega_G = \sqrt{2}\,\gamma\Delta H$, where γ is gyromagnetic constant (1.76×10^7 $G^{-1}\cdot sec^{-1}$).

[11] A.G. Kiselev, M.A. Mokulsky, Yu.S. Lazurkin; Vysokomol, Soedin. 2 1978 (1960)

[12] A.M. Portis; Phys. Rev. 91 1071 (1953)

[13] T.G. Castner, Jr; Phys. Rev. 115 1506 (1959)

[14] H.H. Rossi in; " Radiation Dosimetry " vol.1 p43 Ed. by F.H. Attix and W.C. Roesh, Academic Press (1968) London.

Figure Caption

Fig. 1 Scematic diagram of irradiation facility. The cryostat is placed in the Grazing Hole of the reactor " YAYOI ". Liquid nitrogen is transferred by the transfer tube to the Cu block below the sample chamber. The samples are cooled down to 77 K by operating an Exhaust Pump. The temperature of the samples are monitred by thermocouples and the control of the sample temperature is made in the Preparation Room under the operation of the reactor.

Fig. 2 The changes of the peak intensity of the absorption signal as a function of the microwave power with three different field modulation frequencies, ●; 100 KHz, o; 1 KHz, Δ; 270 Hz.

Fig. 3 Spectra of the first derivatives (a), the absorption (b) and the computer simulated (c) in fast neutron irradiated cyclohexane. Each absorption line is Gaussian one having ∿8G for line width (ΔH). The applied microwave power was 0.01 mW.

(d) Esr spectra of both fast neutron and γ-irradiated polyethylene samples obtained at 0.1 mW.

(e) Esr spectra of both fast neutron and γ-irradiated polymethylmethacrylate samples obtained at 0.1 mW.

Irradiation dose of all samples was set at about 1 Mrad.

Peak intensities indicating by an arrow in the first derivatives are shown in Fig. 4.

Fig. 4 Signal intensity as a function of microwave power. The intensity at the maximum peak of the absorption, the total area of the absorption and the peak intensity at the particular point indicated by an arrow in Fig. 3 are indicated as o, Δ and ●, respectively.

a) fast neutron and b) γ-irradiated cyclohexane.

c) fast neutron and d) γ-irradiated polymethylmethacrylate.

e) fast neutron and f) γ-irradiated polyethylene.

Fig. 5 a) Schematic structure of inhomogeneous system.

b) Intensity of the absorption signal V_r as a function of the reduced microwave field, $X=\gamma H_1(T_1\ T_2)^{\frac{1}{2}}$, calculated from the eq. (3) The value, $\alpha=0$, gives the complete inhomogeneous case.

Fig. 6 Schematical spur and track structure produced by fast neutron (a) and Co-60 γ-irradiation (b). It is noted that the scale of (a) is much larger than (b).

Table I. Obtained relaxation times (T_1, T_2), ratio of the local concentrations, and the separation of produced radicals.

sample	radiation	T_2 (μsec)	A point method		T_2*method	Local concentration ratio	r_{12} (Å)
			$T_1 T_2$ (sec^2)	T_1 (μsec)	T_1 (μsec)		
cyclohexane (C_6H_{12})	fast neutron	0.05	5.6×10^{-13}	11	8.6	3.4	20
	Co 60-γ	0.17	1.7×10^{-12}	10	12		30
Polymethyl-methacrylate (PMMA)	fast neutron	0.067	2.9×10^{-13}	4.3	2.5	6.7	22
	Co 60-γ	0.45	2.2×10^{-12}	4.9	7.5		42
	2MeV proton*	——	2.6×10^{-14}	——	——	≥5.9	—
	Co 60-γ*	——	4.4×10^{-12}	——	——		—
Polyethylene (PE)	fast neutron	0.0067	2.0×10^{-13}	30	4.9	3.3	10
	Co 60-γ	0.022	7.9×10^{-13}	36	8.8		15

* ; reported by Kevan et al from ref. (3)

Table II. The values of LET (linear energy transfer)

radiation	LET(eV/Å)	range
fast-neutron (0.5 MeV)	6 - 7*	——
Proton (2 MeV)	2.4	9 μm*
Co60-γ	0.024	——

* Data for water from ref. (13)

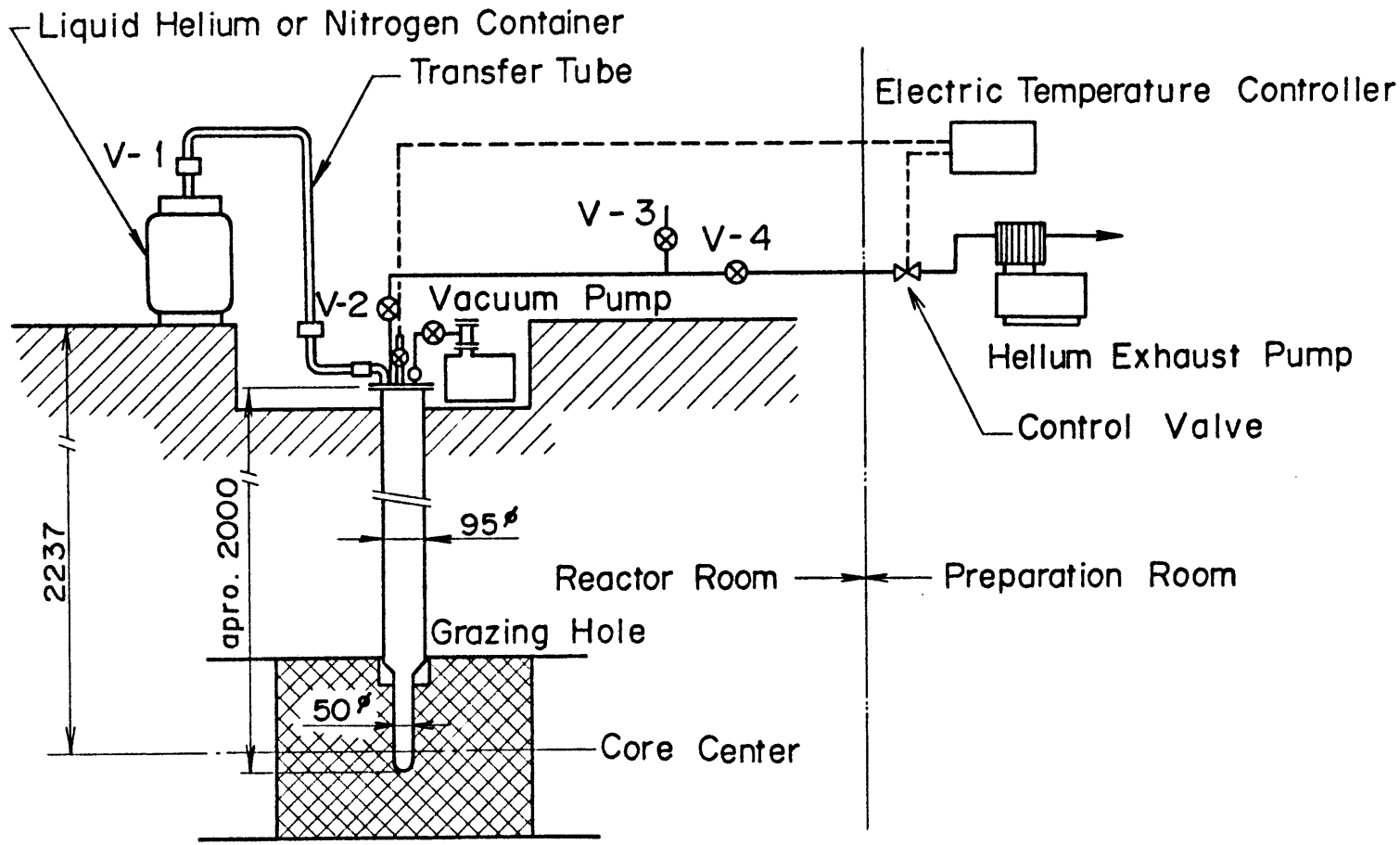
Liquid Helium or Nitrogen Container
Transfer Tube
Electric Temperature Controller
V-1
V-3
V-4
V-2
Vacuum Pump
Hellum Exhaust Pump
Control Valve
2237
apro. 2000
95ϕ
Reactor Room
Preparation Room
Grazing Hole
50ϕ
Core Center

Fig.1

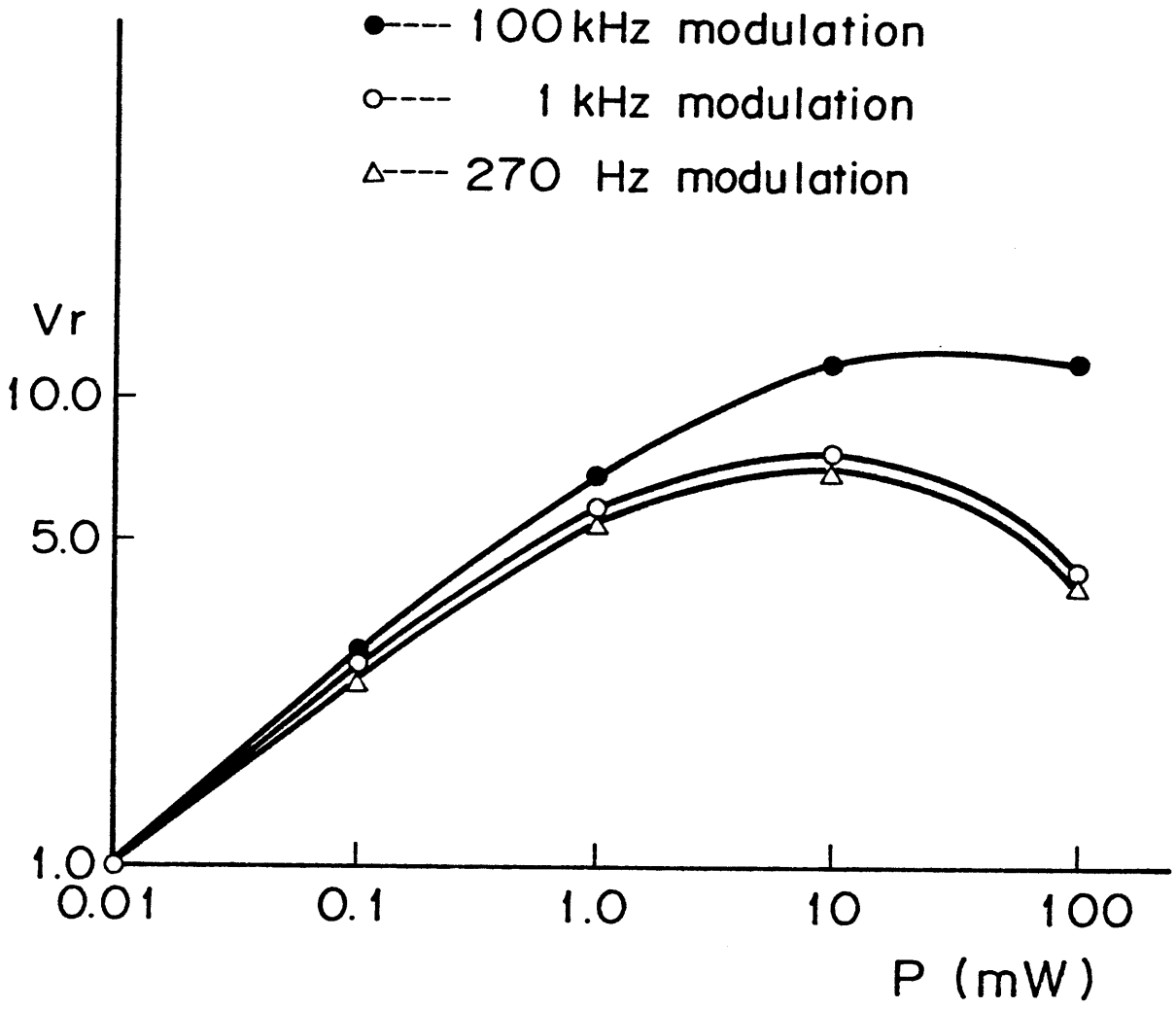
100 kHz modulation
1 kHz modulation
270 Hz modulation
Vr
10.0
5.0
1.0
0.01
0.1
1.0
10
100
P (mW)

Fig.2

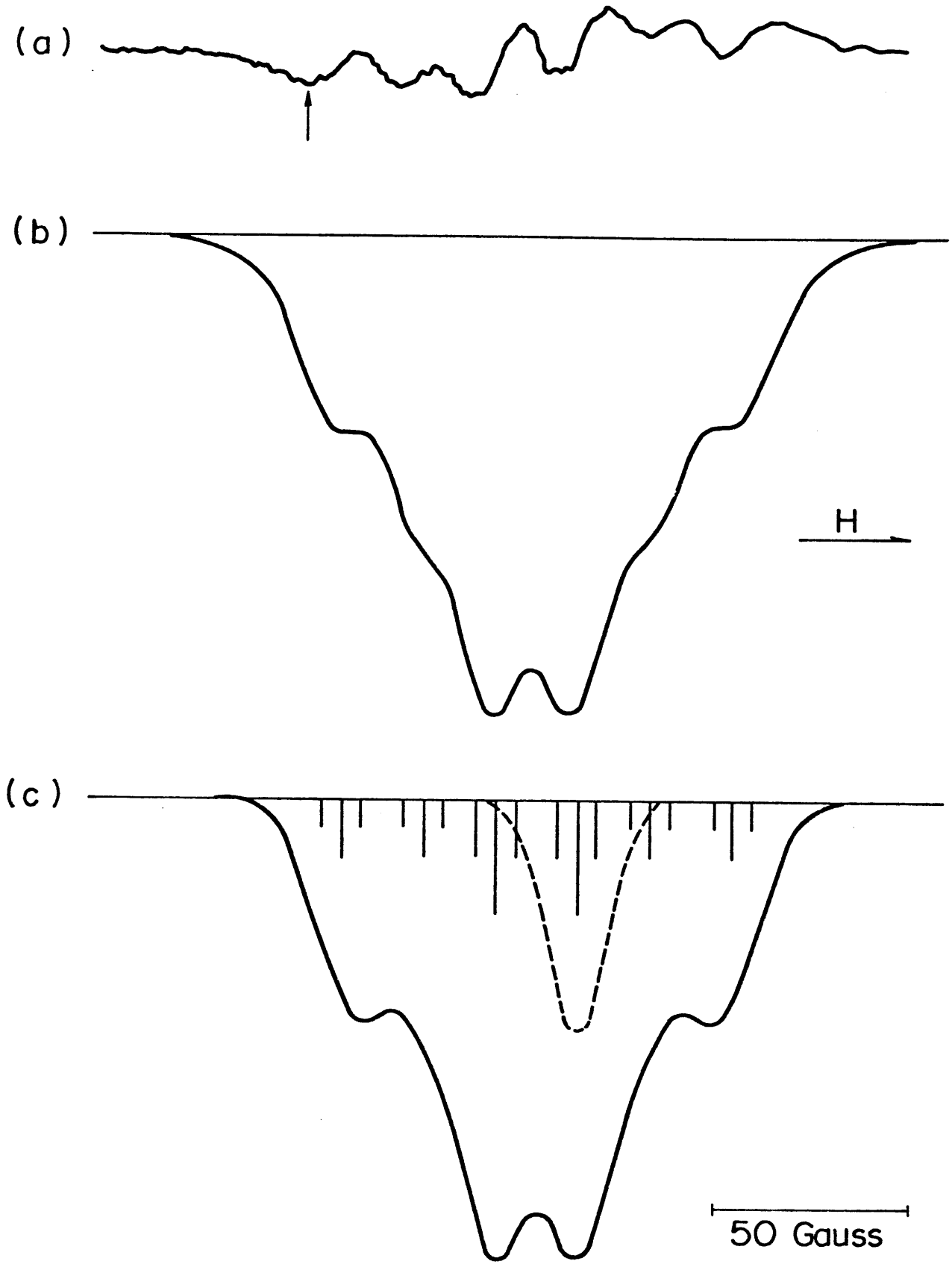

Fig.3 (a),(b) and (c)

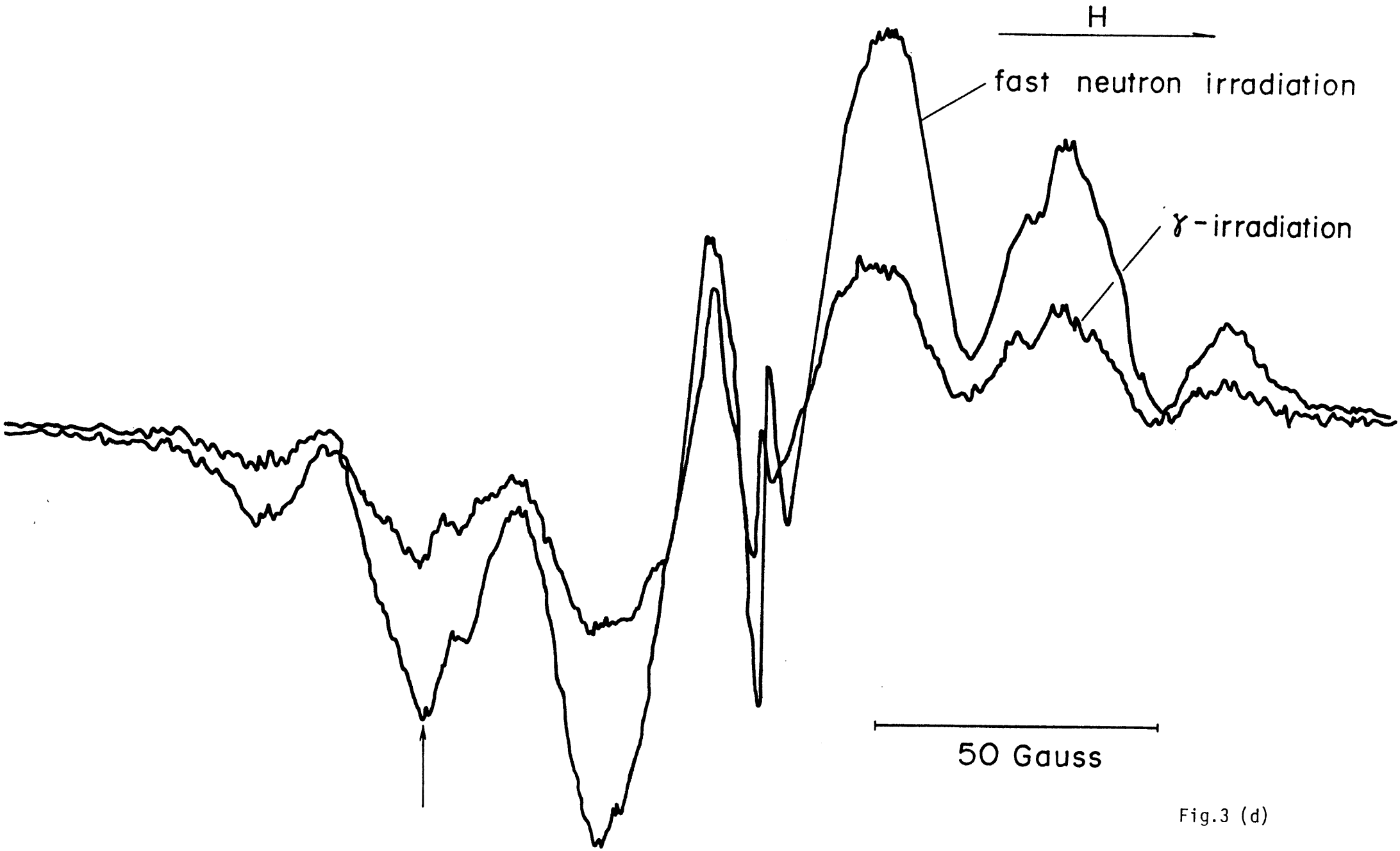

Fig.3 (d)

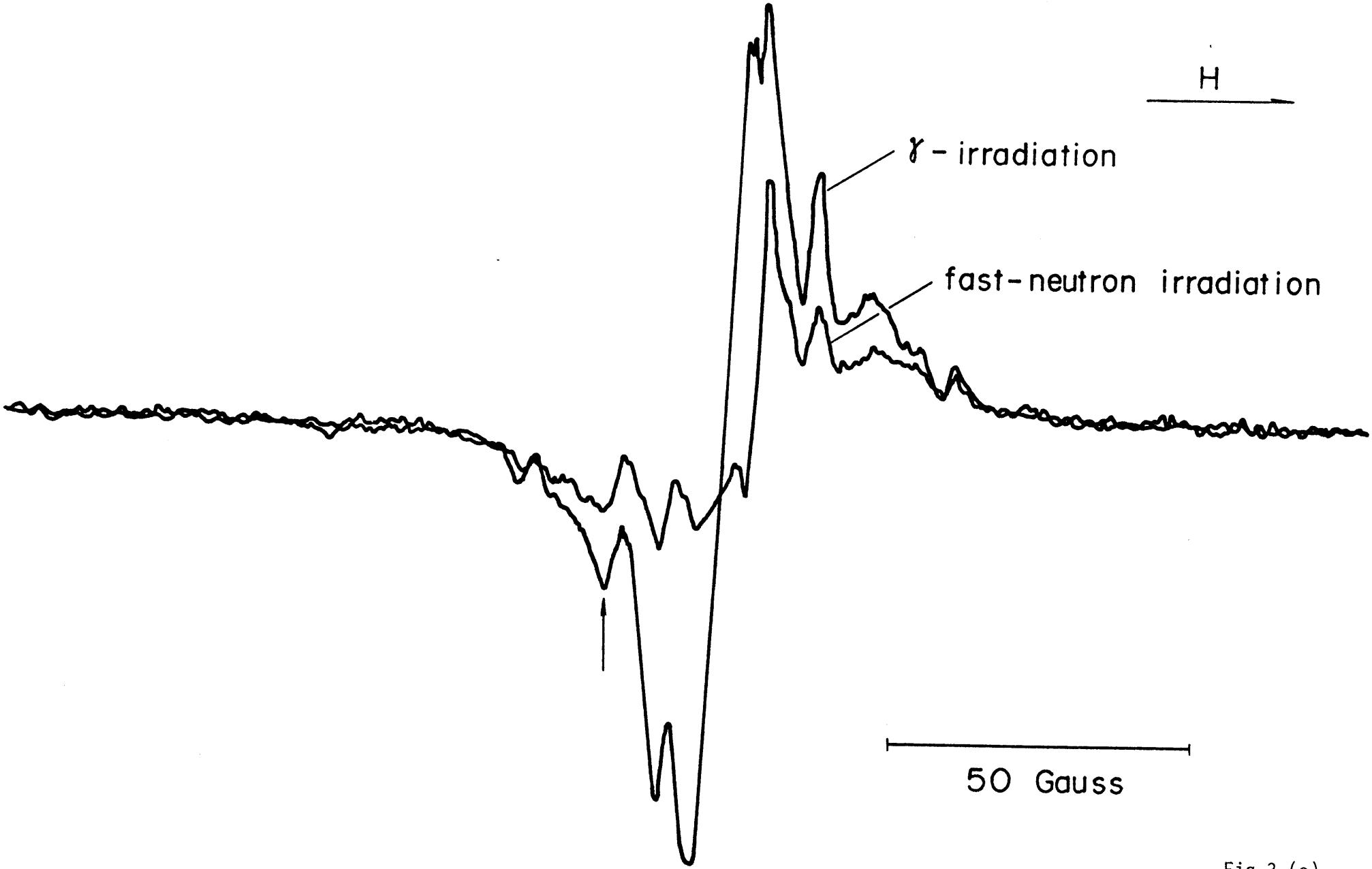

Fig.3 (e)

Fig.4 (a) and (b)

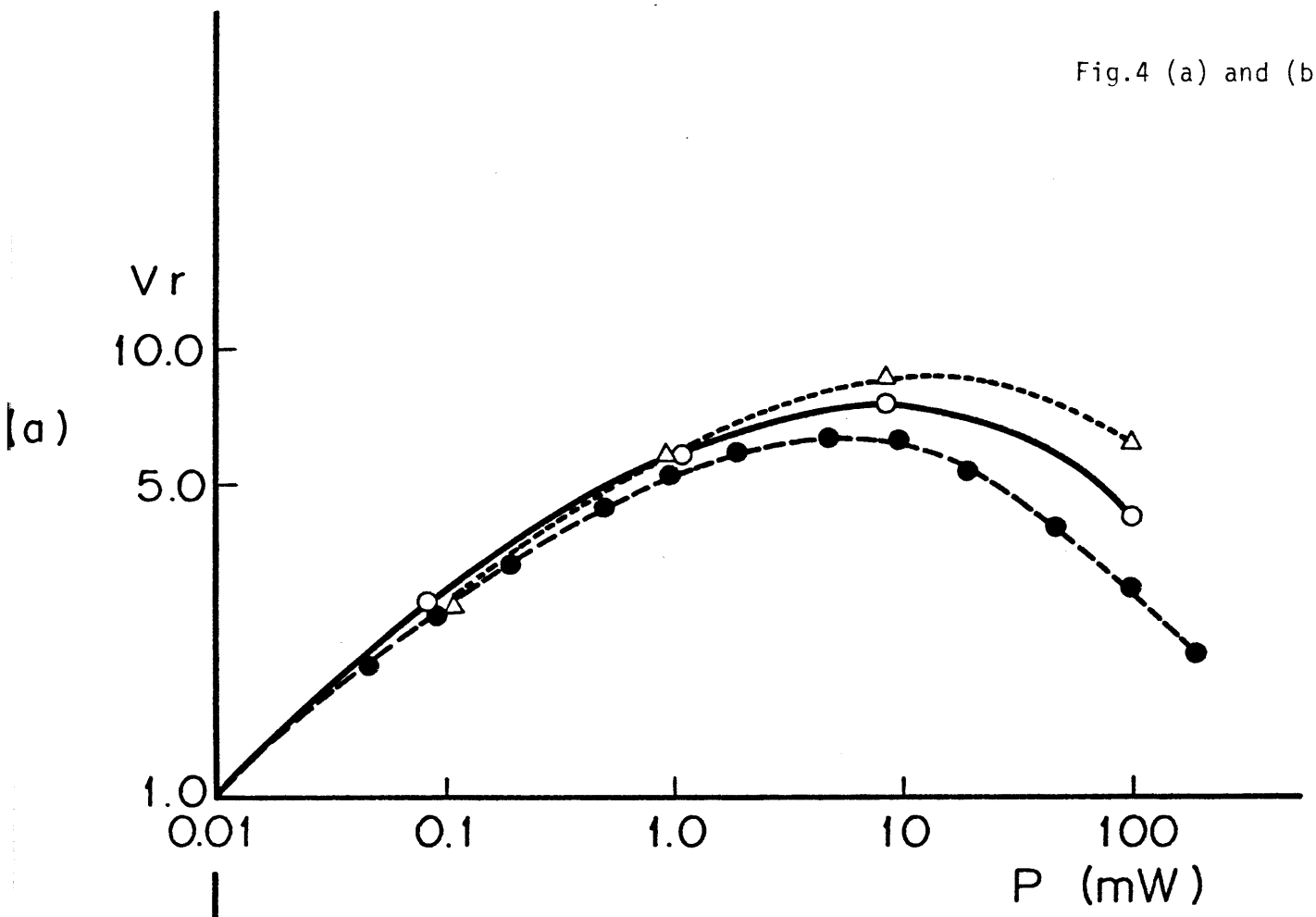
(a)
Vr
10.0
5.0
1.0
0.01
0.1
1.0
10
100
P (mW)

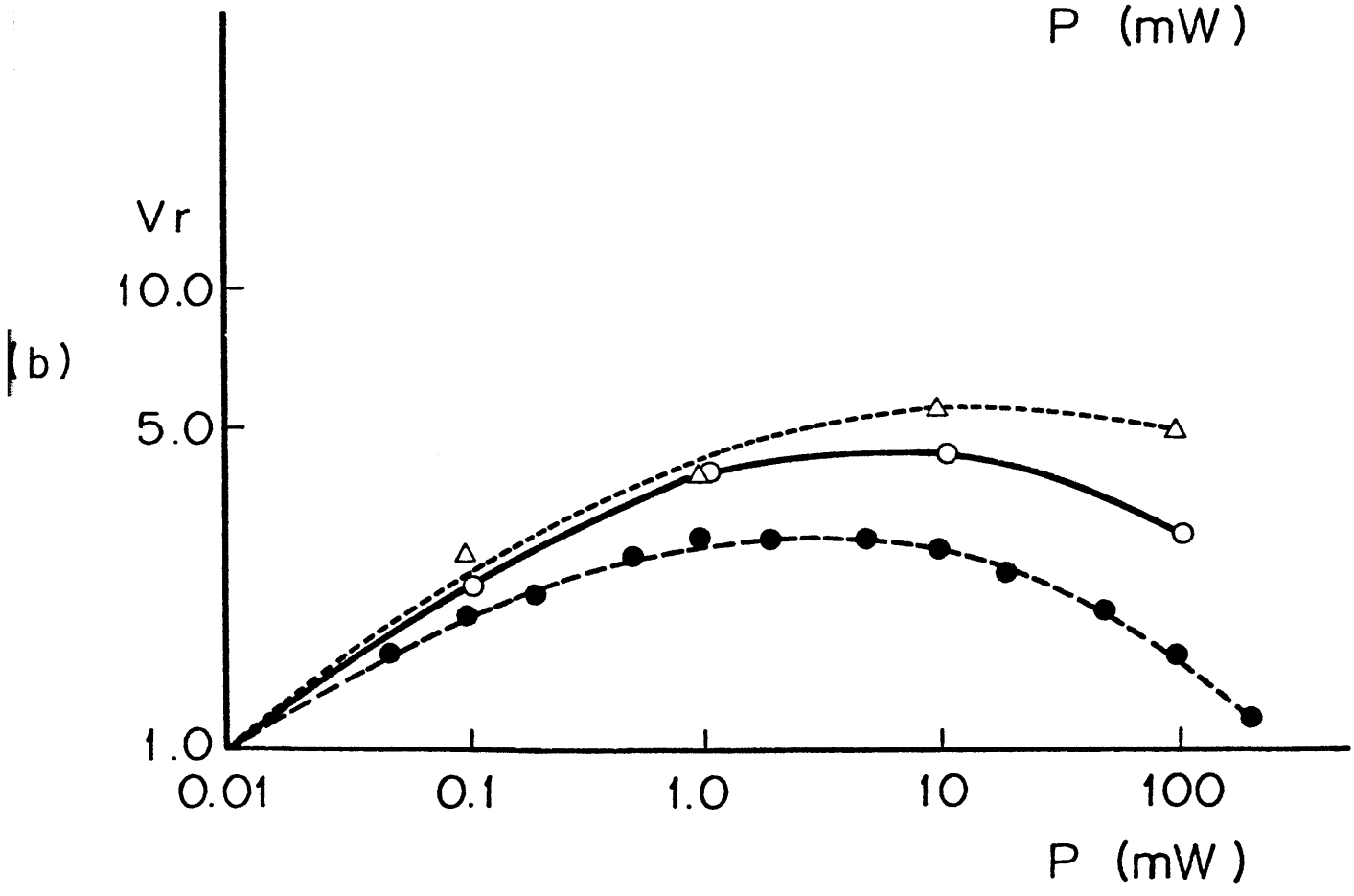
(b)
Vr
10.0
5.0
1.0
0.01
0.1
1.0
10
100
P (mW)

Fig.4 (c) and (d)

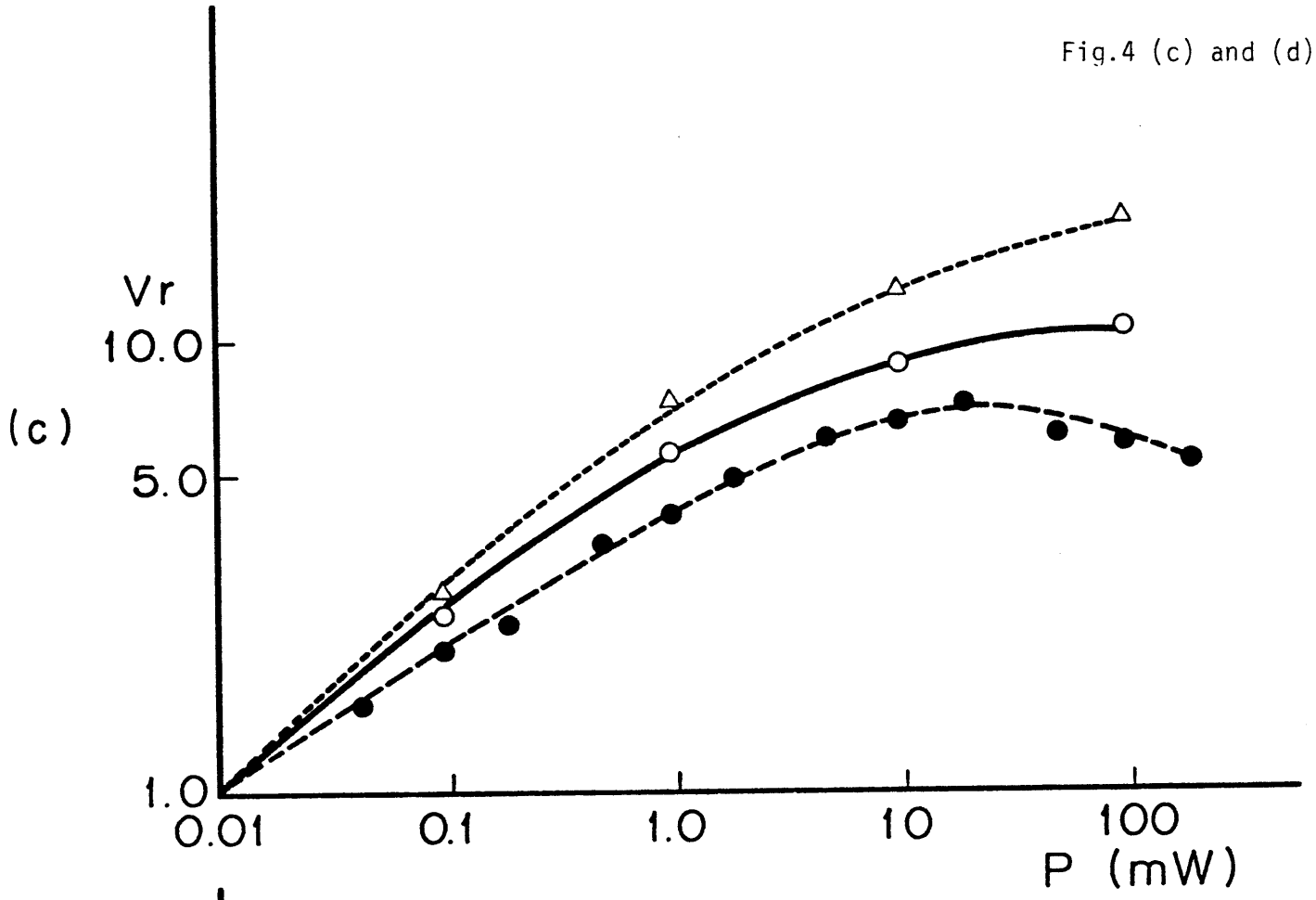
(c)
Vr
10.0
5.0
1.0
0.01
0.1
1.0
10
100
P (mW)

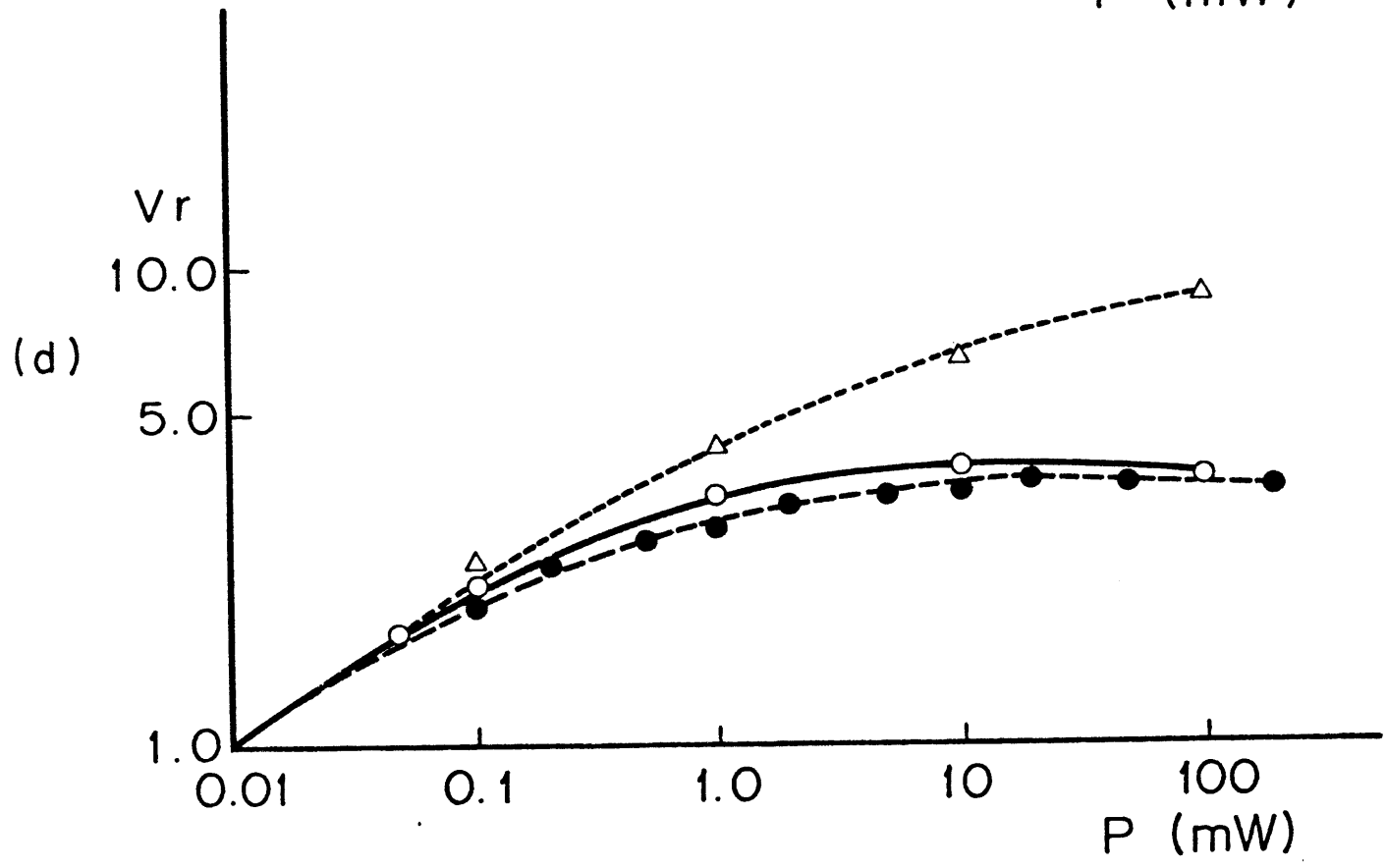
(d)
Vr
10.0
5.0
1.0
0.01
0.1
1.0
10
100
P (mW)

Fig.4 (e) and (f)

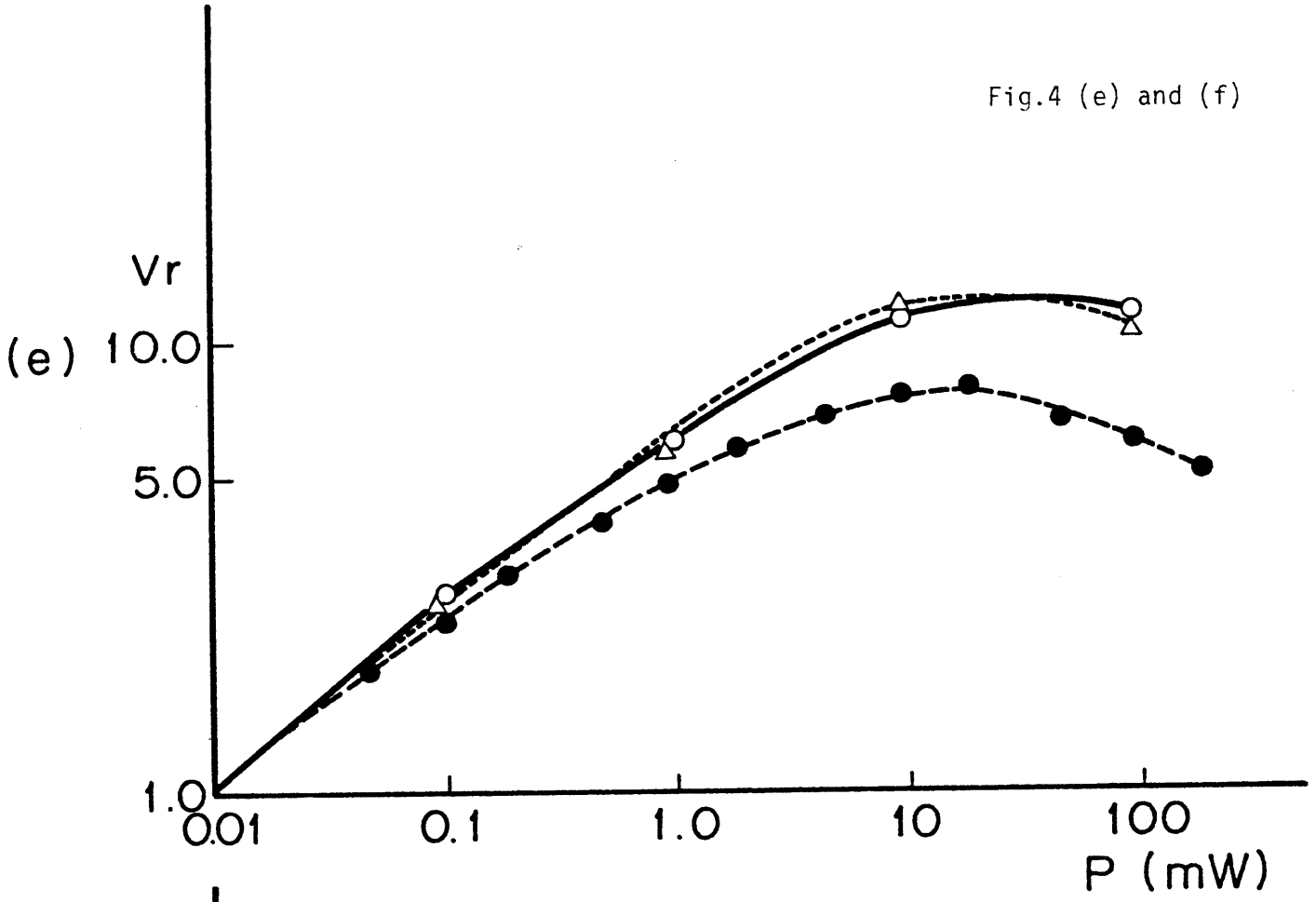
Vr
(e)
10.0
5.0
1.0
0.01
0.1
1.0
10
100
P (mW)

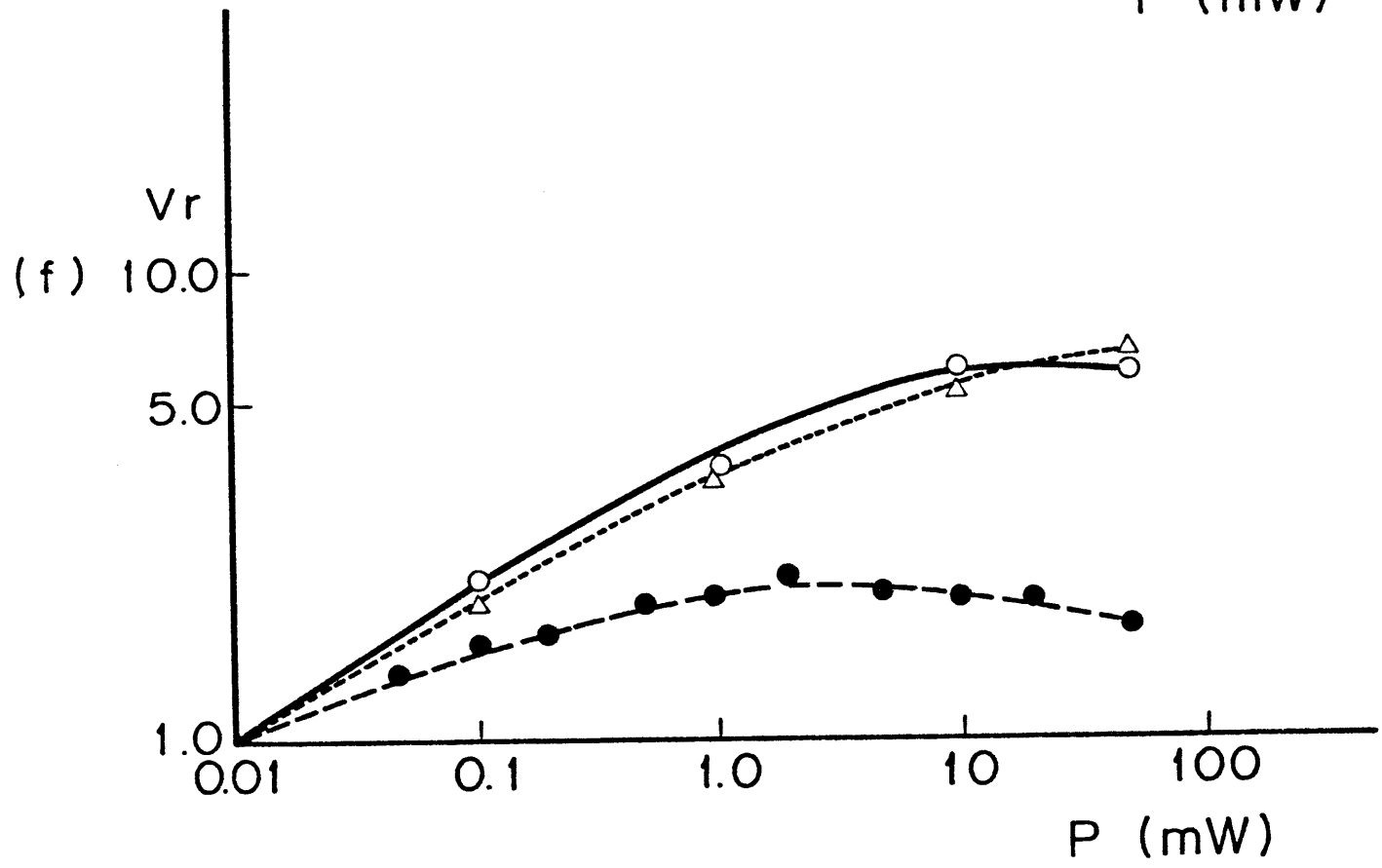
Vr
(f)
10.0
5.0
1.0
0.01
0.1
1.0
10
100
P (mW)

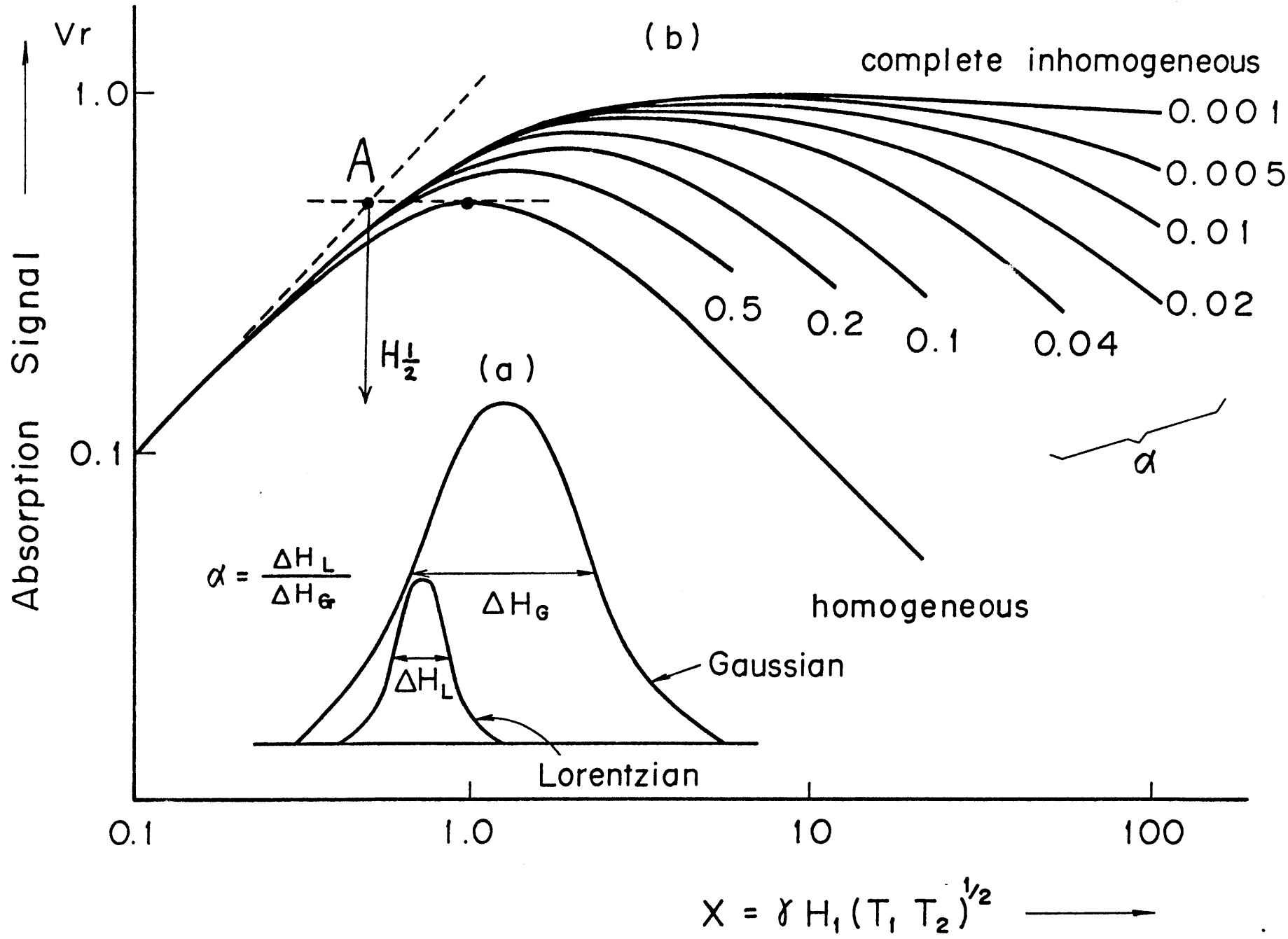
Vr
1.0
0.1
Absorption Signal
(b)
complete inhomogeneous
0.001
0.005
0.01
0.02
0.5
0.2
0.1
0.04
A
$H_{\frac{1}{2}}$
(a)
α
$\alpha = \frac{\Delta H_L}{\Delta H_G}$
ΔH_G
ΔH_L
Gaussian
Lorentzian
homogeneous
0.1
1.0
10
100
$X = \gamma H_1 (T_1 T_2)^{1/2}$

Fig.5 (a) and (b)

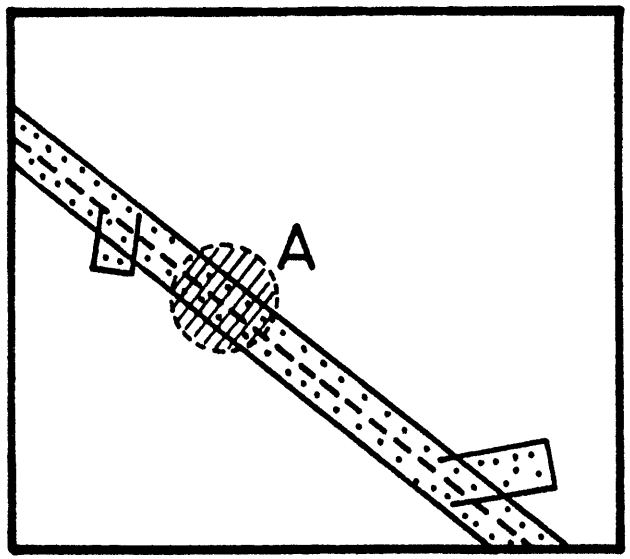

a

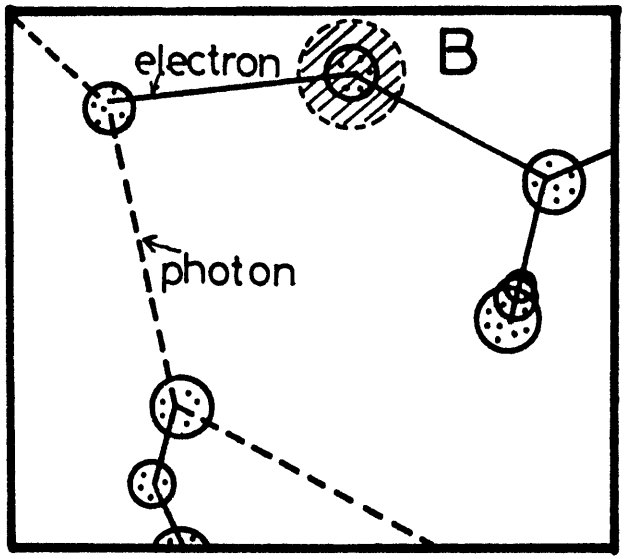

b

Fig.6 (a) and (b)

Chapter 5.

Energy Transfer in Liquid Hydrocarbons

I hope to summarize historical background of energy transfer in liquid hydrocarbons. This subject consists of three sections.

1) Emission spectra and lifetimes of excited states of saturated hydrocarbons.
2) Excimer formation in liquid aromatic hydrocarbons.
3) Energy transfer study by means of steady state photolysis.

I) Emission spectra and lifetimes of excited states of saturated hydrocarbons

For a long time, it has been believed that the fluorescence of excited saturated hydrocarbons can not observed because of its short lifetimes.[1] In 1967, Raymonda and Simpson[2] obtained the absorption band with vibrational structure of saturated hydrocarbons in gas phase below the wavelength of 200 nm. At the same time, Holroyd et al[3] studied photolysis of liquid hydrocarbon such as cyclohexane containing benzene or N_2O by 147 nm light excitation and observed the reduction of H_2 yield. They concluded that the excited state of cyclohexane plays an important role for photolysis and its lifetime is assumed to be order of 1 ns. Recently, similar studies were carried out by Hatano et al[4] and energy transfer rate constant from excited cyclohexane to solute molecules was obtained to be 9∿24 times faster than normal diffusion controlled reaction.

In 1969, fluorescence spectra of saturated hydrocarbons were first observed by excitation with 147 nm light from Xe lamp by microwave excitation by Hirayama and Lipsky.[5] Emission band exists in the wavelength of 180 nm∿250 nm and quantum yield is order of 10^{-3}. They also observed directly the energy transfer phenomena in cyclohexane

containing benzene. In the presence of small amount of benzene, the fluorescence due to benzene molecules having 270 nm∿310 appears and the emission due to the lowest excited state of cyclohexane is reduced.

Based on the emission spectra reported by Lipsky group, many researchers were trying to measure the lifetimes of the excited states. In 1972, Henry and Helman[6] obtained the lifetimes of several kinds of saturated hydrocarbons with X ray pulse and photon counting technique. They studied also quenching rate of CCl_4 in decaline and dodecane and found that the quenching rate is ten times faster than normal diffusion reaction. Using H_2 flash lamp (156 nm), Ware and Lyke[7] obtained the lifetimes of the lowest excited state of hydrocarbons in 1974. The results obtained with flash lamp were somewhat different from those with X ray pulse. Recently, Ware et al[8] constructed a new instrument for gas phase experiment. Preliminary results[9] showed the lifetimes of excited states are dependent on the excited vibrational band in the lowest excited states and the values are rather long compared with results in liquid. Deconvolution techniques applied to data analysis was discussed in a view point of speed and reliability.[10] New technique using Fourier and Laplace transforms appears.[11]

II) Excimer formation in liquid aromatic hydrocarbons

In 1954, the change in emission spectrum of pyrene from structured violet emission in $\sim 10^{-4}$M solution to a broad and structureless blue emission in $\sim 10^{-2}$M solution was first explained by Förster et al as due to the formation of an excited dimer (excimer) from an excited monomer precursor.[12] The concentration dependence of emission behavior is explained as following hypothesis,

1) Main precursor of excimer is excited monomer.

2) Association reaction obeys first order of unexcited monomer concentration.

Equilibrium between monomer and excimer is defined K, equilibrium constant. Large K indicates large excimer population. Since benzene derivatives have smaller K values compared with pyrene, the measurement of emission both from monomer and excimer should be done at low temperature.[13] In 1969, Hirayama and Lipsky observed several alkyl benzene in methylcyclohexane at low temperature and their results showed clear isoemissive points. From these data, they obtained K values and activation energies for sandwich type excimers. This excimer formation is characteristic point in aromatic hydrocarbon system in contrast with in saturated hydrocarbons.

III) Energy transfer in liquid hydrocarbons

In 1955, Kallmann[14] found that solvents could be divided three classes from the view point of scintillation efficiency. In the first class, so-called " effective " solvents are most of aromatics. Second solvent is " moderate " one. " Moderate " solvent have efficiency within a factor of 2-4 of the aromatic ones. Last class is " poor " solvent with efficiecies almost two orders of magnitude lower than that of the " effective " solvents. They thought that double bond in chemical structure of solvent molecule plays an important role for high scintillation efficiency.

In 1971, Hirayama and Lipsky[15] reported energy transfer processes in liquid hydrocarbon with 2,5-diphenyloxazole (PPO) as a solute. They used 147 nm light source. In benzene-PPO system, the change of magnitude of emission at various concentrations could be explained by simple donor-accepter model. On the other hand, the change of energy transfer could not be explained without assuming additional one excited state of solvent in cyclohexane or heptane-PPO solution. This additional excited state was assumed to be triplet of

saturated hydrocarbon solvent. However, obtained energy transfer rate from excited solvent to solute molecules is in a good agreement with our result using a single picosecond electron from a linac at Nuclear Engineering Research Laboratory, Univ. of Tokyo.[16] They also applied their system to radiolysis by Cs^{137} α-irradiation. In radiolysis, obtained transfer rates were somewhat different with those in photolysis. This comparative technique between radiolysis and photolysis were used to evaluate yields of excited singlet state of some saturated hydrocarbon liquid[17] and fraction of geminate ion recombination in excited solute molecules in radiolysis. It is thought that comparative study between radiolysis and photolysis is powerful technique to consider the different points between radiation chemistry and photochemistry.

References

1) for review, S. Lipsky p 495 in " Chemical Spectroscopy and Photochemistry in the Vacuum-Ultraviolet " ed. by C. Sandorfy, P.J. Ausloos and R.B. Robin, D. Reidel, Boston, 1974.

2) J.W. Raymonda and W.T. Simpson; J. Chem. Phys. 47 430 (1967)

3) R.A. Holroyd; J. Am. Chem. Soc. 72, 759 (1968)
R.A. Holroyd, J.Y. Yang and F.M. Serredio; J. Chem. Phys. 46, 4540 (1967)
J.Y. Yang, F.M. Servidio and R.A. Holroyd; J. Chem. Phys. 48, 1331 (1968)

4) J. Nafisi-Movaghar and Y. Hatano; J. Phys. Chem. 78, 1899 (1974)
T. Wada and Y. Hatano; J. Phys. Chem. 79, 2210 (1975)
T. Wada and Y. Hatano; J. Phys. Chem. 81, 1057 (1977)

5) F. Hirayama and S. Lipsky; J. Chem. Phys. 51, 3616 (1969)
F. Hirayama, W. Rothman and S. Lipsky; Chem. Phys. Lett. 5, 296 (1970)
W. Rothman, F. Hirayama and S. Lipsky; J. Chem. Phys. 58, 1300 (1973)

6) M.S. Henry and W.P.Helman; J. Chem. Phys. 56, 5734 (1972)
W.P. Helman; Chem. Phys. Lett. 17 306 (1972)

7) W.R. Ware and R.L. Lyke; Chem. Phys. Lett. 24 195 (1974)

8) R.L. Lyke and W.R. Ware; Rev. Sci. Instrum. 48, 320 (1977)

9) W.R. Ware and D.V. O'Connor; Chem. Phys. Lett. 62, 595 (1979)

10) D.V. O'Connor, W.R. Ware and J.C. Andre; J. Phys. Chem. 83 1333, (1979)

11) J.C. Andre, L.M. Vincent, D.V. O'Connor and W.R. Ware; J. Phys. Chem. 83, 2285 (1979)

12) for review, J.B. Birks, Nature 214, 1187 (1967)

13) M.D. Lumb, and D.A. Weyl; J. Molec. Spec. 23, 365 (1967)
F. Hirayama and S. Lipsky; J. Chem. Phys. 51, 1939 (1969)

14) M. Furst and H. Kallman; J. Chem. Phys. 23, 607 (1955)

15) F. Hirayama and S. Lipsky p 205 in " Organic Scintillators and Liquid Scintillation Counting " Academic Press, New York & London, 1971.

16) S. Tagawa, Y. Katsumura and Y. Tabata; Chem. Phys. Lett. 64 258 (1979)
S. Tagawa, Y. Katsumura and Y. Tabata; Rad. Phys. Chem. 15 287 (1980)
Y. Katsumura, S. Tagawa and Y. Tabata; J. Phys. Chem. 84 833 (1980)
Y. Katsumura, T. Kanbayashi, S. Tagawa and Y. Tabata; Chem. Phys. Lett. 67 183 (1979)
Y. Katsumura, T. Kanbayashi, S. Tagawa and Y. Tabata;
to be published
17) L. Walter and S. Lipsky; Int. J. Radiat. Phys. Chem. 7 175 (1975)
18) L. Walter, F. Hirayama and S. Lipsky; Int. J. Radiat. Phys. Chem. 8 237 (1976)

Chapter 6.
Picosecond Pulse Radiolysis Studies on Excitation Processes in Liquid Cyclohexane

Abstract

Behavior of the scintillation emission from 2,5-diphenyloxazole in liquid cyclohexane was investigated by use of picosecond (~10 psec) electron pulse. The emission was detected by a streak camera with picosecond time resolution. The emission was attributable to the fluorescence of 2,5-diphenyloxazole. From the effect of additives such as CCl_4 and triethylamine, it was found that the formation of excited 2,5-diphenyloxazole composed of faster and slower ones. The slower process was quenched significantly by CCl_4 and triethylamine and this process is considered to be mainly due to the energy transfer from excited cyclohexane molecules to 2,5-diphenyloxazole. The rate constant of the energy transfer is $\sim 4\times10^{11}$ M^{-1} sec^{-1}. It was also found that the lifetime of the excited singlet state of cyclohexane is about 300 psec. On the other hand, in the faster process, the growth of emission is completed within pulse duration and this emission is also affected by quenchers.
In the faster process, the formation of excited 2,5-diphenyloxazole will be discussed in connection with direct excitation by sub-excitation electron, rapid recombination of solute ions, and direct excitation by Čerenkov light.

Introduction

Pulse radiolysis studies on cyclohexane have been carried out by many

investigators[1] in nanosecond time range. Most of all were focused on the study of the formation yields of cation, anion, singlet and triplet of aromatics as solute molecules. There is only few reports with sub-nanosecond time resolution[2],[3]. Difficulties to produce a very short electron pulse and to detect produced very short lifetime transient species with high time resolution prevent such experiment. The main advantage of using a single pulse is that information about time-dependent phenomema can be obtained without any time limitation in contrast with using a pulse train of linac by Hunt et al in aqueous system[4], and by Beck & Thomas in liquid systems[2].

In pure liquid cyclohexane, Henry et al[5] used a pulsed X-ray source for excitation and photon counting technique as the detection method, and reported that the lifetime of the lowest excited state of cyclohexane is 0.3 ns. However, Ware et al[6] reported that the lifetime of cyclohexane in liquid is 0.63 ns by using a 156 nm pulsed light source. Hatano et al[7] investigated the energy transfer from excited cyclohexane to several solutes in liquid phase by means of product analysis. They used a 163 nm light source for the experiment under steady state condition. They found that the rate constant of the energy transfer are larger in a factor of 9∿24 than expected for the diffusion controlled one. This large rate constant was explained by a large effective interaction radius which is estimated to be 10∿20 Å.

The precise mechanism of excitation processes in early stage of radiation chemistry has not yet been made clear. From the scintillation emission of 2,5-diphenyloxazole in cyclohexane, the excitation mechanism has been investigated by use of picosecond single electron pulse with high time resolution down to 10 psec. It was found that in the early stage of emission (<1 nsec), both rapid and slow processes are superimposed[8]. This was not known before. The possibility of excitation of solute molecules by sub-excitation electron, the exsistance of rapid solute ion recombination and the

excitation by Čerenkov light in faster process are discussed.

Experimental

The 35 MeV linear accelerator at the Nuclear Engineering Research Lab. Univ. of Tokyo in Tokai-mura is S-band (2856 MHz) one and it is capable to produce a single picosecond pulse (∿35 MeV) using a subharmonic buncher (SHB) operated at 476 MHz. The pulse duration observed was down to 18 psec from measuring the Čerenkov light accompanied with high energy electorns passing through in the air detected by a streak camera (Fig. 1). Intrinsic time resolution of the streak camera is less than 10 psec. This pulse width observed (18 psec) is larger than the predicted value from theoretical consideration, because the broadening of light pulse distribution mainly occurs due to the difference of flight pathes of Čerenkov light in the air to the detector (streak camera). Recently, the pulse duration was estimated to be ∿17 psec using a correlation method[9]. The electronic trigger pulse synchronized to the electron pulse is now available for the detection system in pulse radiolysis experiment. The time jitter was evaluated to be $\lesssim$22 psec from broadening of pulse occured by accumulating pulses using a streak camera. The repetition of pulses is up to 200 pps. Usually 50, 25, 12.5, and 6.25 pps line synchronization pulses are used and the total charge per single pulse used was ∿500 pC. The details of the 35 MeV Linear Accelerator in Univ. of Tokyo were reported in previous papers.[10]

The detection system is composed of a streak camera (C 979, HTV), a SIT camera (C 1000-12, HTV), an analizer (C 1098 HTV) and a display system of Hamamatsu TV Co. as shown in Fig. 2. To get high S/N ratio, usually 20 signals were accumulated using the analyzer. In the accumulating mode, time resolution of the total detecting system was evaluated to be less than 28 psec from the signal broadening of Čerenkov lights by accumulating repeated pulses.

The time resolution comes from the jitter of both the synchronization circuit of the linac and the detection system including the streak camera.

In observing the spectrum of scintillation emission, a monochrometer (Ritsu MC-10 N) combined with the streak camera was also used. The resolution of the monochrometer was set rather wide as $\Delta\lambda \sim 10$ nm because the emission intensity is low at lower concentration of the solute. The spectral response of the system was calibrated using the relation that the intensity fo Cerenkov light is proportional to $1/\lambda^2$[11].

Cyclohexane and 2,5-diphenyloxazole used were a guaranteed grade from Tokyo Kasei Co. Ltd. Carbontetrachloride and triethylamine purchased from Tokyo Kasei Co. Ltd. were used after distillation. The absorption spectra of the sample solutions were measured by a Shimazu recording spectrometer (UV-360).

As it was found that the emission was not affected by the presence of air, air was not particularly purged.

Results

The emission from excited 2,5-diphenyloxazole in cyclohexane as a function of time is different from that in toluene solution as shown in Fig. 3. The growth of emission in cyclohexane solution is more rapid than that in toluene solution. Emission behavior measured at a lower concentration (0.1 mM) of 2,5-diphenyloxazole in cyclohexane by our detection system with high time resolution is shown in Fig. 4(a). This indicates that the emission is mainly composed of rapid rise. On the other hand, at higher concentrations of 2,5-diphenyloxazole in cyclohexane, the emission was mainly composed of slower rise and the discrimination between rapid growth and slow one was difficult (Fig. 4(b) and (c)). It was also found that the growth time at which emission reaches at maxmum intensity decreases with increasing the concentration of

2,5-diphenyloxazole. Decay time of the emission in cyclohexane is about 1.6 ns, which is agreed with the reported data[12] and it is independent of the concentration of 2,5-diphenyloxazole in cyclohexane solution. However, the apparent lifetime in toluene is significantly dependent on the concentration of 2,5-diphenyloxazole. This difference is considered to be mainly due to the long lifetime of the singlet excited state of toluene molecules and the formation of the excimer in toluene.[13]

The spectrum of emission from excited 2,5-diphenyloxazole in cyclohexane is shown in Fig. 5. In the case of 1 mM 2,5-diphenyloxazole in cyclohexne, the peak of the emission is 360 nm and this spectrum is attributable to fluorescence of 2,5-diphenyloxazole from the lowest singlet excited state to the ground state[14]. However, in the case of 5 mM solution, it was found that the emission peak shifts to higher wavelength, 370 nm. This shift may occur due to absorption of the emission by the red edge of 2,5-diphenyloxazole absorption band. This explanation was also supported by the absorption spectrum of sample solution. The transparency of solution is reduced significantly below 350 nm. It is noted that the spectra of emission do not change with time in different concentrations.

The total emission yield, which means that the emission of 2,5-diphenyloxazole integrated up to ∿10 ns immediately after the electron pulse, is shown in Fig. 6. It is easily seen that the change in total emission with concentration is different between below and above 1 mM concentration of 2,5-diphenyloxazole in cyclohexane. This means that at above 1 mM, the emission from the slower process is dominant. It is also noted that the slope at lower concentration ranges less than 1 mM is ∿0.5. This square root dependence strongly indicates that the formation of excited 2,5-diphenyloxazole occurs by the reaction including charged species.

Since the formation of excimer of 2,5-diphenyloxazole becomes important

at the concentrations larger than 100 mM 2,5-diphenyloxazole[1e], concentration of 2,5-diphenyloxazole is kept below 20 mM.

The effect of quenchers such as CCl_4 and triethylamine on the excitation process was examined. The effect of the scavengers for 20 mM 2,5-diphenyloxazole-cyclohexane solution is shown in Figs. 7(a) and (b). The shaded part in the figure is due to emission of Čerenkov light. It was found that the higher the concentration of quenchers, the faster the dacay of emission due to the quenching of excited 2,5-diphenyloxazole. It was also found that the initial yield of emission is reduced by the additives and the quenching efficiency of CCl_4 is larger than that of triethylamine. By adding CCl_4 and triethylamine at concentrations higher than 100 mM and 400 mM, respectively, the slower emission growth was eliminated completely, and the most of rapid growth within electron pulse duration and consecutive decay were observed.

The emission processes having the slow growth and rapid growth rates will be called the slower process and the faster one, respectively, in the following section. The emission intensity ratio of the faster to the slower process in 1 mM solution is larger than in 20 mM. In the case of 1 mM solution as shown in Figs. 8(a) and (b), it is noted that the reduction of emission by 1 M triethylamine is larger than that by 500 mM CCl_4 in contrast with in the case of 20 mM solution of 2,5-diphenyloxazole. Since the slower process is almost eliminated at these concentrations of scavengers, these results strongly suggest that the quenching for the faster process is very different between two scavengers. This difference can be seen more clearly in the case of 0.1 mM 2,5-diphenyloxazole as shown in Fig. 9(c) (see discussion).

Discussion

The excitation process of 9,10-diphenylanthracene in cyclohexane using pulse trains from a linac was investigated by Beck and Thomas[2]. They con-

cluded that energy transfer process was mainly one process, the transfer from excited solvent molecule to solute one. However, in the present work, it was found that the faster and the slower processes are superimposed and the ratio of these processes is dependent on the concentration of 2,5-diphenyloxazole.

Although oxygen molecules are known to be efficient quenchers, the presence of air in sample solution did not affect the yield in our experimental conditions. There is no significant difference between air-saturated and degassed samples. For only small amount of oxygen less than 2 mM, the quenching by oxygen is considered to be negligible for the fast reaction even if the rate constant of quenching by oxygen assumed to be $\sim 10^{11}$ $M^{-1} \cdot sec^{-1}$.

From the quenching experiment, it is obvious that the additives usually quench more than one process. Quenching of excited 2,5-diphenyloxazole is evaluated from the change in decay of emission. On the other hand, from the reduction of initial emission yield, the formation of excited 2,5-diphenyloxazole can be discussed.

The quenching and inhibition for the formation of excited singlet state of cyclohexane molecule from which the energy is transfered to 2,5-diphenyloxazole molecule are corresponding to the slower process. No color-quenching occurs because the absorption spectrum of the sample solution is not changed by adding quenchers such as CCl_4 and triethylamine at longer wave lenghs than 340 nm, which has the emission band of 2,5-diphenyloxazole. It is seen that the slower and the faster emission growths were reduced by quenchers with different rate constants, respectively, as shown in Figs. 7 and 8. From these results, the total emission yield as a function of concentration of quenchers are shown in Fig. 9. The change of emission yield by additives has different fashion between a higher concentration, 20 mM and a lower concentration, 1 mM 2,5-diphenyloxazole in cyclohexane. In both solutions, a larger reduction in emission was observed by small amount of quenchers and the magnitude of

reduction decreases with increasing the concentration of additives. The slower process is more sensitive by quenchers than the faster process. Addition of CCl_4 is more efficient for the quenching than triethylamine in 20 mM 2,5-diphenyloxazole-cyclohexane solution. However, at lower concentrations such as 1 mM or 0.1 mM 2,5-diphenyloxazole, triethylamine is more efficient than that of CCl_4 in contrast with 20 mM solution. This indicates that at lower concentrations of the solute, the emission from the faster process becomes dominant and the quenching by triethylamine for the faster process is more effecient than for the slower one in contrast with the quenching by CCl_4. It is also clearly seen from Fig. 8 that a remarkable decrease in initial yield and a small change in the decay rate occur in 1 mM 2,5-diphenyloxazole solution containing 100 mM triethylamine. On the other hand, not only decrease in initial yield but also increase in decay rate of emission was observed in 1 mM 2,5-diphenyloxazole solution containing 50 mM CCl_4.

By extraporating the emission to a time immediately after the pulse under different concentrations of scavengers, in Fig. 7 and 8, the emission will be divided into the slower and the faster processes. The faster process is completed within the electron pulse. Although it is not clear whether the faster process obeys the pseudo first order kinetics or not, the rate constant is easily estimated to be $\geq 10^{15}$ M^{-1} sec^{-1} for the faster process if we assume the kinetics.

The slower process for the scintillation emission from 2,5-diphenyloxazole is considered to be mainly due to the energy transfer from excited cyclohexane to 2,5-diphenyloxazole. The mechanism can be explained as following,

$$c\text{-}C_6H_{12} \xrightarrow{\text{very fast}} c\text{-}C_6H_{12}^{*} \quad (1)$$

$$c\text{-}C_6H_{12}^{*} + \underset{(PPO)}{\text{2,5-diphenyloxazole}} \xrightarrow{\beta[PPO]} PPO^{*} \quad (2)$$

$$PPO^{*} \xrightarrow{k} \text{emission} \quad (3)$$

The decay rate of k is obtained from the decay of the emission. The lifetime of excited 2,5-diphenyloxazole is obtained to be 1.6(± 0.1) ns and the decay rate to be $6.3(\pm 0.5) \times 10^{8}$ sec^{-1}. From the above mechanism the emission with time is expressed by following formula,

$$[PPO^{*}](t) = \beta[PPO]/\{(\alpha - k) + \beta[PPO]\} \times \{e^{-kt} - e^{-(\alpha + \beta[PPO])t}\} \quad (4)$$

where α is the lifetime of excited cyclohexane molecule and β is the rate constant of energy transfer from excited cyclohexane to 2,5-diphenyloxazole. From this equation the growth of the emission becomes rapid with increasing the concentration of solute. This is consistent with our observation results at higher concentration ranges. The rate constants, $k=6.3\times10^{8}$ sec^{-1}, $\alpha=3\times10^{9}$ sec^{-1} and $\beta=4\times10^{11}$ $M^{-1}\cdot sec^{-1}$, give the best fit for the experimental observation as shown in Fig. 10 and these values are consistent with our observation results that the emission decay is independent of the solute concentration. These results are agreed with the data reported by Beck and Thomas[2], $\alpha=3.6\times10^{9}$ sec^{-1} $\beta=3.4\times10^{11}$ M^{-1} sec^{-1}. The lifetime of excited state of cyclohexane is 330 psec which is agreed with the measurement by Henry et al[5]. From eq. (4) the total emission yield is obtained as

$$F = \int_0^\infty [PPO^*](t)dt = \frac{\beta[PPO]}{\alpha+\beta[PPO]} \qquad (5)$$

Using eq. (5) the calculated values of total emission yield are shown in Fig. 6. Above 1 mM 2,5-diphenyloxazole, the calculated values coincide with the experimental data. This result is consistent with experimental observation, because at the higher concentration of solute, the emission from the slower process becomes dominant.

The rate constant of energy transfer is one factor larger than the limit of diffusion controlled reaction. There are two explanations for the results. One is that the migration of energy among solvent molecules is very fast, and the transfer rate from solvent to solute seems to be larger than diffusion controlled reaction. The other is that the reaction radius of energy transfer from excited cyclohexane to 2,5-diphenyloxazole is one factor larger than the expected from theoretical consideration. However, it is known that the slower process is eliminated in solid at lower temperatures[8]. Thus, it suggests that the slower process is strongly related to the diffusion or collision of solvent molecules. This conclusion is consistent with the result reported by Hatano et al[7].

Since the lifetime of excited cyclohexane is short and the rate of energy transfer is very fast, the quenching rate of excited 2,5-diphenyloxazole molecules can be obtained directly from the change of decay rate of the emission with adding the quenchers. The rates, $(2\pm1)\times10^9$ M^{-1} sec^{-1} and $0.6(\pm0.5)\times10^8$ M^{-1} sec^{-1}, were obtained for CCl_4 and triethylamine, respectively. The quenching rate of excited cyclohexane molecules by quenchers is estimated, since the change of total emission yield, F, by addition of quenchers in the slower process is expressed as following

$$F \propto \frac{\beta[PPO]}{\alpha+\beta[PPO]+q_3[CCl_4]} \cdot \frac{k}{k+q_1[PPO]+q_2[CCl_4]} \qquad (6)$$

$$c\text{-}C_6H_{12}^{*} + PPO \xrightarrow{\beta[PPO]} PPO^{*} \qquad (2)'$$

$$PPO^{*} \xrightarrow{k} h\nu \qquad (3)'$$

$$PPO^{*} + CCl_4 \xrightarrow{q_2[CCl_4]} PPO \qquad (7)$$

$$PPO^{*} + PPO \xrightarrow{q_1[PPO]} (PPO_2)^{*} \qquad (8)$$

$$c\text{-}C_6H_{12}^{*} + CCl_4 \xrightarrow{q_3[CCl_4]} c\text{-}C_6H_{12} \qquad (9)$$

where q_1 and q_2 are the quenching rate constants of PPO^{*} by PPO and CCl_4 (or triethylamine), respectively, and q_3 is the quenching rate of $c\text{-}C_6H_{12}^{*}$ by CCl_4 (or triethylamine). The value of q_1 is the rate of excimer formation and $5.6(\pm1.4)\times10^{9}$ M^{-1} sec^{-1} is reported by Dainton et al(1e). In the case of 20 mM 2,5-diphenyloxazole, the emission is assumed to be composed of mainly the slower process, the quenching rate of $c\text{-}C_6H_{12}^{*}$ by quenchers (q_3) was estimated by using eq. (6). The result is shown in Fig. 9(a) and q_3 are $\sim(3\pm1)\times10^{11}$ and $\sim(1\pm1)\times10^{11}$ M^{-1} sec^{-1} for CCl_4 and triethylamine, respectively. These values are also larger in a factor of 10 than that expected in diffusion controlled reaction. It is also found that the quenching rates of $c\text{-}C_6H_{12}^{*}$ by CCl_4 and triethylamine are much larger than the rate of PPO^{*} by them, but the same order of the rate constant of the energy transfer from excited cyclohexane to 2,5-diphenyloxazole. From these results, the large rate constant is considered to be due to the rapid migration of excitation energy among cyclohexane solvent molecules. The value $\sim(3\pm1)\times10^{11}$ M^{-1} sec^{-1} for CCl_4 obtained in the present work is about four times larger than that reported by Hatano et al in their photolysis and product analysis experiments(7). This discrepancy is thought to be intrinsic one arising from the differencies

between the observation of the emission by the pulse radiolysis and the analysis of products from the steady state photolysis.

It is noted that above kinetics is based on the assumption that the formation of excited state of cyclohexane is very fast and its formation is not affected by quenchers. It seems that this assumption is hardly applicable for the system, because the inhibition of the formation of the excited cyclohexane[15] may actually occur. In order to clarify the excitation processes, inhibition of formation of excited cyclohexane and deactivation of formed excited cyclohexane by quenchers are desirable to be clearly distinguished. However, it is not so easy. In spite of some ambiguities mentioned above, an overall analysis induding both two processes makes it possible to evaluate the effect of quenching. The rate constant q_3 includes both inhibition of formation and quenching of formed excited state of cyclohexane.

The faster process is very rapid and the growth of emission is completed within pulse duration. Rapid emission growth contains different formation processes of PPO^*.

Yield of excited 2,5-diphenyloxazole obtained by calculation using the absorbed dose and G-value of PPO^* formation[1,e] was compared with that only due to the absorption of Čerenkov light induced in sample medium by an electron pulse. It is made clear from comparison that the former is more than 10^2 times larger than the latter. From these consideration, a large part of the faster process could not be explained as due to direct excitation of Čerenkov light in the present experiments. However, at lower concentrations ($\leq 10^{-5}$ M) of 2,5-diphenyloxazole, the contribution of direct excitation by Čerenkov light may become important.

For the faster process, quenchers also affect the initial yield of emission. The emission from 0.1 mM 2,5-diphenyloxazole in cyclohexane is

considered to be mainly due to the faster process. It is clearly seen that the reduction of emission by quenchers occurs as shown in Fig. 9(c). This result strongly suggests that the charged species play an important role in the faster process. It is well known that CCl_4 is one of the typical electron scavengers and triethylamine is a hole scavenger. Ion recombination processes are considered to form the excited solute molecules rapidly. Recombinations of the positive hole with solute anion, and of solute cation with electron are expected to be affected by ion scavengers. In 0.1 mM 2,5-diphenyloxazole solution presence of CCl_4 more than 100 mM, the change in the decay of emission yield can be explained only by quenching excited 2,5-diphenyloxazole. Addition of CCl_4 at concentrations up to about 100 mM reduces the initial yield of emission. At more than 100 mM, initial yield of emission is not affected furthermore and only decay rate of emission increases. This result suggests that fast formation of solute excited state is composed of two parts, one is sensitive to CCl_4 and the other is insensitive. On the other hand, the initial yield of emission decreases with increasing the concentration of triethylamine to a smaller extent than that in the case of CCl_4. Triethylamine can scavenge selectively holes and cations, while CCl_4 can scavenge the counter ion, electrons.

Although the energy transfer from higher excited state of cyclohexane to other solvent molecules is expected to be very fast, its contribution to the faster process is thought to be negligiblly small. If energy transfer from the higher excited states occurs, the formation process of the excited state of 2,5-diphenyloxazole should be competition between relaxation of the higher excited state of cyclohexane to the lowest one and the energy transfer from this higher excited solvent molecules to solute. Therefore, the yield of the emission must increase with increasing the concentration of solute.

Furthermore, quenching by additives is expected to be very efficient, because the competition between the quencher and the solute is determined by the ratio of $k_t[PPO]/k_q[Q]$, where k_t and k_q are the rate constants of the energy transfer and quenching, respectively and [Q] is the concentration of quencher. In the quenching experiment of 0.1 mM 2,5-diphenyloxazole solution, the concentration ratio ([PPO]/[Q]) is $\lesssim \frac{1}{500}$. If the rate constants are assumed to be the same order between k_t and k_q, the obtained results can not be explained. Thus, the possibility of the energy transfer from the higher excited state of cyclohexane to solvent molecules may be excluded.

Another possibility of the faster process is direct excitation of solute by sub-excitation electrons. As sub-excitation electrons have enough energy to excite the solute molecules but not enough to excite the solvent molecules, it is difficult to scavenge. This mechanism is not excluded from the fast formation processes of excited solute molecules at present.

Pulse radiolysis studies on similar systems using electron pulses from L-band linac are in progress at Argonne National Laboratory in USA.[16]

References

[1] a) P.O'Neil, G.A. Salmon and R. May; Proc. R. Soc. Lond. A 347 61 (1975)

b) J.K. Thomas; J. Rad. Phys. Chem. 8 1 (1976)

c) S.J. Rzad; J. Phys. Chem. 76 3722 (1972)

d) E. Zader, J.M. Warman and A. Hummel; Chem. Phys. 62 3897 (1975)

e) Sir. F. Dainton, M.B. Ledger, R. May and G.A. Salmon; J. Phys. Chem. 77 45 (1973)

[2] G. Beck and J.K. Thomas; J. Phys. Chem. 76, 3356 (1972)

G. Beck and J.K. Thomas; Chem. Phys. Lett, 16 318 (1972)

[3] M.S. Henry and W.P. Helman; J. Chem. Phys. 56, 5734 (1972)

[4] M.J. Bronskill and J.W. Hunt; J. Phys. Chem. 72, 3762 (1968)

[5] M.S. Henry and W.P. Helman; J. Chem. Phys. 56, 5734 (1972)

[6] W.R. Ware and R.L. Lyke; Chem. Phys. Lett. 24 195 (1974)

[7] T. Wada and Y. Hatano; J. Phys. Chem. 81 1057 (1977)

T. Wada and Y. Hatano; J. Phys. Chem. 79 2210 (1975)

[8] S. Tagawa, Y. Katsumura, T. Ueda and Y. Tabata; Chem. Phys. Lett. 68 276 (1979)

S. Tagawa, Y. Katsumura, and Y. Tabata; Rad. Phys. Chem. 15 287 (1980)

[9] K. Hasegawa and Y. Hosono; private comunication

[10] Y. Tabata, S. Tagawa, Y. Katsumura, T. Ueda, K. Hasegawa and J. Tanaka; J. Atomic Energy Soc. Japan, 20, 473 (1978)

Y. Tabata, J. Tanaka, S. Tagawa, Y. Katsumura, T. Ueda, K. Hasegawa; J. Fac. Eng. of Univ. of Tokyo 34, 619 (1978)

[11] J.V. Jelley, " Čerenkov radiation and its application, " Pergamon Press (1958)

[12] F.J. Lynch; Argonne National Laboratory Rpt. ANL-7247 (1966)

J.B. Birks, H.Y. Najjar and M.D. Lumb; J. Phys. B: Atom. Molec. Phys. 4 1516 (1971)

[13] Y. Katsumura, T. Kanbayashi, S. Tagawa and Y. Tabata;

[14] I.B. Berlman " Hand book of fluorescence Spectra of Aromatic Molecules " Academic Press (1971)

[15] L. Walter, F. Hirayama and S. Lipsky; Int. J. Radiat. Phsys. Chem. 8 237 (1976)

[16] C.D. Jonah; Chem. Phys. Letts. 63 535 (1979)

Figure Captions

Fig. 1 The single picosecond electron pulses measured by the detection of Čerenkov light induced in the air.

a) The fine structure of 2 ns pulse detected by a streak camera. The separation of these pulses is 350 psec. From this value, the duration is estimated to be 18 psec. The duration is considered to be overestimated because the broadening mainly due to the difference of flight pathes of Čerenkov light.

b) The single picosecond electron pulse used for the present experiment. No sattellite pulse is observed.

Fig. 2 Block diagram of the detection system. The synchronous trigger to the electron beam is fed from the pulse generator to the streak camera. Total time response and jitter are considered to be 18 psec and $\leq$22 psec, respectively. The beam intensity is monitered with beam moniter behind the sample cell in the experiment.

Fig. 3 The emission behaviors of 2,5-diphenyloxazole in cyclohexane (a) and toluene (b) obtained under the same condition. The concentration of 2,5-diphenyloxazole is 5 mM in both solutions. The apparant decays of the emission are $\sim$1.6 ns and $\sim$4.0 ns in cyclohexane and toluene solution, respectively. Time division is 110 psec.

Fig. 4 The growths of emission in different concentration of 2,5-diphenyloxazole in cyclohexane. The concentrations of 2,5-diphenyloxazole are a) 0.1 mM b) 5 mM c) 10 mM.
The Čerenkov light from the sample is clearly seen in 0.1 mM 2,5-diphenyloxazole-cyclohexane system. It is found that the growth time decreases with increasing the concentration of 2,5-diphenyloxazole.

Fig. 5 The spectra of the emission from the lowest excited state of 2,5-diphenyloxazole. The —— lines are in the case of 1 mM diphenyloxazole at 1; (●), 2; (▲) and 3ns; (×) after the pulse. The --- lines are in the case of 5 mM at 1; (o), 2; (△) and 3ns; (*) after the pulse. The peak shift at higher concentration is discussed in the text.

Fig. 6 The total emission ($\int_0^\infty [PPO^*]dt$) from the excited state of 2,5-diphenyloxazole obtained as the function of the concentration of 2,5-diphenyloxazole in cyclohexane. The behavior above and below 1 mM is different. The --- lines are calculated yield of 2,5-diphenyloxazole formed by the energy transfer from the excited state of cyclohexane molecules to 2,5-diphenyloxazole.

Fig. 7 The change of the emission of the excited state of 2,5-diphenyloxazole in 20 mM 2,5-diphenyloxazole in cyclohexane. The shaded parts in the figure is the emission from Čerenkov light.

a) The effect of CCl_4. The concentrations are ●; 0 mM, ▲; 50 mM, ■; 100 mM, o; 200 mM, ×; 300 mM and ●; 500 mM CCl_4.

b) The effect of triethylamine. The concentrations are ●; 0 mM, ▲; 100 mM, ■; 200 mM, o; 400 mM, ×; 600 mM and ●; 1 M.

Fig. 8 The change of the emission of the excited state of 2,5-diphenyloxazole in 1 mM 2,5-diphenyloxazole in cyclohexane. The shaded parts in the emission from Cerenkov light.

a) The effect of CCl_4. The concentration are ●; 0 mM, ▲; 50 mM, ■; 100 mM, o; 200 mM, ×; 300 mM and ●; 500 mM CCl_4.

b) The effect of triethylamine. The concentrations are ●; 0 mM, ▲; 100 mM, ■; 200 mM, o; 400 mM, ×; 600 mM and ●; 1 M triethylamine.

Fig. 9 The change of total emission yield, F, from the excited state of 2,5-diphenyloxazole obtained as the function of added CCl_4 and triethylamine. The concentration of 2,5-diphenyloxazole are 20 mM in (a), 1 mM in

(b) and 0.1 mM in (c). In each case, the total emission yield of 2,5-diphenyloxazole solution containing no scavenger was defined as Fo.

Fig. 10 The discrimination of the emission into the faster and slower process and the simulation using the values, $\alpha=3\times10^{9}$ sec^{-1}, $\beta=4\times10^{11}$ M^{-1} sec^{-1} and $k=6.3\times10^{8}$ sec^{-1}.

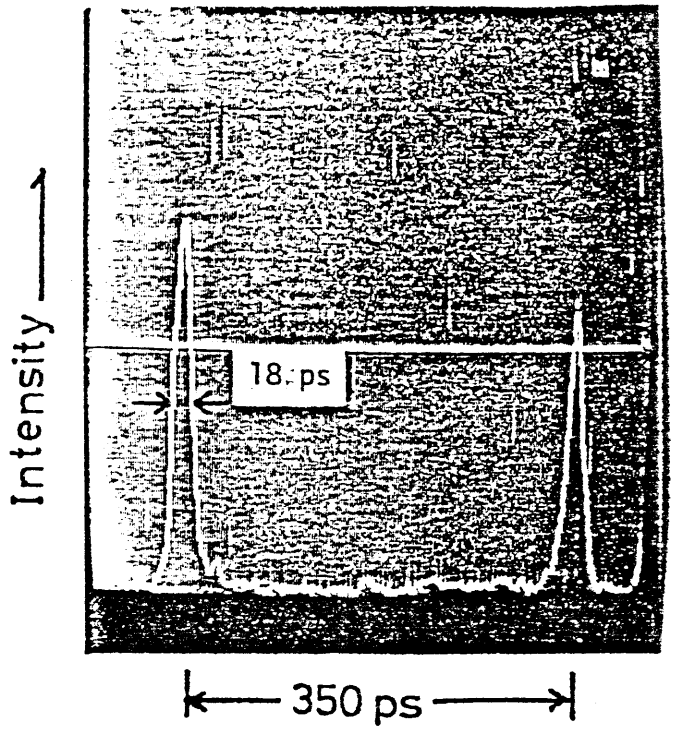

(a)

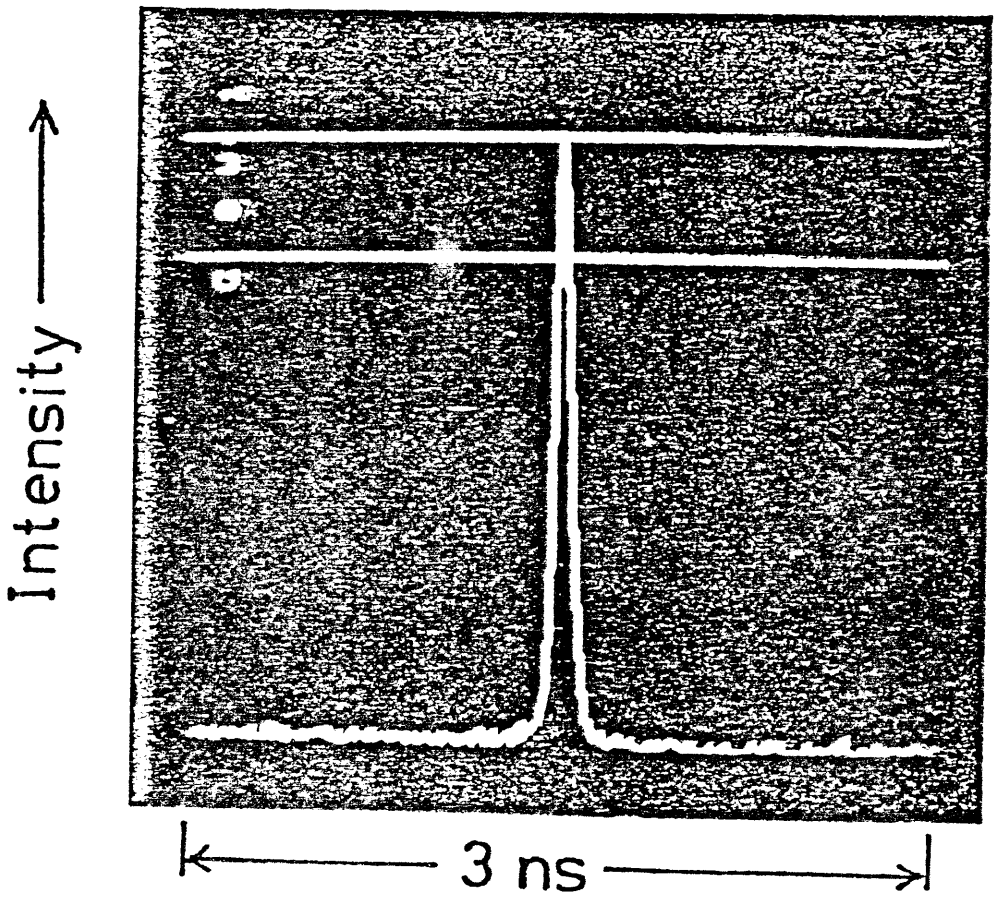

(b)

Fig.1

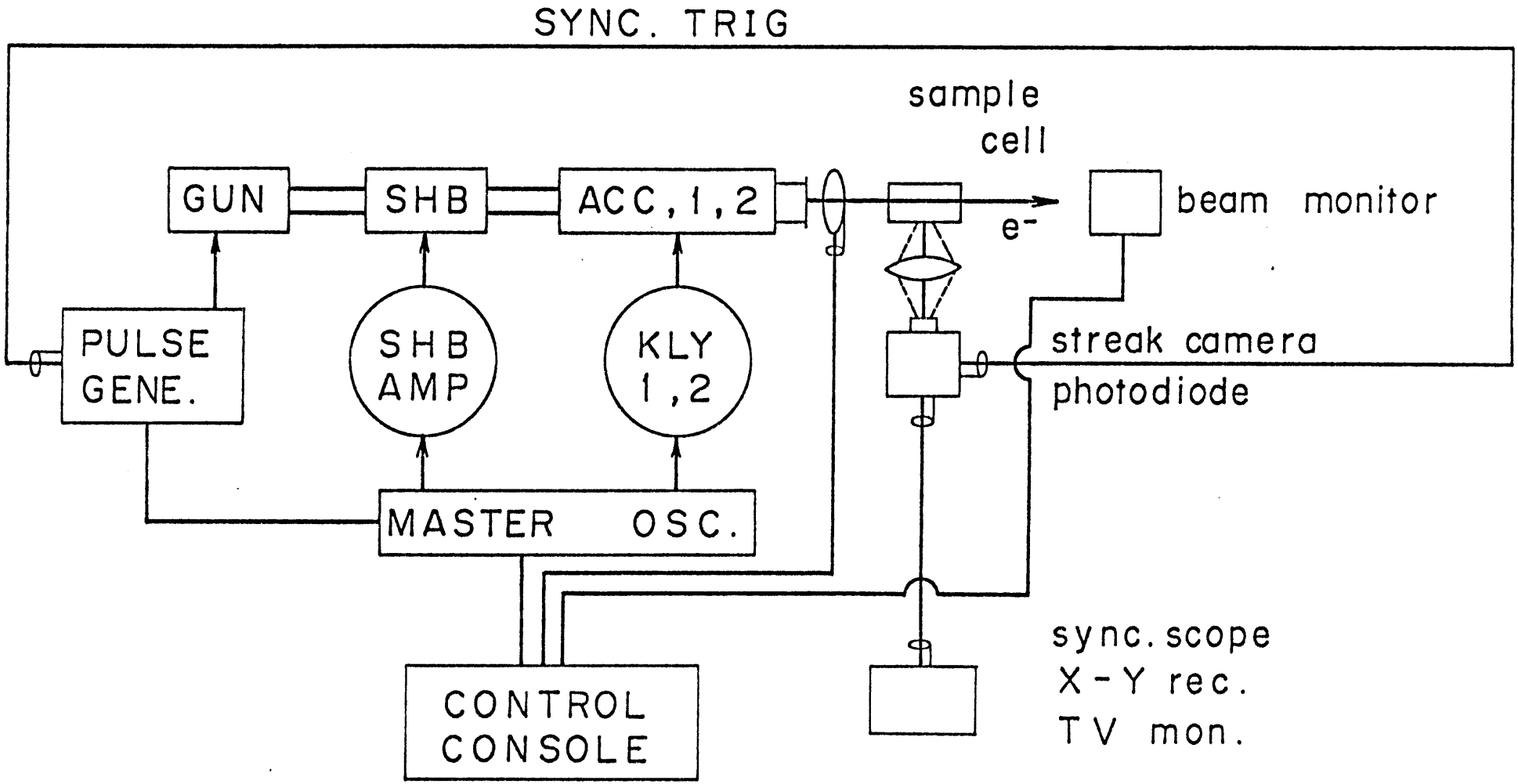
SYNC. TRIG
sample
cell
GUN
SHB
ACC, 1, 2
e-
beam monitor
PULSE
GENE.
SHB
AMP
KLY
1, 2
streak camera
photodiode
MASTER OSC.
sync. scope
X-Y rec.
TV mon.
CONTROL
CONSOLE

Fig.2

Scintillation Emission of PPO

Fig.3

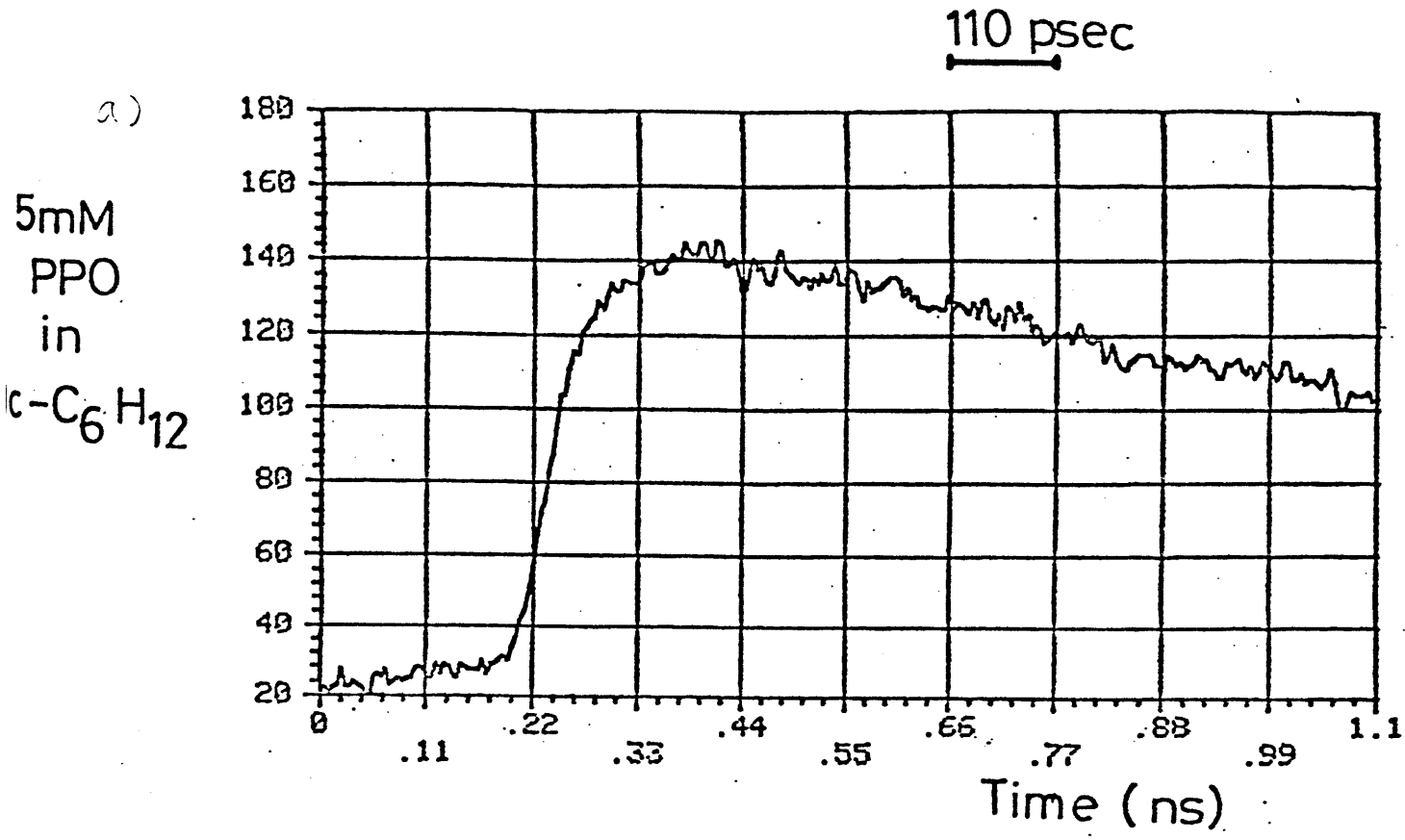

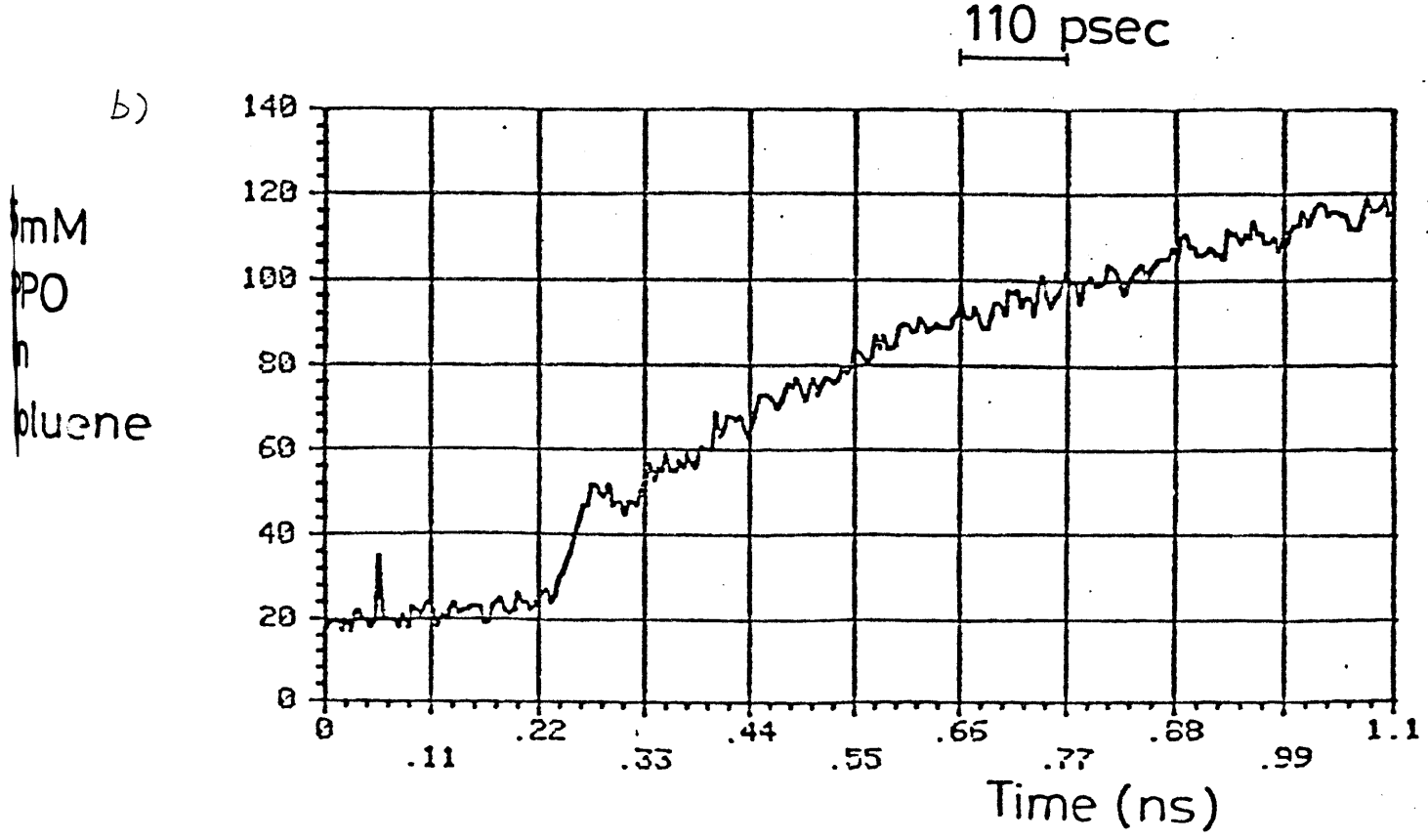

Fig.4 (a),(b) and (C)

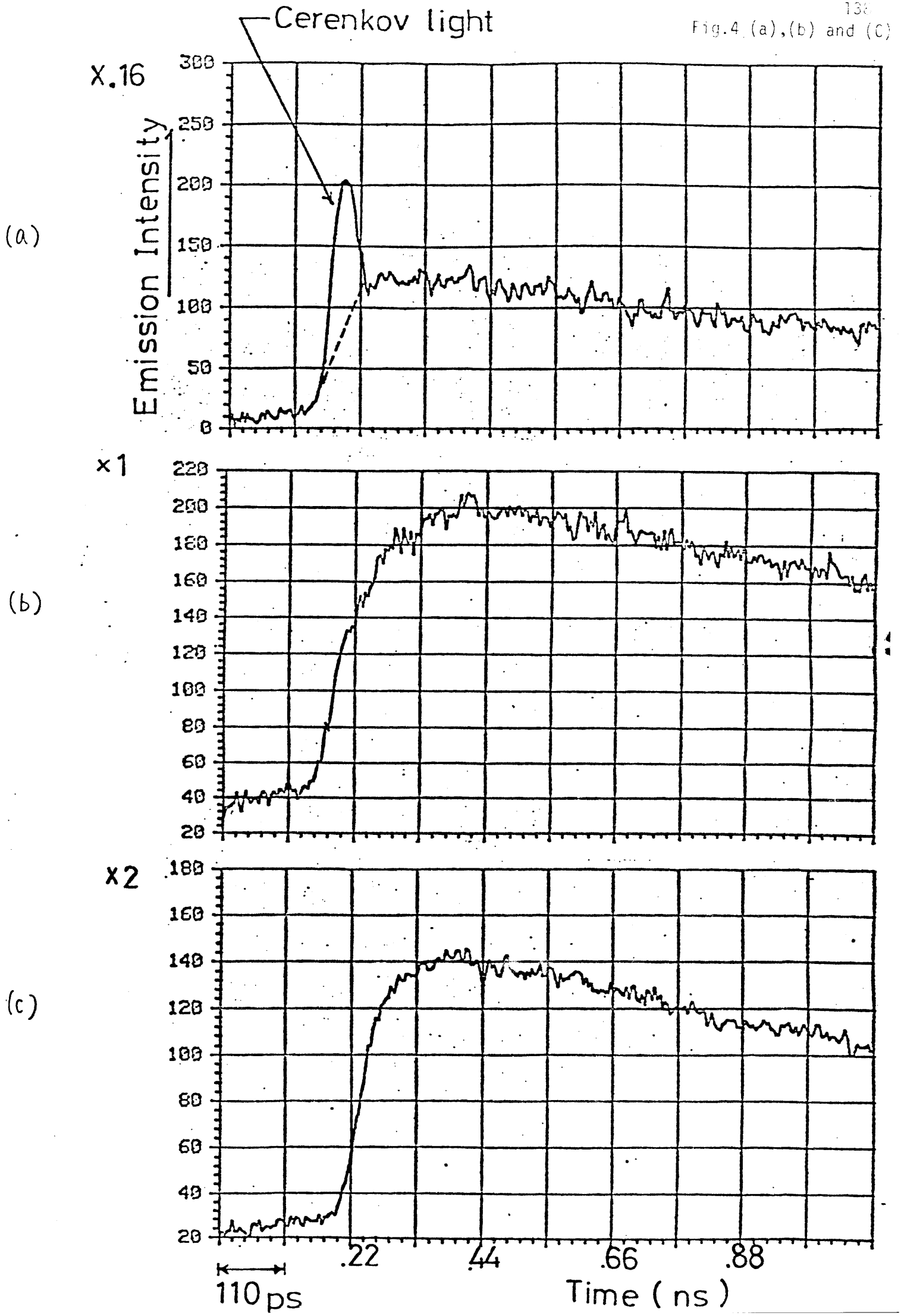
Čerenkov light
X.16
Emission Intensity
300
250
200
150
100
50
0
(a)
x1
220
200
180
160
140
120
100
80
60
40
20
(b)
x2
180
160
140
120
100
80
60
40
20
(c)
.22
.44
.66
.88
110 ps
Time (ns)

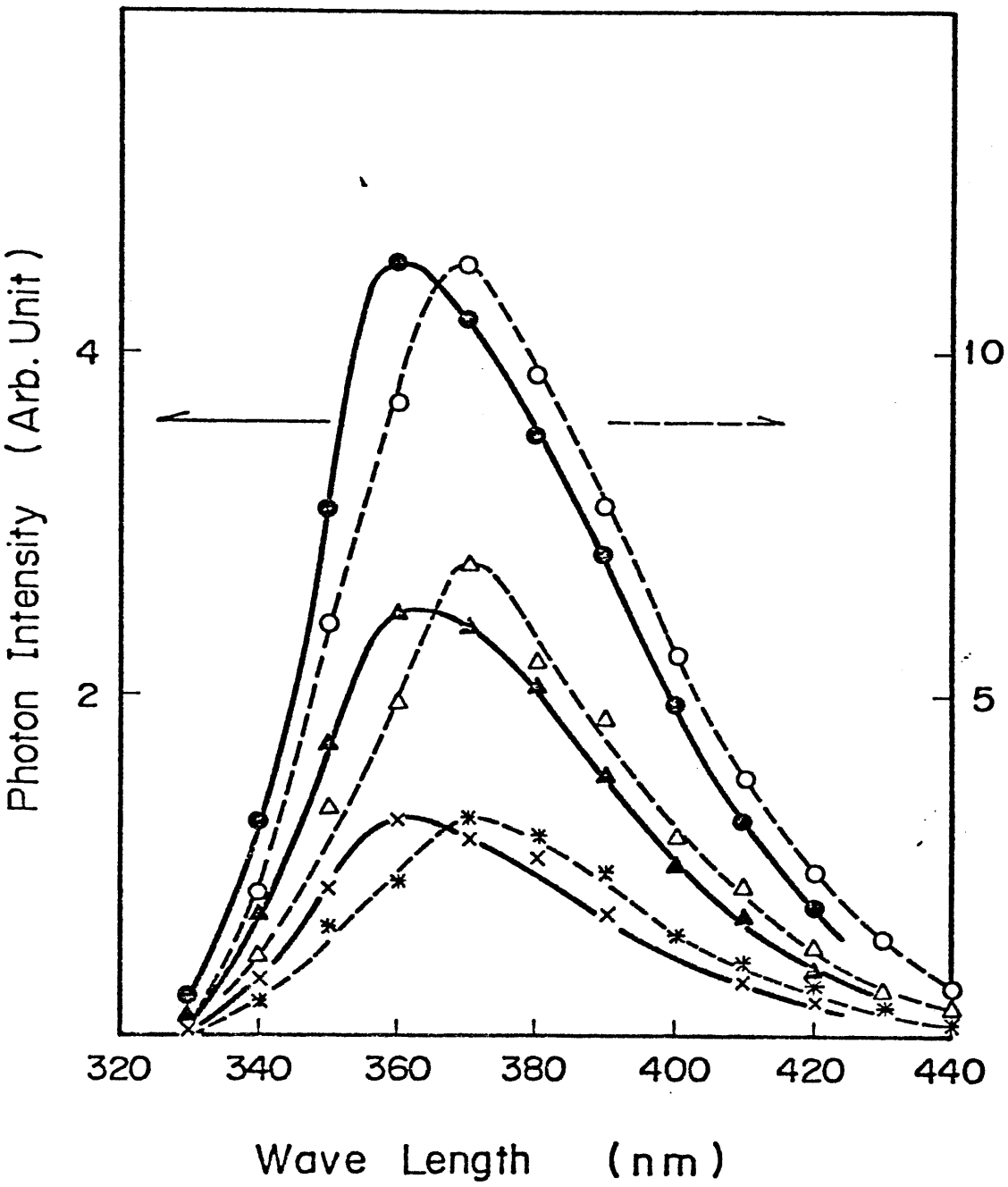
Photon Intensity (Arb. Unit)
4
2
10
5
320
340
360
380
400
420
440
Wave Length (nm)

Fig.5

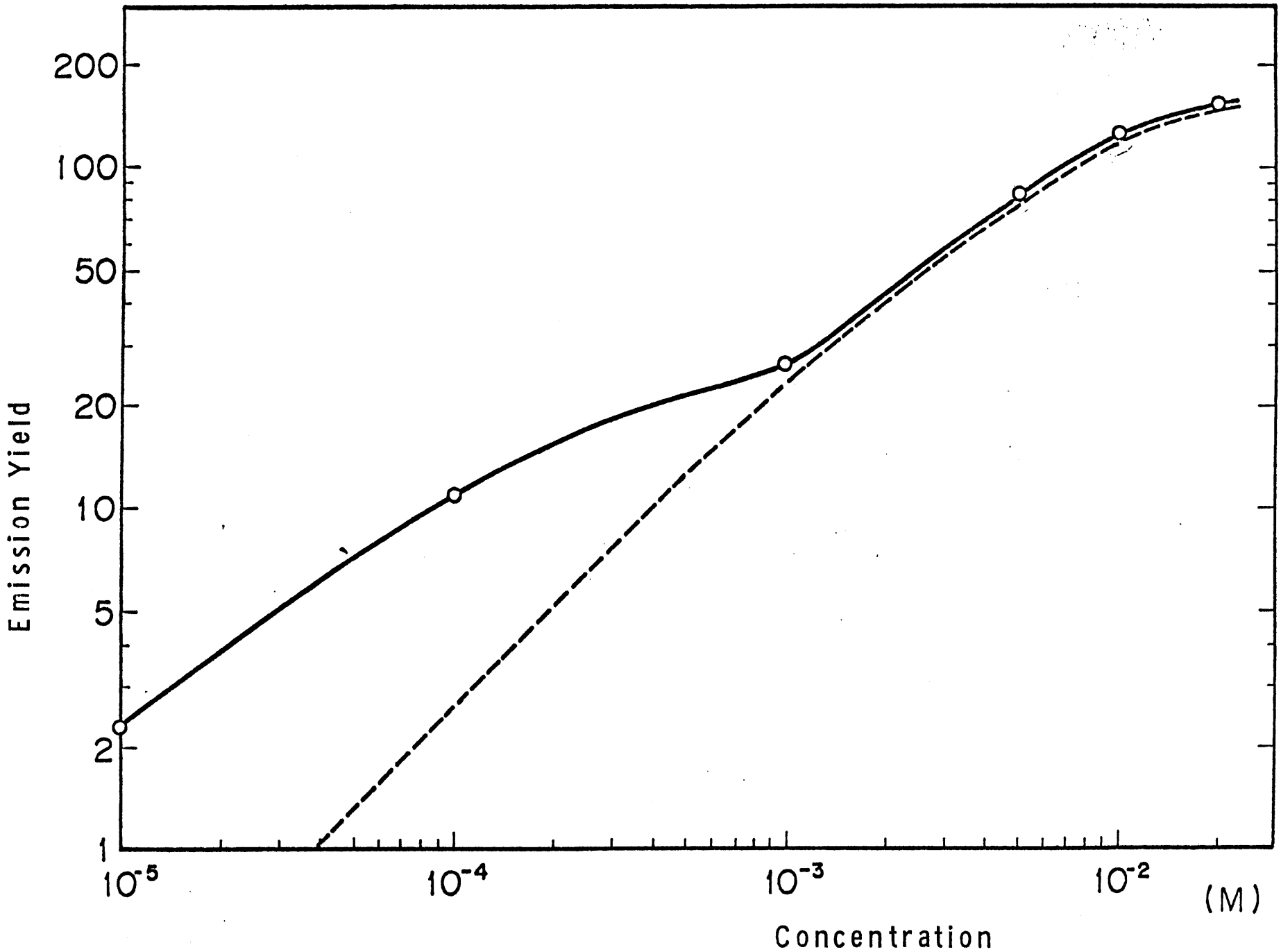
200
100
50
20
10
5
2
1
Emission Yield
10^{-5}
10^{-4}
10^{-3}
10^{-2}
(M)
Concentration

Fig.6

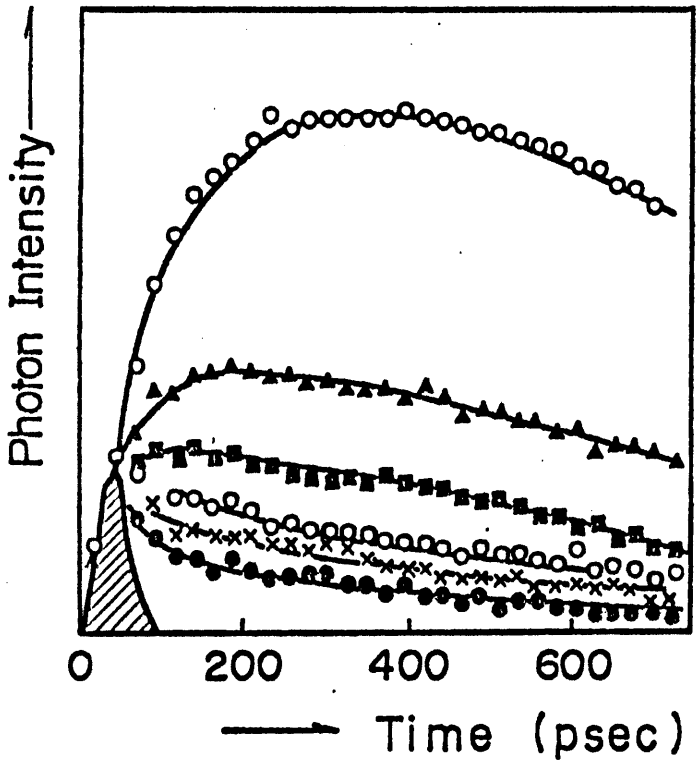
Photon Intensity
0
200
400
600
Time (psec)

(a)

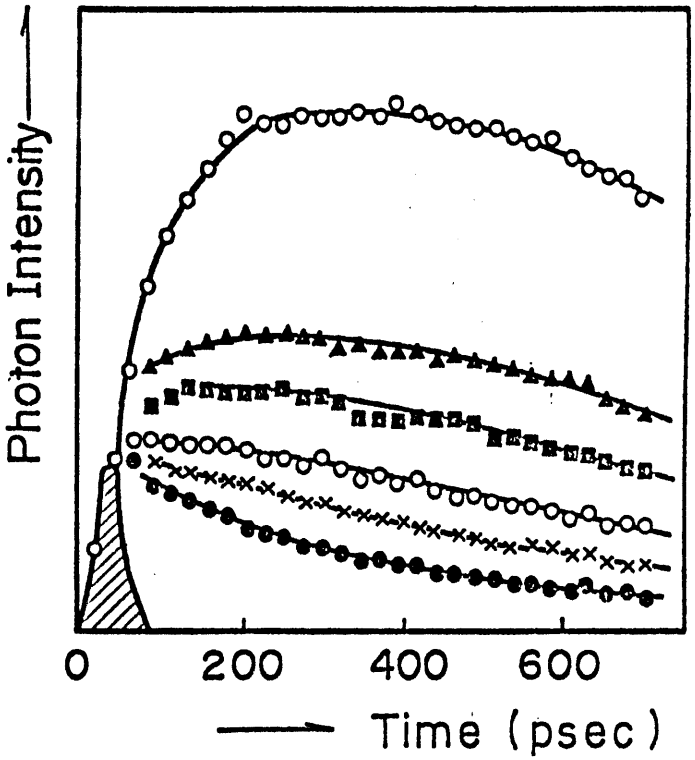
Photon Intensity
0
200
400
600
Time (psec)

(b)

Fig.7

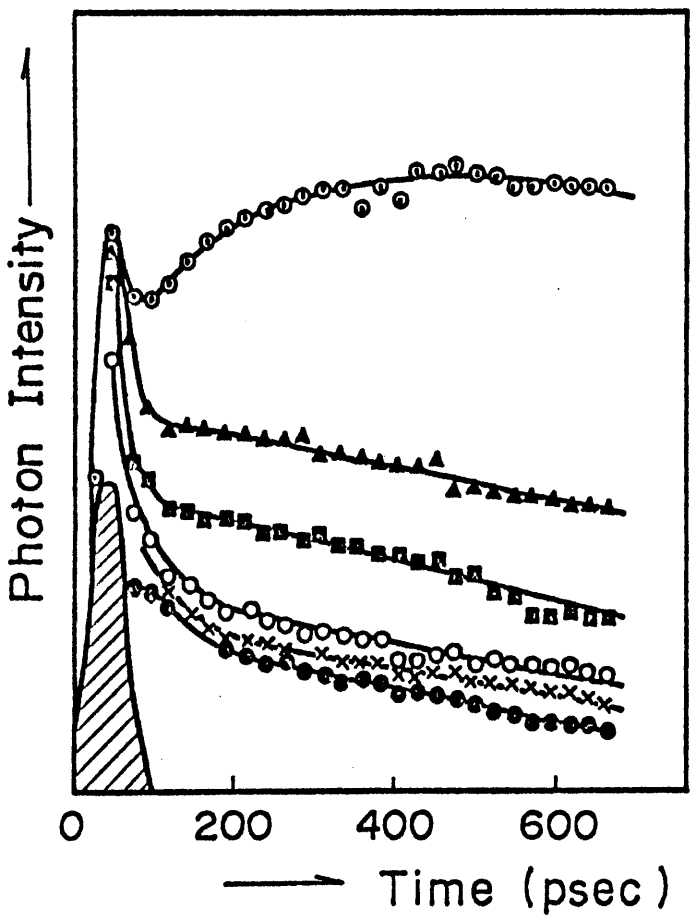
Photon Intensity
0
200
400
600
Time (psec)

(a)

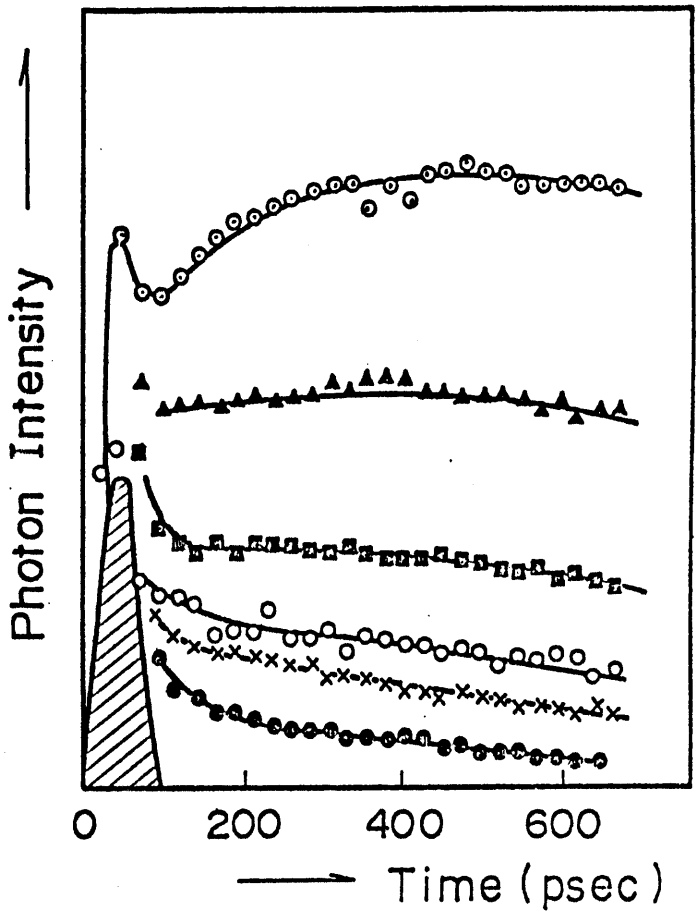
Photon Intensity
0
200
400
600
Time (psec)

(b)

Fig.8

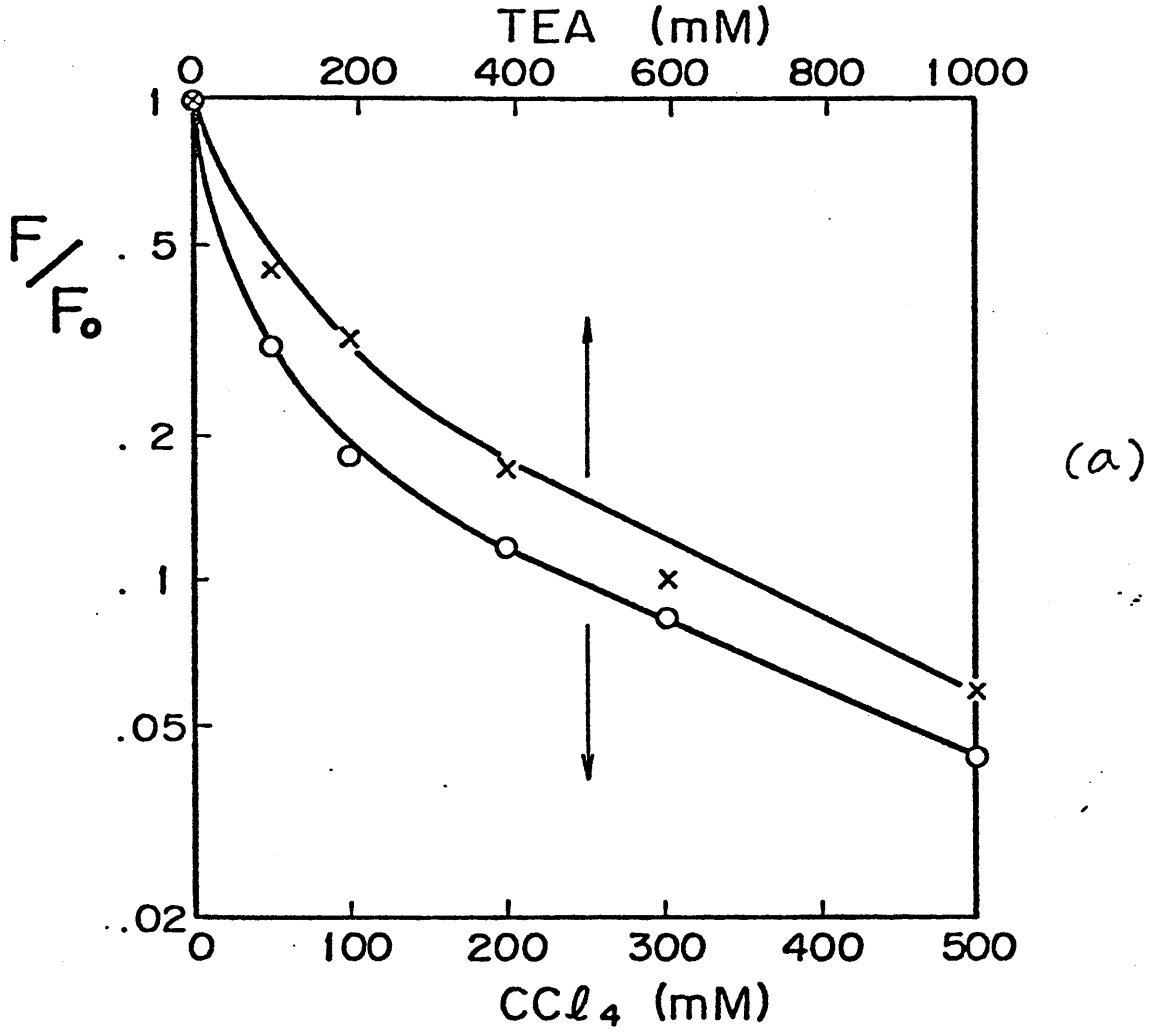
TEA (mM)
0
200
400
600
800
1000
1
.5
.2
.1
.05
.02
F/Fo
0
100
200
300
400
500
CCℓ4 (mM)

(a)

Fig.9 (a)

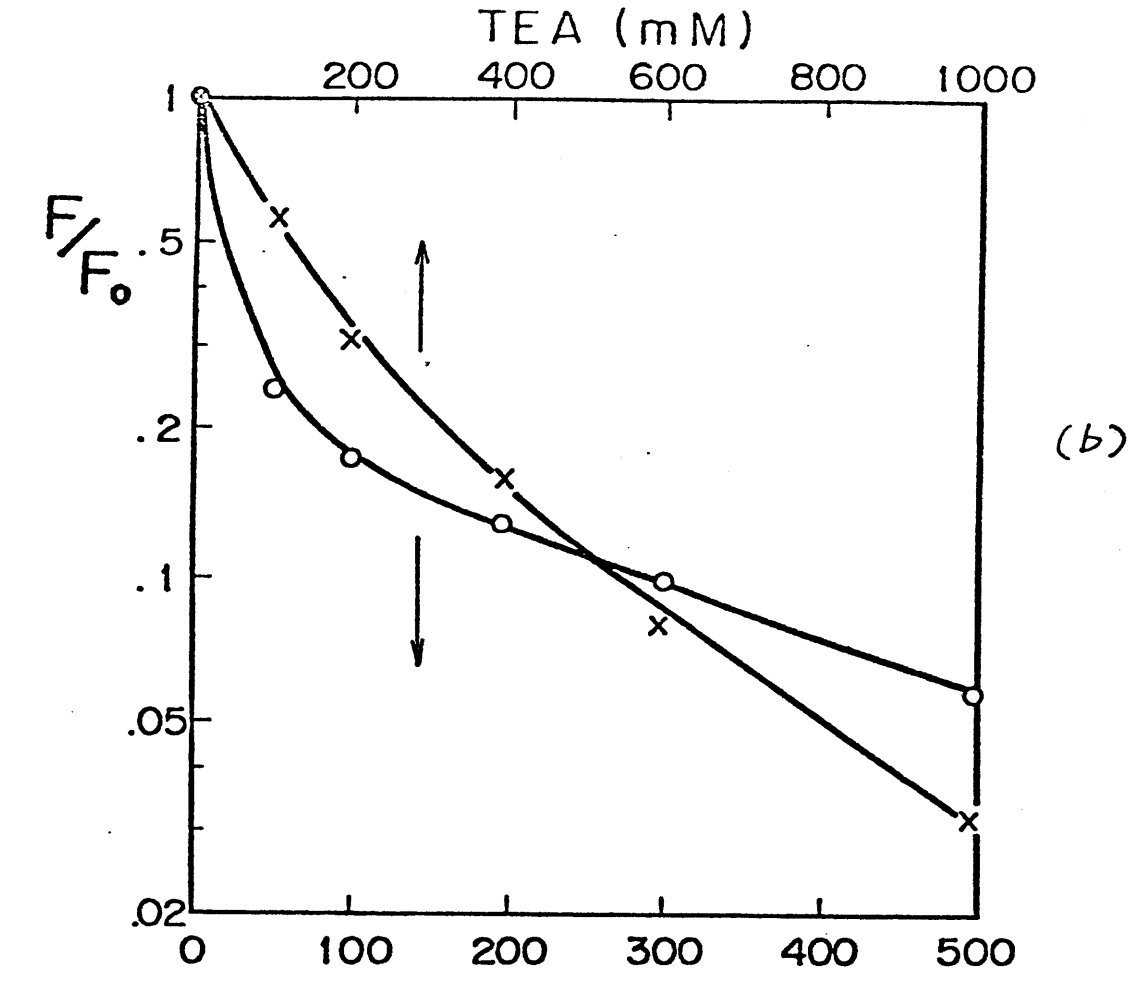

(b)

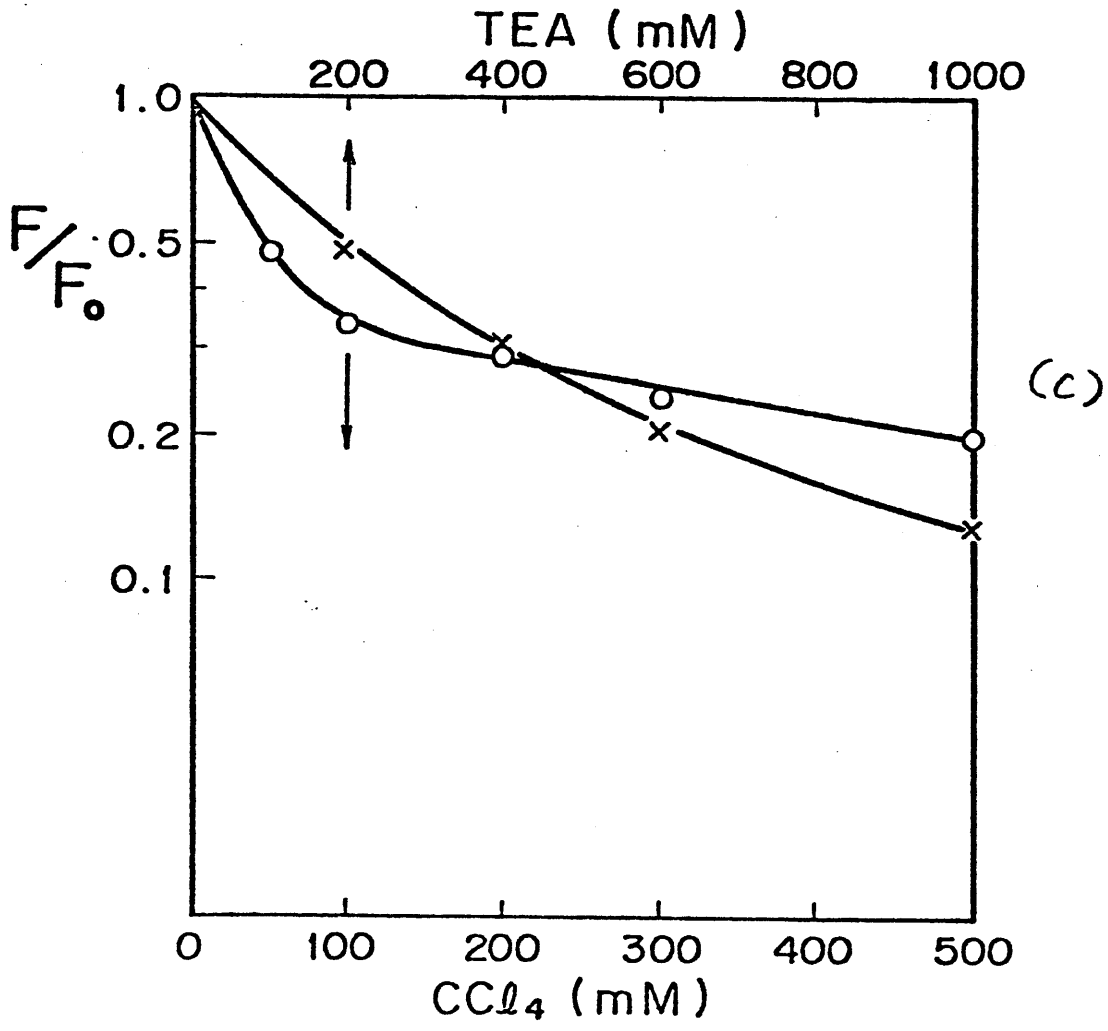

(c)

Fig.9 (b) and (c)

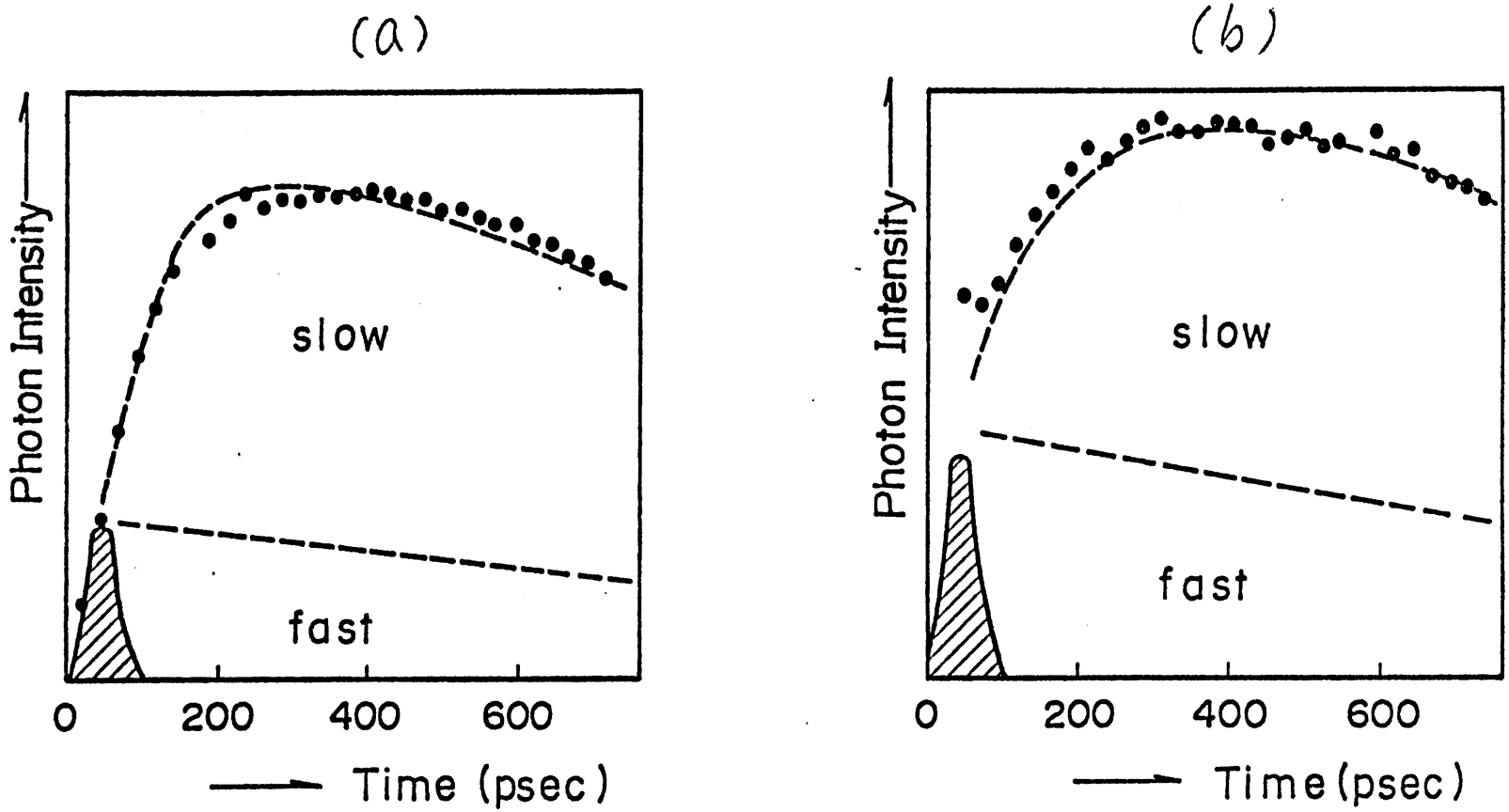
(a)
Photon Intensity
slow
fast
0
200
400
600
Time (psec)
(b)
Photon Intensity
slow
fast
0
200
400
600
Time (psec)

Fig.10 (a) and (b)

(C)

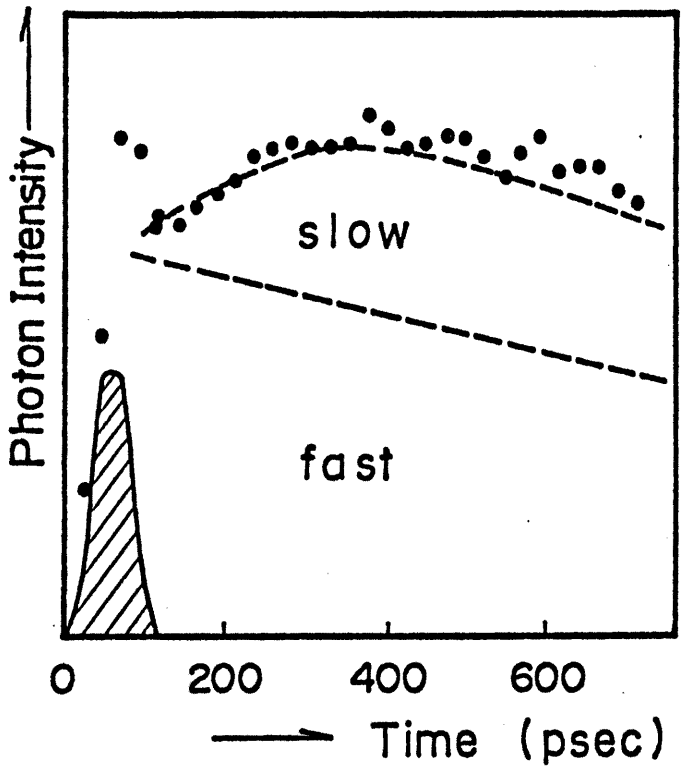

Fig.10 (c)

Chapter 7.

Direct Observation of Energy Transfer from Excited Cyclohexane Molecules to Toluene by Means of Picosecond Pulse Radiolysis

Summary

Direct observation of emissions from excited toluene molecules were made by means of picosecond single electron pulse radiolysis.

Energy transfer from excited cyclohexane to toluene was investigated by the same method, and the rate constant was obtained to be $\sim 8\times10^{10}$ $M^{-1}sec^{-1}$.

The fluorescence spectra from saturated hydrocarbons were reported by Hirayama and Lipsky[1]. They found that, in the presence of a small amount of benzene in cyclohexane, the intensity of fluorescence from the lowest excited state of cyclohexane decreases and at the same time the emission from excited benzene appears. This is one of the evidences that the energy transfer occurs from excited cyclohexane molecules to benzene.

Baxendale and Mayer[2] observed emissions from both cyclohexane and benzene excited state, and obtained the yield of solvent excited state from the energy transfer. They obtained a value, 2.8×10^{11} M^{-1} sec^{-1} for the rate of energy transfer and concluded that the yield of excited state of cyclohexane is not greater than 0.3.

Beck and Thomas[3] also obtained the rate constant of energy transfer from excited cyclohexane molecules to benzene by measuring the quenching of the emission from 9,10-diphenylanthracene in the presence of benzene molecules and the lifetime of the excited cyclohexane molecules. The rate constant of the energy transfer and the decay rate for excited cyclohexane were estimated to be 2.2×10^{11} $M^{-1}sec^{-1}$ and 3.6×10^{9} sec^{-1}, respectively.

Hatano et al[4] investigated energy transfer from excited cyclohexane to several solutes in liquid phase by means of product analysis. They found that rate constants of the energy transfer are larger than in a factor of 9∿24 than values expected for an ordinary diffusion controlled process.

As for the direct measurement of the lifetime of cyclohexane, Henry and Helman[5] obtained the lifetime in pure liquid to be 0.3 ns by a photon counting technique using a pulse X-ray source. However, Ware and Lyke[6] reported that the lifetime of the lowest excited cyclohexane in liquid is 0.68 ns by using a 156 nm pulse light source for the excitation. They also reported the lifetime of the lowest excited cyclohexane in gas phase in their latest paper.[7]

Recently, the emission from the lowest excited state of 2,5-diphenyloxazole in cyclohexane has been investigated by means of picosecond pulse radiolysis by the present authors. It was found that the emission is composed of the faster and the slower formation processes and the slower process is predominant at higher concentration of solute molecules (>1 mM).[8] The slower process is explained fairly well by energy transfer process.

Direct observation of emission from both excited cyclohexane molecule in the pure liquid and monomer excited toluene molecules in cyclohexane solution containing a small amount of those molecules are reported in the present paper.

The cyclohexane solution containing small amount of toluene (0.5∿2.0 vol %) was irradiated by picosecond single electron pulse (∿10 psec) from a linear accelerator at the Nuclear Engineering Research Laboratory, Univ. of Tokyo. The emission was observed by a streak camera with picosecond time resolution. In nsec time regions, a photomultiplier (HV R1194X) was also used. The details of the detection system and the accelerator were reported in our previous papers.[8] Although the emission from the excited state of cyclohexane is

very weak because of low fluorescence quantum yield, the lifetime was obtained to be ∿350 psec. The obtained lifetime is in good agreement with the values by Henry et al[5] and Beck et al.[3]

The emission form irradiated cyclohexane solution containing a small amount of toluene was attributable to monomer excited state of toluene. The lifetime of monomer excited state is obtained to be 34 ns, which is in a good agreement with liturature value. In pure liquid toluene, the emission spectrum has a tail at longer wave length, 320 nm ∿ 350 nm, compared with that in cyclohexane solution as shown in Fig. 1. Emission at longer wavelength is attributed to excimer of toluene. Total emission spectrum is composed of both monomer and excimer excited states of toluene. The lifetimes of two excited states in liquid toluene is a few nsec shorter than the value obtained Beck and Thomas[9] by laser photolysis.

The emissions from the excited toluene at different concentrations at 300 nm are shown in Fig. 2. Čerenkov radiation induced in the target solution by the electron pulse and the growth of the emission due to the formation of the lowest excited state of toluene molecules are clearly seen in the figure. These formation processes can be explained by energy transfer mechanism.

$$c\text{-}C_6H_{12} \xrightarrow[\text{very fast}]{\sim\sim\sim} c\text{-}C_6H_{12}^{*} \xrightarrow{\alpha} \text{decay} \qquad (1)$$

$$c\text{-}C_6H_{12}^{*} + \Phi CH_3 \xrightarrow{\beta[\Phi CH_3]} \Phi CH_3^{*} \xrightarrow{k} h\nu \qquad (2)$$

Since the lifetime of the excited cyclohexane is 330 psec[8] and that of monomer excited toluene is 34 ns, the rate constant (β) of the energy transfer, $\sim 8\times10^{10}\ M^{-1}\ sec^{-1}$, can be obtained. The formation of monomer excited state, (F(t)), in early stage is experessed as following.

$$F(t) \propto \frac{\beta[s]}{\alpha+\beta[s]} (1 - \exp\{-(\alpha+\beta[s]\}t) \qquad (3)$$

By using eq. (3), obtained simulation curve of the emissions are also shown Fig. 2. Obtained rate constant ($\sim 8\times10^{10}$ M^{-1} sec^{-1}) is in agreement with the rate constant of energy transfer reported by Baxendale et al[2] and Beck et al[3].

The emission from the faster processes discussed in scintillation system is considered to be negligibly small in this experiment.

References

[1] F. Hirayama and S. Lipsky; J. Chem. Phys. 51 3616 (1969)

[2] J.H. Baxendale and J. Mayer; Chem. Phys. Letts. 17 458 (1972)

[3] G. Beck and J.K. Thomas; J. Phys. Chem. 76 3856 (1972)

[4] T. Wada and Y. Hatano; J. Phys. Chem. 81 1057 (1977)

T. Wada and Y. Hatano; J. Phys. Chem. 79 2210 (1975)

[5] M.S. Henry and W.P. Helman; J. Chem. Phys. 56 5734 (1972)

[6] W.R. Ware and R.L. Lyke; Chem. Phys. Letts. 24 195 (1975)

[7] W.R. Ware and D.V. O'Conner; Chem. Phys. Letts. 62 595 (1979)

[8] S. Tagawa, Y. Katsumura, T. Ueda and Y. Tabata; Chem. Phys. Letts. 68 276 (1979)

S. Tagawa, Y. Katsumura and Y. Tabata; Rad. Phys. Chem. 15 287 (1980)

Y. Katsumura, S. Tagawa and Y. Tabata; J. Phys. Chem. 84 833 (1980)

Y. Katsumura, Y. Kanbayashi, S. Tagawa and Y. Tabata; to be submitted for publication

[9] G. Beck and J.K. Thomas; J. Chem. Soc. Farad. Trans. I, 72 2610 (1976)

[10] J.V. Jelley, "Čerenkov radiation and its application," Pergamon Press (1958)

Figure caption

Fig. 1 The emission spectrum (Δ) at 10 ns after the pulse in irradiated cyclohexane solution containing 1 vol% toluene. The spectral response of the system was calibrated by measuring the Cerenkov light based on the relation that the distribution of Cerenkov light intensity is proportional to $1/\lambda^2$[10]. The resolution of monochrometer was set as $\Delta\lambda\sim 10$ nm. The emission spectrum (o) at 10 ns in pure liquid toluene is also indicated. In pure toluene, the emission has a tail at longer wave length due to excimer formation.

Fig. 2 The emissions from excited toluene molecules due to energy transfer from excited states of cyclohexane in toluene solutions of cyclohexane with various concentrations. The emission was measured in a wave length at 300 nm by a streak camera. It is clearly seen that the emissions grow during or after the Cerenkov lights from the target solution, depending on the toluene concentration. Simulated curve (---) obtained by using the values, $\alpha = 3\times10^{9}$ sec^{-1} $\beta = 8\times10^{10}$ M^{-1} sec^{-1} and 34 ns for the lifetime of the excited toluene molecules.

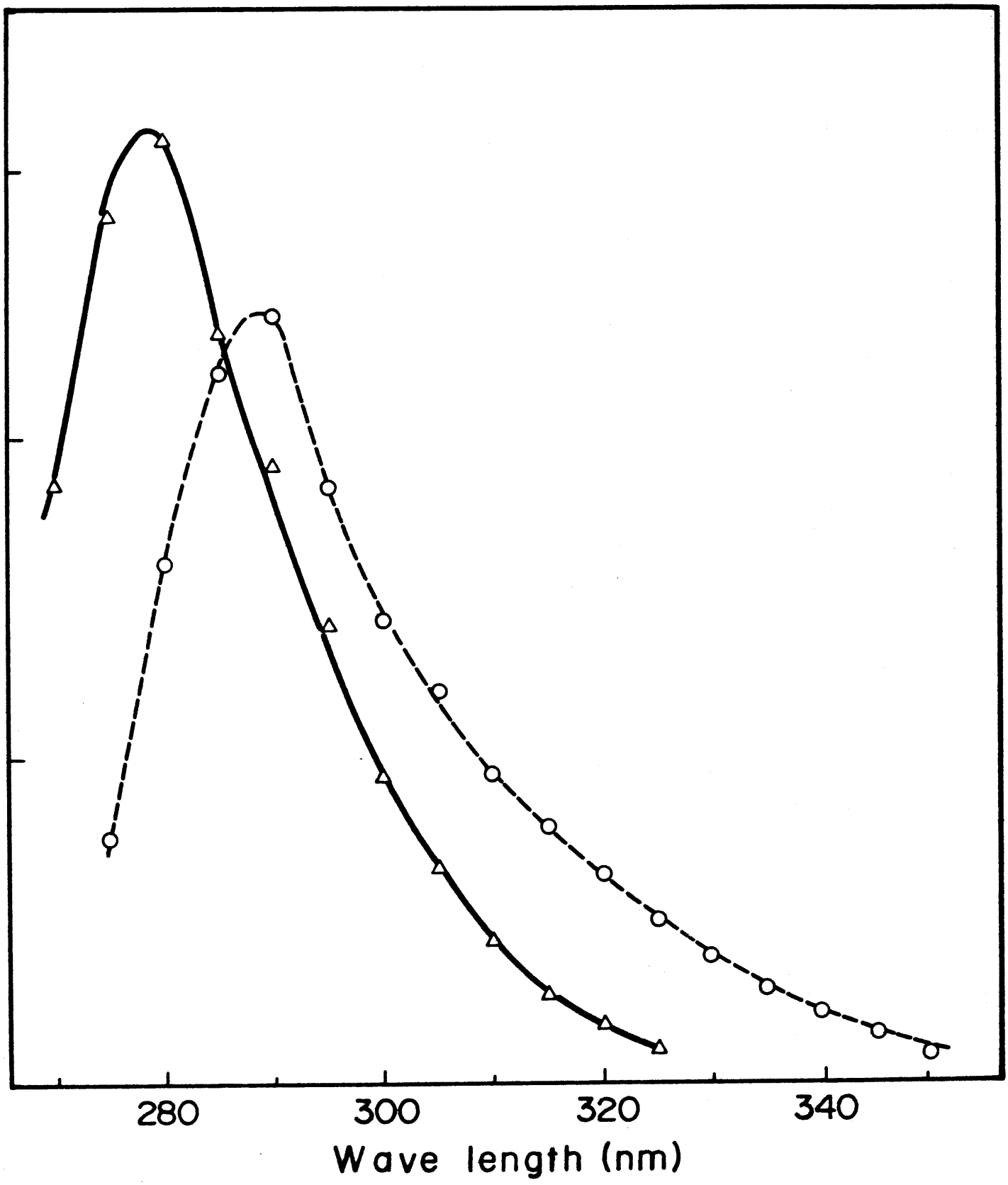

Fig.1

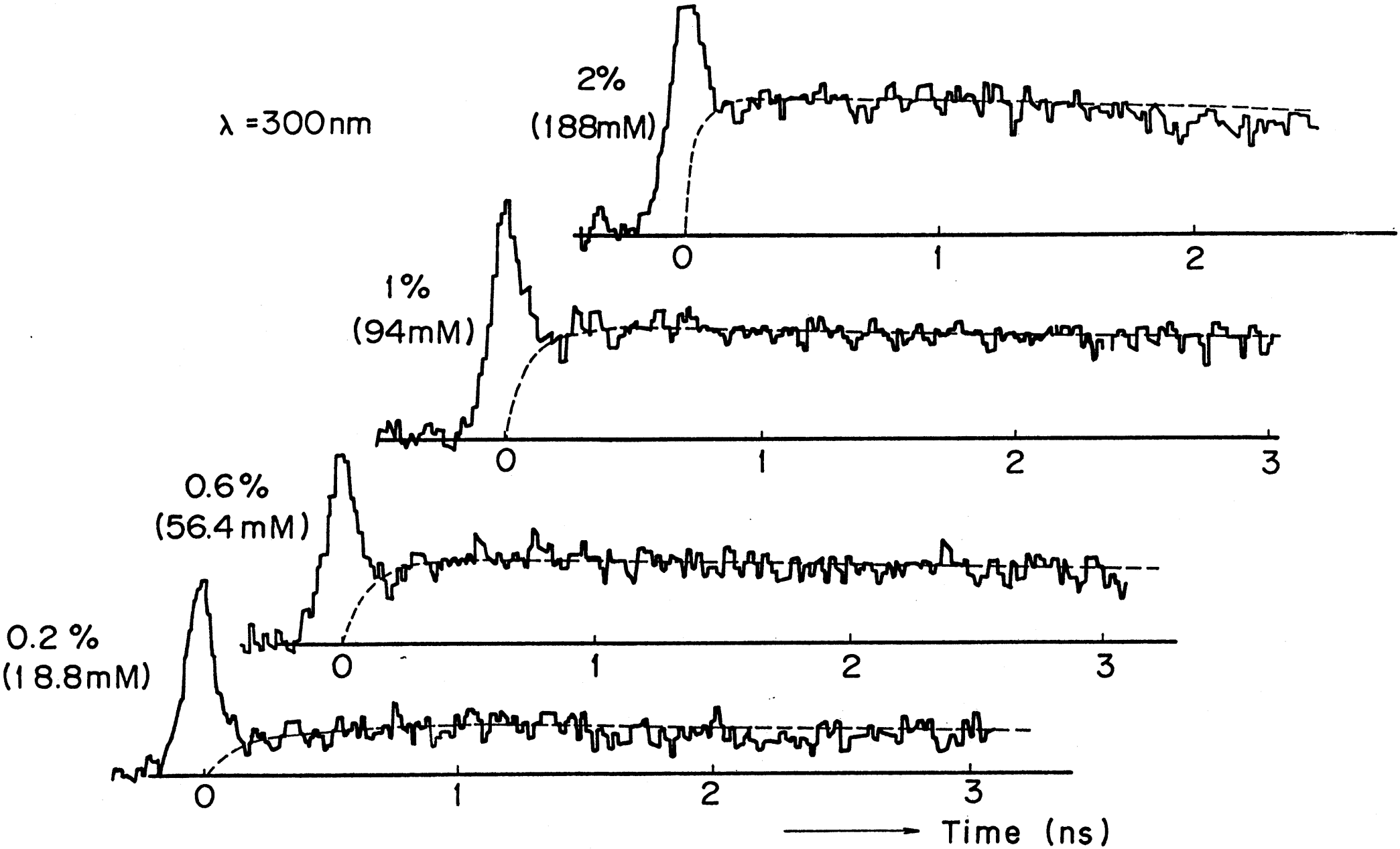

Fig.2

Chapter 8.

Studies on Energy Transfer Process in Liquid Toluene by Picosecond Pulse Radiolysis

Abstract

Emission from 2,5-diphenyloxazole in liquid toluene has been investigated by means of picosecond pulse radiolysis technique. The emission is attributable to the fluorescence of 2,5-diphenyloxazole. It was found that the decay of emission is strongly dependent on the concentrations of 2,5-diphenyloxazole. At lower concentrations of 2,5-diphenyloxazole, some fraction of the solute excited state is formed immediately after the pulse and gradual growth is also observed over one nanosecond. At higher concentrarions of 2,5-diphenyloxazole in toluene, gradual growth of emission becomes predominant and this formation process is explained fairly well based on energy transfer from both the lowest excited states of toluene and toluene excimer to 2,5-diphenyloxazole. Its rate constant was obtained to be $\sim 6 \times 10^{10} M^{-1} sec^{-1}$.

Introduction

Formation processes of solute excited states in liquid hydrocarbon produced by irradiation with high energy radiation have been widely investigated.[1] In aromatic solvents such as benzene, toluene and xylene many investigations have been carried out by photoexcitation[2] and irradiation, and formation mechanism of solute excited state by energy transfer from excited state of solvent molecules produced by photoexcitation and irradiation to solute

molecules has been widely accepted.[3] As for energy transfer process in liquid toluene, Birks et al[4] investigated on quenching of excited state of solvent and solute molecules using 2,5-diphenyloxazole (PPO) and obtained the rate parameters of solvent-solute energy transfer by photoexcitation. However, most of the studies were based on steady state method and a few studies with high time resolution were reported.

Recently, Beck et al[5] studied excited states of 9,10-diphenylanthracene in toluene with subnanosecond resolution using a Van de Graaf accelerator. They suggested that the probability of reaction of higher excited states of toluene molecules with 9,10-diphenylanthracene increases at lower temperature. They also used two photon excitation with laser pulses[6] and electron irradiation with L-band linear accelerator[7] for the study.

We have reported in our previous papers[8] that two formation processes of solute excited state in liquid hydrocarbons such as cyclohexane and toluene, can be clearly observed by means of picosecond pulse radiolysis with 30 psec time resolution. Those formation processes are called the slower and the faster processes from the view point of the formation time of excited solute molecules. Main part of the slower process is explained fairly well based on the energy transfer from the lowest excited state of solvent molecules to solute molecules. On the other hand, the faster process, in which the growth of the emission is completed immediately after the electron pulse ($\leq$18 psec), is thought to be mainly due to the rapid recombination of solute and solvent charged species. From these observations, various kinds of solvents have been classified into three groups from the points of combination of these two processes and emission efficiency.[9]

In liquid toluene, not only the excited state monomer but also the excimer are formed by irradiation. Existence of both the excited state monomer and the excimer in toluene gives a different aspect in the energy transfer process

from saturated hydrocarbon such as cyclohexane in which only monomer type excited state is formed. In the present paper, the excitation process in toluene containing 2,5-diphenyloxazole is discussed.

It is well known that formation yield of excited state of solute molecules such as 2,5-diphenyloxazole, para-terphenyl in aromatic solvents is very high as compared with that in saturated hydrocarbons,[9] and aromatic solvents have been widely used in liquid scintillation counters.[10] To get new scintillation counters having rapid rise, rapid decay and high efficiency, it is thought that studies on the formation processes of solute excited state in liquid aromatics with high time resolution is very important.

Experimental

The 35 MeV linear accelerator at the Nuclear Engineering Research Laboratory, University of Tokyo is capable of producing a single picosecond (∿10 psec) electron pulse by means of a subharmonic buncher. The pulse width is estimated to be ∿18 psec. The value of pulse width, 18 psec, is obtained by using a streak camera to detect Čerenkov light arising from electrons passing through air. The detection system is composed of the streak camera and its analyzing systems. The time resolution of the detection system is estimated to be less than 18 psec. The details of the linac and detection system (Hamamatsu TV Co.Ltd.) are reported in previous papers.[11]

For the measurement with high time resolution, the streak camera was mainly used. In time regions longer than nsec, a photomultiplier (R1194X, Hamamatsu TV Co.Ltd.) was also used. The risetime of this photomultiplier is found to be ∿250 psec (from 10 % to 90 %) from observing Čerenkov light with a sampling oscilloscope (TEKTRONIX, 4S sampling head).

In observing the spectrum of emission, a monochrometer (Ritsu MC-10 N) combined with the streak camera or the photomultiplier was also used.

The spectral response which depends on wavelength in the detection system including the monochrometer was calibrated using Cerenkov light as a standard light source. It is well known that the intensity of Cerenkov light is propotional to $1/\lambda^2$.[12]

The toluene, cyclohexane and 2,5-diphenyloxazole used were guaranteed grade from Tokyo Kasei Co. Ltd. The samples were degassed by connecting them with a vacuum line.

Results

By using the streak camera, the growth curves of emissions from excited 2,5-diphenyloxazole in toluene solutions at various concentrations were obtained. They are shown in Fig. 1. It is seen that the growth of the emission varies very much by changing the concentration of 2,5-diphenyloxazole. At lower concentrations, both the rapid growth and the following slow one are clearly seen. These formation processes are called the faster process and the slower one, respectively. From observing emissions at different concentraions, it was found that the faster process is dominant at lower concentrations, and that the ratio of the slower process to the total process in the intensity of emission increases with increasing concentration of solute and the slower process becomes predominant above 1 mM concentration of the solute.

The emission spectra from 2,5-diphenyloxazole at different time after the pulse are shown in Fig. 2. The spectra obtained is slightly different between above 5 mM and below 1 mM of the solute. Below 1 mM, the spectra are the same with those of fluorescence obtained from photolysis study.[13] However, in the case of 5 mM, the peak of the spectra shifts to a longer wavelength. This red-shift is caused by reabsorption of emissions by 2,5-diphenyloxazole itself at higher concentrations. These results obtained in liquid toluene are similar to those in liquid cyclohexane.[8] It is noted

that changes of the spectra with time do not occur, as indicated in Fig. 2.

In longer time regions, the decays of these emissions were obtained with the photomultiplier. Emission at 380 nm was detected and obtained apparent decay is strongly dependent on the concentration of the solute, as shown in Fig. 3. The decay at higher concentrations is faster than that at lower concentrations. It is also noted that decays can not be written by a single exponential term, because the decay curves are not linear as indicated in Fig. 3 for the semi-logarithmic plot.

These results obtained in liquid toluene are very different from those in liquid saturated hydrocarbon. In cyclohexane, the decay of emission is independent of the concentration and the decay is almost the same with the natural lifetime of 2,5-diphenyloxazole, 1.6 ns.[13]

In pure liquid toluene containing no solute, the emissions due to both the monomer excited state and the toluene excimer were observed in a wavelength region of 275 nm ∿ 350 nm, as shown in Fig. 4(a). The decay rates were found to be (∿25±3) ns and ∿(28±3) ns for 280 nm and 360 nm, respectively. These values are slightly smaller than those obtained in photolysis and pulse radiolysis studies [6],[7] Since quantum yields of excited toluene and toluene excimer are rather low, and lifetimes are over 20 nsec, the emission intensities are weak and the data obtained with the streak camera have a poor S/N ratio. However, it is clearly seen that formation of these toluene excited states are completed immediately after the electron pulse, as shown in Fig. 4.

Discussion

At higher concentration ranges of solute, gradual growth of the emission becomes predominant and its growth and decay can be explained by energy transfer mechanism. Mechanism of energy transfer is assumed that the energy donor, solvent excited states, is produced very fast within pulse duration by irradiation

and energy transfer ocurrs from excited solvent molecules to solute molecule, as shown following.

$$M \xrightarrow{\sim\sim} M^* \qquad (1)$$

$$M^* \xrightarrow{\alpha} \text{decay} \qquad (2)$$

$$M^* + S \xrightarrow{\beta[S]} S^* \qquad (3)$$

$$S^* \xrightarrow{k} \text{emission} \qquad (4)$$

where M, M^*, S, S^*, α, β and k are the solvent molecule, the excited state of the solvent molecule, the solute molecule, the excited state of the solute molecule, the decay rate of M^*, the rate of energy transfer from M^* to S, and the decay rate of S^*, respectively. The intensity of emission from S^* with time is expressed by the following equation.

$$F \propto \frac{\beta[S]\cdot k}{\{(\alpha+\beta[S])-k\}} \left[\exp(-kt) - \exp\{-(\alpha+\beta[S])t\}\right] \qquad (5)$$

If the value of $\alpha+\beta[S]$ is larger than k. Therefore, the decay of emission from 2,5-diphenyloxazole is independent of the concentration of solute and is proportional to exp(-kt) at longer times. These predictions are consistent with our observed results in cyclohexane.[8]

In cyclohexane-toluene, since the lifetime of toluene monomer excited stated is much larger than that of 2,5-diphenyloxazole and consequent value of k is rather small compared with the case of 2,5-diphenyloxazole in pure cyclohexane, the second term is also eliminated in the longer time range, and the emission is also proportional to exp(-kt). On the other hand, the growth of emission is expressed as $\{\beta[S]\cdot k/(\alpha+\beta[S])\}(1-\exp\{-(\alpha+\beta[S])t\})$ in the shorter time range as reported in a previous paper.[8]

As for 2,5-diphenyloxazole in toluene solution, k is larger than the term $\alpha+\beta[PPO]$ in diluted solutions, because k is $6.3\times10^8 (=(1.6\ ns)^{-1})$, and

α^{-1} is over 20 nsec. However, with increasing concentration of 2,5-diphenyloxazole, the term $\alpha+\beta[PPO]$ becomes larger. If the value of β is about $10^{11}M^{-1}\cdot sec^{-1}$, the term $\alpha+\beta[PPO]$ becomes nearly equal to k at 5 mM of PPO. Hence, the intensity of emission with time is predicted to be strongly dependent on the concentration of 2,5-diphenyloxazole. Furthermore, the time dependencies of emission intensity can be expressed by not a single exponential term but two exponential terms.

In pure liquid toluene, it was found that both the monomer lowest excited state and the toluene excimer are formed within the pulse duration. Not only the excited monomer but also the toluene excimer have enough energy to transfer the energy from themselves to solute molecules. Therefore, both the lowest excited monomer and the toluene excimer should be sources of energy transfer to the solute molecules independently. However, since the decay times of both excited states have almost the same values, it can be assumed for simplification that dynamic equilibrium is achieved very rapidly between the excited state monomer and the toluene excimer. This assumption is reasonable because the formation of these two excited states is completed during the pulse duration, and those emissions from them start immediatly after the pulse, as shown in Fig. 4.

Since the slower process is predominant at higher concentrations, the best parameter for fitting the observed results in the higher concentration region is found to be $\beta=6\times10^{10}M^{-1}sec^{-1}$, when α and k are assumed to be $(27\ ns)^{-1}$ and $(1.6\ ns)^{-1}$, respectively. Decay of emission from excited 2,5-diphenyloxazole at 10, 5, 1 mM are fairly well simulated as shown in Fig. 5. At 0.1 mM of 2,5-diphenyloxazole, the observed intensity is larger than calculated one. Considering that the faster process is predominant at lower concentrations as indicated in Fig. 1, the observed emission is composed of a large fraction of the faster process and a small fraction of the slower process. However,

contribution of the faster process is predominant at short times and decay of emission at longer times should be obey the prediction because emission due to the faster one decays rapidly. If fact, the decay behavior from simulation agrees well with the experimental result at 0.1 mM solution. Therefore, this discrepancy is resonable. At higher concentrations the slower process is predominant, and a good fit to the observed results can be obtained. The rate constant of energy transfer, 6×10^{10} M^{-1}, is in a reasonable agreement with literature values of 4.7×10^{10} M^{-1} sec^{-1}(2), 1.1×10^{11} M^{-1} sec^{-1}(5) and 7×10^{10} M^{-1} sec^{-1}.(7)

Evidence of higher excited states of toluene in energy transfer reactions at lower temperatures, suggested by Beck and Thomas, has not been obtained directly in our present experiment. Our observed results can be explained by an energy transfer mechanism without considering higher excited states of toluene.

In scintillation systems, the faster and the slower processes are observed. For slower processes in 2,5-diphenyloxazole solution of toluene, the emission is fairly well explained by energy transfer from excited solvent to solute molecules. This energy transfer mechanism plays an important role in early processes of scintillation system, especially in aromatic solvents.

As for the faster process, it is predominant in the lower concentration range of solute, and the precise mechanism for the fast formation of excited 2,5-diphenyloxazole within the pulse duration has not yet been made clear. However, several possibilities for the fast formation of the solute excited state are under consideration. At present, it is thought that rapid recombination of solute charged species plays an important role for the faster process.

References

1) J.K. Thomas; Int. J. Radiation Phys. Chem. 8 1 (1976)

2) J.B. Birks "Photophysics of Aromatic Molecules" Wiley-Interscience (1970)

3) F. Hirayama and S.Lipsky in "Organic Scintillators and Scintillation Counting" ed. by D.L. Horrocks and C-T. Peng p205, Academic Press 1971.

4) J.R. Greenleaf, M.D. Lumb and J.B. Birks; J. Phys. B, II 1157 (1968)
J.B. Birks, H.Y. Najjar and M.D. Lumb; J. Phys. B, Molec. Phys. 4 1516 (1971)

5) G. Beck, J.T. Richards and J.K. Thomas; Chem. Phys. Lett. 40 300 (1976)

6) G. Beck and J.K. Thomas; J. Chem. Soc. Farad. Trans. I, 72 2610 (1976)

7) G. Beck A. Ding, and J.K. Thomas; J. Chem. Phys. 71 2611 (1979)

8) S. Tagawa, Y. Katsumura and Y. Tabata; Chem. Phys. Lett. 64 258 (1979)
S. Tagawa, Y. Katsumura and Y. Tabata; Rad. Phys. Chem. 15 287 (1980)
Y. Katsumura, S. Tagawa and Y. Tabata; J. Phys. Chem. 84 833 (1980)

9) Y. Katsumura, T. Kanbayashi, S. Tagawa and Y. Tabata; to be published

10) for example; "Liquid Scintillation Counting" vol.1∿6 Proceedings of a Symposium on Liquid Scintillation Counting, Heyden & Son Ltd.

11) Y. Tabata, J. Tanaka, S. Tagawa, Y. Katsumura, T. Ueda and K. Hasegawa; J. Fac. Engi. Univ. Tokyo 34 619 (1978)

12) J.V. Jelly, "Cerenkov radiation and its application," Pergamon Press (1958)

13) I.B. Behman "Hand-book of Fluorescence Spectra of Aromatic Molecules" Academic Press (1971)

Figure Captions

Fig. 1 Growth of emissions from 2,5-diphenyloxazole of several concentrations in liquid toluene detected with the streak camera. Concentrations of (a)∿(d) are 0.1, 1, 5 and 10 mM, respectively. In both 0.1 and 1 mM solutions, Čerenkov light produced in sample medium by electron pulse is clearly seen at the injection of electron pulse. It is noted that some fraction of the formation of excited 2,5-diphenyloxazole is already completed immediately after the Čerenkov light. These data are obtained by accumulation of 20 signals. Time resolution of this accumulation mode is estimated to be less than 30 psec.

Fig. 2 Emission spectra of 5 mM; (a) and 1 mM; (b) 2,5-diphenyloxazole in toluene. Values of time in figures indicates the time after irradiation by electron pulses. No change of emission spectra with time is observed. It is also noted that the emission of 5 mM solution decays faster than that of 1 mM solution. Defference of emission spectra is discussed in text.

Fig. 3 Semi-logarithmic plot of emission at 380 nm from the lowest excited state of 2,5-diphenyloxazole in liquid toluene. Decay time strongly depends on the concentration of solute.

Fig. 4 a) Emission spectra obtained at 10 ns after electron pulse in pure toluene (o) and cyclohexane containing 0.5 vol% toluene (Δ) measured under the same condition by the photomultiplier. The latter spectram is similar to the emission from toluene monomer excited state, reported by Berlman.[14]

b) Emission from two excited states of toluene obtained with streak camera. At 320 nm the emission is attributable to mainly that from excimer to toluene. However, the emission at 300 nm is

composed of two emissions from the excited monomer toluene and the excimer. The formations of two excited states of toluene are completed at the end of Čerenkov light produced in sample medium by electron pulse.

Fig. 5 Simulated curve fitting to the experimental results, obtained by using following parameters $\alpha=3.70\times10^{7}sec^{-1}$, $\beta=6\times10^{10}M^{-1}sec^{-1}$, and $k=6.3\times10^{8}sec^{-1}$ and eq. (5). Agreement between simulation and experimental reaults is fairly well, except 0.1 mM 2,5-diphenyloxazole solution.

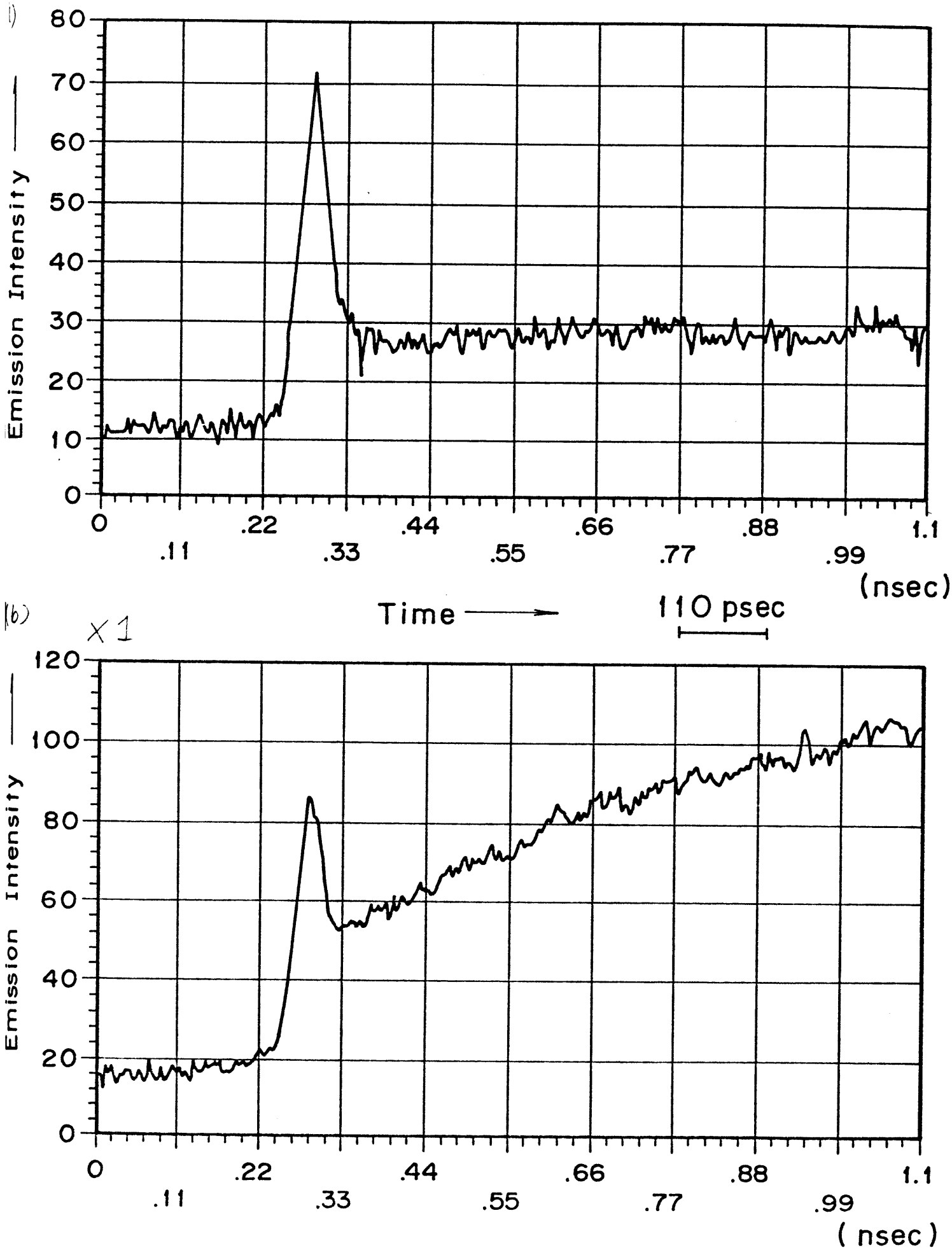
(a)
Emission Intensity
80
70
60
50
40
30
20
10
0
0
.11
.22
.33
.44
.55
.66
.77
.88
.99
1.1
(nsec)
(b)
Time
110 psec
X 1
Emission Intensity
120
100
80
60
40
20
0
0
.11
.22
.33
.44
.55
.66
.77
.88
.99
1.1
(nsec)

Fig.1 (a) and (b)

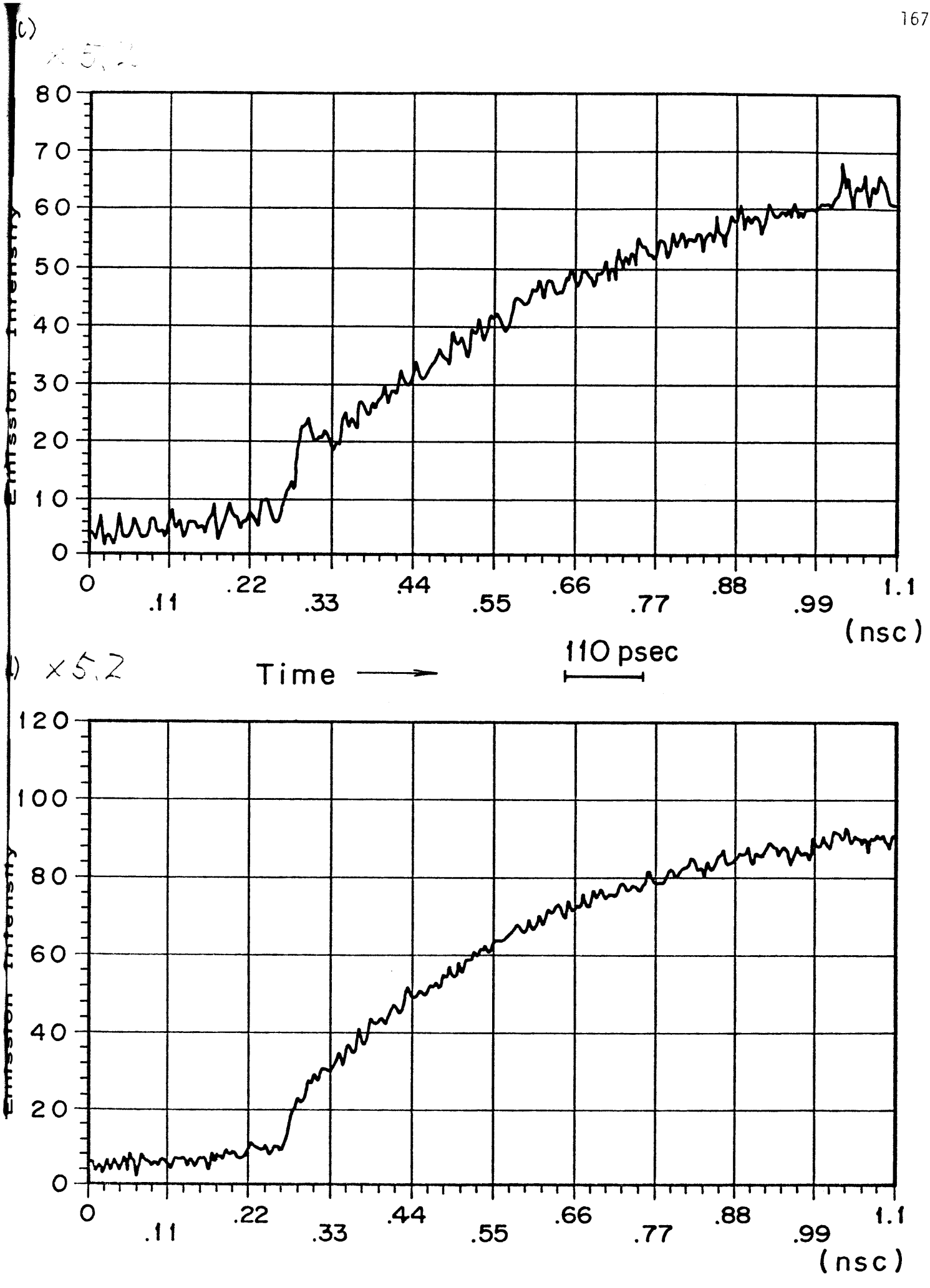
(c)
Emission Intensity
80
70
60
50
40
30
20
10
0
0
.11
.22
.33
.44
.55
.66
.77
.88
.99
1.1
(nsc)
(d) ×5.2
Time
110 psec
Emission Intensity
120
100
80
60
40
20
0
0
.11
.22
.33
.44
.55
.66
.77
.88
.99
1.1
(nsc)

Fig.1 (c) and (d)

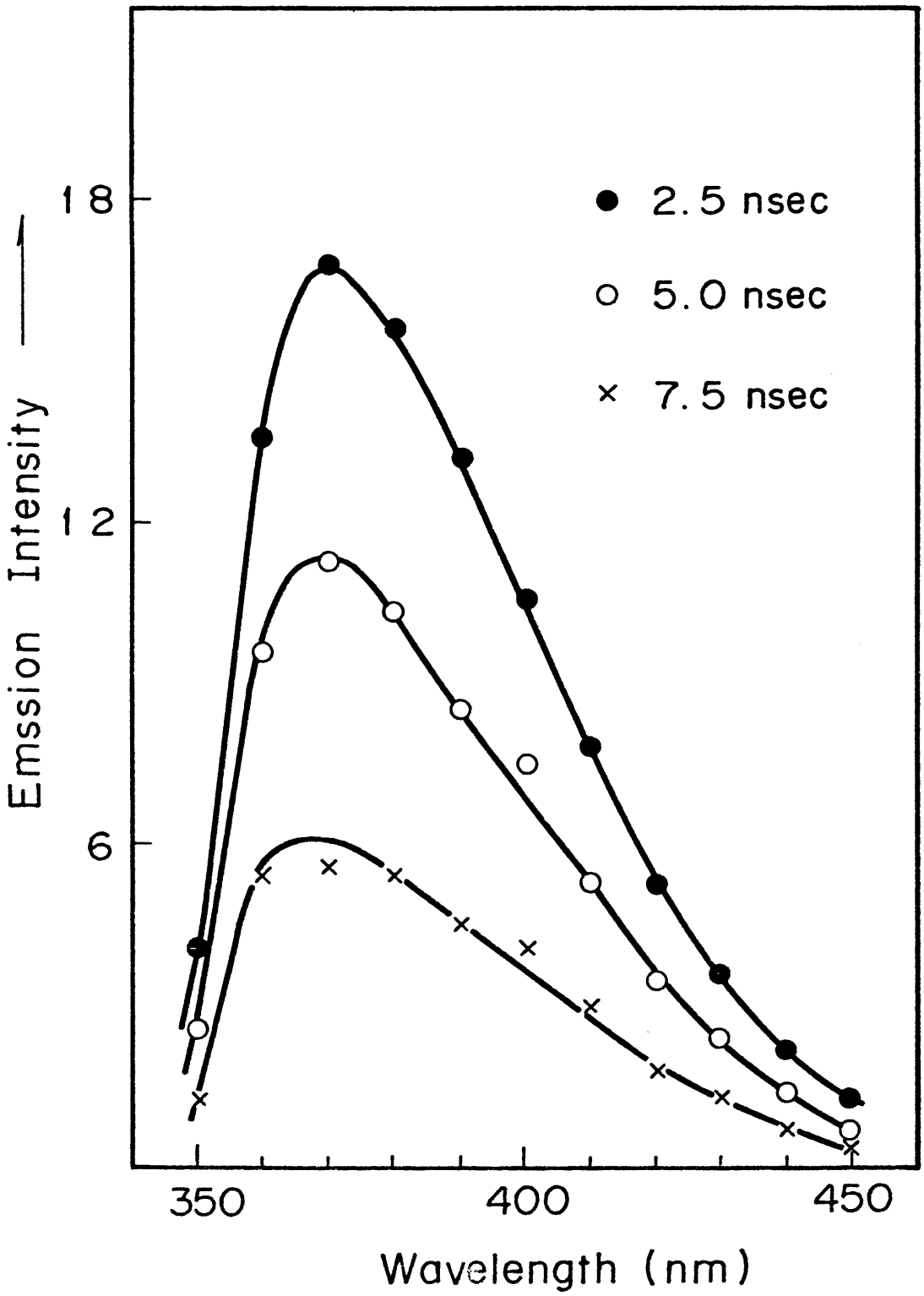
18
12
6
Emssion Intensity
2.5 nsec
5.0 nsec
7.5 nsec
350
400
450
Wavelength (nm)

Fig.2 (a)

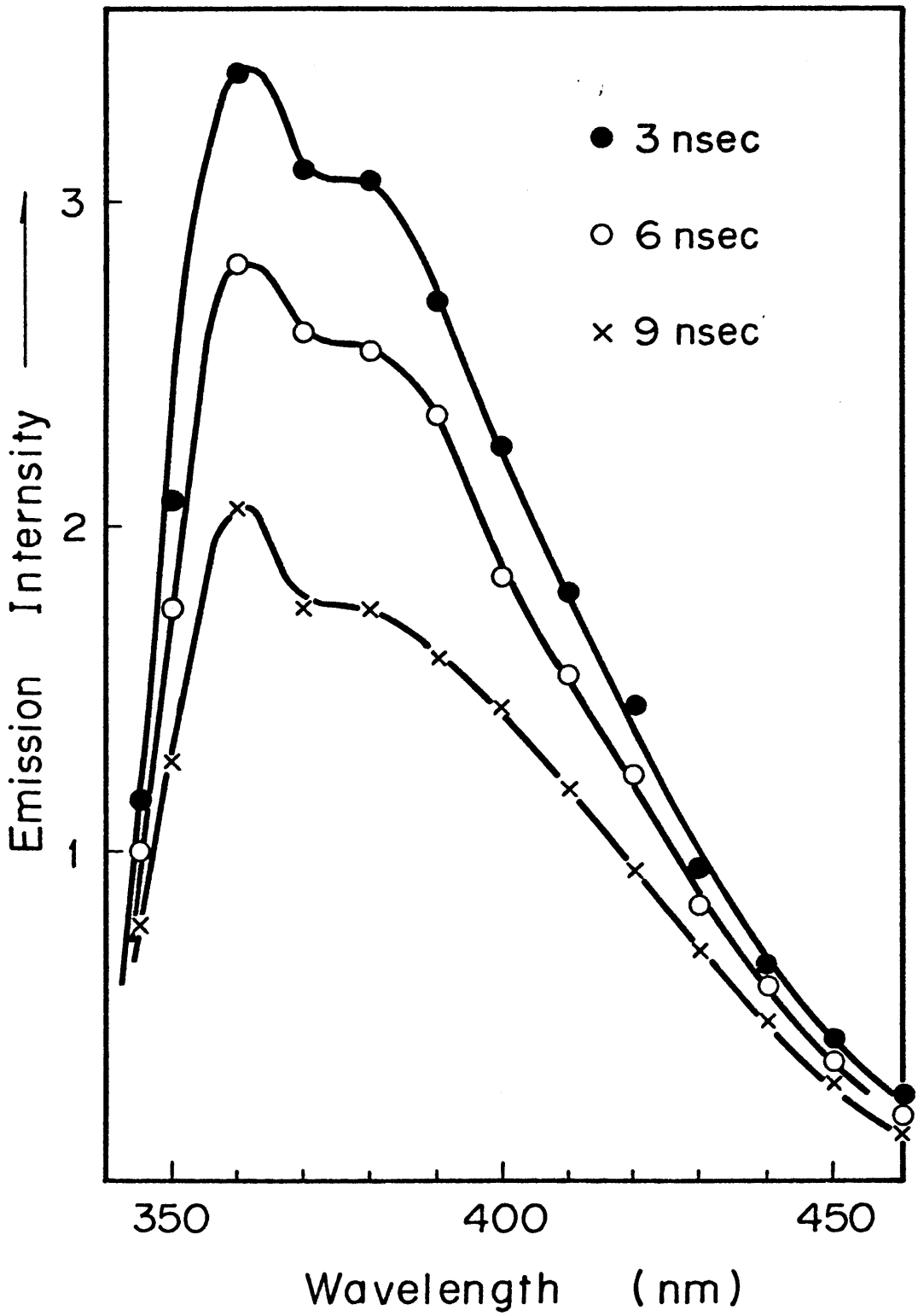
3 nsec
6 nsec
9 nsec
Emission Internsity
1
2
3
350
400
450
Wavelength (nm)

Fig.2 (b)

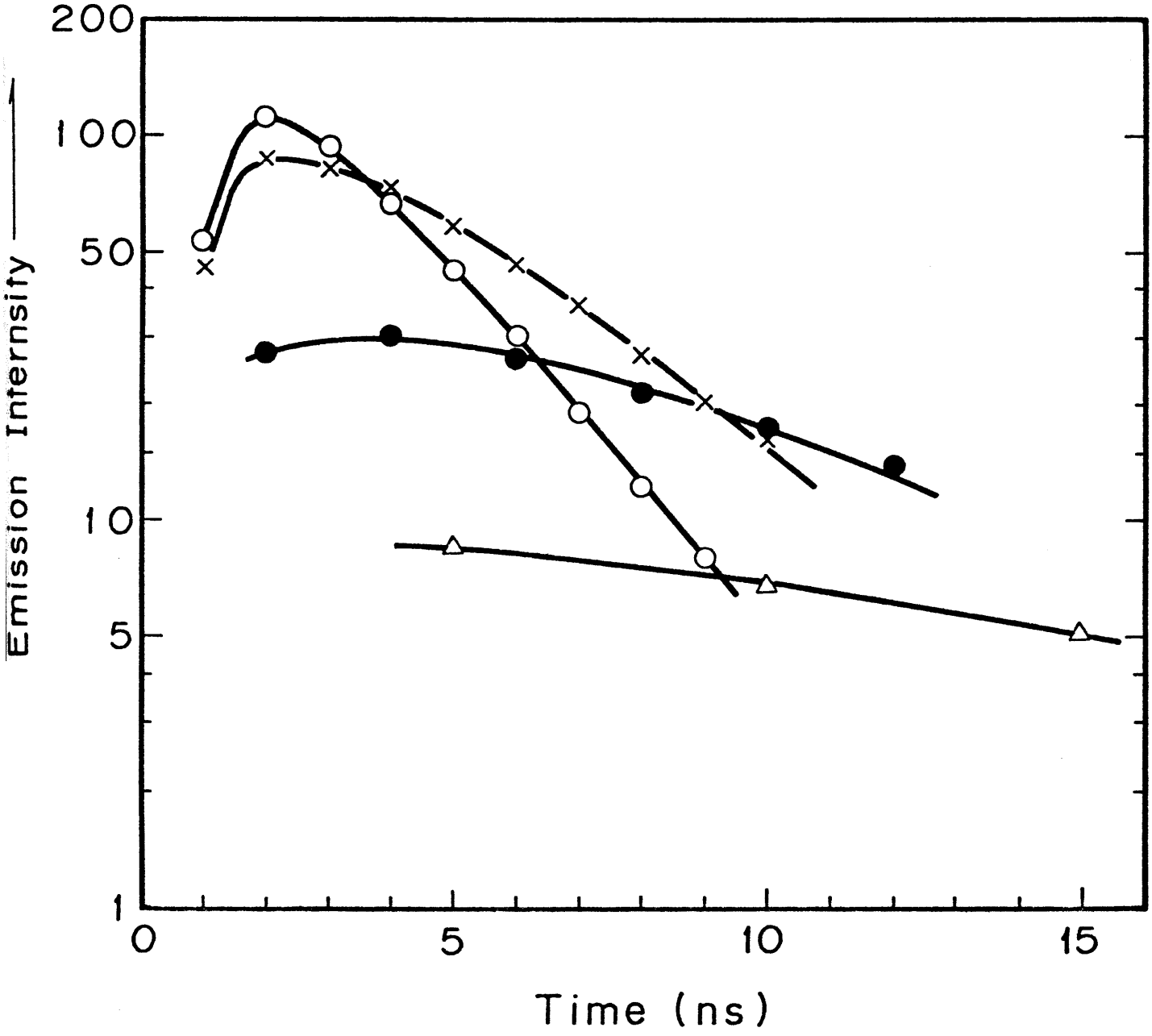

Fig.3

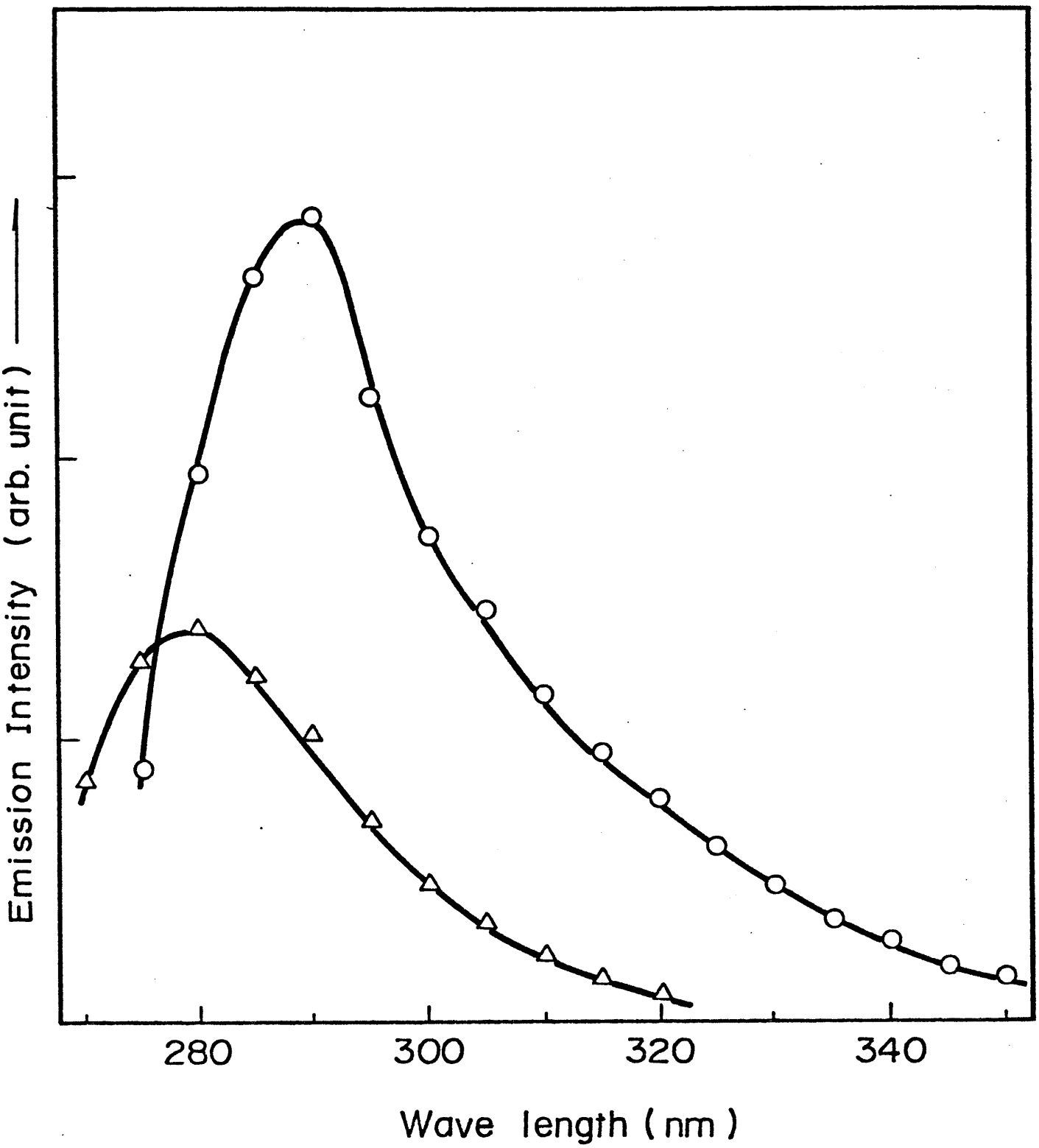

Fig.4 (a)

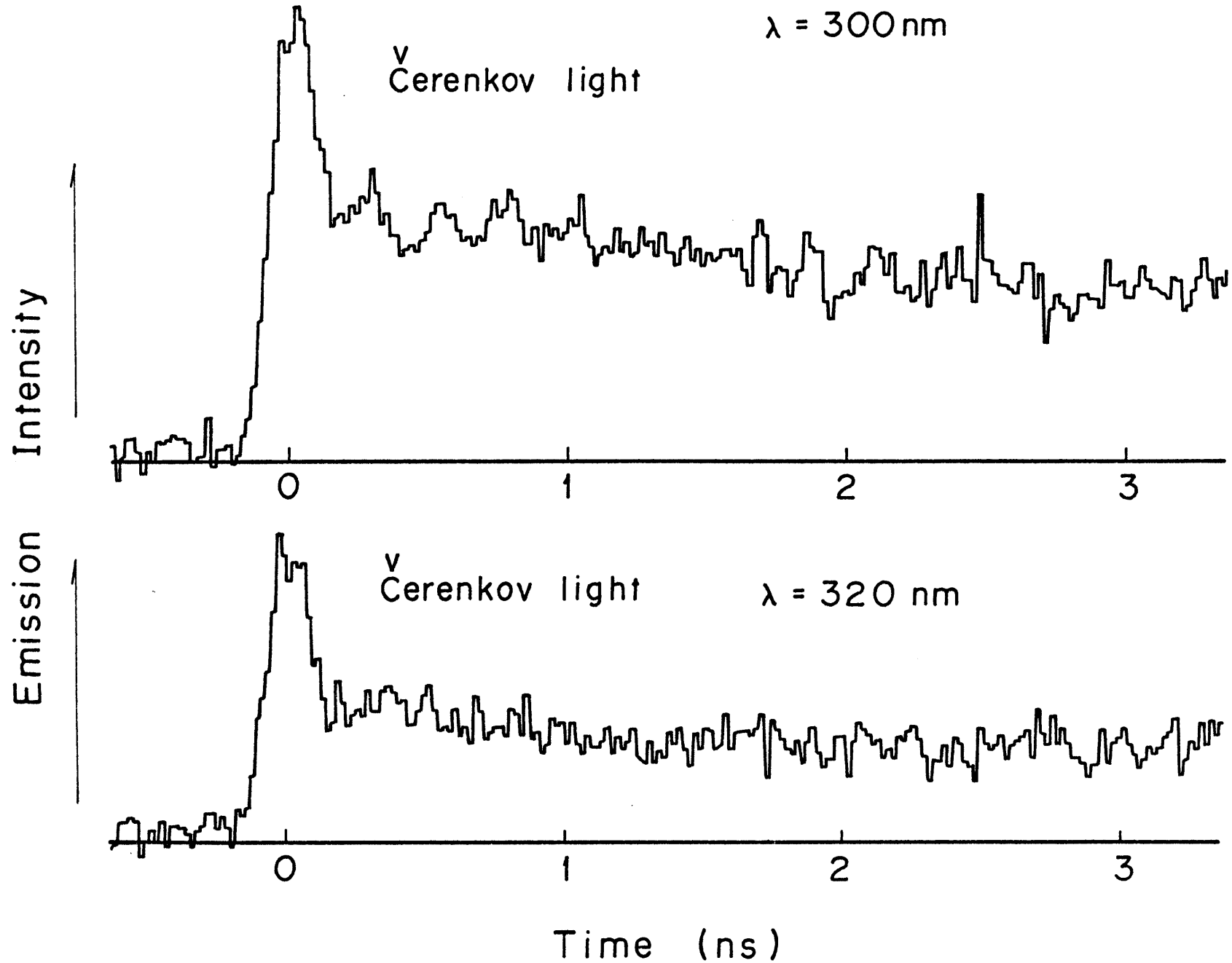
λ = 300nm
ν
Cerenkov light
Intensity
0
1
2
3
Emission
ν
Cerenkov light
λ = 320 nm
0
1
2
3
Time (ns)

Fig.4 (b)

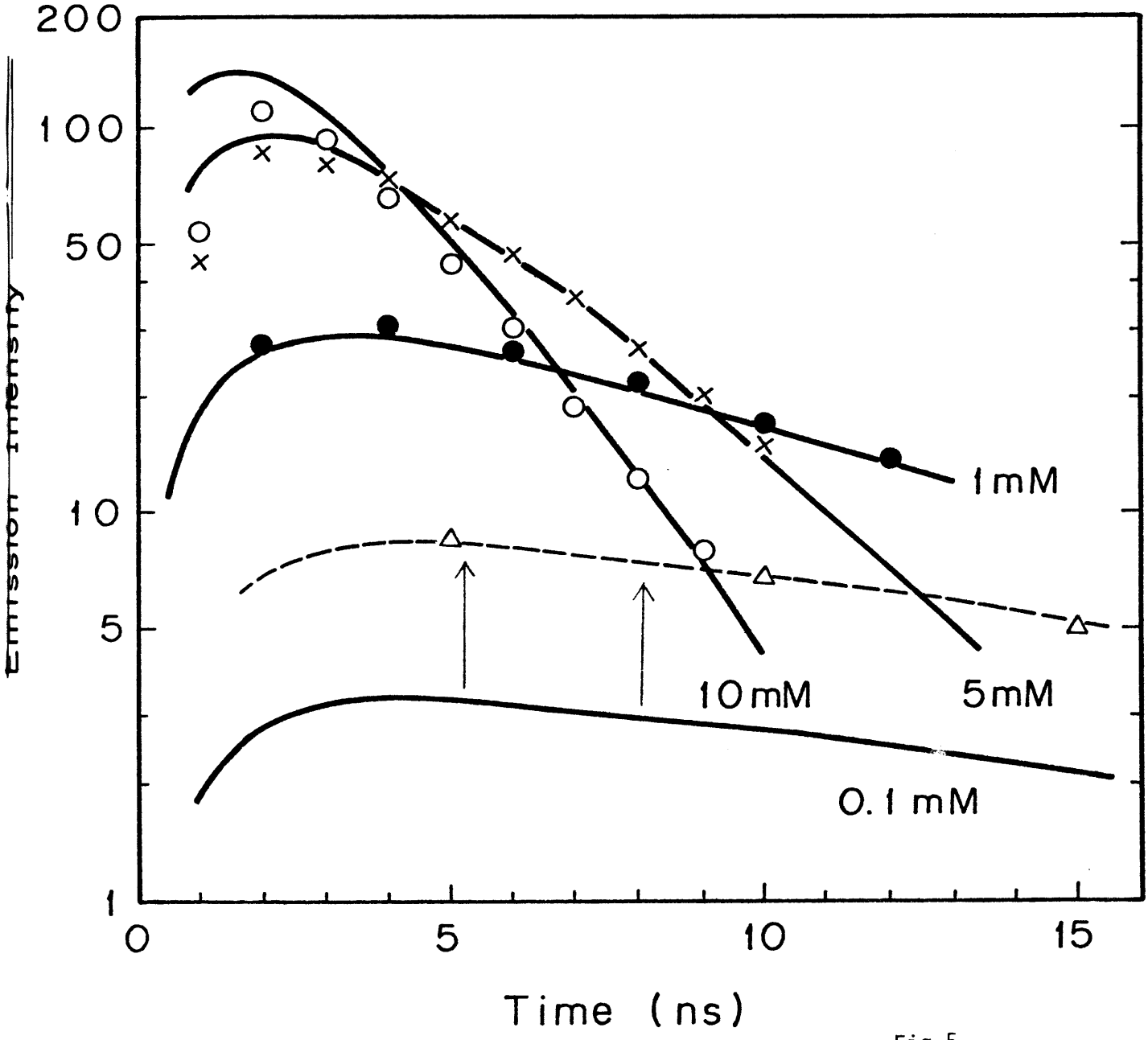
200
100
50
10
5
1
0
5
10
15
Emission Intensity
Time (ns)
1mM
10mM
5mM
0.1mM

Fig.5

Chapter 9.

Studies on Scavenging Effect for Faster Formation Processes of Solute Excited State in Cyclohexane by Means of Picosecond Pulse Radiolysis

Summary

By means of picosecond pulse radiolysis, emission from excited 2,5-diphenyloxazole in liquid cyclohexane was observed. In the diluted solution, the growth of emission is very fast and completed within 30 psec. Addivives such as chloride compounds reduce the yield of the fast formation of excited solute molecules, which is so called the faster process. By adding several kinds of electron scavengers and toluene, the changes of initial yield were measured as a function of scavenger concentration in 0.1 mM 2,5-diphenyloxazole cyclohexane solution.

In the presence of scavenger such as CCl_4 the emission intensity is reduced efficiently by the scavenger below about 100 mM, but above 100 mM to 400 mM the intensity does not decrease any more and the emission intensity is remained constant. The plateau value of the initial intensity is dependent on the kind of scavenger. It was found that the most efficient scavenger is CCl_2:CCl_2 among them. The observed result strongly suggests that a selective capture of electron by scavenger occurs in liquid hydrocarbon at early stages after electron irradiation. Mechanism of the faster formation process through the reduction of initial yield of emission by additives will be discussed in connection with the electron attachment cross section as a function of electron energy obtained in the gas phase.

Introduction

The formation yields of anion, cation, singlet and triplet have been widely studied with nanosecond time resolution.[1] Mobilities of charged carriers produced in irradiated liquid hydrocarbons have also been measured by means of microwave conductivity method.[2] Recently, evaluations of geminate ion decay and following homogeneous recombination were made.[3]

By means of picosecond pulse radiolysis, the formation process of solute excited state in a liquid hydrocarbon such as cyclohexane was observed by Beck and Thomas in 1972.[4] Since they used pulse trains from a L-band linac, information from the experiment was limited from 60 psec to 770 psec. The pulse to pulse separation is 770 psec for the L-band linac. They found out that excited solute molecules are produced by energy transfer from the lowest excited states of solvent molecules and that the rate constant fo this process was one factor larger than that expected based on the diffusion controlled reaction. They also observed the emission at low temperatures in toluene.[5] Similar experiments were carried out by Jonah et al.[6] However, the result is somewhat different from Beck and Thomas's data.

Recently, using single picosecond electron pulses from a S-band (2856 MHz) linac with about 30 psec time resolution, observation of the emission from liquid scintillation systems such as 2,5-diphenyloxazole in cyclohexane and toluene has been made by the present authors without any time limitation after electron irradiation.[7] It was also found from our experiments that slower formation of solute excited states can be explained based on energy transfer from excited solvent molecules to solute molecules, as already reported by Beck and Thomas.[4] This is consistent with the steady state photolysis data reported by Hirayama and Lipsky.[8] However, at lower concentrations, another ultra fast formation process unknown before has been found by our experiments and its rate constant was estimated to be $\geq 10^{15} M^{-1} sec^{-1}$,

if this process obeys pseudo first order kinetics. We have been calling these two processes as the slower and the faster ones from the view point of formation rate of excited solute molecules. It was confirmed that the ratio of these two formation processes is dependent on the concentration of solute, and the faster process is predominant at lower solute concentrations ($\leq$1 mM). The following possible explanations for the faster process have been suggested.

(1) Direct excitation of solute molecule by subexcitation electrons.

(2) Energy transfer from unrelaxed excited solvent molecules.

(3) Direct excitation of solute by absorbing Čerenkov light produced in matrix medium by electron beam.

(4) Fast recombination of positive holes and anions, and/or cations and electrons.

The contribution to the direct excitation by Čerenkov light can be estimated. G-value for the formation of excited 2,5-diphenyloxazole in cyclohexane at 1 mM was reported to be 0.25 by Dainton et al.[9] In our experimental condition, the dose per pulse was roughly estimated to be 500 rad/pulse[10] and resultant yield of excited 2,5-diphenyloxazole to be $\sim 8\times10^{13}$ molecules/g. On the other hand, photons of Čerenkov light induced in a wave range of 250 nm to 350 nm, in which an absorption band of 2,5-diphenyloxazole in cyclohexane solution is placed, can be calculated to be $\sim 2\times10^{12}$ per/pulse. The formation yield of excited solute molecules by absorption of Čerenkov light shorter than 200 nm is assumed to be negligible, because the absorption coefficient of cyclohexane as a matrix becomes large below 200 nm. Taking the absorbance of the Čerenkov light by 1 mM 2,5-diphenyloxazole[11] solution in cyclohexane solution into consideration, the produced Čerenkov light in a wave range from 250 nm to 350 nm is completely absorbed by solute molecules. Therefore, the expected yield of excited 2,5-diphenyloxazole by absorbing the Čerenkov light is equal to the number of photons of Čerenkov light produced in the same wave range. Comparing these

two values, the formation yield of excited 2,5-diphenyloxazole by the absorbed dose is much larger than that due to Čerenkov light produced in cyclohexane medium. It is concluded that the main part of the faster process can not be explained by direct excitation with Čerenkov light. This conclusion is supported by the experimental result that the initial yield of excited solute molecules is quenched to some extent by electron scavenger such as CCl_4. Because direct formation of excited solute molecules by absorbing Čerenkov light is expected to be not affected by the presence of electron scavengers.

In general, electron scavengers affect both the formation and decay processes of the solute excited state. In order to clarify the process of the electron-induced luminecence, some additional experiments of photo-excitation were also carried out.

In the present paper, the effect of electron scavengers on the initial formation of excited 2,5-diphenyloxazole in cyclohexane and its mechanism are mainly discussed.

Experimental

Details of our linac and detection systems were reported elsewhere.[7] Measurements were made at room temperature. Since no difference in the emission yield at short times ($\leq$1 nsec) between air saturated and degassed samples was observed, most samples used were air saturated ones. Additives used were toluene, $CHCl_3$, CCl_4, CH_3CCl_3, t-CHCl:CHCl, c-CHCl:CHCl, CCl_2:CCl_2, and triethylamine.

Quenching rates of the lowest excited state of 2,5-diphenyloxazole by different additives were evaluated by means of photofluorescence analysis. A spectro-photofluorometer, Hitachi model MPF-4, was used for the experiment.

Results

It has been already reported that the faster process is predominant at diluted solution of 2,5-diphenyloxazole in cyclohexane or toluene.[7] Instead of 2,5-diphenyloxazole, para-terphenyl was used as a solute in cyclohexane. The result is indicating similar behavior to 2,5-diphenyloxazole, as shown in Fig. 1. At lower solute concentrations Čerenkov light pulse induced in the solvent of cyclohexane overlaps with emission from the solute excited state. From Figs. 1(a) and 1(b), it is easily to discriminate the Čerenkov light pulse produced by electron irradiation in cyclohexane medium at lower concentrations from the total emission. However, at higher concentrations, the emission from the lowest excited state of the solute molecules becomes large, and it is difficult to discriminate the Čerenkov light pulse from the emission due to fluorescence of the solute. Above 1 mM concentration of the solute, emission due to the slower process becomes predominant. These results are similar to that of 2,5-diphenyloxazole in cyclohexane.

In iso-octane the emission from excited 2,5-diphenyloxazole and para-terphenyl is somewhat different from that in cyclohexane as shown in Figs. 2 and 3. The ratio of the faster process to the slower one in iso-octane is larger than that in cyclohexane. Even at a concentration of 1 mM of solute, the emission corresponding to the faster process is dominant in iso-octane. It is concluded from these experimental results that both the faster and the slower processes can be observed normally in any kind of scintillater and solvent (saturated and aromatic hydrocarbons)[12], but the ratio of these two processes depends upon the kind of solvent.

All streak traces were obtained by a streak camera without monochrometer. Because the intensity of emission becomes weak in diluted solute samples. The emission due to excited 2,5-diphenyloxazole is strong in a region of 340∿420 nm. As the sensitivity of the detection system decreases in a factor

of 20 % at longer wavelengths and it is known that growth and decay of the emission with time at each wavelength is similar, emission of the solute excited state obtained without monochrometer is assumed to be the same as that with monochrometer. However, the Čerenkov light obtained was mainly due to a region of 250 nm to 450 nm. Therefore, the intensity of Čerenkov light pulse observed was enhanced in diluted solute samples.

In the case of 0.1 mM 2,5-diphenyloxazole in cyclohexane, the emission is assumed to be mainly due to the faster process (Fig. 4). This initial formation yield (Yo in Fig. 4(b)) is clearly proportional to the electron charge per pulse, namely dose per pulse, as shown in Fig. 5. It was found that electron scavengers such as CCl_4 reduce the initial formation yield of emission and accelerate the decay of the emission as shown in Fig. 4(c). In the presence of electron scavengers, absorption of the emission by the additives (color quenching) was not detected, that is, no change of emission spectra from solute excited state in the presence of additives was observed. In Fig. 6, the emission spectra in several samples are shown. Since the intensities of emission were very weak at 0.1 mM concentration of 2,5-diphenyloxazole, S/N ratio of the signals was not so good. However, all spectra were the same as the original spectrum (without electron scavengers) within experimental errors.

By using different kinds of additives, the reduction of initial emission yield was also observed. The results are shown in Fig. 7. From these results, it was found that the presence of those additives reduces appreciably the initial formation yield of excited 2,5-diphenyloxazole up to 100 mM of the additives. However, above concentrations 100 mM to 400 mM of additives, the initial yields are almost constant. They are saturated at higher concentrations. The saturated yields are dependent on the kind of scavenger. It is noted that the presence of toluene reduces also the yield in a similar fashion to other electron scavengers such as t-CHCl:CHCl. When binary mixtures

of cyclohexane and benzene or toluene are used as the solvent,[13] benzene or toluene acts as a scavenger just like chloride compounds at low concentration.

Triethylamine reduces the emission intensity as well. The reduction is pronaunced more than the chloride compounds, and continues over a wide range of the scavenger concentration without any plateau, as shown in Fig. 8. It is well known that triethylamine is one of the typical hole scavengers.[14] It is interesting to compare triethylamine with electron scavengers. Quenching by the electron scavengers in 2,5-diphenyloxazole-isooctane solution was similar to that in cyclohexane solution.

Effects by mixtures of two different electron scavengers on the luminescence have been also examined. When a equimolar mixture of two electron scavengers (200 mM for each) was put into a 0.1 mM PPO cyclohexane solution no additional effect by the 2nd scavenger which is weaker than the other (1st one) was observed: that is, the effect was equivalent to that of the first one of 200 mM. These experimental results suggest that a selective capture of electron by the first scavenger plays an important role for the scavenging process. However, in the case of binary mixtures of toluene and halogen compounds, some additional and combined effects have been observed. Not only selective electron capture but also certain interaction between the two scavengers must be taken into consideration for the latter case.

Cyclohexane solutions of 0.1 mM 2,5-diphenyloxazole containing chloride compounds were illuminated by 335 nm light, which is corresponding to the absorption band of 2,5-diphenyloxazole, and the fluorescence yield from the excited solute was measured. Only the yield in a solution containing 0.4 M CCl_4 decreased significantly. The reduction was 45 % compared with the solution without CCl_4. However, other chloride compounds of 0.4 M concentration reduced the emission in a factor of about 10 % in most cases.

Considering the lifetime of the lowest excited state of 2,5-diphenyloxazole to be ∿1.6 ns, quenching rates of the lowest solute excited state by CCl_4 and other chloride additives were obtained to be $2\times10^9 M^{-1}\cdot sec^{-1}$ and $\leq 10^8 M^{-1}\cdot sec^{-1}$, respectively. These quenching rates are in good agreement with the radiolysis results. The emission decay rate was strongly effected only by CCl_4.

From comparison of the photo excitation experiments with those of pulsed electrons, it is confirmed that the emission yield of solute excited state is reduced by electron scavengers during or before the formation process of the excited state for the latter case as shown in Figs. 7 and 8.

Discussion

The lowest excited state of 2,5-diphenyloxazole (PPO) in liquid hydrocarbon is assumed to be produced by several patways, as shown in the following,

$$M \rightsquigarrow M^+ + e^- \longrightarrow M^* \quad (1)$$

$$M \rightsquigarrow M^* \quad (2)$$

$$PPO + M^* \longrightarrow PPO^* + M \quad (3)$$

$$PPO + M^+ \longrightarrow PPO^+ + M \quad (4)$$

$$PPO + e^- \longrightarrow PPO^- \quad (5)$$

$$PPO^- + PPO^+ \longrightarrow PPO^* + PPO \quad (6)$$

$$PPO^+ + e^- \longrightarrow PPO^* \quad (7)$$

$$PPO^- + M^+ \longrightarrow PPO^* + M \quad (8)$$

where M is solvent molecule.

In a higher concentration range of 2,5-diphenyloxazole in cyclohexane, the growth of formation of the solute excited state was clearly observed and the formation process is called " slower process ". This slower process is assumed to be mainly due to both energy transfer from excited solvent molecules

to the solute molecules and geminate recombination reaction.[7] At lower concentrations of the solute, the formation of the excited solute molecules is completed during the electron pulse. This is called " faster process ". Recombination of ion-paris as eq. (6) in a longer time region from nanosecond to several tens nanosecond was confirmed by Sargent, Brocklehurst et al.[15] They observed magnetic field effect on the emission from excited naphthalene molecules in the squalane solution. Recently, the recombination process has been detected with a very high sensitivity by an optical method through the magnetic resonance phonomenon.[16] However, process expressed by eq. (6) may not be important in a short time range, because the concentrations of formed PPO^+ and PPO^- are very low and the mobilities of these species are assumed to be much smaller than that of electron. Therefore, mechanisms through eqs. (4), (5), (7) and (8) are preferable to explain the faster process. Possibility of direct excitation by Čerenkov light has been recognized to be less important for the formation of the excited state, as mentioned in the previous section. If excited 2,5-diphenyloxazole in cyclohexane is formed through mechanisms, eqs. (4), (5), (7) and (8), the yield of solute excited state should be influenced by the presence of electron scavengers. It was already shown that various electron scavengers reduce the initial formation yield of excited 2,5-diphenyloxazole in a concentration range less than 100 mM of scavenger in 0.1 mM 2,5-diphenyloxazole solution in cyclohexane. Above 100 mM concentration of the scavengers, the reduction in the initial yield becomes rapidly insignificant and the yield is saturated. The saturated values depend on the kind of scavenger, as shown in Fig. 6. These results are suggesting that each scavenger captures electrons in different ways among different scavengers.

Scavenging yield in hydrocarbons as a function of scavenger concentration was well established experimentally. The value of scavenged ion, G, depends on scavenger concentration C according to the empirical formula[17]

$$G = G_{fi} + G_{gi} \frac{(\alpha_s C)^{1/2}}{1+(\alpha_s C)^{1/2}} \qquad (9)$$

where G_{fi}, G_{gi}, α_s are free ion yield, yield of geminate ion pair per 100 eV and empirical parameter for each scavenger having a dimension M^{-1}. These values were obtained experimentally. Based on eq. (9), a functional discription of the lifetimes of the ion pairs in the radiolysis of pure hydrocarbons was derived by use of Laplace transformation.[18] This discription has been applied to analyze the behaviors of solute and solvent charged species obtained in hydrocarbon pulse radiolysis.[19] It is noted that time is considered to be measured from the time at which the electron becomes thermalized one in this theory. It seems that it is difficult to analyze our experimental results by above theories, because selective reduction of the formation which depends on scavenger was observed. At higher concentrations of those scavengers in 0.1 mM 2,5-diphenyloxazole-cyclohexane solution, the number ratio of the solute to the scavenger molecules is up to 1:4000, and a certain fraction of the excited solute molecules is not quenched, irrespective of such high concentration. This results strongly suggests that the formation of the lowest excited 2,5-diphenyloxazole occurs not homogeneously in the medium but in localized space such as spur and that spatial distribution of holes, electrons and solute molecules seems to play very important roles for the faster formation of the solute excited states. There are some evidences that a rapid formation of solute anions in cyclohexane[4] and a rapid electron capture in aqueous solution occurs before electron thermalization.[20] Therefore, it can be speculated that only electrons having a specific energy distribution are effectively scavenged by a particular scavenger.

It is thought that there is a certain relationship between magnitude of the reduction in emission from solute excited state in the presence of electron scavenger and attachment rate of electrons to the scavenger as a function of electron energy. In gas phase, electron attachment rates

corresponding to the electron attachment cross sections as a function of electron energy for various molecules were obtained by swarm method by Christophorou et al.[21] The attachment rates of thermal electron to three different chloride molecules, and the energies, ε_1 and ε_2, of the first and second maxima in the attachment cross section were obtained. Those results are shown in Table I. It is known that the molecule of $CHCl{:}CCl_2$ has a similar distribution of attachment rates as a function of electron energy to that of $CCl_2{:}CCl_2$.[22] In Table I, the distribution of attachment rates to $CHCl{:}CCl_2$ can be assumed to be the same as $CCl_2{:}CCl_2$. Among three chlorides, CCl_4 is the most effecient and $CHCl{:}CCl_2$ is the weakest scavenger for thermal electrons. However, it was found in the present experiment that $CCl_2{:}CCl_2$ is the most efficient scavenger. If it is assumed that reaction rates of scavengers in liquid cyclohexane is similar to those in gas phase, thermal electrons may not play an important role for the inhibition of the faster formation process of excited 2,5-diphenyloxazole in cyclohexane. Since it is reasonably assumed that a certain energetic electron can be selectively captured by a particular scavenger, it is interesting to examine whether any correlation between the magnitude of reduction for the faster process and the distribution of attachment rates of electrons to these chlorides as a function of their energy exist or not. In Fig. 9 the attachment rate, $\alpha w(\varepsilon)$, as a function of electron energy, ε, is shown. If an energy spectrum of electrons in which the excited solute will be preferably formed is assumed to be $p(\varepsilon)$, the effectiveness of electron capture, which may corresponds to the reduction of emission, R, is proportional to the overlapping of both distributions, $\alpha w(\varepsilon)$ and $p(\varepsilon)$.

$$R(C) \propto C(c) \int_0^\infty \alpha w(\varepsilon)\, p(\varepsilon)\, d\varepsilon \qquad (10)$$

using the relation, $\sigma(\varepsilon)=\alpha w(\varepsilon)/N_0(2/m)^{1/2}\varepsilon^{1/2}$, where m is the electron mass and N_0 is the number of molecules per cm^3 per Torr, we get following equation.

$$R(C) \propto C'(c) \int_0^\infty \sqrt{\varepsilon}\cdot\sigma(\varepsilon)\ p(\varepsilon)\ d\varepsilon \qquad (11)$$

where C(c) and C'(c) are concentration parameters and $\sigma(\varepsilon)$ is the cross section of electron attachment, respectively. By comparing $\alpha w(\varepsilon)$ with the magnitude of reduction obtained from the experiment, the distribution function $p(\varepsilon)$ will be determined. If $p(\varepsilon)$ has peak around 0.6∿0.7 eV as shown in Fig. 9(b), the magnitude of emission unaffected by the presence of scavenger is explained qualitatively by the value from eq. (10). This correlation may be in a good agreement with the energy distribution of electron attachment cross section of CH_3CCl_3 in gas phase. Since the attachment rate of electrons to CH_3CCl_3 in an energy range of 0.5∿1.0 eV is smaller than that of CCl_2CCl_2, the difference observed between those two scavengers may be qualitatively understood from the explanation mentioned above.

Allen and Holroyd[23] measured chemical reaction rate of quasifree electrons in nonpolar liquids. They obtained a correlation between reaction rate of the electrons with good electron scavengers and the quantity Vo, the energy level of the mobile conduction electrons. They concluded that the scavengers that require more energetic electrons than thermal one for reaction in the gas phase react more rapidly in solvents of positive Vo such as cyclohexane than in those of more negative Vo such as neopentane and tetramethylsilane. It seems that the magnitude of the rate constants of $CHCl_3$, CCl_4 and C_2HCl_3 with electrons obtained by Allen et al is parallel to the magnitude of the reduction of the solute excited state by these additives obtained in the present experiment. Schmidt et al[24] obtained the rate constant for electron attachment to electron scavengers in liquid Ar and Xe as a function of an external electric field. Rough estimate of energy dependence of the attachment cross section of electron based on the Cohen-Lekner theory

was correlated with gas phase data. It seems that the scavenging efficiency of additives in liquid phase is reflected by the electron attachment cross section of those materials. Although there is neither an accurate knowledge of the changes in the magnitude and energy dependece of the $\sigma(\varepsilon)$ function in going from the gas to liquid,[25] nor the true energy distribution of electron which is the precursor of excited solute, the scavenging tendency could be reasonable explained through the principle.

The possibility of the formation of solute excited state by subexcitation electron can not be excluded completely. As for the effect of toluene, the mechanism of reduction is also not yet clear. However, it is expected that a small amount of toluene in cyclohexane may give a profound effect on the transport of electrons and holes in the medium.

It is concluded that the fast recombination reaction of positive holes and anions, or cations and electrons mainly occurs in the faster formation of solute excited state. Additional experiments using other type of scavengers on the formation process of solute excited state in liquid hydrocarbons are in progress, and more precise mechanisms will be discussed in near future.

Acknowledgement

The authors are grateful to Mr. H. Kobayashi, Mr. T. Ueda and Mr. T. Kobayashi for their help during the course of this experiment. Spectro-photofluorometory was carried out at Faculty of Engineering, Univ. of Tokyo. We thanks to Dr. F. Toda.

References

1) J.K. Thomas, K. Johnson, T. Klippert and R. Lowers; J. Chem. Phys. 48 1608 (1968)

J.W. Hunt and J.K. Thomas; J. Chem. Phys. 46 2954 (1967)

J.H. Baxendale and P. Wardman; Trans. Faraday Soc. 67 2997 (1971)

R. Cooper and J.K. Thomas; J. Chem. Phys. 48 5097 (1968)

A. Hummel and L.H. Luthjens; J. Chem. Phys. 59 654 (1973)

J.K. Thomas; Int. Rad. Phys. Chem. 8 1 (1976)

Erika Zador, J.M. Warman and A. Hummel; J. Chem. Phys. 62 3897 (1975)

PO'Neill, G.A. Salmon and R. May; Proc. R. Soc. Lond. A 347 61 (1975)

2) J.M. Warman, P.P. Infelta, M.P. de Haas and A. Hummel; Can. J. Chem. 55 2249 (1977) references herein

3) C.A.M. van den Ende, L. Nyikos, J.M. Warman and A. Hummel; J. Rad. Phys. Chem.

4) G. Beck and J.K. Thomas; J. Phys. Chem. 76 3359 (1972)

G. Beck and J.K. Thomas; Chem. Phys. Letts. 16 318 (1972)

5) G. Beck and J.T. Richards, J.K. Thomas; Chem. Phys. Lett. 40 300 (1976)

G. Beck, A. Ding and J.K. Thomas; J. Chem. Phys. 71 2611 (1979)

6) C.D. Jonah, M.C. Sauer, R. Cooper and A.D. Trifunac; Chem. Phys. Lett. 63 535 (1979)

7) S. Tagawa, Y. Katsumura and Y. Tabata; Chem. Phys. Letts. 64 258 (1979)

S. Tagawa, Y. Katsumura, T. Ueda adn Y. Tabata; Rad. Phys. Chem. 15 287 (1980)

Y. Katsumura, S. Tagawa and Y. Tabata; J. Phys. Chem. 84 833 (1980)

Y. Katsumura, T. Kanbayashi, S. Tagawa and Y. Tabata; Chem. Phys. Letts. 67 183 (1979)

Y. Katsumura, T. Kanbayashi, S. Tagawa and Y. Tabata; submitted for publication

8) F. Hirayama and S. Lipsky p205 in " Organic Scintillators and Liquid Scintillation Counting " Academic Press, 1971.

9) Sir F. Dainton, M.B. Ledger, R. May and G.A. Salmon; J. Phys. Chem. 77 45 (1973)

10) Dosimetry was carried out by measuring the optical absorption of the solvated electron in a 10^{-2} M NaOH, 1 M ethanol aqueous solution. Absorption was measured at 634 nm ($G(e_{aq})=1.34\times10^{4}$ M^{-1} sec^{-1}, $G(e_{aq})=3.4/100$ eV) using pulse Xe lamp and photomultiplier.

11) I.B. Berlman " Handbook of Fluorescence Spectra of Aromatic Molecules " Academic Press (1971)

12) Emission behaviors in various kind of liquid organic compound will be reported elsewhere.

13) S. Tagawa, T. Kanbayashi, and Y. Tabata; to be submitted.

14) It was found that a certain fraction of triethylamine may react with the lowest excited state of 2,5-diphenyloxazole and they may be formed an exciplex in special concentration range. The emission spectra from the exciplex seems to be similar to the fluorescence spectra of 2,5-diphenyloxazole. However, it is assumed that the formation of the exciplex will be neglected immediately after the pulse in this paper.

15) F.P. Sargent, B. Brocklehurst, R.S. Dixson, E.M. Gardy, V.J. Lopata and Ajit Singh; J. Phys. Chem. 81 815 (1977)

16) O.A. Anisimov, V.M. Grigoryants, V.K. Molchanoc and Yu. N. Molin; Chem. Phys. Lett. 66 265 (1979)

17) J.M. Warman, K.D. Asmus and R.H. Schuler; J. Phys. Chem. 73 931 (1969)
R.H. Schuler and P.P. Infelta; J. Phys. Chem. 76 3812 (1972)

18) A. Hummel; J. Chem. Phys. 49 4840 (1968)
M. Tachiya; J. Chem. Phys. 56 4377 (1972)
M. Tachiya; J. Chem. Phys. 70 238 (1979)

19) S.J. Rzad, P.P. Infelta, J.M. Warman and R.H. Schuler; J. Chem. Phys. 52 3979 (1970)

20) J.W. Hunt " Advances in Radiation Chemistry " ed. M. Burton and J.L. Magee vol.5 p.186 John Wiley & Sons 1976.

21) L.G. Christophorou, " Atomic and Molecular Radiation Physics " Wiley-Interscience, New York. N.Y., 1971.

22) J.P. Johnson, L.G. Christophorou and J.G. Carter; J. Chem. Phys. 67 2196 (1977)

23) A.O. Allen and R.A. Holroyd; J. Phys. Chem. 78 796 (1974)
A.O. Allen, T.E. Gangwer and R.A. Holroyd; J. Phys. Chem. 79 25 (1975)

24) G. Bakale, U. Sowada and W.F. Schmidt; J. Phys. Chem. 80 2556 (1976)

25) L.G. Christophorous; Chem. Rev. 76 409 (1976)

Figure Captions

Fig. 1 Čerenkov light from pure cyclohexane, (a), and emissions from cyclohexane containing para-terphenyl, (b)∿(e), under the same irradiated condition. Concentrations are 0.01; (b), 0.1; (c), 1; (d) and 5 mM; (e). In diluted solution, Čerenkov light from sample matrix produced by electron pulse irradiation is clearly seen.

Fig. 2 Čerenkov light from pure iso-octane, (a), and emissions from iso-octane containing 2,5-diphenyloxazole, (b)∿(f), under the same irradiated condition. Concentrations are 0.05; (b), 0.1; (c), 0.5; (d), 1; (e) and 10 mM; (f).
In iso-octane, the faster formation of solute excited state is larger than the slower formation at rather high concentration range of solute molecule in contrast with cyclohexane as a solvent.

Fig. 3 Čerenkov light from pure iso-octane, (a), and emissions from iso-octane containing para-terphenyl 0.01, 0.1, ; and 3 mM for (b), (c), (d), and , (e) and (e'), respectively, under the same irradiated condition. It is noted that time scale of (e') is different from others. It was found that the width of Čerenkov light produced by electron irradiation is slightly dependent on the arrangement of the optical paths in detection system. The width of Čerenkov light in Fig. 3 is slightly sharper than these of Figs. 1 and 2.

Fig. 4 Emissions from pure cyclohexane; (a), cyclohexane with 0.1 mM 2,5-diphenyloxazole; (b), and cyclohexane with 0.1 mM 2,5-diphenyloxazole containing 400 mM CCl_4; (c) under the same irradiated condition. Values, Y_0 and Y, were difined as shown in (b) and (c).

Fig. 5 Dose dependence of initial yield of excited 2,5-diphenyloxazole (PPO^*). It was thought that dose per pulse is proportional to electron charge per pulse.

Fig. 6 Emission spectra of excited 2,5-diphenyloxazole without additive (o), with 400 mM CCl_4 (•) and with 400 mM CCl_2:CCl_2 (Δ) in 0.1 mM 2,5-diphenyloxazole-cyclohexane solution. Spectra resolution was set rather large to be ∿10 nm, because the emission intensity was weak.

Fig. 7 Change of initial emission yield (Y/Y_0) as a function of concentrations of additives in 0.1 mM 2,5-diphenyloxazole-cyclohexane solution. The values, Y and Y_0, were defined as shown in Fig. 4.

Fig. 8 Change of initial emission yield (Y/Y_0) as a function fo concentrations of additives in 0.1 mM 2,5-diphenyloxazole-cyclohexane solution.

Fig. 9 (a) Monoenergetic electron attachment rate, $\alpha w(\varepsilon)$ [$sec^{-1} \cdot Torr^{-1}$] as a function of electron energy (ε) [eV] (from ref. 16) and (b) an assumed function of $p(\varepsilon)$.

Table I. Energies, ε_1 and ε_2, of the first and second maxima and thermal value, $(\alpha w)_{th}$, in electron attachment cross section obtained in gas phase (from ref. 25).

Molecule	ε_1(eV)	ε_2(eV)	$(\alpha w)_{th}(s^{-1} \cdot torr^{-1})$
CCl_4	~ 0	0.2	8.5×10^9
			9×10^9
			13.3×10^9
CCl_3H	0.1	0.44	1.3×10^8
$CHClCCL_2$ (CCl_2:CCl_2)	0.2	0.76	7.8×10^7

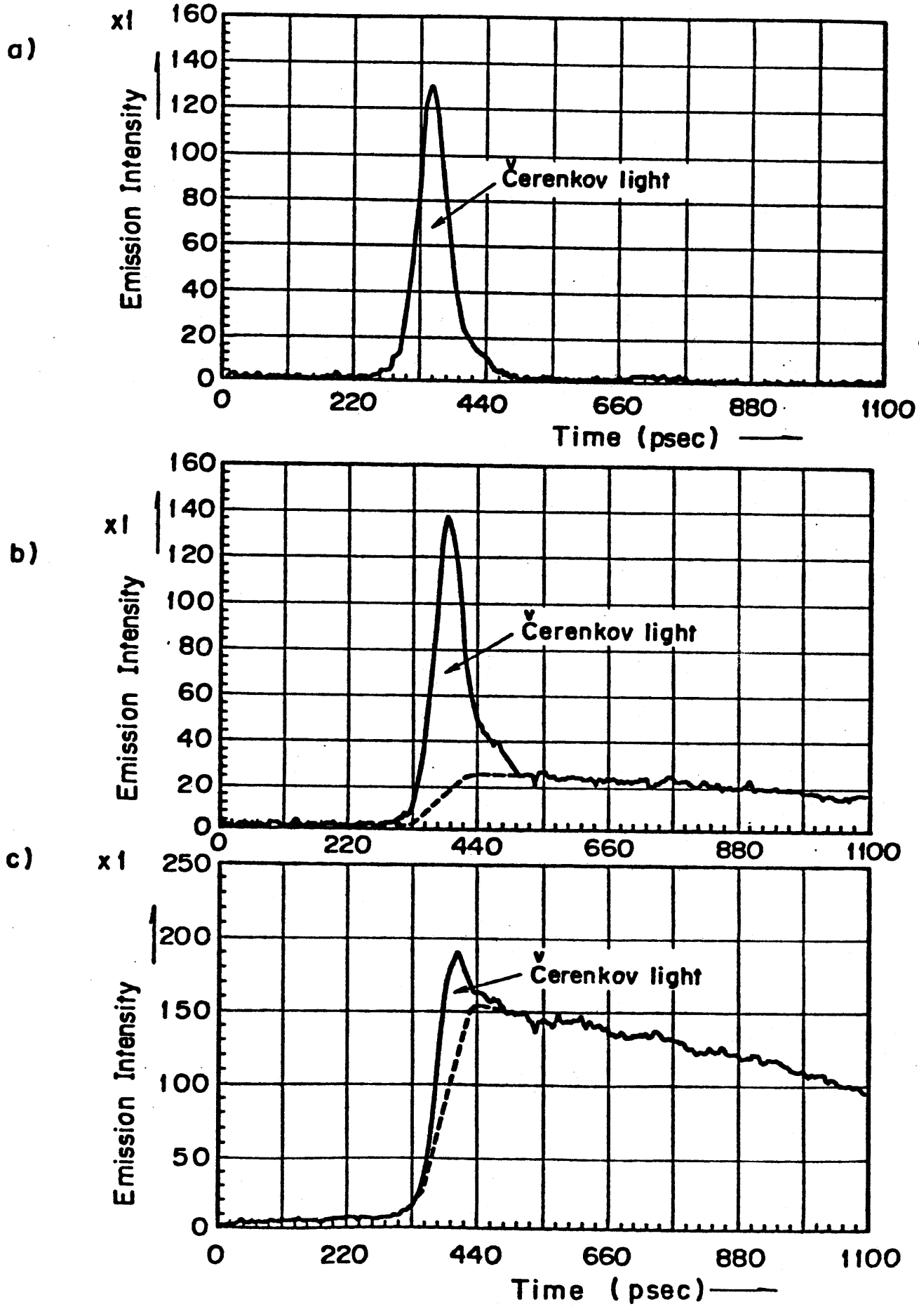
a)
x1
160
140
120
100
80
60
40
20
0
Emission Intensity
Čerenkov light
0
220
440
660
880
1100
Time (psec)
b)
x1
160
140
120
100
80
60
40
20
0
Emission Intensity
Čerenkov light
0
220
440
660
880
1100
c)
x1
250
200
150
100
50
0
Emission Intensity
Čerenkov light
0
220
440
660
880
1100
Time (psec)

Fig.1 (a),(b) and (c)

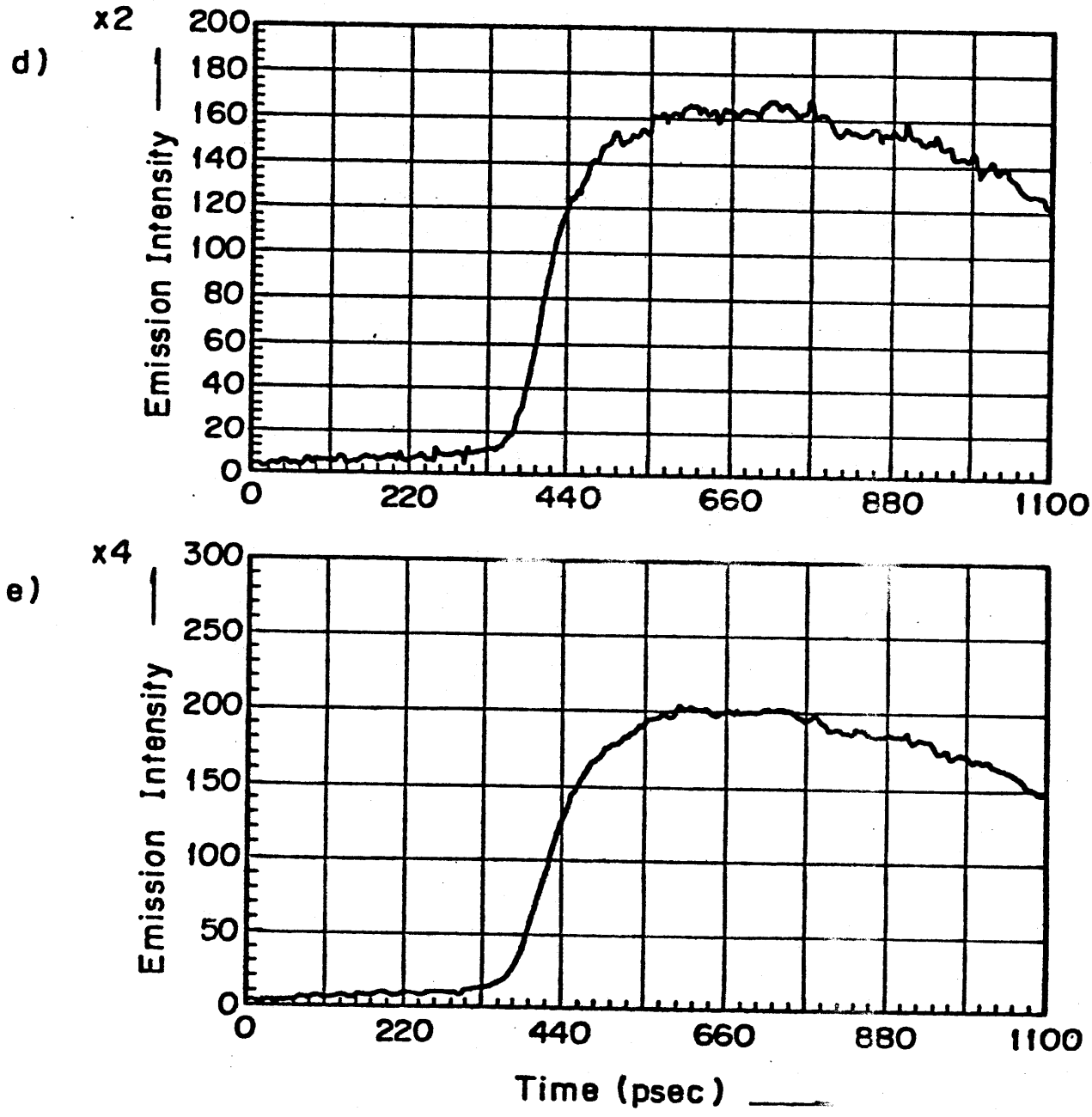
d)
x2
Emission Intensity
200
180
160
140
120
100
80
60
40
20
0
0
220
440
660
880
1100
e)
x4
Emission Intensity
300
250
200
150
100
50
0
0
220
440
660
880
1100
Time (psec)

Fig.1 (d) and (e)

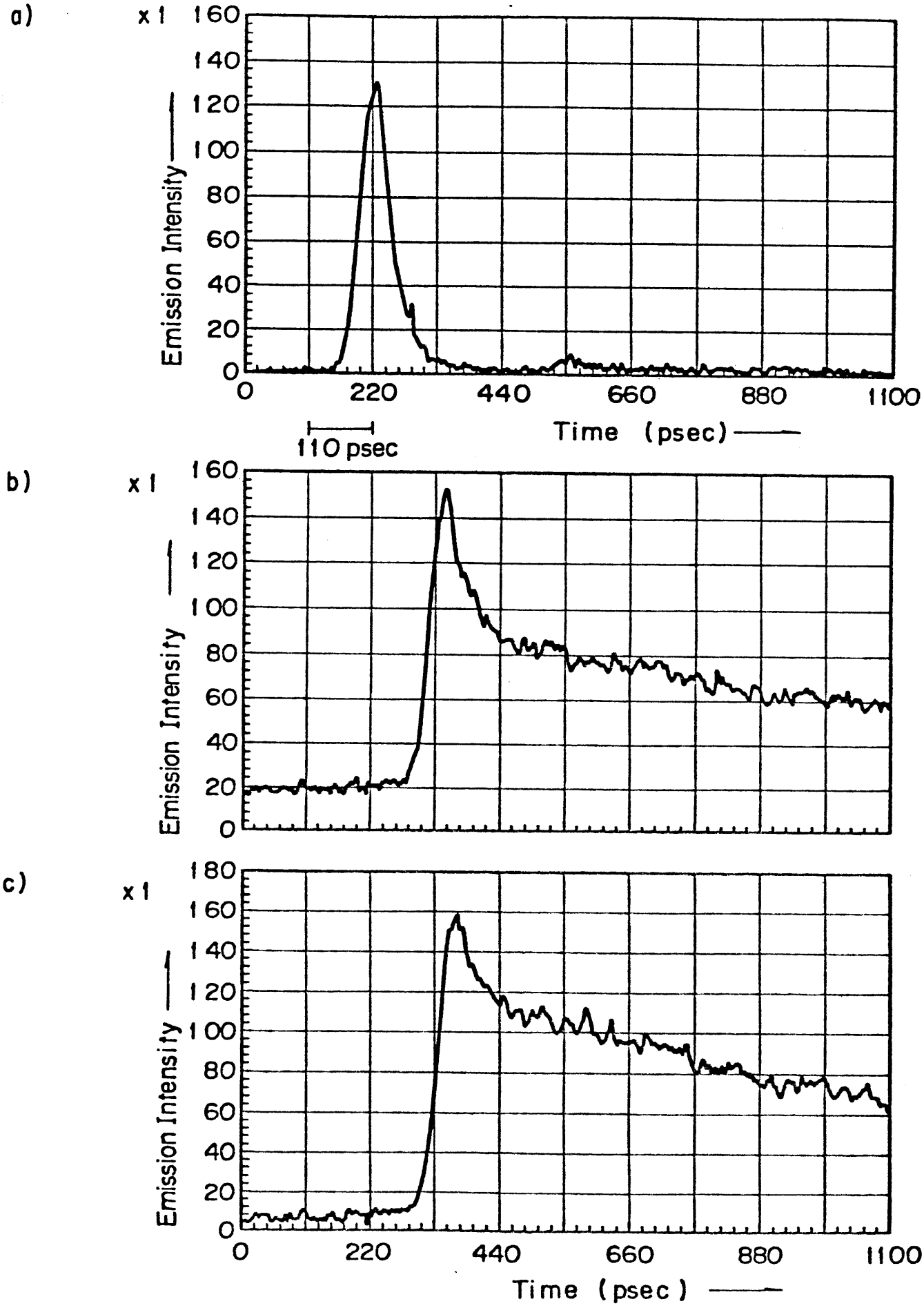
a)
x1
160
140
120
100
80
60
40
20
0
Emission Intensity
0
220
440
660
880
1100
Time (psec)
110 psec
b)
x1
160
140
120
100
80
60
40
20
0
Emission Intensity
c)
x1
180
160
140
120
100
80
60
40
20
0
Emission Intensity
0
220
440
660
880
1100
Time (psec)

Fig.2 (a),(b) and (c)

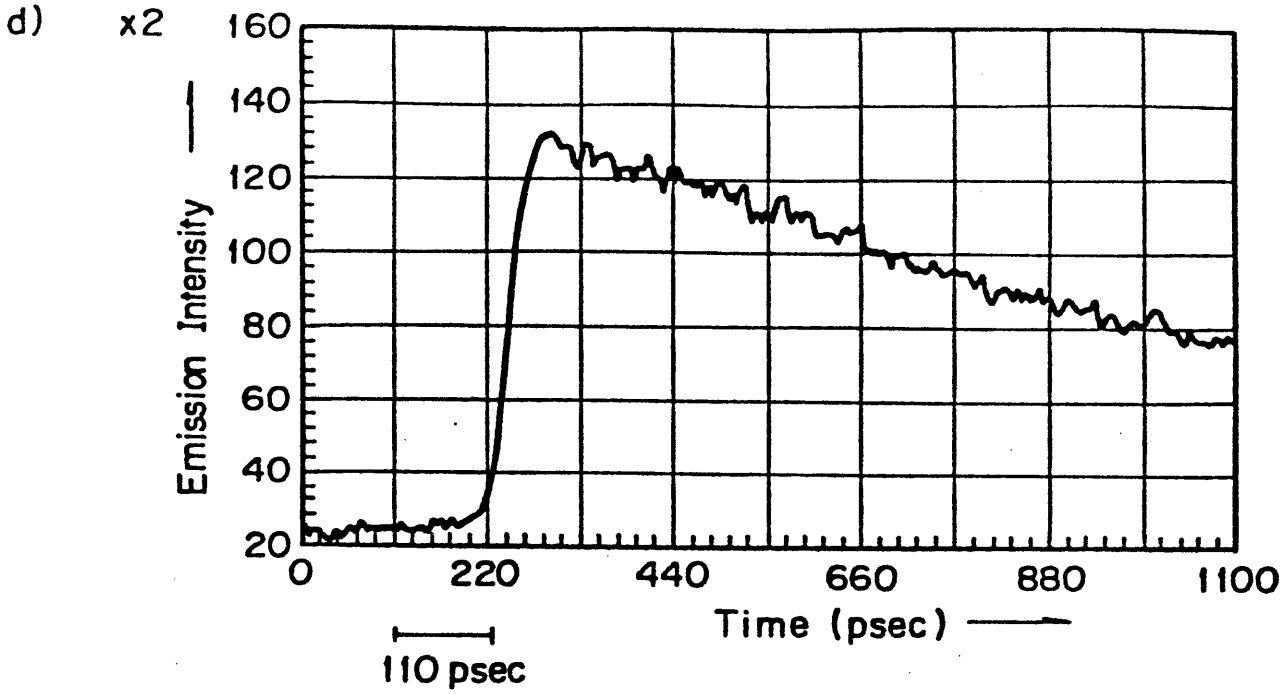
d)
x2
Emission Intensity
160
140
120
100
80
60
40
20
0
220
440
660
880
1100
Time (psec)
110 psec

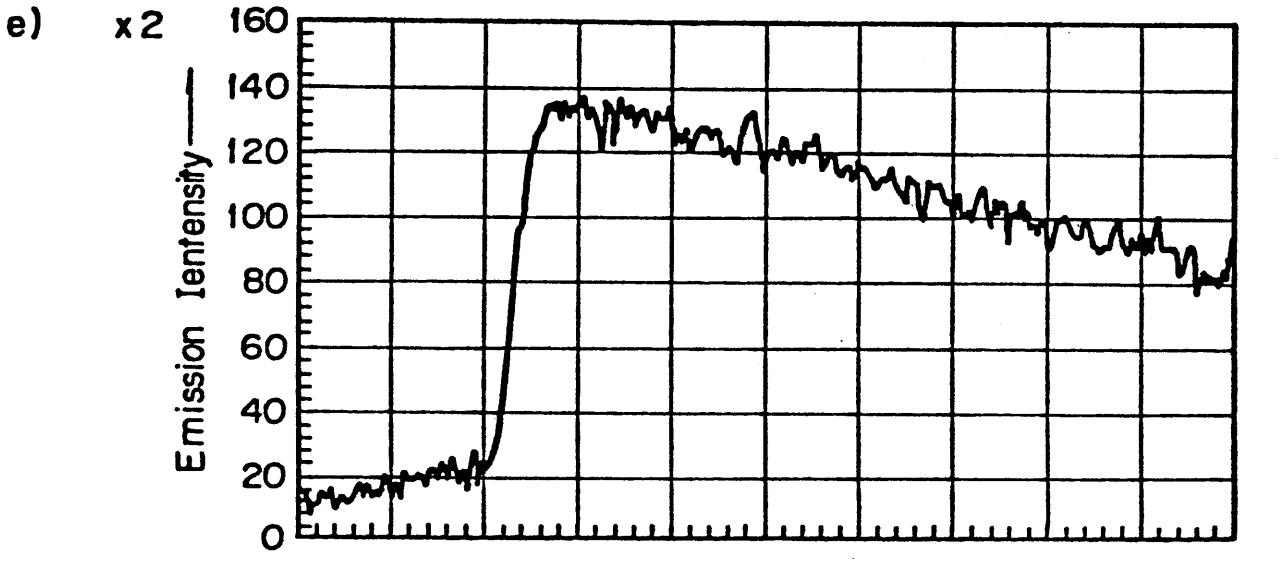
e)
x2
Emission Intensity
160
140
120
100
80
60
40
20
0

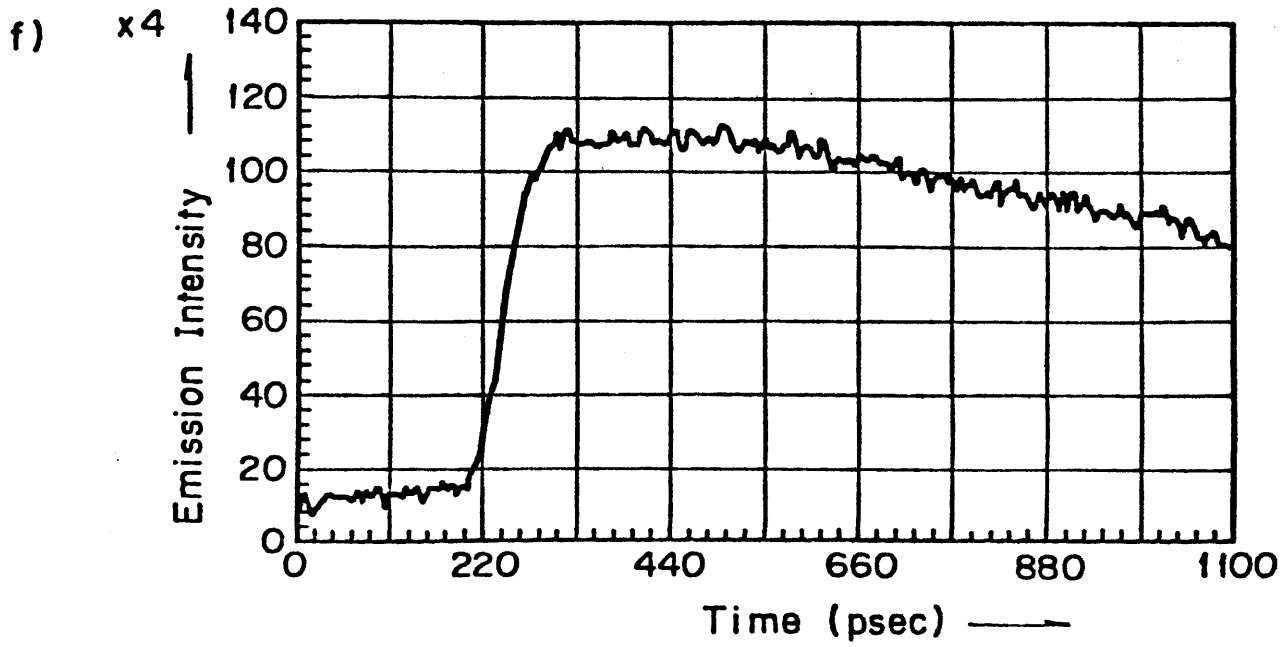
f)
x4
Emission Intensity
140
120
100
80
60
40
20
0
220
440
660
880
1100
Time (psec)

Fig.2 (d),(e) and (f)

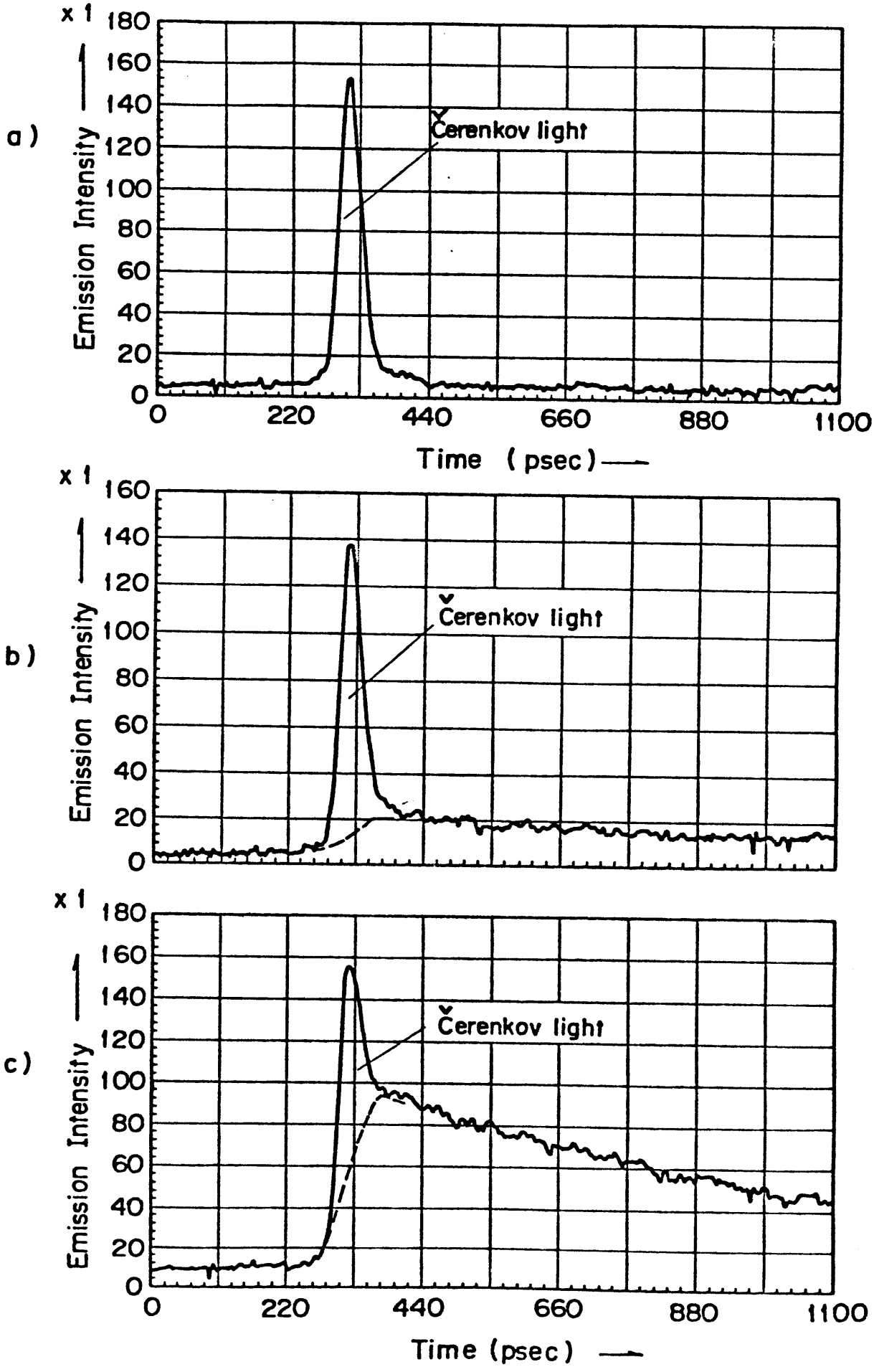
a)
x 1
Emission Intensity
Čerenkov light
Time (psec)
b)
x 1
Emission Intensity
Čerenkov light
c)
x 1
Emission Intensity
Čerenkov light
Time (psec)

Fig.3 (a),(b) and (c)

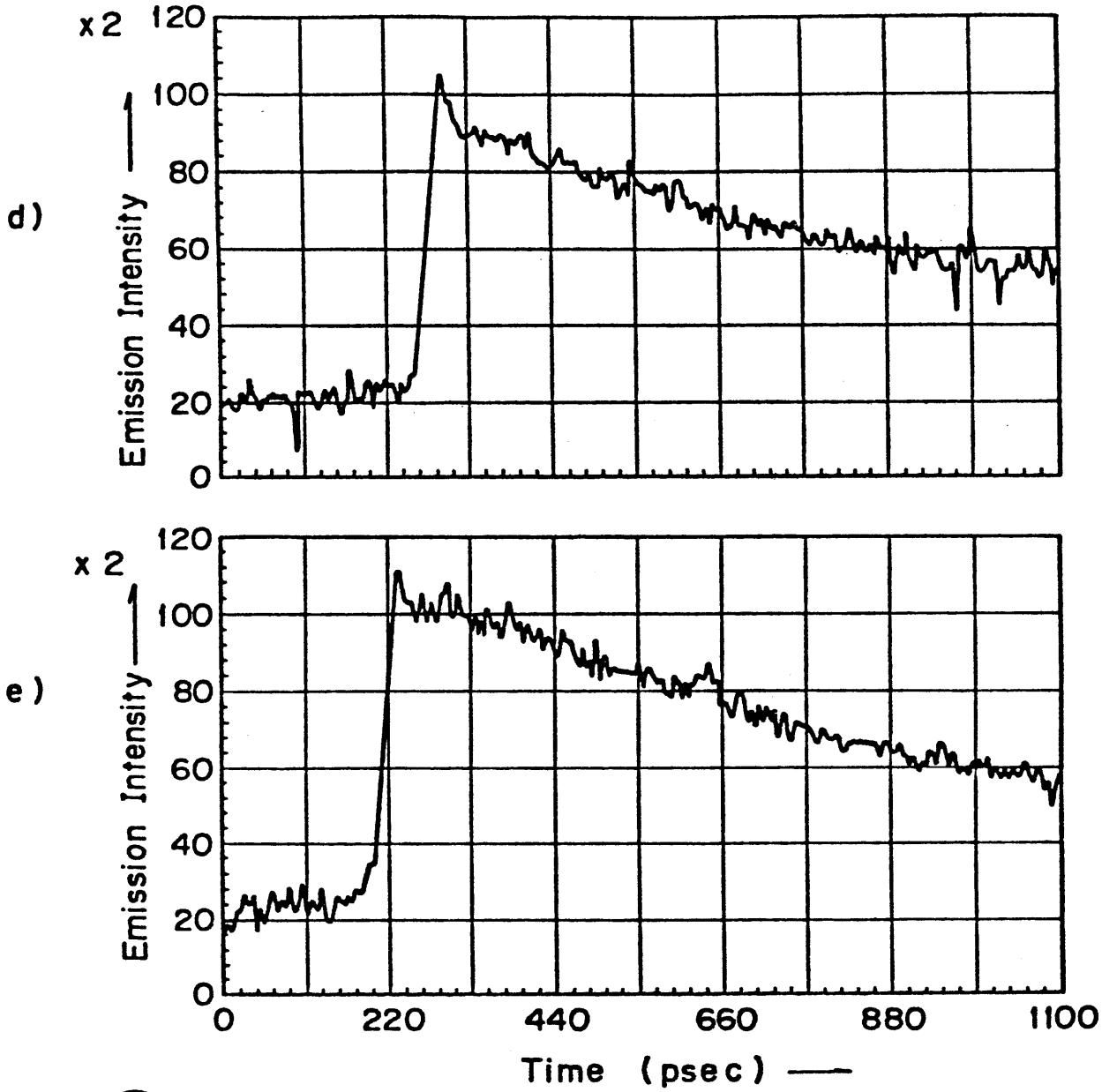
d)
x2
120
100
80
60
40
20
0
Emission Intensity

e)
x 2
120
100
80
60
40
20
0
Emission Intensity
0
220
440
660
880
1100
Time (psec)

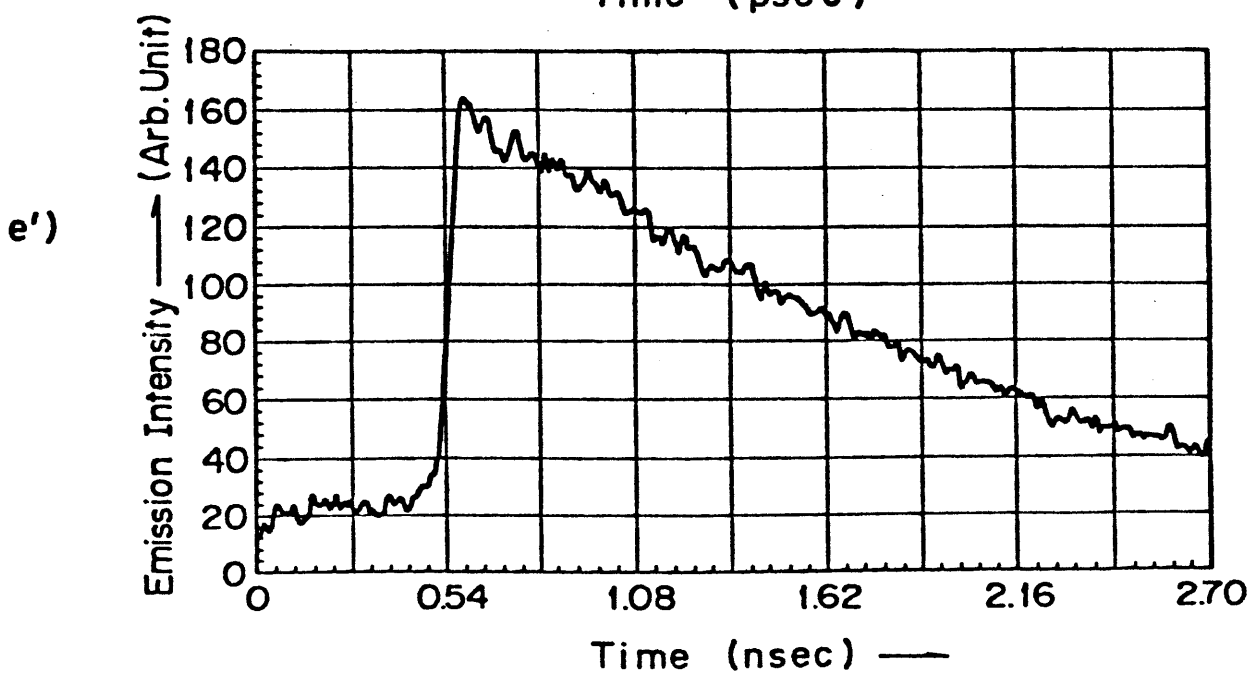
e')
180
160
140
120
100
80
60
40
20
0
Emission Intensity (Arb.Unit)
0
0.54
1.08
1.62
2.16
2.70
Time (nsec)

Fig.3 (d),(e) and (e′)

a)

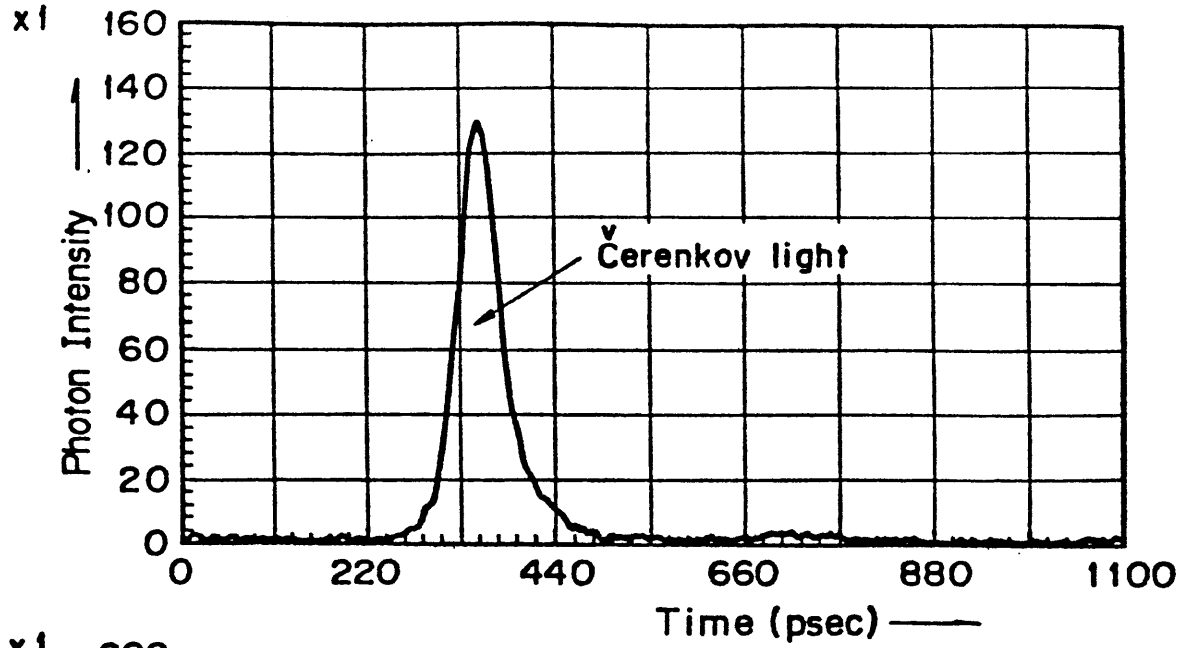

b)

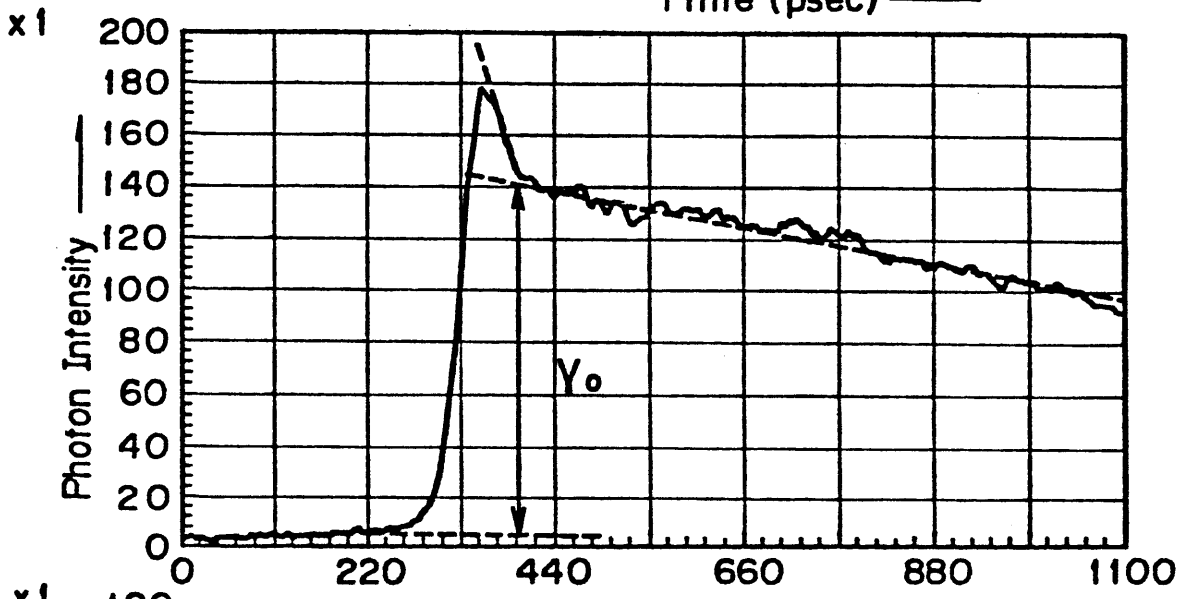

c)

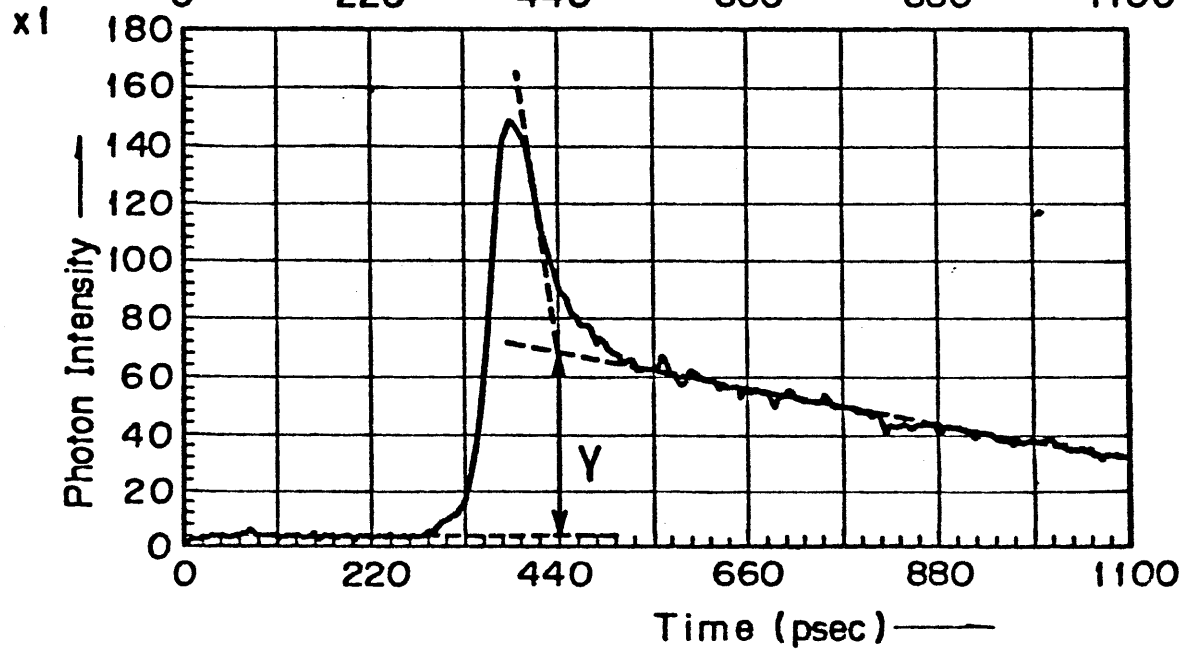

Fig.4 (a),(b) and (c)

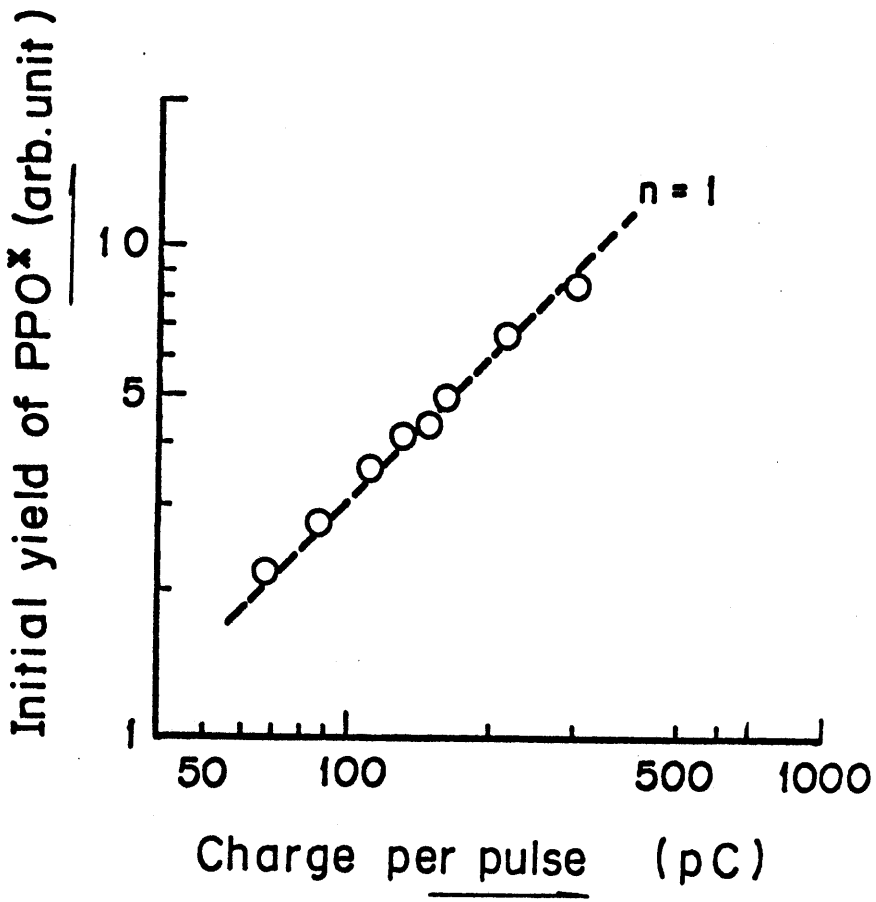
Initial yield of PPO* (arb.unit)
10
5
1
n = 1
50
100
500
1000
Charge per pulse (pC)

Fig.5

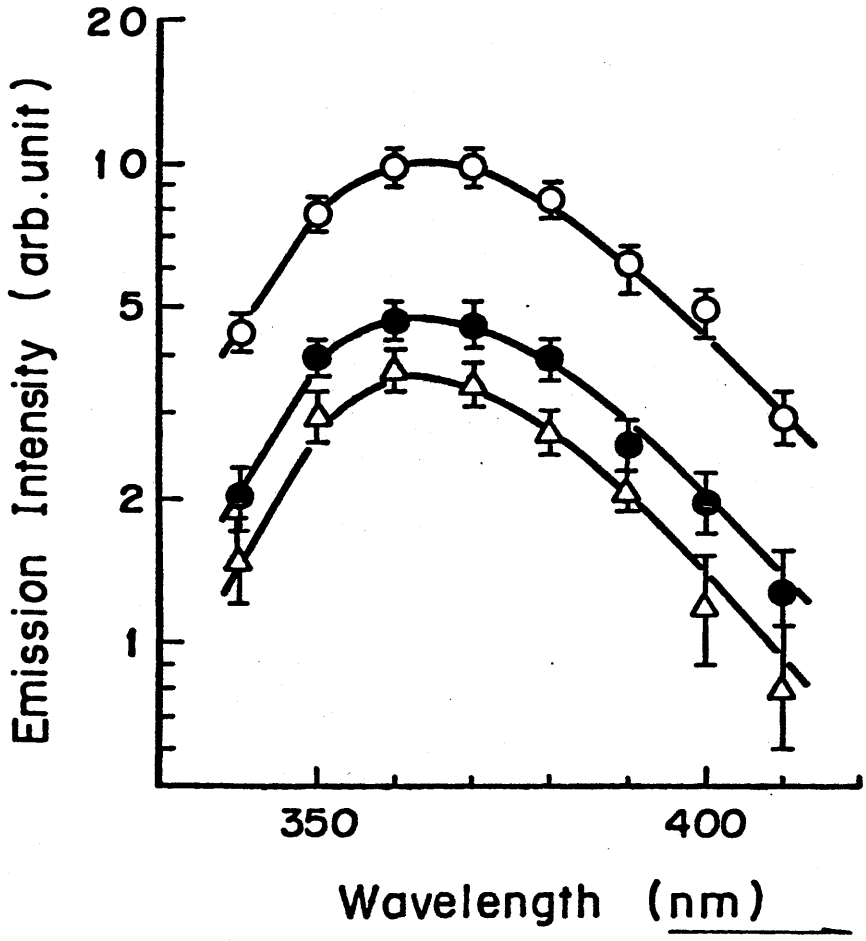

Fig.6

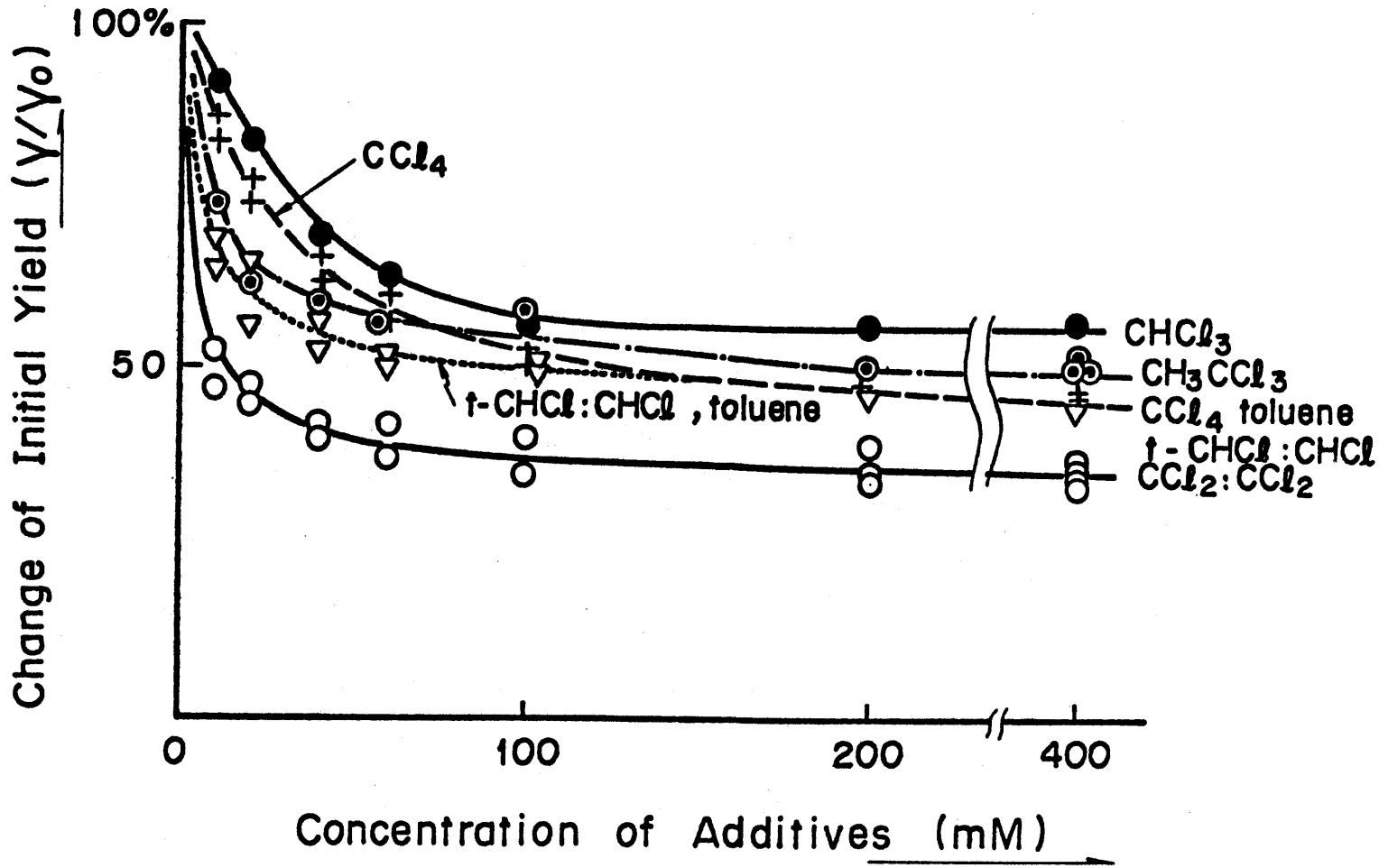
100%
50
Change of Initial Yield (Y/Y0)
CCl4
t-CHCl:CHCl , toluene
CHCl3
CH3CCl3
CCl4 toluene
t-CHCl:CHCl
CCl2:CCl2
0
100
200
400
Concentration of Additives (mM)

Fig.7

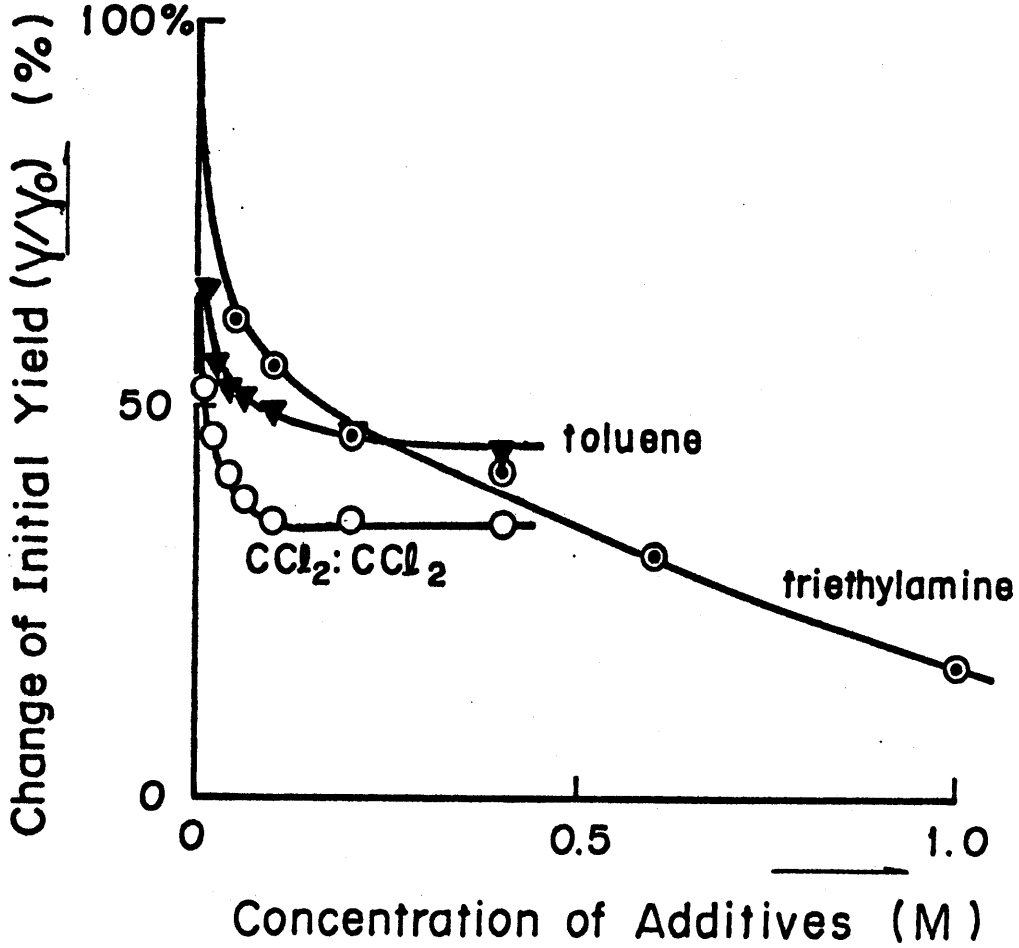
100%
50
0
0
0.5
1.0
Change of Initial Yield (γ/γ0) (%)
Concentration of Additives (M)
toluene
CCl2: CCl2
triethylamine

Fig.8

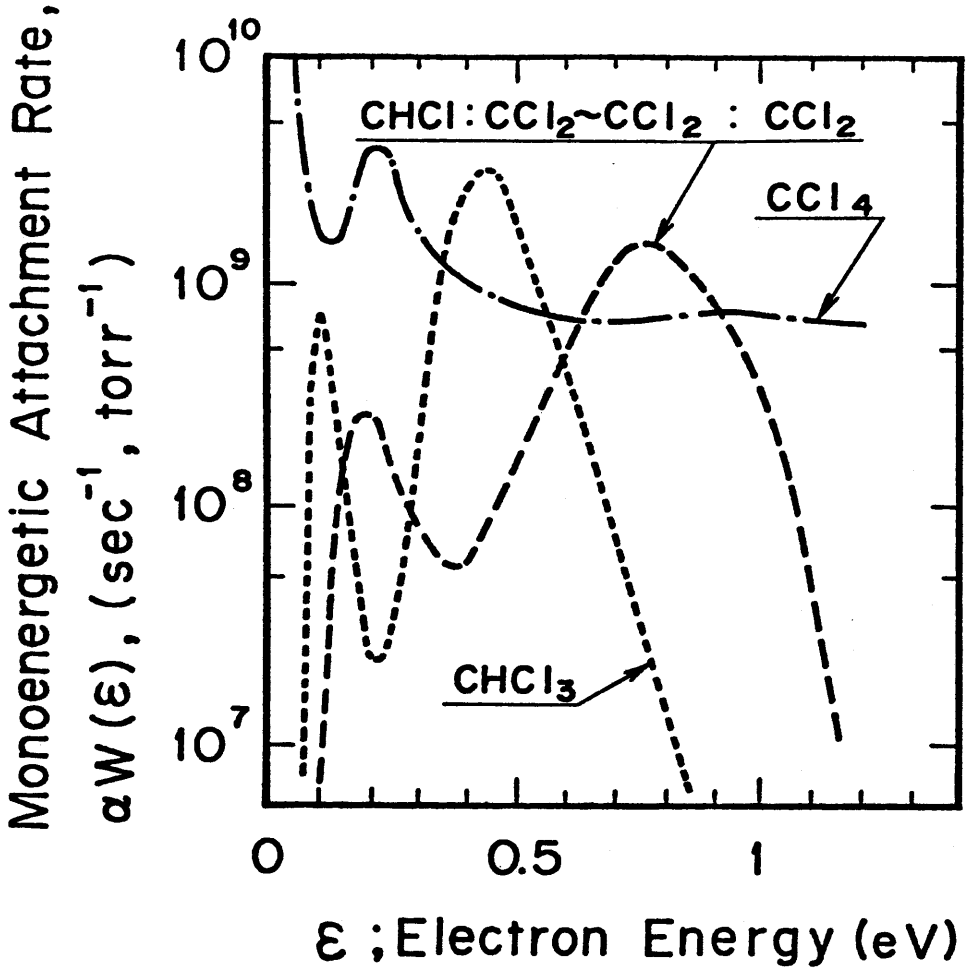
Monoenergetic Attachment Rate,
αW(ε), (sec⁻¹, torr⁻¹)
10¹⁰
10⁹
10⁸
10⁷
CHCl : CCl₂~CCl₂ : CCl₂
CCl₄
CHCl₃
0
0.5
1
ε ; Electron Energy (eV)

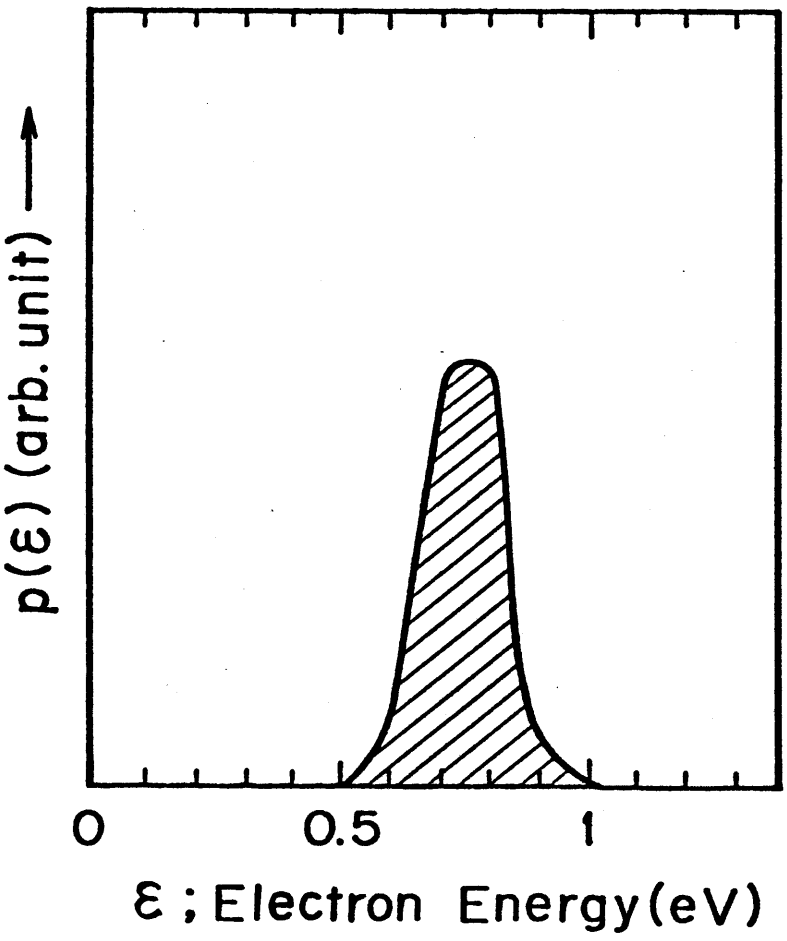
p(ε) (arb. unit)
0
0.5
1
ε ; Electron Energy(eV)

Fig.9 (a)and (b)

Chapter 10.

Studies on Scintillation Emissions in Various Kinds of Solvents by Means of Picosecond Pulse Radiolysis

Abstract

By using picosecond single electron pulse, scintillation behavior of excited 2,5-diphenyloxazole (PPO) in various kinds of solvents has been observed with 30 picosecond time resolution. The emission from solute excited states could be divided into two formation processes, faster and slower ones, from the view point of formation speed. From the points of combination of these two processes and emission efficiancy, solvents could be classified into three groups; effective, moderate and poor ones. This classification is in a good agreement with Kallmann's one.

Introduction

Liquid scintillation counting is widely used for the radioassay of biological and other materials labelled with carbon-14, tritium or other radio-isotopes.[1] Since the discovery of liquid organic solution scintillators in 1949, many combinations of solvents and solutes have been tested, and a great variety of scintillators have been prescribed and used. In 1955, Furst and Kallmann[2] reported that solvents could be divided into three classes of scintillation efficiency; effective, moderate, and poor.

Most of the aromatic compounds were included in " effective " solvents. In a second class, so called " moderate " solvents, saturated hydrocarbons were placed with efficiencies within a factor of 2∿4 of aromatic compounds. The third class of " poor " solvents includes alcohols and normal aliphatic ethers and ketones with efficiencies almost two orders of magnitude lower than that of the " effective " solvents.

The effective solvents such as benzene, toluene and p-xylene have been most extensively studied and the mechanism of the scintillation process, that excited singlet state of solute molecules are formed by energy transfer from excited state of solvent molecules produced by irradiation to solute molecules, has been widely accepted. In saturated hydrocarbons such as cyclohexane and n-heptane, Hirayama and Lipsky[3] studied by means of both photolysis and radiolysis and confirmed that the energy transfer plays a main role for the formation of solute excited states. Since most of the studies were based on steady state photolysis and radiolysis, scintillation behaviors with time are not yet known clearly.

Recently, studies on the formation of solute excited state in hydrocarbons by means of pulse radiolysis technique with single electron pulse (10 psec duration) from S-band linac by the present authors.[4] Emissions from solute excited state were detected with 30 psec time resolution. It was found experimentally that there are two formation processes, which we have been calling slower and faster processes. So-called " faster " formation process is completed within pulse duration (10 psec) and the " slower " formation process continues over a few nanoseconds after pulse irradiation. These two processes exist normally in any kinds of saturated and aromatic hydrocarbons. However, the ratio of these processes are significantly dependent on kinds of solvents and concentrations of solute molecules. The slower process was explained mainly based on the energy transfer from solvent excited state to solute molecules in liquid toluene.[4] Although the slower

process is not necessarily equivalent to the energy transfer one, it is thought that a large fraction of the slower process can be explained by the energy transfer mechanism. On the other hand, there are several possible mechanisms[4] for the faster formation process. One possible explanation was a direct formation of solute excited state by absorbing Čerenkov light induced by electron pulse in the matrix medium. This formation process is expected to be very fast one, because Kaiser et al[5] reported that risetime of emission from excited dimethyl-POPOP, which is one of the liquid scintillator, was measured to be less than 2 psec in both liquid and vapor phases by laser excitation. However, it is concluded that direct formation by Čerenkov light may not be predominant process, by comparing the number of solute excited state molecules produced and photons induced as Čerenkov light in sample solution. At present, it is thought that ion recombination of charged species may play an important role in the faster formation process.

In the present paper, behavior of scintillaiton emission of excited 2,5-diphenyloxazole (PPO) as a solute in various kinds of solvents is examined by means of pulse radiolysis with about 30 psec time resolution and the solvents will be reclassified from the view point of both above two formation processes and scintillaiton efficiency.

Experimental

Used over 30 solvent materials were saturated and aromatic hydrocarbons, alcohols, ketones, and ethers. Most of them were supplied from Tokyo Kasei Co. Ltd. As a solute, 2,5-diphenyloxazole (PPO) was used. PPO is one of the typical scintillator, which has been widely used as a solute for liquid scintillation counters. Concentrations of the most sample solutions were set at from 0.1 to 10 mM. As oxygen in air does not significantly affect the emission behavior in a short time ($\leq$1 nsec) after electron pulse irradiation,

most of the sample solutions used were air-saturated ones.

Emissions from sample solutions were detected by a streak camera (HTV) which has intrinsic time resolution of less than 10 psec. Normally 20∿100 streak traces were accumulated for increasing S/N ratio and consequent time resolution of the detection system was reduced to 30 psec in this accumulation mode. Most sample solutions were detected at room temperature (∿20°C).

The emission of the solute is fluorescence emitted from 340 nm to over 400 nm. The peak of the emission spectrum is around 360∿370 nm.[6] Because it is known that growth and decay of the emission with time at each wavelength is similar and sensitivity of the streak camera is almost flat with wavelength for the emission band, obtained traces without monochrometer are assumed to be the same with the emission at each wavelength. Then, streak traces of the samples having a large concentration ranges could be obtained by the streak camera without monochrometer.

Details of the linac[7] and the detection systems[4] were already reported elsewhere.

Results and Discussion

1) Faster and Slower Process

In Fig. 1, emissions from excited 2,5-diphenyloxazole in acetone, cyclohexane and phenylcyclohexane are shown. In liquid acetone which is one of the poor solvents, growth of emission from the solute excited state was completed at the end of Čerenkog light induced by electron pulse and the emissions decay gradually. As a lifetime of excited 2,5-diphenyloxazole in ethylalcohol was reported to be 1.6 nsec,[6] above experimental results suggest that most of the solute excited states are already formed immediately after the pulse. This rapid growth of emission has been called the faster formation of solute excited state. In phenylcyclohexane

which is palced in effective solvents, at lower solute concentration, Čerenkov light is clearly seen and at the end of Čerenkov light some fraction of excited states are already formed and gradual growth is also seen over 1 nsec. This gradual growth has been called slower formation process. At 10 mM of 2,5-diphenyloxazole in phenylcyclohexane, ratio of the slower formation to the faster one becomes large and the faster one can not be discriminated. On the other hand, in cyclohexane, both the slower and the faster formation can be seen, but the growth of the emission corresponding to the slower formation is relatively rapid as compared with those in phenylcyclohexane. In precise inspection, it was found that the time at which the emission intensity reaches to its maximum value becomes shorter with increase of solute concentration in cyclohexane.

2) Aromatic Solvents

In aromatic solvents; benzene, toluene (shown in Fig. 6(c)), p-xylene, ethylbenzene, isodurene, cumene, p-cymene and tetralin, the emission behaves similarly to that in phenylcyclohexane. Precise discussions of the slower formation process were reported in 2,5-diphenyloxazole-toluene[4] and 9,10-diphenylanthracene-toluene and cumene.[8] The slower process could be explained by energy transfer from solvent excited states to solute molecules. As the lifetime of solvent excited states is over 10 nanoseconds[6] and rate constant of energy transfer from excited solvent molecules to solute molecules is about 6×10^{10} M^{-1} sec^{-1},[4),8)] the growth of emission continues to over one nanosecond at 10 mM of solute concentration. This long growth time in aromatic solutions is different from that in saturated hydrocarbon solution. It was also found that the formation yields of the excited solute molecules due to the faster formation process in aromatic solutions are normally smaller than those in saturated hydrocarbons at the same concentration of solute.

3) Saturated Hydrocarbons

Used saturated hydrocarbons are cyclohexane, methylcyclohexane, trans-decalin, n-hexane, 3-methylpentane, and isooctane. In all solvents, both the faster and the slower formation process could be seen. Normally, at lower concentration ranges of the solute, the faster formation process is predominant and at over 1 mM, the slower formation one become large and it is difficult to discriminate the faster one from the total emission as already shown in Fig. 1.

The fraction of the faster process in isooctane is relatively large as compared with other saturated hydrocarbons. Up to 10 mM of solute concentration, the faster process is predominant as shown in Fig. 2, but emission intensity is somewhat smaller than that in cyclohexane. In other solvents, fraction ratios of these processes are almost the same with that in cyclohexane. At 10 mM concentration in saturated hydrocarbons, the total emission yields are 4∿5 times smaller than those of in aromatic solvents, as already reported by Kallmann.[1] In these saturated hydrocarbon solvents, emission efficiency is also dependent on each solvent and cyclohexane has the largest efficiency among them.[11]

In the case of binary mixture of cyclohexane and benzene as a solvent, change of the emission with time as a function of solvent mole fraction was precisely discussed in our previous papers.[4] It is noted that the faster formation of solute excited state in cyclohexane is reduced to some extent by adding small amount of benzene or toluene.[11]

4) Alcohols

In methylalcohol or ethylalcohol, the formation and decay behavior of the emission are similar to those in acetone as shown in Fig. 3. However, in benzylalcohol having a phenyl ring, the emission behavior as a function of time is somewhat different from that in ethylalcohol or methylalcohol but similar to that in aromatic solvents. Fig. 4 shows the emissions in

benzylalcohol. The slower process can be clearly seen, but the intensity due to the slower one is smaller than that in aromatic compounds. From comparing the emissions between in ethylalcohol and benzylalcohol, it seems that phenyl ring in solvent molecules may play a very important role for observing the slower formation process.

At 10 mM concentration of solute in methyl or ethylalcohol, only the emission due to the faster process can be seen and emission yield of the solute excited state is about 10 times smaller than that in aromatic compounds. The yield of the emission is saturated at higher concentration of solute.

5) Ethers

Ethylether, phenylethylether, di-benzylether, di-phenylether and benzylphenylether were used as ether solvents. The solute emissions are much different and dependent on the kinds of solvents, as shown in Fig. 5. In ethylether and benzylphenylether, no clear slower formation process could not be observed. In di-benzylether, most emission corresponds to the faster process, but small amount of emission due to slower one could be observed at 10 mM of 2,5-diphenyloxazole. In phenylethylether and di-phenylether, the emissions are similar to that in aromatic solvents. It is noted that samples of di-phenylether and benzylphenylether were measured at 35°C and 53°C, respectively, because they form solid phase at room temperature ($\sim$20°C).

Although phenyl ring in solvent moleculer structure is important for observing the slower formation process, as mentioned before, no clear slower formation one could not observed in benzylphenylether or di-benzylether. This point will be discussed later.

The solute emissions in cyclic-ethers were also investigated. In tetrahydrofuran and 2-methyltetrahydrofuran, the solute excited state forms similarly to that in acetone. In p-dioxane, the emission due to the slower process like in aromatics is predominant, but the contribution of this

slower one is several times smaller than that in aromatics. This result shows a drastic difference from that in tetrahydrofuran, as shown in Fig. 6.

6) Chlorides and Amine

It is well known that carbontetrachloride and chloroform are typical electron scavengers and triethylamine is a hole scavenger. They are also strong quenchers for excited states. In these liquids, no emission but only Čerenkov light could be observed even at 10 mM of solute concentrations. By other experiment using photoexcitation emission due to formation of the solute excited states in these liquid could be observed, but the yield is very low because these liquid behave as quenchers. It was also found that if some amount of the solute excited state is formed, the emission from the excited states should be observed. Therefore, the results obtained from pulse radiolysis study strongly suggest that the formation yields of the solute excited states in these solutions are significantly low or negligiblly small.

7) Classification of Solvents

It was already reported that solvents could be divided into three classes of scintillation efficiency by Kallmann et al.[2] Our experimental results are consistent with their classification. Solvents could be reclassified by not only scintillation efficiency but also behavior with time, as shown in Table 1. Most of the aromatic compounds are included in effective solvents, in which the solute excited states are formed by the slower and the faster processes. Although emissions have two formation processes in most of the saturated hydrocarbons, the saturated hydrocarbons are placed in moderate solvents. Because the emission yield in them is several times smaller than that in effective ones. On the other hand, no emission due to the slower process could not be observed in poor solvents. In chlorides or amines, which are also in poor solvents, even the faster formation could not be observed exceptionally.

8) Energy Transfer in Solvents

It was already noted that the most compounds which have a phenyl ring in chemical structure are placed in effective or moderate ones and large slower formation processes can be seen in them. Typical contrast of scintillation with time could be observed between in methyl or ethylalcohol and benzylalcohol, and diethylether and phenylethylether. These results strongly suggest that the phenyl ring in solvent molecular structure plays an energy donor to solute molecules. As energy transfer in aromatic solvents was confirmed in photolysis study,[3] this consideration seems to be reasonable.

However, all the solvents having phenyl ring in their chemical structures do not necessarily behave like benzene or toluene. In fact, in diphenylether and benzylphenylether which have phenyl ring in their molecular structures, large contribution of slower process could not be observed as shown in Figs. 5(b) and (d). In these liquids, it can be speculated that the energy on phenyl ring is rapidly lost before energy transfer, the rate constant of energy transfer is very small, and/or formation yield of excited solvent molecules as an energy donor is negligiblly small as compared with other solvents in which large contribution due to slower formation was observed.

It is known that the excited state of p-dioxane emits fluorescence between 220 nm∿330 nm[9] and its lifetime is obtained to be ∿2.2 nsec.[10] However, in tetrahydrofuran and 2-methyltetrahydrofuran, no fluorescence was reported. From our experimental results, both the slower and the faster formation process of solute excited states could be observed in p-dioxane but only the faster one could be observed in tetrahydrofuran and 2-methyltetrahydrofuran. Therefore, it is reasonable that the slower process in p-dioxane can be explained mainly by energy transfer from the lowest solvent excited state to solute molecules. This concludion is consistent with the fact that small emission correspounding to the fluorescence of the solvent could be observed in neat p-dioxane.

9) Faster Formation Processes

Emissions due to the faster process could be observed normally in the most solvents at lower concentration of solute. Although the intensity of the emission is dependent on the kinds of solvents and is saturated over 10 mM concentration of solute. It was found that emissions due to the faster formation in alcohols and ethers are smaller than that in saturated and aromatic solvents. In isooctane, the faster formation process is predominant even at higher concentration ranges as shown in Fig. 2, but its intensity is also saturated at higher solute concentrations. It seems that contribution of the faster process depends on the kind of solvents.

Since it was found that the faster formation process is reduced by addition of electron and hole scavengers such as CCl_4, $CHCl_3$ and triethylamine,[4] it is assumed that rapid recombination of solute and solvent charged species play an important role. Precise mechanism of the faster process is not yet made clear at present, and further discussions are in progress.[11]

Conclusion

By means of picosecond pulse radiolysis, scintillation emissions in various kinds of solvents have been observed with about 30 picosecond time resolution. It was found that normally emissions have two formation processes; the slower and the faster one. The faster formation of solute excited state is completed within pulse duration and the slower formation of it continues after electron pulse over 1 nsec. Solvents could be divided into three classes; effective, moderate and poor ones, by not only scintillation efficiency but behavior with time. This classification is in a good agreement with Kallmann's one. As for the slower formation process in aromatic solvents, phenyl ring in solvent molecular structure or the lowest excited state may play an energy donor to solute as an accepter. On the other hand the mechanism of the faster formation process is not yet made clear at present.

References

1) for example, " Liquid Scintillation Counting " ed by P.E. Stanley and B.A. Scoggins, Academic Press, 1974.
" Liquid Scintillation Counting " vol. 1~6 Proceedings of a Symposium on Liquid Scintillation Counting, Heyden & Son Ltd.

2) M. Furst and H. Kallmann; J. Chem. Phys. 23 607 (1955)

3) F. Hirayama and S. Lipsky, " Organic Scintillators " ed by D.L. Horrocks, Academic Press, New York, 1970, p.205

4) S. Tagawa, Y. Katsumura and Y. Tabata; Chem. Phys. Letts. 64 258 (1979)
S. Tagawa, Y. Katsumura and Y. Tabata; Rad. Phys. Chem. 15 287 (1980)
Y. Katsumura, S. Tagawa and Y. Tabata; J. Phys. Chem. 84 833 (1980)
Y. Katsumura, T. Kanbayashi, S. Tagawa and Y. Tabata;
to be published

5) B. Kopainsky and W. Kaiser; Chem. Phys. Letts. 66 39 (1979)

6) I.B. Berlman " Handbook of Fluorescence Spectra of Aromatic Molecules " Academic Press (1971)

7) Y. Tabata, J. Tanaka, S. Tagawa, Y. Katsumura, T. Ueda and K. Hasegawa; J. Fac. Eng. Univ. of Tokyo. 34 619 (1978)
Y. Tabata, S. Tagawa, Y. Katsumura, T. Ueda, K. Hasegawa and J. Tanaka; J. Atomic Energy Soc. Japan, 20 473 (1978)

8) G. Beck and J.K. Thomas; J. phys. Chem. 76 3856 (1972)
G. Beck and J.K. Thomas; Chem. Phys. Letts. 16 318 (1972)
G. Beck and J.K. Thomas; J. Chem. Phys. 71 2611 (1979)

9) F. Hirayama, G.W. Lawson and S. Lipsky; J. Phys. Chem. 74 2411 (1970)

10) A.M. Halpern and W.R. Ware; J. Phys. Chem. 74 2413 (1970)

11) S. Tagawa, Y. Katsumura, T. Kanbayashi and Y. Tabata;
to be published
Y. Katsumura, S. Tagawa and Y. Tabata; to be published

Figure Captions

Fig. 1 Scintillation emissionsof 2,5-diphenyloxazole (PPO) in acetone; (a) (b), phenylcyclohexane; (c) (d) (e) and cyclohexane; (f) (g). Concentrations of 2,5-diphenyloxazole are 1 mM at (a), (c), (f) and 10 mM at (d), (e), (g). It is noted that vertical scale and horizontal scale of (e) are different from others. Vertical scales of 1.1 nsec sweep traces are comparable with Figs. 3, 4 and 5.

Fig. 2 Scintillation emissionsof 2,5-diphenyloxazole (PPO) in isooctane. Cerenkov light induced in pure isooctane is shown in (a). Concentrations of (b), (c), (d), (e) and (f) are 0.05 mM, 0.1 mM, 0.5 mM, 1 mM and 10 mM, respectively. It is noted that vertical scales are different from Figs. 1, e, 4, 5 and 6.

Fig. 3 Scintillation emissions of 2,5-diphenyloxazole (PPO) at 0.1 mM; (a) and 1 mM; (b) and 10 mM; (c) in ethylalcohol.

Fig. 4 Scintillation emissions of 2,5-diphenyloxazole (PPO) at 10 mM in benzylalcohol. In (b), holizontal scale is larger than that in (a).

Fig. 5 Scintillation emissions of 10 mM 2,5-diphenyloxazole (PPO) in ethylether; (a), phenylethylether; (b), dibenzylether; (c), diphenylether; (d) and benzylphenylether; (e). Diphenylether was measured at 35°C. Other samples were at room temperature (∿20°C).

Fig. 6 Scintillation emissions of 10 mM 2,5-diphenyloxazole (PPO) in tetrahydrofuran; (a), p-dioxane; (b) and toluene; (c) under the same irradiated condition. It is noted that vertical scales are different from Figs. 1, 2, 3, 4 and 5.

Table. 1 Classification of Solvents

	faster process	slower process	Emission Yield *	Solvents
effective	Yes	Yes	~ 1	aromatics; benzene, toluene, ethylbenzene p-xylene, cumene, p-cymene tetraline, phenylcyclohexane isodurene ethers; phenylethylether, diphenylether p-dioxane
moderate	Yes	Yes	$1/4 \sim 1/5$	saturated hydrocarbon cyclohexane, methylcyclohexane 3-methylpentane, transdecaline n-hexane, isooctane alcohol; benzylalcohol
Poor	Yes	No	$\sim 1/10$	alcohol; ethylalcohol, methylalcohol ketone; acetone ether; ethylether, dibenzylether** benzylphenylether tetrahydrofuran methyltetrahydrofuran
	No	No	$\ll \frac{1}{10}$	chloride; CCl_4, $CHCl_3$ amine; triethylamine

* In precise inspection, the emission yield depends on each solvent and solute concentration.
Only the relative efficiency between these four groups at 10 mM of solute concentration is shown.

** Small contribution of the slower process could be observed, but emission intensity is very low.
Therefore, dibenzylether is placed in poor group.

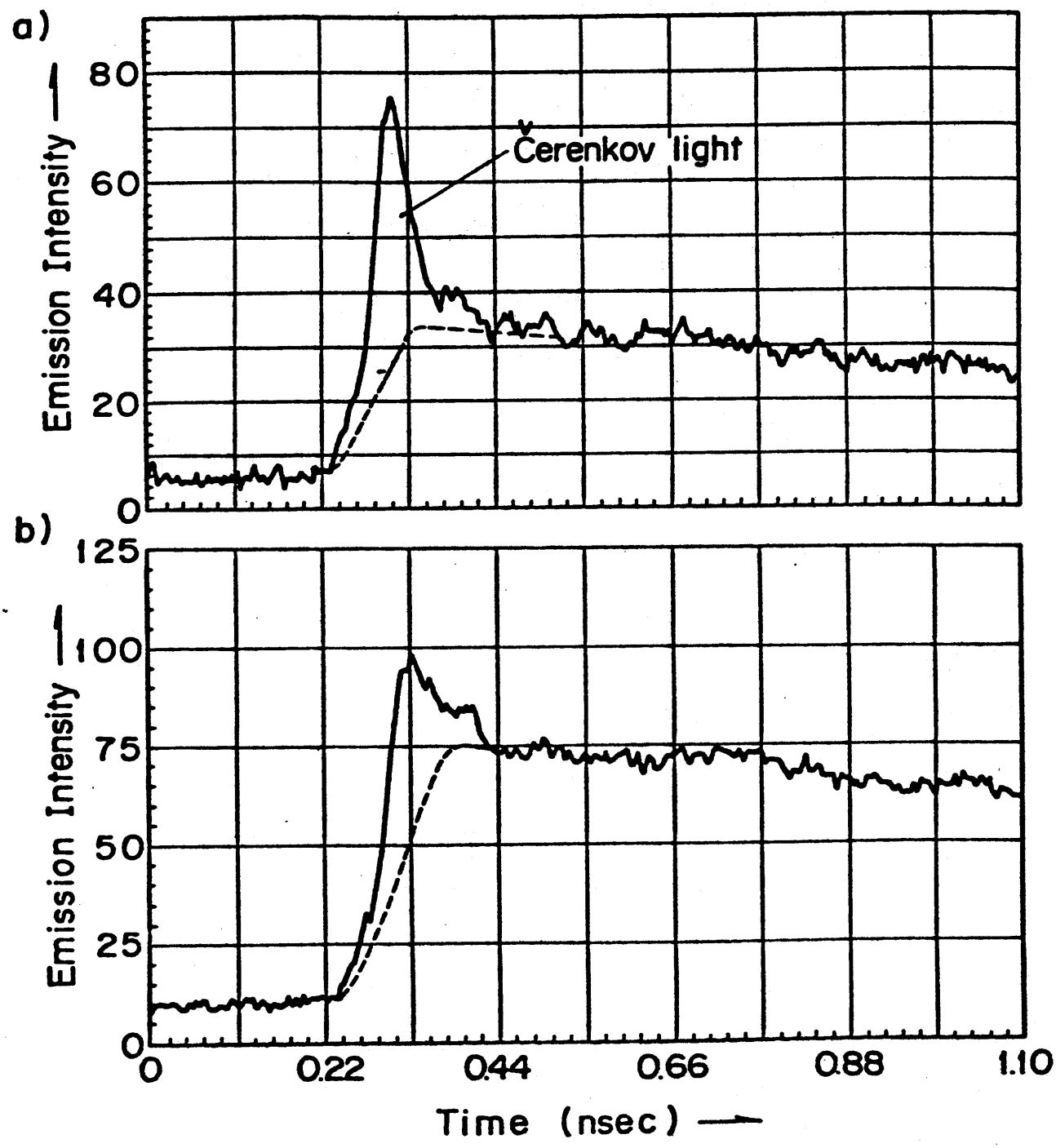
a)
Emission Intensity
80
60
40
20
0
Čerenkov light
b)
Emission Intensity
125
100
75
50
25
0
0
0.22
0.44
0.66
0.88
1.10
Time (nsec)

Fig.1 (a) and (b)

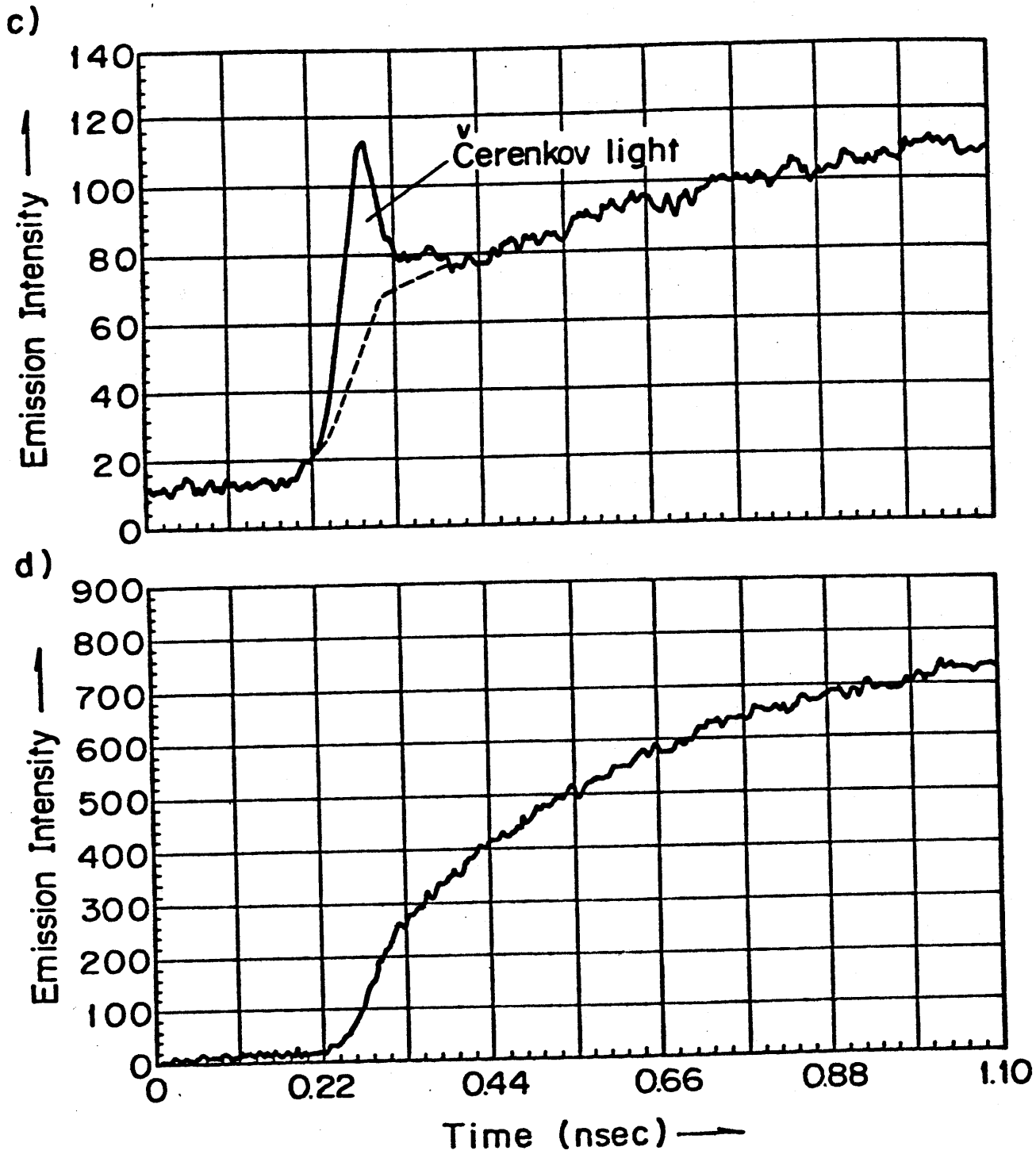
c)
Emission Intensity
140
120
100
80
60
40
20
0
Čerenkov light
d)
Emission Intensity
900
800
700
600
500
400
300
200
100
0
0
0.22
0.44
0.66
0.88
1.10
Time (nsec)

Fig.1 (c) and (d)

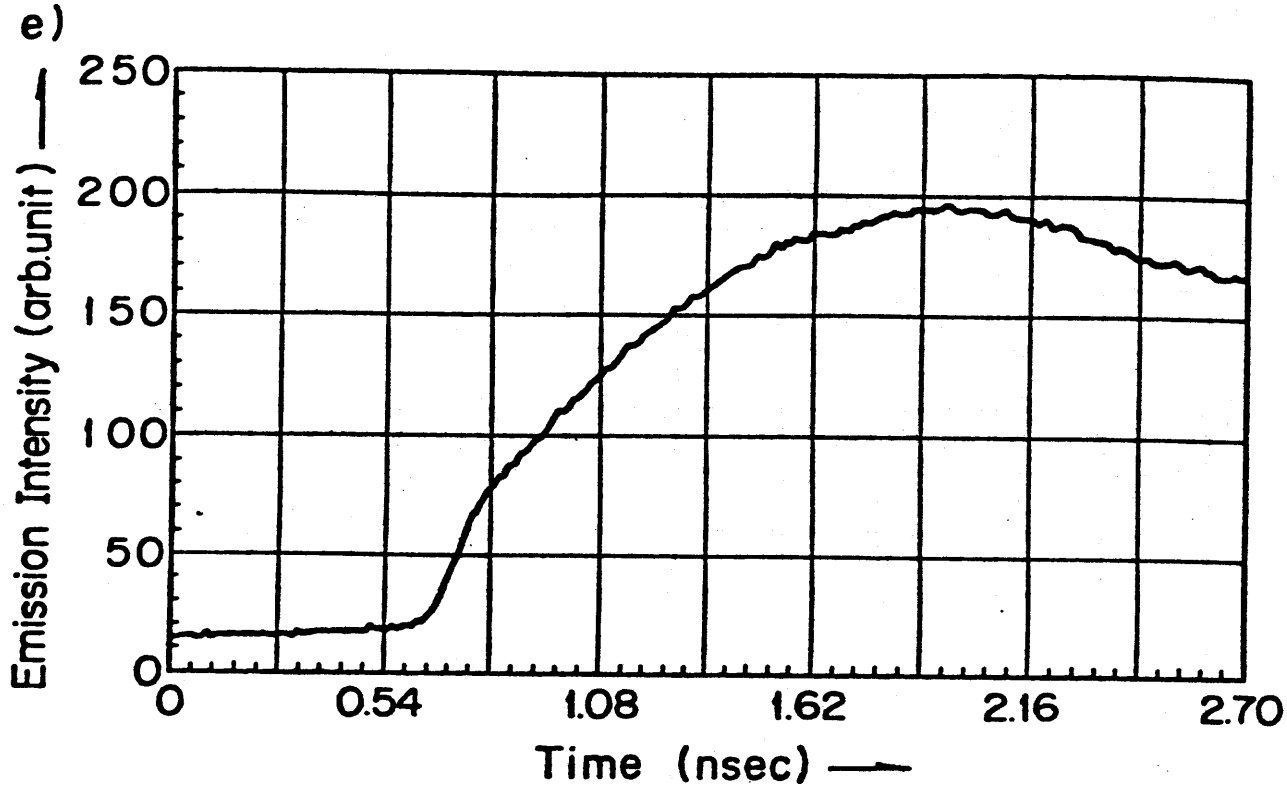
e)
Emission Intensity (arb.unit)
250
200
150
100
50
0
0
0.54
1.08
1.62
2.16
2.70
Time (nsec)

Fig.1 (e)

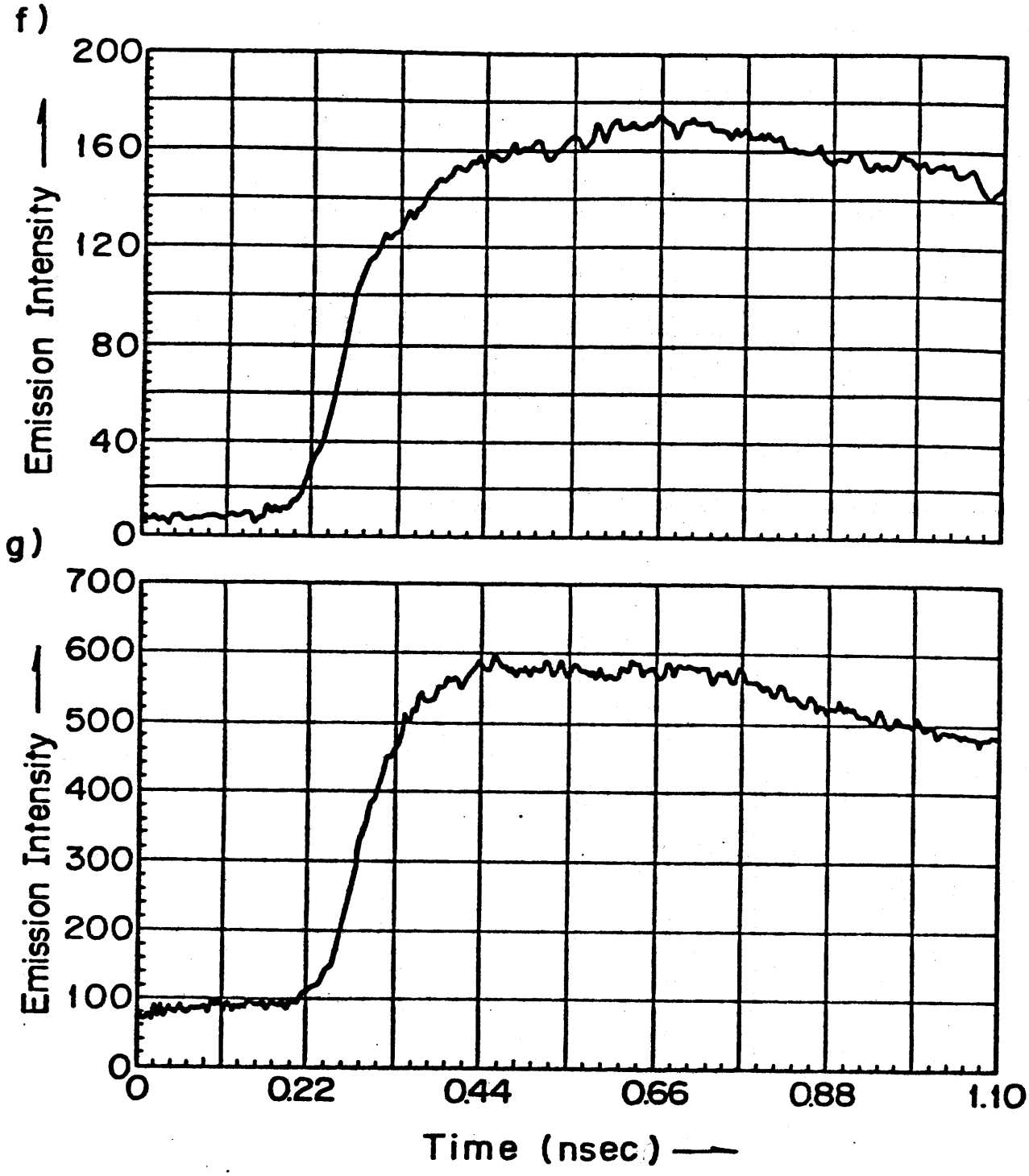
f)
200
160
120
80
40
0
Emission Intensity
g)
700
600
500
400
300
200
100
0
Emission Intensity
0
0.22
0.44
0.66
0.88
1.10
Time (nsec)

Fig.1 (f) and (g)

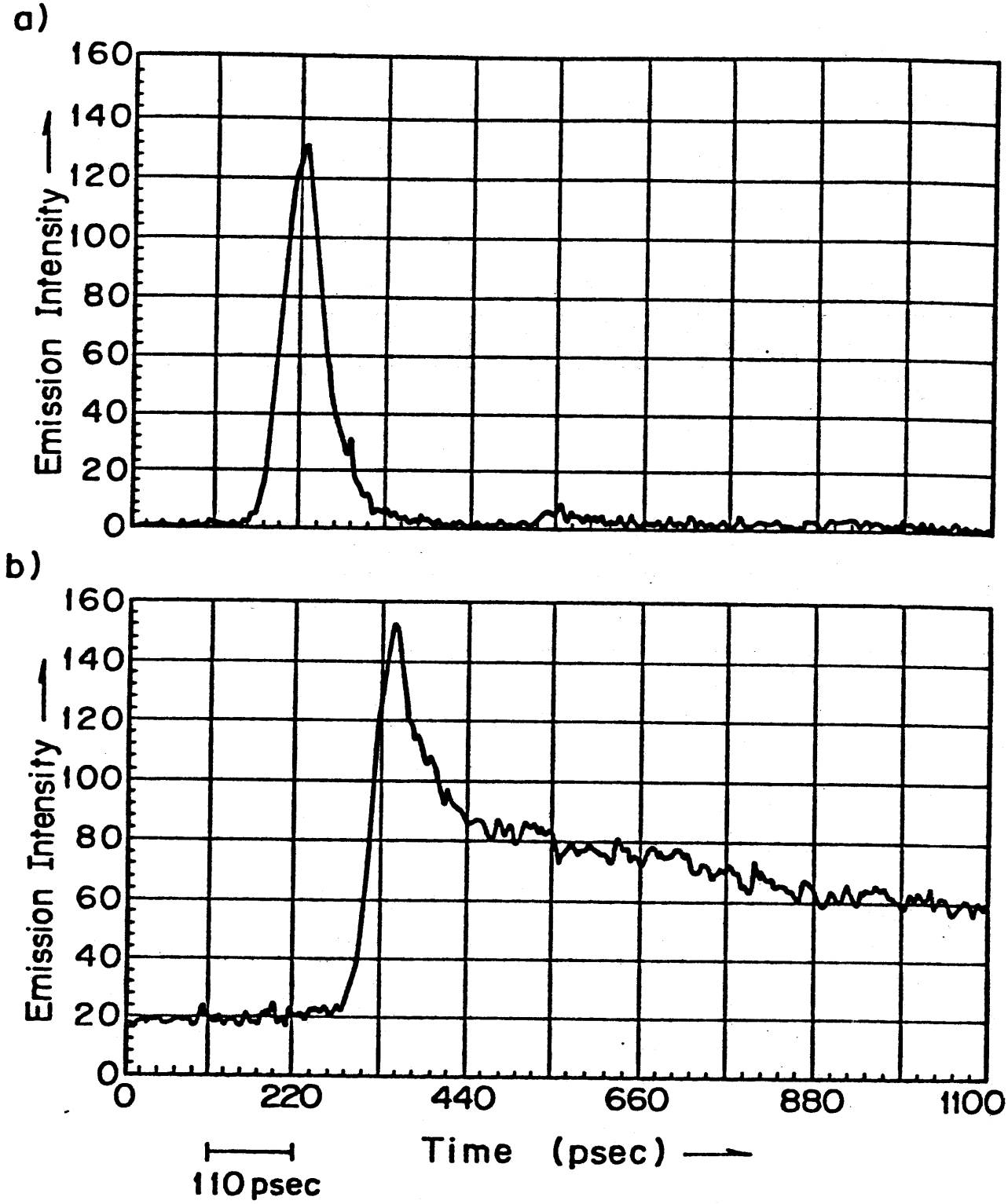
a)
160
140
120
100
80
60
40
20
0
Emission Intensity
b)
160
140
120
100
80
60
40
20
0
Emission Intensity
0
220
440
660
880
1100
Time (psec)
110 psec

Fig.2 (a) and (b)

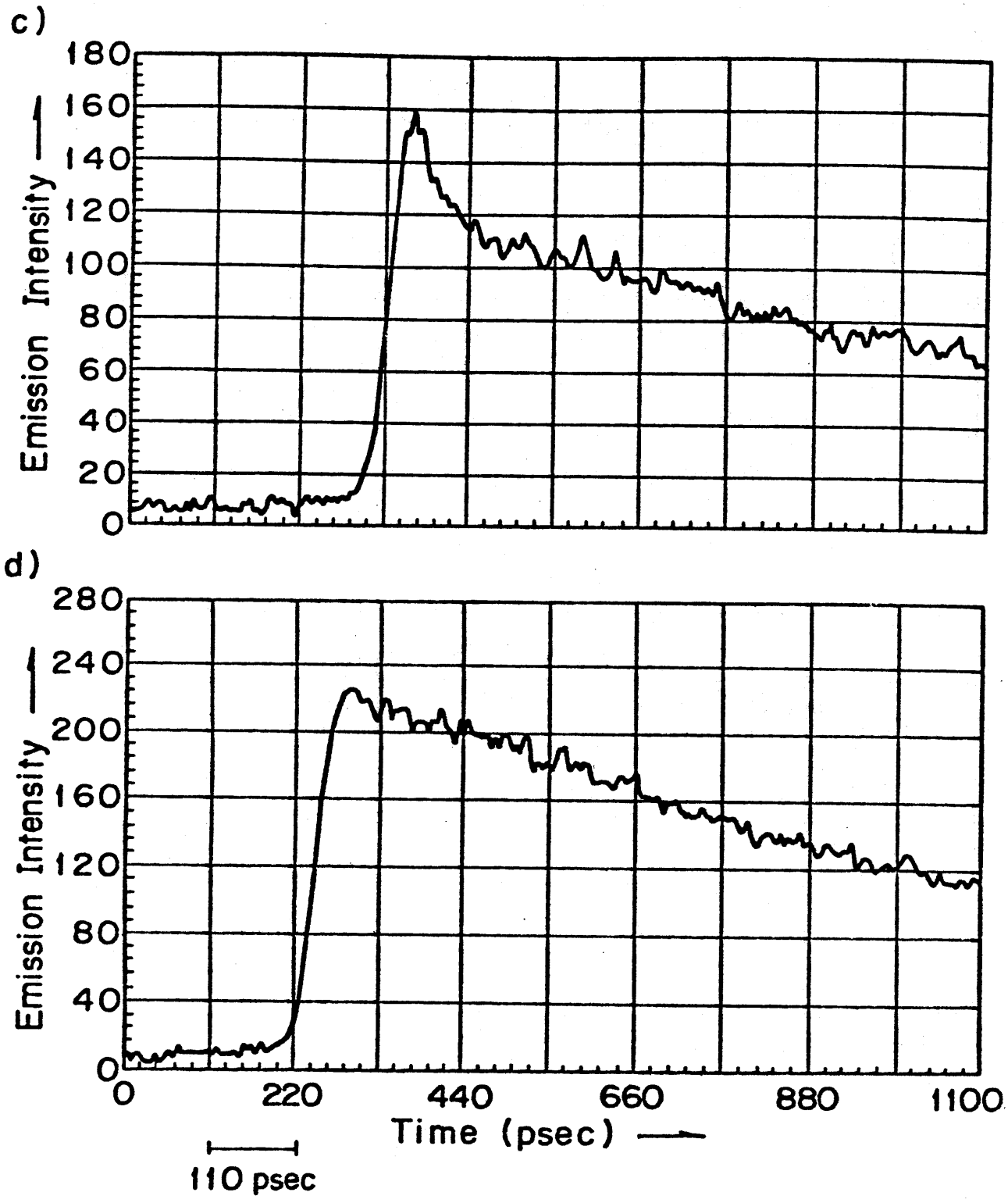
c)
Emission Intensity
180
160
140
120
100
80
60
40
20
0
d)
Emission Intensity
280
240
200
160
120
80
40
0
0
220
440
660
880
1100
Time (psec)
110 psec

Fig.2 (c) and (d)

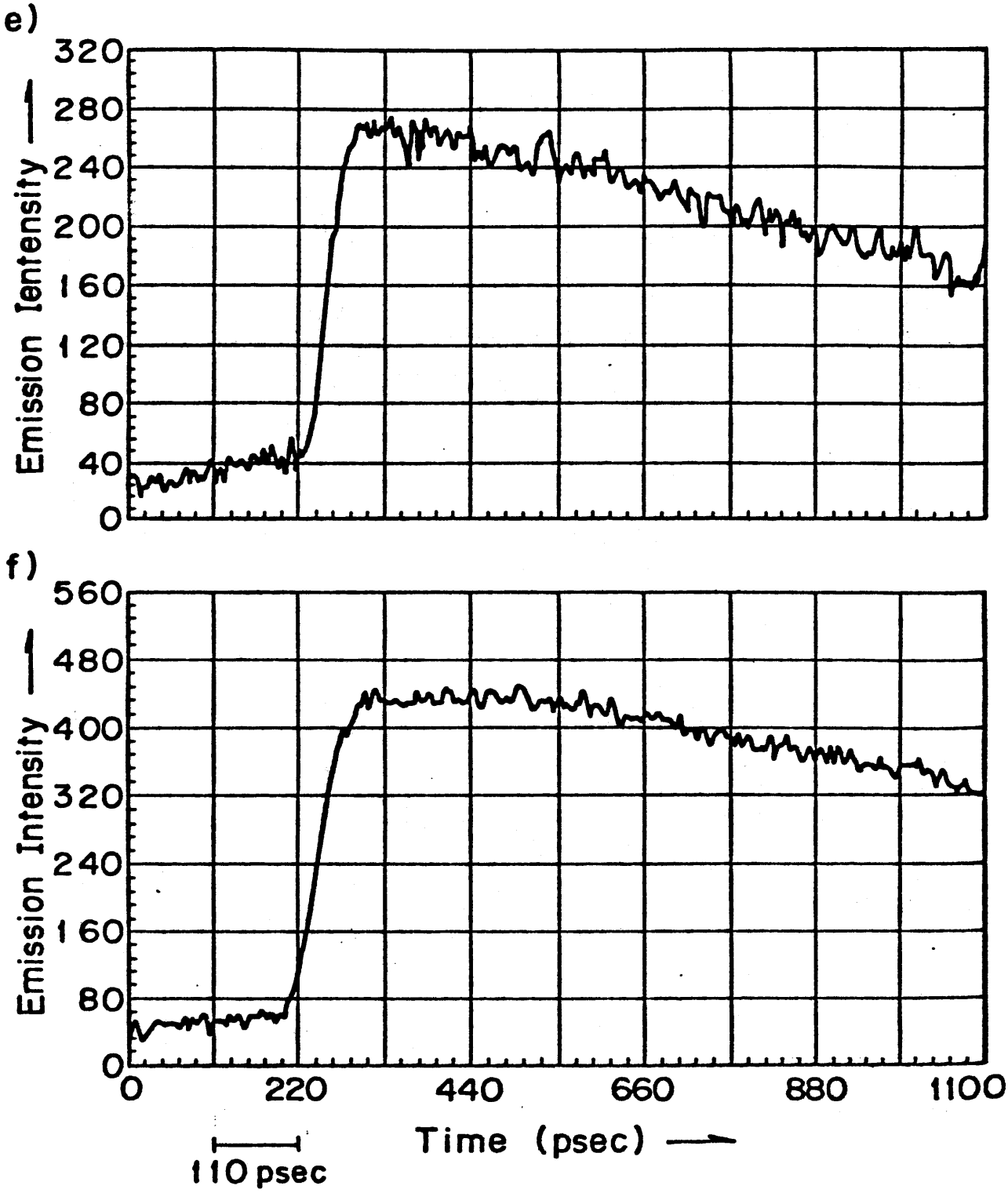
e)
Emission Intensity
320
280
240
200
160
120
80
40
0
f)
Emission Intensity
560
480
400
320
240
160
80
0
0
220
440
660
880
1100
Time (psec)
110 psec

Fig.2 (e) and (f)

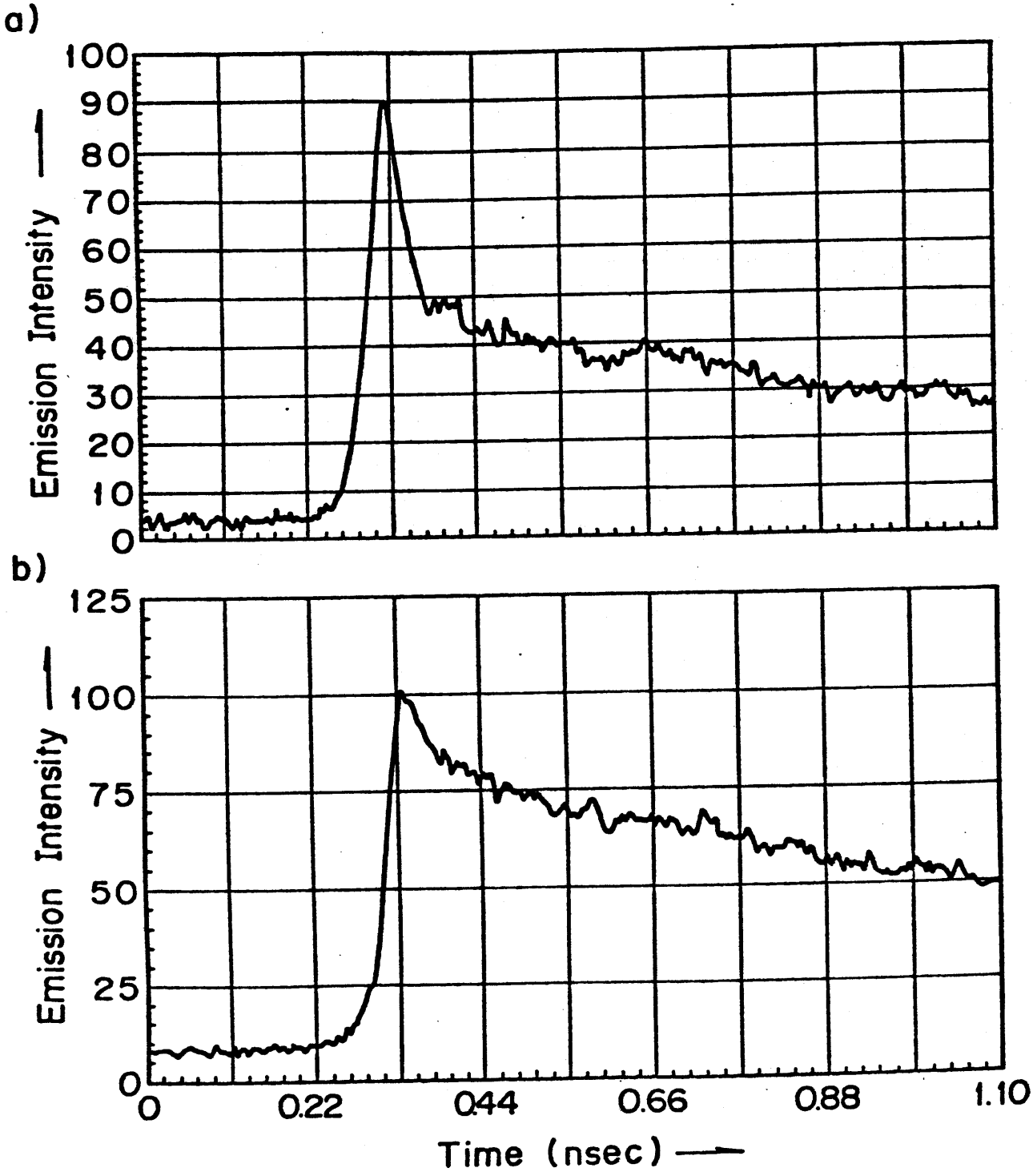
a)
Emission Intensity
100
90
80
70
60
50
40
30
20
10
0
b)
Emission Intensity
125
100
75
50
25
0
0
0.22
0.44
0.66
0.88
1.10
Time (nsec)

Fig.3 (a) and (b)

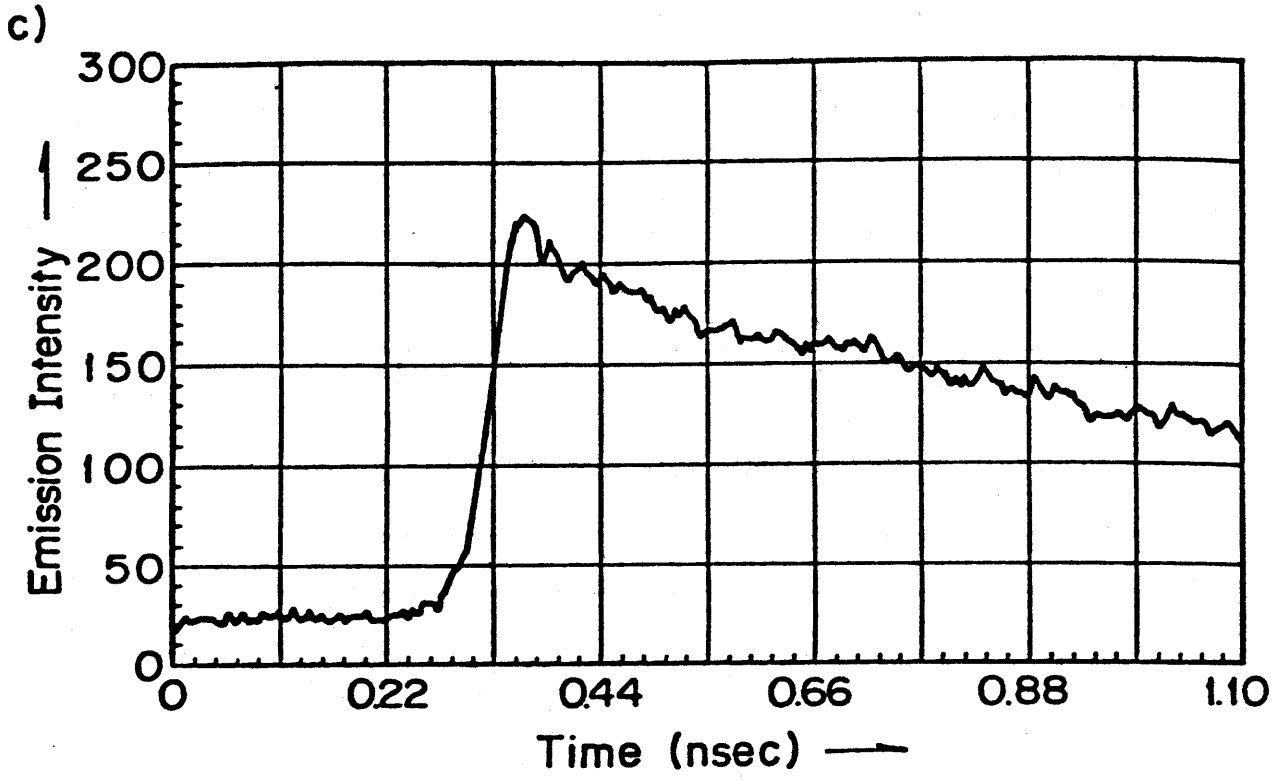
c)
300
250
200
150
100
50
0
Emission Intensity
0
0.22
0.44
0.66
0.88
1.10
Time (nsec)

Fig.3 (c)

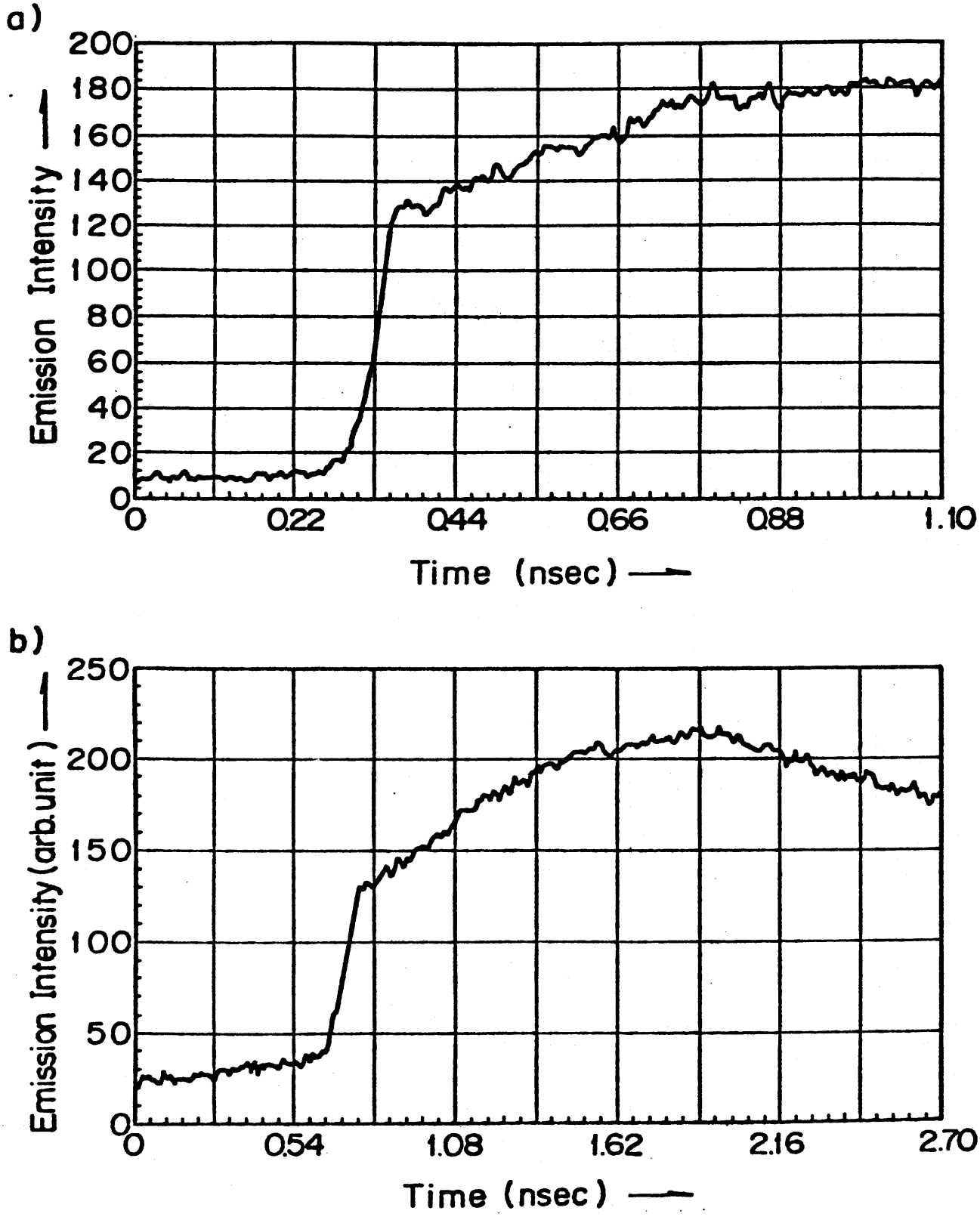
a)
Emission Intensity
200
180
160
140
120
100
80
60
40
20
0
0
0.22
0.44
0.66
0.88
1.10
Time (nsec)
b)
Emission Intensity (arb.unit)
250
200
150
100
50
0
0
0.54
1.08
1.62
2.16
2.70
Time (nsec)

Fig.4 (a) and (b)

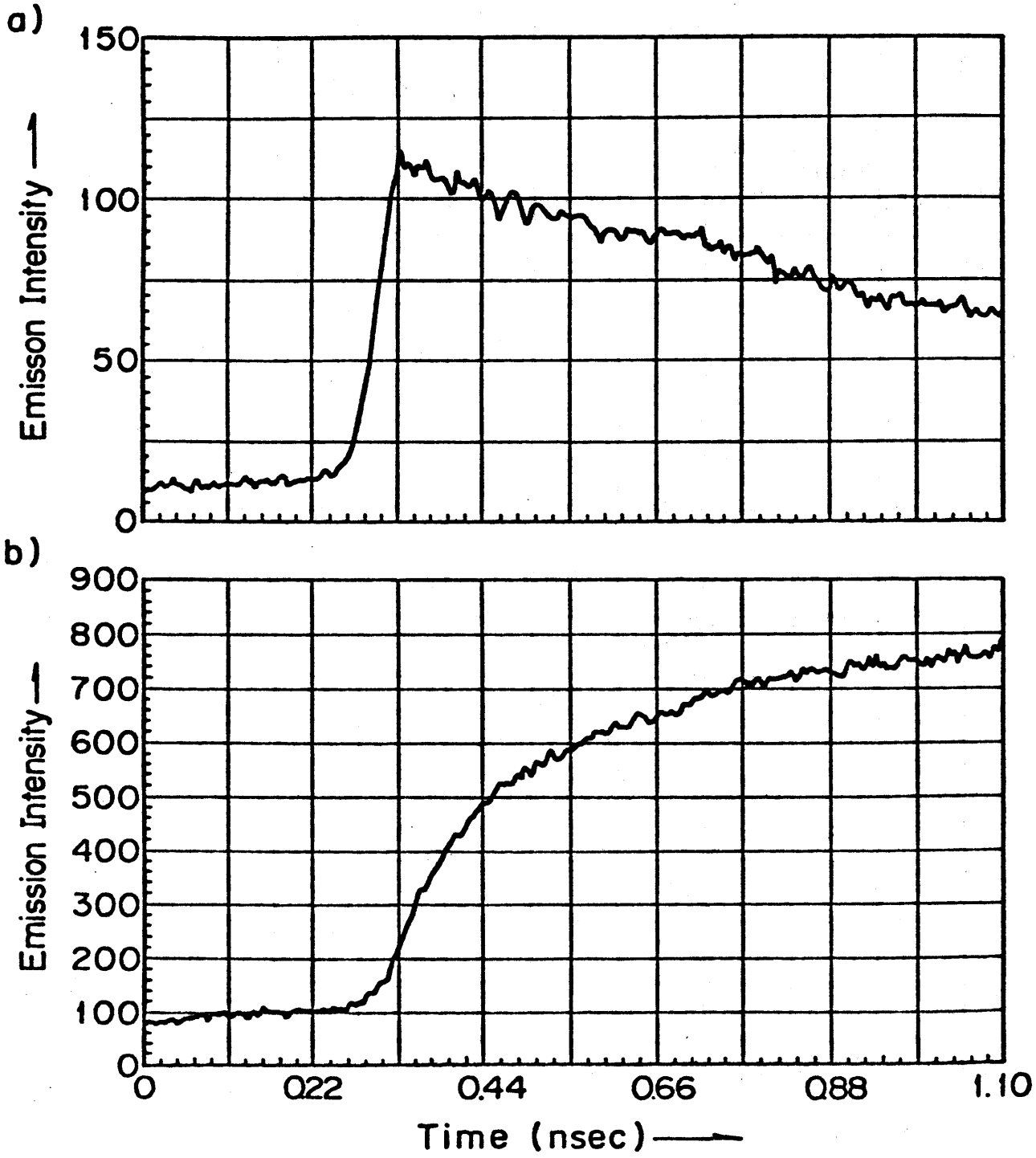
a)
150
100
50
0
Emisson Intensity
b)
900
800
700
600
500
400
300
200
100
0
Emission Intensity
0
0.22
0.44
0.66
0.88
1.10
Time (nsec)

Fig.5 (a) and (b)

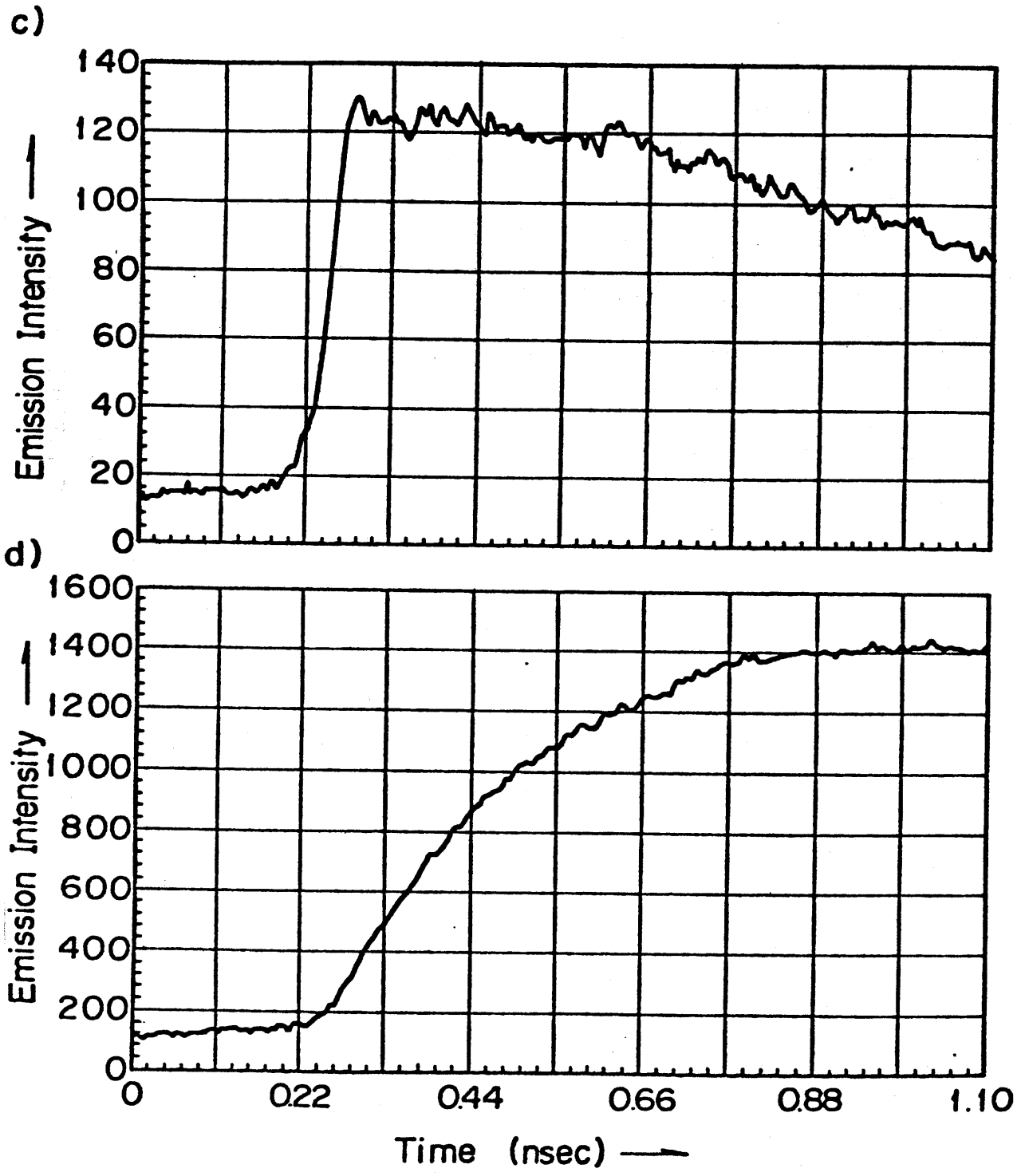
c)
140
120
100
80
60
40
20
0
Emission Intensity
d)
1600
1400
1200
1000
800
600
400
200
0
Emission Intensity
0
0.22
0.44
0.66
0.88
1.10
Time (nsec)

Fig.5 (c) and (d)

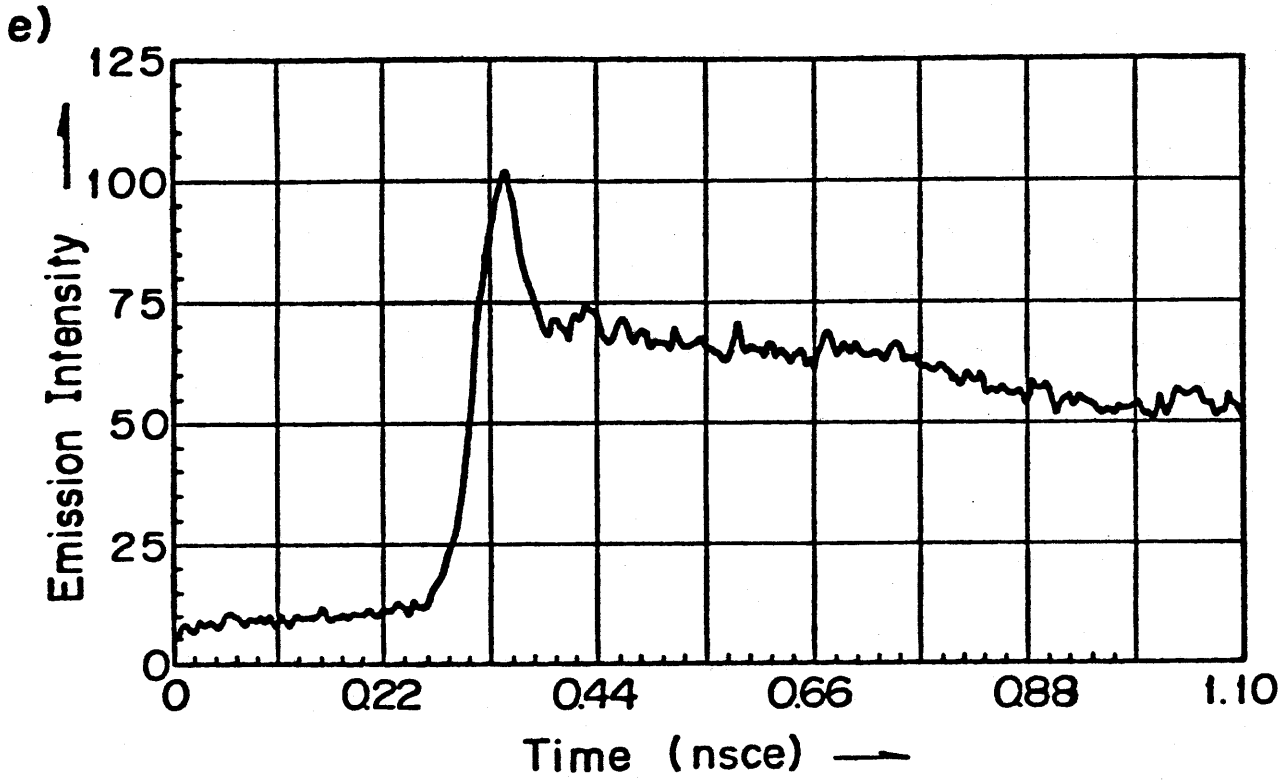
e)
125
100
75
50
25
0
Emission Intensity
0
0.22
0.44
0.66
0.88
1.10
Time (nsce)

Fig.5 (e)

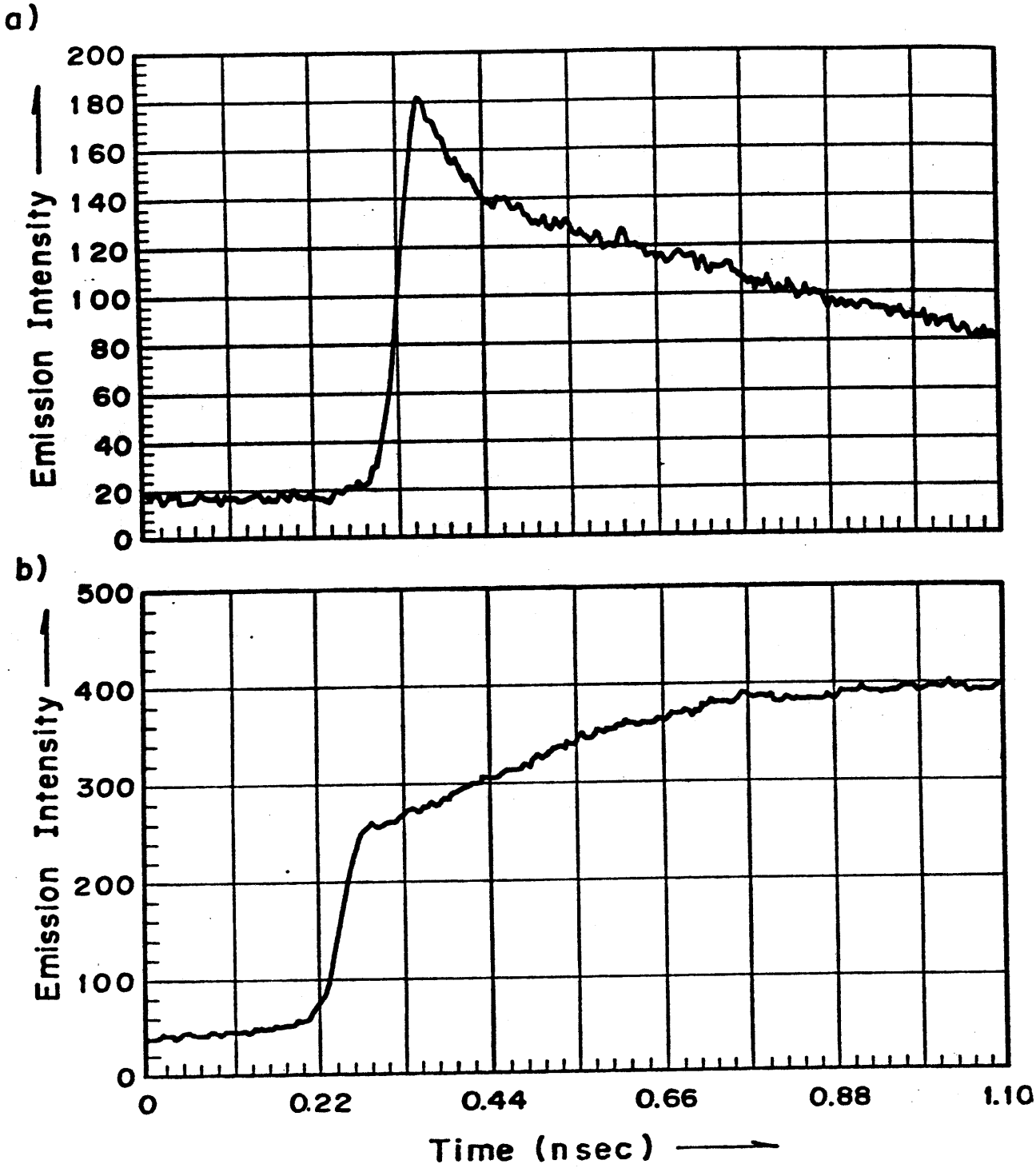
a)
Emission Intensity
200
180
160
140
120
100
80
60
40
20
0
b)
Emission Intensity
500
400
300
200
100
0
0
0.22
0.44
0.66
0.88
1.10
Time (nsec)

Fig.6 (a) and (b)

c)

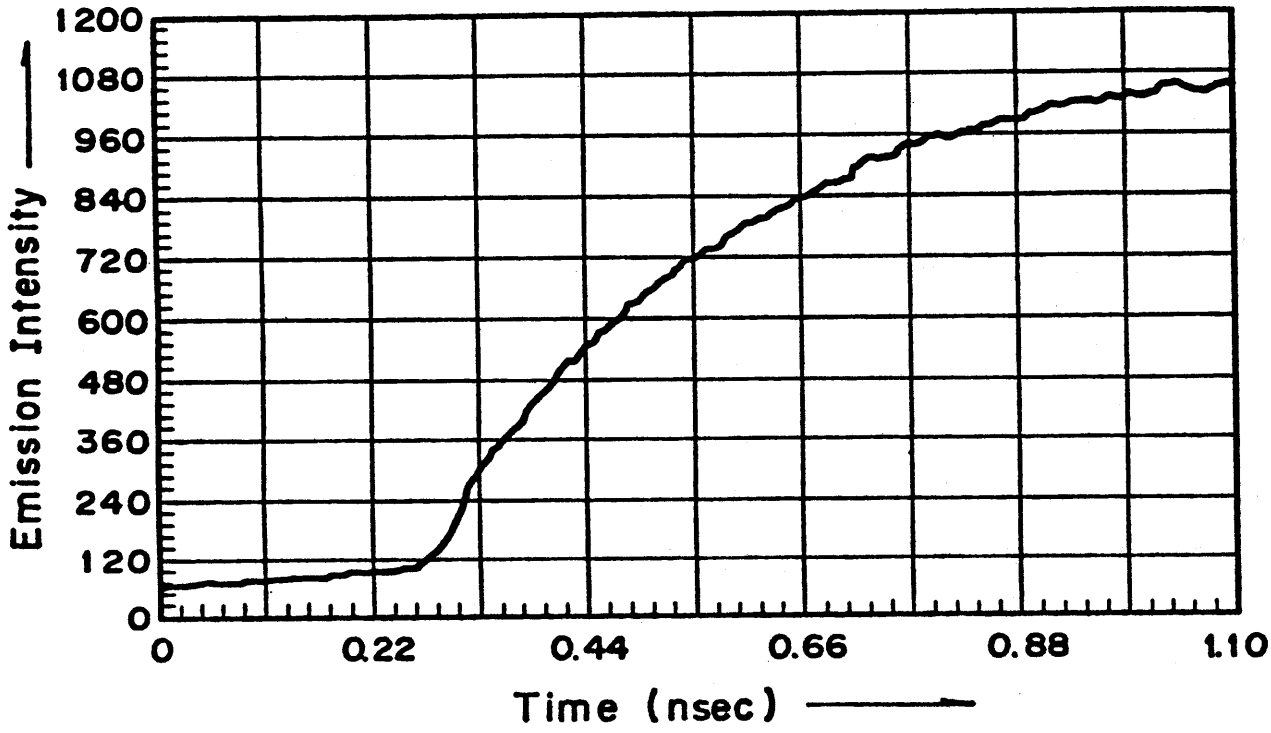
1200
1080
960
840
720
600
480
360
240
120
0
Emission Intensity
0
0.22
0.44
0.66
0.88
1.10
Time (nsec)

Fig.6 (c)

Chapter 11.

Excimer Formation of Hexafluorobenzene by Means of Picosecond Pulse Radiolysis

It is well known that excited aromatic moleucles form excimer in liquid phase [1]. As for various kind of alkylbenzenes, Hirayama and Lipsky [2] observed emission from monomers and excimers as a function of aromatic concentration over the temperature range from 25 to -100 °C. They found a clear isoemissive point and discussed the details of the monomer-excimer kinetics. The excimer emission is found to be weak as compared to higher polyacene such as pyrene.

Hexafluorobenzene has been reported to have an electron affinity between 1 and 2 eV [3] and to have large cross section of electron attachment at ∿0.0 and ∿0.73 eV in gas phase [4]. Therefore, C_6F_6 has been used frequently for an electron scavenger in liquid phase for the studies on early processes in radiation chemistry [5].

Recently, studies of the formation of excited solute molecules in liquid hydrocarbons by means of a single picosecond electron pulse radiolysis technique with 30 psec time resolution have been carried out by the authors [6]. It was found that C_6F_6 forms excimer more easily than other alkylbenzene derivatives, and decay time of excimer emission was measured.

Guaranteed hexafluorobenzene are used as received from Tokyo Kasei and PCR Research Chemicals, Inc. Steady state absorption and emission spectra of hexafluorobenzene solution was measured by using Shimazu UV 360 and

Hitachi MPF-4, respectively. Details of pulse radiolysis system and detection system were reported elsewhere [6].

In Fig. 1, absorption and emission spectra of hexafluorobenzene in isooctane are shown. It was found that emission spectra have two peaks, ∿276 nm and ∿355 nm. The former decreases and the latter increases with increase of C_6F_6 concentration. They show a clear isoemissive point at 303 nm. Above two emission bands, 276 nm and 355 nm, are identified as monomer and excimer one. From theoretical consideration [2], the value, $(\psi_s/\psi_m)/(\psi_L/\psi_e)$ equals to $1+1/\bar{K}_c$, where ψ_s and ψ_L, ψ_m and ψ_e, $\bar{K}$ and c are monomer and excimer emission yields, monomer and excimer intrinsic emission quantum yield, equilibrium constant and solute (C_6F_6) concentration, respectively. Above plot of this system shows a clear straight line as shown in Fig. 2 and the value of $\bar{K}=7(\pm2)\times10^2$ [M^{-1}] was obtained. A large $\bar{K}$ implies substantial excimer emission at relatively low monomer concentration as above results. This fact is very different from other non-fluorinated benzene alkyl derivatives [2] and monofluorobenzene [7].

Excimer emissions at 360 nm and 308 nm in pure C_6F_6 liquid irradiated electron pulse at room temperature observed by a streak camera are shown in Fig. 3(a) and (b). It is noted that a spike of emission superimposed is Čerenkov light induced by electron pulse in sample medium. In the pure C_6F_6 liquid, formation of the excimer is completed within 100 psec. However, monomer emission around 280 nm could not observed because the emission is significantly weak. The lifetime of the excimer emission in pure liquid was obtained to be 2.2(±0.1) ns. Although, in 1.74 mM C_6F_6-cyclohexane solution, the emission becomes weak, growth of emission at 360 nm is clearly observed over 1 ns after the Čerenkov light as shown in Fig. 4. In diluted solution, the decay of excimer emission is almost the same with in pure C_6F_6. These results clearly show that these two excited states form dynamic equilibrium very rapidly. Precise analysis is in progress at present.

References

[1] J.B. Birks p301 in "Photophysics of Aromatic Molecules" Wiley-Interscience 1970.

[2] F. Hirayama and S. Lipsky; J. Chem. Phys. 51 1939 (1969)

[3] C. Lifshitz, T.O. Tierman and B.M. Hughes; J. Chem. Phys. 59 318 (1973)

[4] K.S. Gant and L.G. Christophorou; J. Chem. Phys. 65 2977 (1976)

[5] L. Nyikos, C.A.M. Van den Ende, J.M. Warman and A Hummel Preprints at Collogue Weyl V Aciemore Scotland 25-29 June 1979.

[6] S. Tagawa, Y. Katsumura and Y. Tabata; Chem. Phys. Lett. 64 258 (1979)
Y. Katsumura, T. Kanbayashi, S. Tagawa and Y. Tabata; Chem. Phys. Lett. 67 183 (1979)
Y. Katsumura, S. Tagawa, and Y. Tabata; J. Phys. Chem; 84 833 (1980)

[7] I.B. Berlman "Handbook of Fluorescence spectra of Aromatic Molecules" Academic Press 1971.

Figure Captions

Fig. 1 (a) Absorption spectrum of C_6F_6 in isooctane .

(b) Emission spectra of C_6F_6 in isooctane by 255 nm photo-excitation. It is clearly seen isoemissive point at ∿304 nm.

Fig. 2 Ratio of the emission at 276 nm to that at 360 nm as a function of [concentration]$^{-1}$.

Fig. 3 Emission from pure C_6F_6 liquid irradiated by electron beam (∿10 psec duration) at 360 nm (a) and 308 nm (b).

Fig. 4 Emission at 360 nm from 1.74 mM C_6F_6 in cyclohexane by electron irradiation. Growth of emission is clearly observed after irradiation.

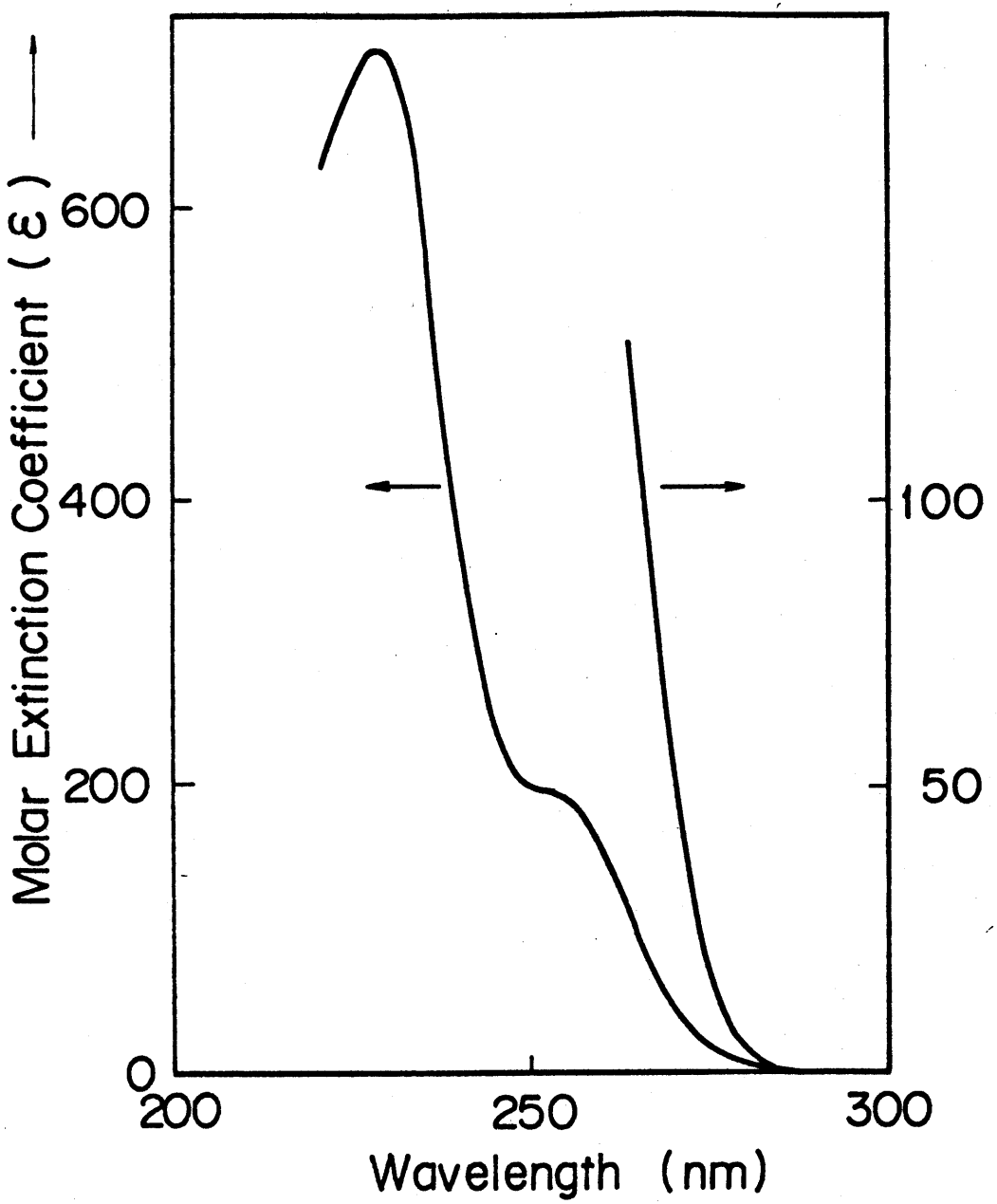
Molar Extinction Coefficient (ε)
600
400
200
0
100
50
200
250
300
Wavelength (nm)

Fig.1 (a)

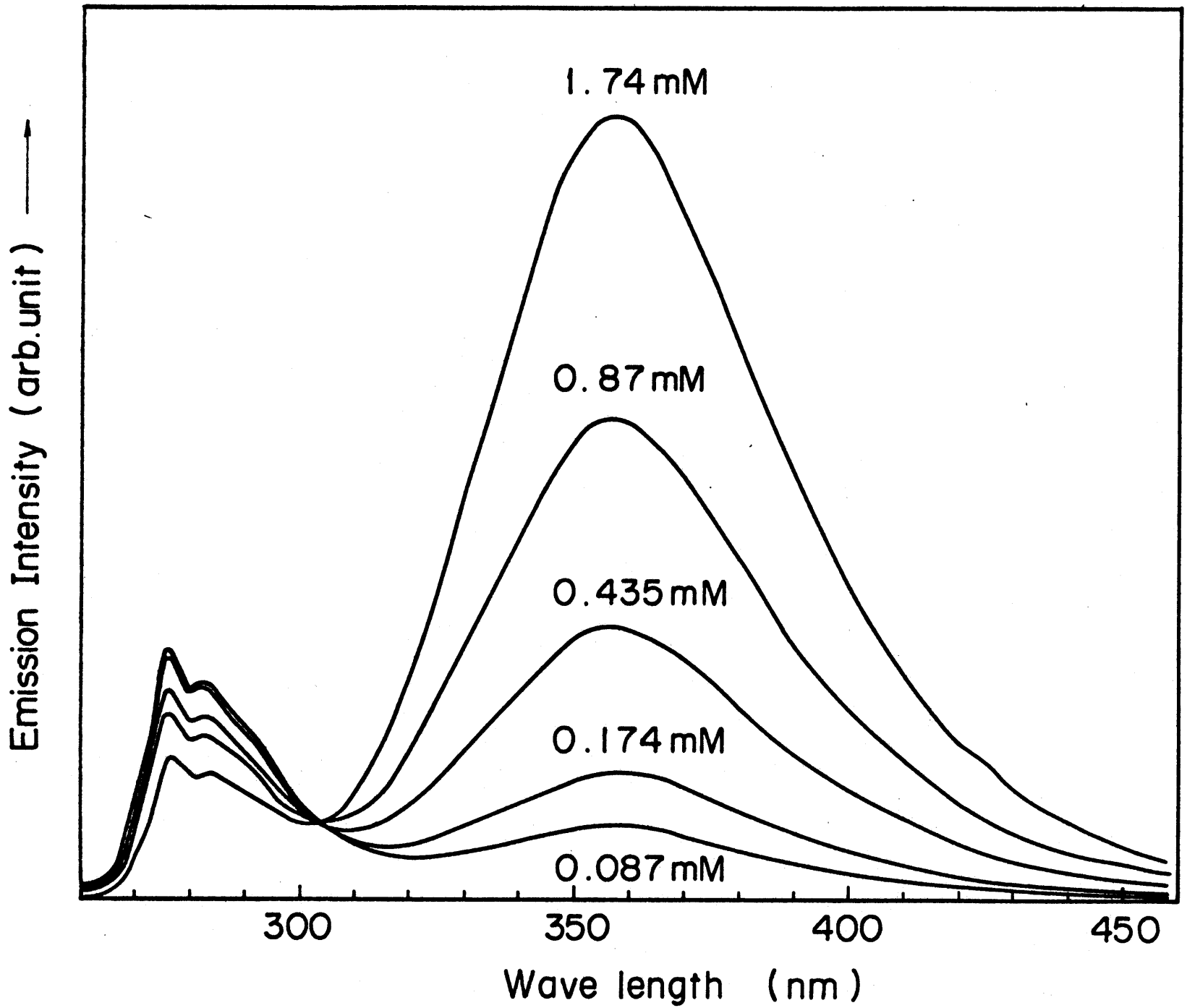
1.74 mM
0.87 mM
0.435 mM
0.174 mM
0.087 mM
Emission Intensity (arb.unit)
300
350
400
450
Wave length (nm)

Fig.1 (b)

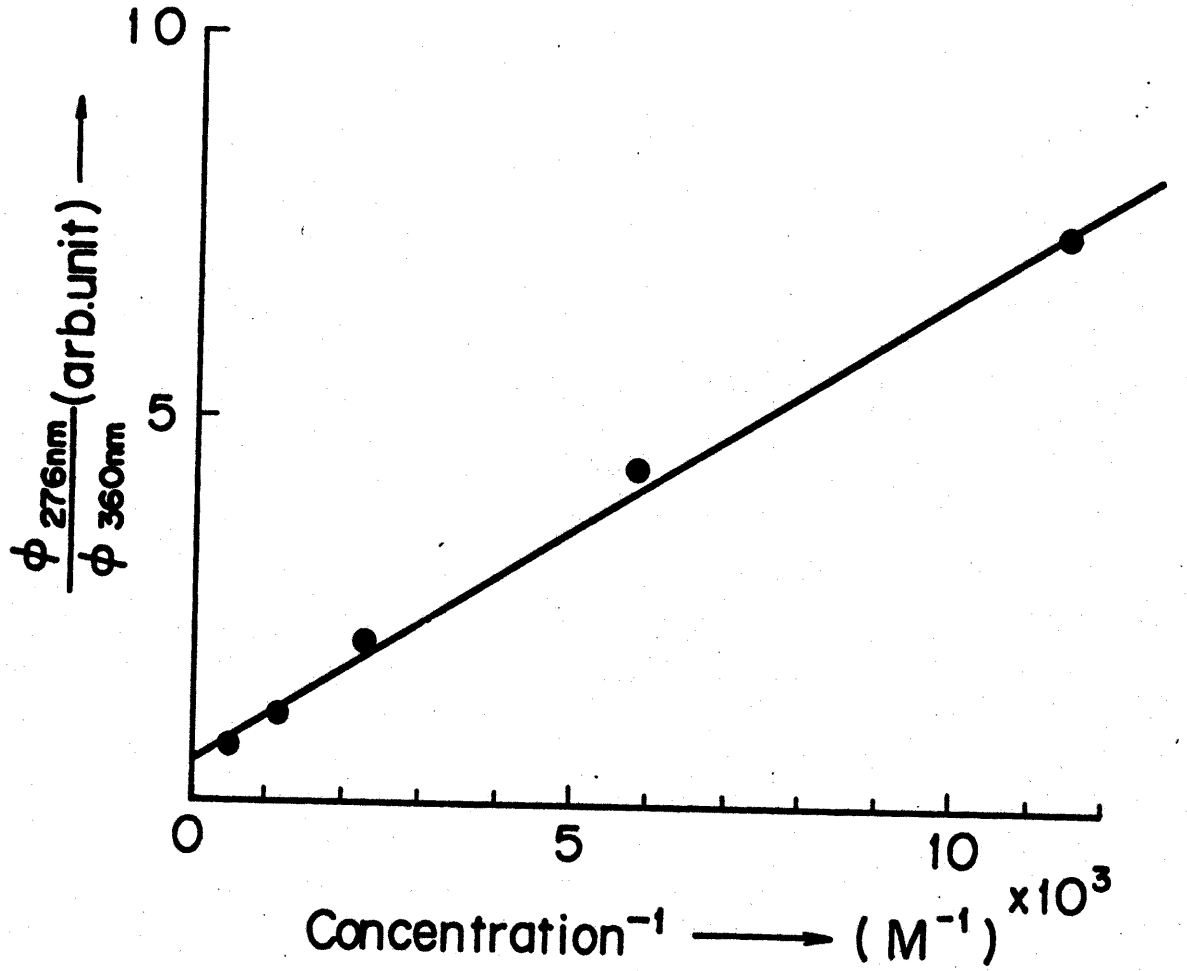
10
5
0
5
10
$\frac{\phi_{276nm}}{\phi_{360nm}}$(arb.unit) ⟶
Concentration^{-1} ⟶ (M^{-1}) x10^3

Fig. 2

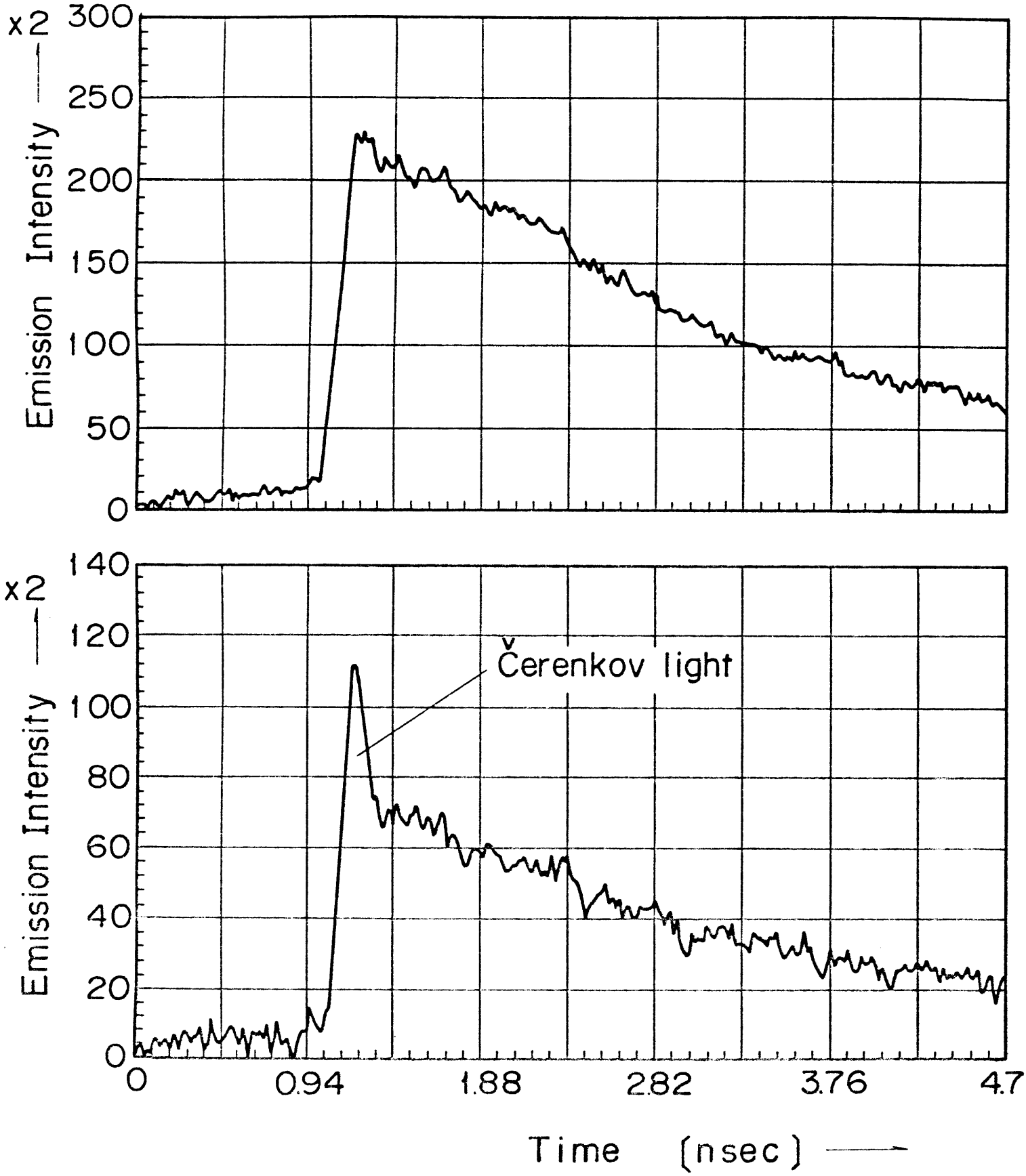
x2
300
250
200
150
100
50
0
Emission Intensity
x2
140
120
100
80
60
40
20
0
Emission Intensity
Čerenkov light
0
0.94
1.88
2.82
3.76
4.7
Time (nsec)

Fig. 3
(a) and (b)

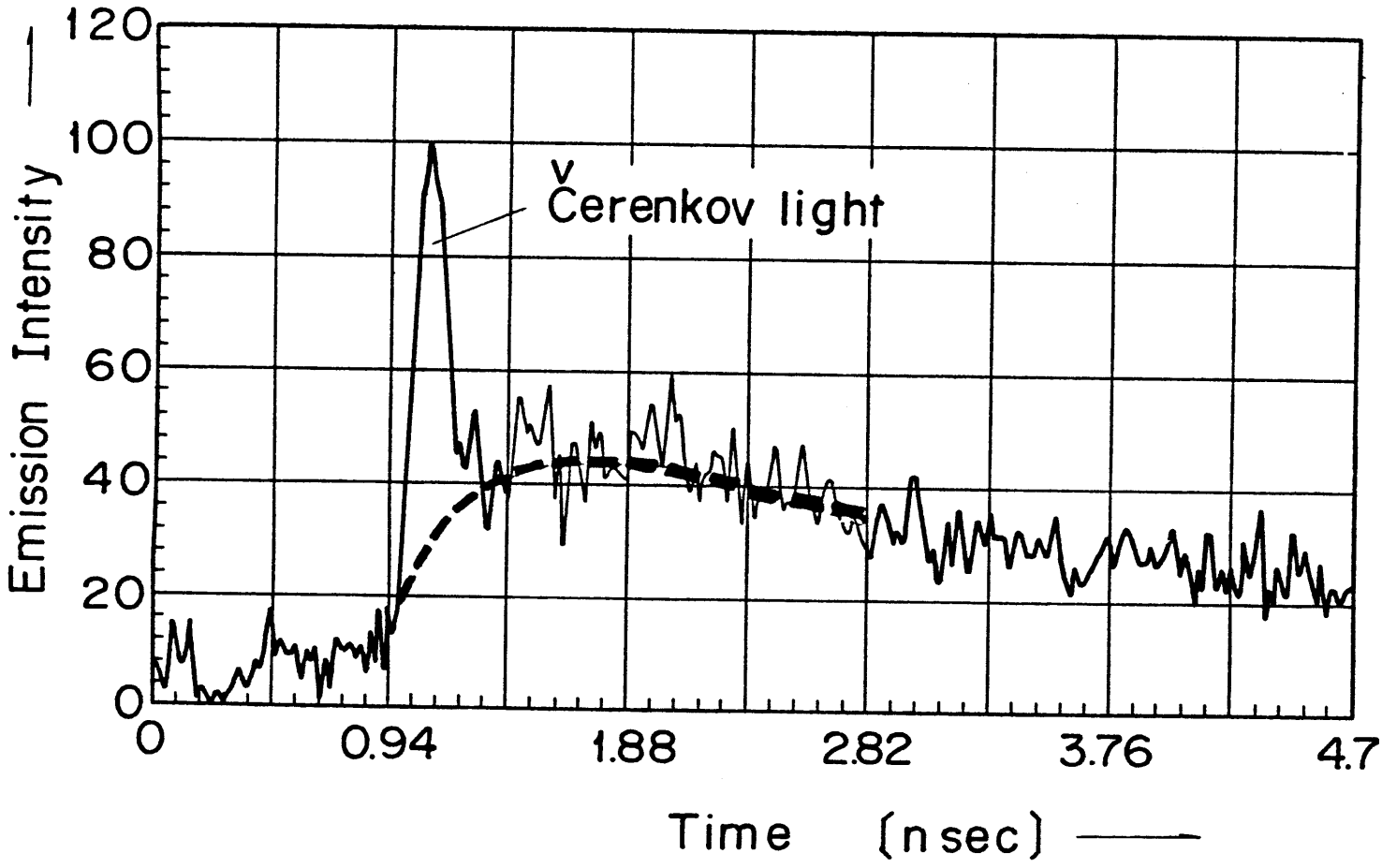
120
100
80
60
40
20
0
Emission Intensity
v
Čerenkov light
0
0.94
1.88
2.82
3.76
4.7
Time (nsec)

Fig. 4